

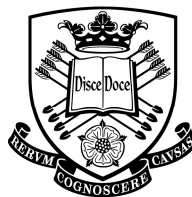
**The Functional Role of
ADAMTS-1 and -15 in
Prostate Cancer Progression**

PhD Thesis

Chidiebele N. Molokwu MBBS, MRCS

**Academic Unit of Molecular Medicine
&
Academic Urology Unit
School of Medical and Biomedical Sciences
University of Sheffield**

October 2011



**The
University
Of
Sheffield.**

CONTENTS

Summary of Thesis.....	6
Sources of Funding.....	8
Acknowledgements.....	9
Dedication.....	11
Prizes, Publications and Presentations.....	12
List of Abbreviations.....	14
List of Tables and Figures.....	16
1. Introduction.....	24
1.1 Epidemiology of Prostate Cancer.....	25
1.2 Aetiology and Predisposing Factors.....	26
1.3 The Prostate Gland.....	28
1.3.1 Anatomy	
1.3.2 Prostate Cells	
1.3.3 Extracellular Matrix	
1.3.4 Prostatic Secretions	
1.3.5 Androgen Regulation	
1.4 Pathology of Prostate Cancer.....	36
1.4.1 Pathogenesis	
1.4.2 Histopathological Grading	
1.4.3 Staging	
1.4.4 Role of the Androgen Receptor	
1.5 Management of Prostate Cancer.....	44
1.6 The Role of Proteinases in Prostate Cancer	45
1.6.1 Tumourigenesis	
1.6.2 Cell Proliferation and Invasion	
1.6.3 Cell Motility and Invasion	
1.6.4 Angiogenesis	
1.6.5 Establishment of Metastasis	
1.6.6 Clinical Management	
1.6.7 Summary of Proteinase Activity in Prostate Cancer	
1.7 ADAMTS Proteinases.....	61
1.7.1 Introduction to ADAMTS Enzymes	
1.7.2 ADAMTSs in Cancer	
1.7.3 Structure of ADAMTS-1 and -15	
1.7.4 Functions of ADAMTS-1 and -15	
1.8 Inflammation in Prostate Cancer.....	76
1.8.1 Immune Cells and Cytokines	

1.8.2 TNF Receptor Signalling	
1.9 ADAMTS Expression in Inflammatory Disease.....	78
1.10. Aims and Hypotheses	78
2. Materials and Methods.....	81
2.1 Cell Lines and Culture.....	82
2.2 RNA Extraction.....	83
2.3 cDNA Synthesis.....	84
2.4 Real-time RT-PCR.....	84
2.5 Protein Extraction from Cultured Cells.....	87
2.5.1 Extraction using Mammalian Cell Lysis Kit (RIPA Buffer)	
2.5.2 Extraction using Triton X-100	
2.6 Protein Quantification.....	88
2.7 Immunoprecipitation with Protein A-Agarose.....	88
2.8 Precipitation with Heparin-Agarose.....	90
2.9 SDS-PAGE.....	91
2.9.1 Resolving Gel Preparation	
2.9.2 Stacking Gel Preparation	
2.9.3 Sample Preparation	
2.9.4 Electrophoresis	
2.10 Western-Blotting.....	94
2.10.1 Protein Transfer	
2.10.2 Immuno-probing	
2.11 Horseradish Peroxidase Detection.....	96
2.12 PVDF Membrane Stripping.....	96
2.13 Densitometry.....	97
2.14 Fluorescence Immunocytochemistry.....	97
2.15 Regulation of ADAMTS-1, -15 and TIMP-3 by DHT.....	99
2.16 Identification of Putative AREs	100
2.17 Regulation of ADAMTS-1, -15 and TIMP-3 by TNF.....	101

2.18 Transfection Protocols.....	102
2.18.1 Electroporation	
2.18.2 Calcium Phosphate	
2.18.3 Lipid-based Methods	
2.19 Transient Knock-down of ADAMTS-1 and -15.....	105
2.20 Stable Knock-down of ADAMTS-1.....	106
2.21 Proteolysis Assays.....	108
2.22 Chemotaxis Assay.....	109
2.23 Proliferation Assays.....	111
2.23.1 Haemocytometer Counts	
2.23.1 MTT Assay	
2.24 Migration Assays.....	112
2.24.1 Migration using the Scratch Assay	
2.24.1 Migration using the Boyden Chamber	
2.25 Invasion Assays.....	114
2.26 Statistical Analyses.....	116
3. Imaging of Proteolysis in 3-Dimensional Culture	118
3.1 Introduction.....	119
3.2 Gelatinolytic Activity of Multicellular Tumour Spheroids.....	119
3.3 Gelatinolytic Activity of PC3 Cells in Monolayer Culture.....	122
3.4 Co-Culture of PC3 Cells and Prostate Stromal Cells.....	123
3.5 Chemotactic Effect of Stromal Cell-Conditioned Media.....	124
3.6 Discussion	126
4. Expression of ADAMTS-1, -15 and TIMP-3 in Prostate Cells.....	129
4.1 Introduction.....	130
4.2 ADAMTS-1, -15 and TIMP-3 mRNA Expression.....	130
4.3 ADAMTS-1 and -15 Protein Expression	134
4.3.1 Probing for ADAMTS-1 in Cell Lysates	

4.3.2 Test of Specificity of Anti-ADAMTS-1 Antibody	
4.3.3 Probing for ADAMTS-15 in Cell Lysates and Media	
4.3.4 Validation of Anti-ADAMTS-15 Antibody	
4.3.5 Heparin-Agarose Precipitation and Probing for ADAMTS-15	
4.4 Fluorescence Immunocytochemistry for Detection of ADAMTS-15...	151
4.5 Discussion	158
5. Regulation of ADAMTS-1 and -15 by DHT and TNF.....	165
5.1 Introduction.....	166
5.2 Regulation of ADAMTS-1, ADAMTS-15 and TIMP-3 by DHT.....	168
5.2.1 Regulation of PSA mRNA by DHT	
5.2.2 Regulation of ADAMTS-1 mRNA by DHT	
5.2.3 Regulation of ADAMTS-15 mRNA and Protein by DHT	
5.2.4 Regulation of TIMP-3 mRNA by DHT	
5.3 Putative AREs in the <i>ADAMTS1</i> and <i>ADAMTS15</i> Genes.....	175
5.4 Regulation of ADAMTS-1, ADAMTS-15 and TIMP-3 by TNF.....	178
5.4.1 Regulation of ADAMTS-1 mRNA by TNF	
5.4.2 Regulation of ADAMTS-15 mRNA by TNF	
5.4.3 Regulation of TIMP-3 mRNA by TNF	
5.5 Discussion.....	184
6. Knock-down of ADAMTS-1 and -15 and effect on Proliferation, Migration and Invasive Potential of PC3 Cells.....	191
6.1 Introduction.....	192
6.2 ADAMTS-1 and -15 Knock-down	193
6.2.1 Transient Knock-down	
6.2.2 Stable Knock-down	
6.3 Functional Assays	199
6.3.1 Proliferation	
6.3.2 Migration	
6.3.3 Invasion	
6.4 Discussion	218
7. General Discussion, Limitations and Future Directions.....	222
7.1 General Discussion and Limitations.....	223
7.1.1 Proteolytic Activity of Prostate Cells	
7.1.2 Detection of ADAMTS-1 and -15 Protein	
7.1.3 Androgen Regulation of ADAMTS-15 and TIMP-3	

7.1.4 TNF Regulation of ADAMTS-15 and TIMP-3	
7.1.5 ADAMTS-1 and -15 Gene Silencing and Functional Assays	
7.1.6 Relevance of ADAMTS-15 Cleavage Products	
7.2 Future Work.....	238
7.3 Conclusions.....	240
8. References	241
9. Appendix	283
Appendix A: Peer-Reviewed Publication	284
Appendix B: Copyright Permissions	297
Appendix C: List of Suppliers	303

SUMMARY OF THESIS

Introduction: Prostate cancer is a leading cause of cancer death in men. Death is usually a consequence of castration resistant tumour progression. Some metalloproteinases are implicated in the process of cancer progression. ADAMTS proteinases (A Disintegrin And Metalloproteinase with ThromboSpondin motifs) are metalloproteinases that play diverse roles in tissues. Prostate cancer cells express ADAMTS-1 and -15 but the role played by these proteinases in prostate cancer progression is unknown. This study was designed to determine the role of ADAMTS-1 and 15 in prostate cancer progression.

Materials & Methods: Prostate cancer and stromal cell tumour spheroids were grown in 3-dimensional culture in ECM gel containing a quenched-fluorescent substrate. The tumour spheroids were observed for evidence of proteolytic activity. Prostate cancer cells were treated with DHT and TNF. Changes in expression of ADAMTS-1 and -15 were analysed. ADAMTS-1 and -15 expression was knocked-down in PC3 prostate cancer cells and the effect of knock-down on proliferation, migration and invasion was analysed.

Results: Tumour spheroids emitted fluorescence after approximately 24 hours in culture, indicating proteolytic activity. DHT and TNF down-regulated ADAMTS-15 expression in LNCaP cells and stromal cells respectively. The validated anti-ADAMTS-15 antibody detected 50kDa bands, suggesting a novel cleavage site within the disintegrin-like domain of ADAMTS-15. ADAMTS-1 and 15 knock-down had no effect on proliferation, migration or invasion of PC3 prostate cancer cells.

Conclusions: Prostate cancer and stromal cells degrade components of the surrounding ECM. ADAMTS-15 but not ADAMTS-1 expression is androgen and TNF-regulated. ADAMTS-1 and 15 expression do not affect the proliferation, migration or invasive

potential of PC3 cells *in vitro*. Cleavage of ADAMTS-15 in the disintegrin-like domain results in the release of a C-terminal fragment with potential anti-angiogenic properties. Down-regulation by DHT in prostate cancer cells suggests that ADAMTS-15 could be playing an anti-tumour role in prostate cancer progression.

SOURCES OF FUNDING

Funding for this project was obtained from three main sources. The Ian Sunter Charitable Trust provided support through a competitive fellowship award from the Royal College of Physicians and Surgeons of Glasgow. BMI Thornbury Hospital, Sheffield provided support in form of a grant for consumable supplies over three years, and personal support which allowed me to spend 75% of my time on this project. The work was also supported by the National Cancer Research Institute through a grant awarded to Professor F.C. Hamdy for the ProMPT study.

ACKNOWLEDGEMENTS

My interest in prostate cancer research began when I was drafted into a group as a medical student to do a community health project studying the variations in PSA levels between ethnic groups in Trinidad, West Indies. Following that experience, Professor Hylton McFarlane encouraged me to explore the possibility of doing further research on prostate cancer. I owe many thanks to him for his support and guidance at that stage of my career. A multitude of thanks to Dr. Dave Buttle and Prof. Freddie Hamdy for their supervision of this thesis. Dr. Buttle provided laboratory supervision and provided a suitable learning environment that made this work possible. Prof. Hamdy provided invaluable support, guidance and mentorship that helped to bring this work to completion. I am grateful to Ms. Jumoke Adeniji for her help and friendship and for sharing vital tips on various experimental protocols. I would like to acknowledge the help of Dr. Elizabeth Waterman Dr. Neil Cross and Mrs. Nicola Jokonya for introducing me to laboratory techniques and cell culture. Dr. Colby Eaton deserves my appreciation for being a valuable source of advice as my academic mentor. Thanks to Prof. Nicola Woodroffe, Dr. Ingunn Holen, Prof. Claire Lewis and Prof. Gerry Wilson for help from their group members at various stages of this work. Funding for this project was provided by BMI Thornbury Hospital, the Royal College of Physicians and Surgeons of Glasgow and the National Cancer Research Institute via the ProMPT funding mechanism. Their generosity provided the resources necessary to carry out this study.

On a personal note, I am grateful to my family and friends for support throughout the period of this study. Mostly I am grateful to my wife, Amaka, for her care and understanding especially during the busiest and most stressful periods. My three year old daughter, Miriam, helped in her own way to edit my thesis by clicking random keys

on my laptop in my absence. My parents were a constant source of support and encouragement throughout my education and more so during this project. I couldn't ask for more from them. I am also grateful to my clinical mentors on the East of Scotland Training Programme in Urology, Ms. Justine Royle, Mr. Chris Goodman and Mr. Antony Riddick for their constant support and advice while writing up this thesis.

Lastly, I am grateful to God for giving me the intellectual and physical ability to carry out this work, and the inner strength to persevere when things were not going to plan. I hope that my effort will help in some way to prevent or alleviate the burden of prostate cancer on men all over the world.

DEDICATION

This thesis is dedicated to the memory of my father, Eliezer Molokwu, who died in September 2010 after living with prostate cancer for ten years. He succumbed after battling with metastatic disease and the associated complications. His life is a constant source of inspiration to me. Coming from humble beginnings, reaching the peak of his career as a veterinary reproductive physiologist, and at the same time being a caring and dedicated father. He is greatly missed.

PRIZES, PUBLICATIONS & PRESENTATIONS

PRIZES & AWARDS

HRH The Princess Royal Prize for 2nd Best Presentation

Royal College of Physicians & Surgeons of Glasgow Triennial Conference, Nov 2008, SECC, Glasgow

Ian Sunter Charitable Trust Research Fellowship (£40,000)

Royal College of Physicians & Surgeons of Glasgow. Jul 2006

Prize for 2nd Best Scientific Presentation, British Prostate Group Autumn Meeting, Royal College of Surgeons, London. Dec 2005

PUBLICATIONS

PEER-REVIEWED

Molokwu CN, Adeniji OO, Chandrasekharan S, Hamdy FC, Buttle DJ. Androgen regulates *ADAMTS15* gene expression in prostate cancer cells. *Cancer Investigation* 2010; 28(7):698-710.

ABSTRACTS

Molokwu CN, Adeniji OO, Chandrasekharan S, Hamdy FC, Buttle DJ. Regulation of *ADAMTS15* by dihydrotestosterone in prostate cancer cells and identification of putative androgen response elements. *BJU International* 2009; 103(S4):20

Molokwu CN, Adeniji OO, Hamdy FC, Buttle DJ. Regulation of ADAMTS expression in prostate cancer and stromal cells by androgen and TNF: P040. *International Journal of Experimental Pathology* 2007; 88(6):A95

Molokwu CN, Adeniji OO, Hamdy FC, Buttle DJ. Imaging proteolysis in prostate cancer and stromal cells: P039. *International Journal of Experimental Pathology* 2007; 88(6):A95

Adeniji OO, **Molokwu CN**, Waterman EA. Cross NA, Hamdy F C, Buttle D J. TIMP-3 expression in prostate stromal and tumour cells is regulated by androgen and TNF: P034. *International Journal of Experimental Pathology* 2007; 88(6):A93-A94

Adeniji OO, **Molokwu CN**, Waterman EA, Cross NA, Hamdy FC, Buttle DJ. Evaluating the role of ADAMTS proteoglycanases and TIMP-3 in prostate cancer progression: P8. *International Journal of Experimental Pathology* 2007; 88(4):A58

PRESENTATIONS

Molokwu CN, Adeniji OO, Hsu Y, Hamdy FC, Buttle DJ. Regulation of *ADAMTS15* by dihydrotestosterone in prostate cancer cells and identification of putative androgen

response elements. Poster & Oral Presentation, British Association of Urologic Surgeons Annual Meeting, Glasgow. June 2009

Molokwu CN, Adeniji OO, Hsu Y, Hamdy FC, Buttle DJ. Regulation of *ADAMTS15* by Androgen and Identification of Putative Androgen Response Elements. Poster Presentation, American Association of Cancer Research Centennial Conference, Colorado Convention Centre, U.S.A. April 2009

Molokwu CN, Adeniji OO, Hamdy FC, Buttle DJ. Regulation of *ADAMTS15* by Androgen and Identification of Putative Androgen Response Elements. Poster Presentation, Royal College of Physicians & Surgeons of Glasgow Triennial Conference, Glasgow. Nov 2008

Molokwu CN, Adeniji OO, Waterman EA, Cross NA, Hamdy FC, Buttle DJ. Evaluating the Role of ADAMTS Enzymes & TIMP-3 in Prostate Cancer Progression. Poster Presentation, National Cancer Research Institute Conference, Birmingham. Oct 2006

Molokwu CN, Hamdy FC, Buttle DJ. Evaluating the Role of ADAMTS-1 in Prostate Cancer Invasion. Poster Presentation, American Society for Clinical Oncology Prostate Cancer Symposium, San Francisco Marriott, U.S.A. Feb 2006

Molokwu CN, Hamdy FC, Buttle D.J. Evaluating the Role of ADAMTS-1 in Prostate Cancer Invasion. Poster Presentation, British Prostate Group Autumn Meeting, Royal College of Surgeons, London. Dec 2005

Molokwu CN, Hamdy FC, Buttle DJ. Imaging of Proteolysis in Prostate Cancer Cells. Poster presentation, Prostate Cancer: Roadmap to the Future, Roswell Park Cancer Institute, Buffalo, New York, U.S.A. July 2005

LIST OF ABBREVIATIONS

3D	3-Dimensional
aa	Amino Acid
ADAM	A Disintegrin and Metalloproteinase
ADAMTS	A Disintegrin and Metalloproteinase with Thrombospondin Motifs
ADT	Androgen Deprivation Therapy
ANOVA	Analysis of Variance
APS	Ammonium persulphate
AR	Androgen Receptor
ARE	Androgen Response Element
bFGF	Basic Fibroblast Growth Factor
bp	Base Pair
BPH	Benign Prostatic Hyperplasia
BSA	Bovine Serum Albumin
CaP	Prostate Cancer
cDNA	Complementary Deoxyribonucleic Acid
CRPC	Castration-resistatant Prostate Cancer
CS	Chondroitin Sulphate
CSPG	Chondroitin Sulphate Proteoglycans
Da	Daltons
DBD	DNA-binding domain
DEPC	Diethyl pryrocarbonate
DHT	Dihydrotestosterone
DMEM	Dulbecco's modification of Eagle's medium
DNA	Deoxyribonucleic Acid
dNTP	Deoynucleotide triphosphate
DTT	Dithiothreitol
EDTA	Ethylenediaminetetraacetic Acid
ECM	Extracellular Matrix
EGF	Epidermal Growth Factor
FCS	Foetal Calf Serum
FOLH1	Folate Hydrolase 1
GAPDH	Glyceraldehyde3-phosphate dehydrogenase
GRE	Glucocorticoid Response Element
hKLLK3	Human Kallikiein 3
HRE	Hormone Response Element
HRP	Horse Radish Peroxidase
HRPC	Hormone-refractory Prostate Cancer
HS	Heparan Sulphate
HSP	Heat Shock Protein
HSPG	Heparan Sulphate Proteoglycans
Ig	Immunoglobulin
IL	Interleukine
kDa	Kilodaltons
LBD	Ligand-binding Domain
LPS	Lipopolysaccharide
MMP	Matrix Metalloproteinase
mRNA	Messenger Ribonucleic Acid

NF- κ B	Nuclear factor- κ B
NR3C	Nuclear Receptor 3C
NTD	Amino-terminal domain
PBS	Phosphate-buffered Saline
PIN	Prostatic Intraepithelial Neoplasia
Pol II	RNA Polymerase II
PSA	Prostate Specific Antigen
Rh	Recombinant Human
RT-PCR	Reverse Transcriptase Polymerase Chain Reaction
SD	Standard Deviation
SEM	Standard Error of the Mean
siRNA	Short Interfering Ribonucleic Acid
Slp	Sex-limited Protein
TAM	Tumour Associated Macrophage
TBS	Tris-buffered Saline
TEMED	Tetramethylethylenediamine
TGF- β	Transforming Growth Factor Beta
TIMP	Tissue Inhibitor of Metalloproteinases
TME	Tumour Micro-environment
TNF	Tumour Necrosis Factor
TNFR	Tumour Necrosis Factor Receptor
TSP	Thrombospondin
Tween-20	Polyoxylenesorbitan sulphate
VEGF	Vascular Endothelial Growth Factor
VEGFR	Vascular Endothelial Growth Factor Receptor
WT	Wild-type

LIST OF TABLES & FIGURES

Chapter 1

Table 1.1: Summary of the TNM staging system for prostate cancer.....	39
Table 1.2: Established management options for patients with prostate cancer.....	44
Table 1.3: Classification of proteinases according to the amino acid residue at the catalytic site.....	45
Table 1.4: Expression of proteinases in prostate cancer and correlation with Gleason score.....	46
Table 1.5: Summary of some known and putative biological activity of proteinases in prostate cancer.....	47
Table 1.6: Summary of the expression of ADAMTS proteins in human cancer tissue and cells compared with non-malignant tissue.....	69
Table 1.7: Similarities between ADAMTS-1 and -15 domain length and configuration.	
Figure 1.1: Anatomy of the male genito-urinary system.....	29
Figure 1.2: Zonal anatomy of the prostate.....	30
Figure 1.3: Cells of the prostate gland.....	31
Figure 1.4: Production and regulation of androgens.....	36
Figure 1.5: Progression of prostate cancer.....	37
Figure 1.6: The Gleason grading system.....	38
Figure 1.7: Magnetic resonance imaging of the pelvis of a prostate cancer patient.	40
Figure 1.8: Local progression of prostate cancer.....	40
Figure 1.9: Radio-nuclide bone scintigraph of a prostate cancer patient with advanced disease.....	41
Figure 1.10: Activation cascade of some of the proteolytic enzymes involved in tumour metastasis.....	52

Figure 1.11: Schematic diagram of the prostate and bone micro-environment showing the role of proteinases in primary and secondary tumour sites.....	61
Figure 1.12: Domain structure of MMPs, ADAMs and ADAMTSs.....	62
Figure 1.13: Phylogenetic tree of the ADAMTS proteins.....	64
Figure 1.14: Generic structure of ADAMTS-1 and -15.....	70
<u>Chapter 2</u>	
Table 2.1: Gene, primer and amplicon data for primer products supplied by Applied Biosystems and used with SYBR-Green as the reporter dye.....	86
Table 2.2: Gene, assay, probe, reporter and amplicon data for Taqman primer products supplied by Applied Biosystems.....	86
Table 2.3: DNA sequences of six HREs that have been experimentally verified and shown to be functional AR binding sites.....	100
Table 2.4: Sequence data for siGENOME SMARTpool siRNA from Dharmacon showing the sequence ID and nucleotide sequence for each of the siRNA duplexes.....	106
Figure 2.1: Method of performing immunoprecipitation using protein A-agarose beads.....	89
Figure 2.2: Method of performing precipitation using heparin-agarose beads.....	91
Figure 2.3: shRNA sequences designed for stable knock-down of ADAMTS-1....	107
Figure 2.4: Schematic representation of transient and stable knock-down of ADAMTS-1 and ADAMTS -15.....	108
Figure 2.5: Cleavage of quenched fluorescent gelatin by proteolysis.....	109
Figure 2.6: Modified Boyden chamber used for chemotaxis assays....	110
Figure 2.7: Cell migration using the scratch assay.....	113
Figure 2.8: Modified Boyden chamber used for invasion assays.....	115

Chapter 3

Figure 3.1: PC3 multicellular tumour spheroid grown in 3D culture in ECM gel containing 25mg/ml DQ-Gelatin.....	120
Figure 3.2: LNCaP multicellular tumour spheroid grown in 3D culture in ECM gel containing 25mg/ml DQ-Gelatin.....	121
Figure 3.3: BPH45 (stromal cell) multicellular tumour spheroid grown in 3D culture in ECM gel containing 25mg/ml DQ-Gelatin.....	121
Figure 3.4: PC3 cells in monolayer 3D culture in ECM gel containing 25mg/ml DQ-Gelatin....	122
Figure 3.5: PC3 cells in Figure 3.4 at higher magnification.....	123
Figure 3.6: PC3 and BPH45 stromal cell co-culture in ECM gel containing 25mg/ml DQ-Gelatin.....	124
Figure 3.7: PC3 and BPH45 stromal cell co-culture from Figure 3.6 at higher magnification.....	124
Figure 3.8: Chemotaxis assay showing the chemo-attractive force on PC3 cells by DMEM conditioned by BPH45 stromal cells.....	125

Chapter 4

Table 4.1: Relative expression of ADAMTS-1 and GAPDH in PC3 cells determined by realtime RT-PCR following knock-down of ADAMTS-1 and GAPDH.....	137
Figure 4.1: ADAMTS-1 mRNA expression levels in PC3, LNCaP, C4-2b4, PCAF, U373 and MDA-G8 cell lines.....	131
Figure 4.2: ADAMTS-15 mRNA expression levels in PC3, LNCaP, C4-2b4, PCAF, U373 and MDA-G8 cell lines.....	132
Figure 4.3: TIMP-3 mRNA expression levels in PC3, LNCaP, C4-2b4, PCAF, U373 and MDA-G8 cell lines.....	133

Figure 4.4: Western blotting of U373, MDA-G8, PC3, LNCaP, C4-2b4 and PCAF cell lysates using a rabbit polyclonal antibody (Abcam, ab39194) raised against the C-terminus of ADAMTS-1.....	135
Figure 4.5: Western blotting of U373, MDA-G8, PC3, LNCaP, C4-2b4 and PCAF cell lysates using a mouse monoclonal antibody (R&D Systems, MAB2197) raised against the catalytic domain of ADAMTS-1.....	136
Figure 4.6: Test of specificity of the mouse monoclonal anti-ADAMTS-1 catalytic domain antibody (R&D Systems, MAB2197).....	139
Figure 4.7: Detection of ADAMTS-15 in U373, MDA-G8, PC3, LNCaP, C4-2b4 and PCAF cell lysates using the rabbit polyclonal cysteine-rich domain antibody (Abcam, ab28516).....	141
Figure 4.8: Immunoprecipitation and western blotting for ADAMTS-15 on cell lysate and conditioned medium from PC3 and LNCaP cells.....	143
Figure 4.9: Probing of PVDF membranes with either anti-ADAMTS-15 primary and HRP-labelled secondary antibodies or TBST as primary and HRP-labelled secondary antibody.....	144
Figure 4.10: Western blot to determine the source of bands detected on lysates after immunoprecipitation.....	146
Figure 4.11: Western blotting for ADAMTS-15 in U373, MDA-G8, PC3, LNCaP, C4-2b4 and PCAF cell lysates using a rabbit polyclonal propeptide domain antibody (Abcam ab45047).....	148
Figure 4.12: Validation of the specificity of the rabbit polyclonal anti-ADAMTS-15 antibody (Abcam ab45047).....	150
Figure 4.13: Fluorescence immunocytochemistry for detection of ADAMTS-15 expression in non-targeting knock-down PC3 cells.....	153

Figure 4.14: Fluorescence immunocytochemistry probing for ADAMTS-15 in ADAMTS-15 knock-down PC3 cells.....	154
Figure 4.15: Fluorescence immunocytochemistry for detection of GAPDH expression in non-targeting knock-down PC3 cells.....	156
Figure 4.16: Fluorescence immunocytochemistry probing for GAPDH in GAPDH knock-down PC3 cells.....	157
<u>Chapter 5</u>	
Table 5.1: Densitometric analysis of 50kDa bands detected on western blots.....	174
Table 5.2: Positions, orientation, sequence and similarity score of the AREs detected in the <i>ADAMTS1</i> gene.....	176
Table 5.3: Positions, orientation, sequence and similarity score of the AREs detected in the <i>ADAMTS15</i> gene.....	177
Figure 5.1: Relative expression of PSA mRNA in LNCaP cells treated with DHT and the non-steroidal androgen antagonist flutamide.....	169
Figure 5.2: Expression of ADAMTS-1 mRNA in LNCaP cells treated with DHT and the non-steroidal androgen antagonist flutamide.....	170
Figure 5.3: Expression of ADAMTS-15 mRNA in LNCaP cells treated with DHT and the non-steroidal androgen antagonist flutamide.....	172
Figure 5.4: Expression of ADAMTS-15 protein in LNCaP cells treated with DHT.....	173
Figure 5.5: Expression of TIMP-3 mRNA in LNCaP cells treated with DHT and the non-steroidal androgen antagonist flutamide.....	175
Figure 5.6: Putative AREs identified in the <i>ADAMTS1</i> gene.....	176
Figure 5.7: Putative AREs identified in the <i>ADAMTS15</i> gene.....	177

Figure 5.8: Expression of ADAMTS-1 mRNA in PC3, LNCaP and BPH45 cells treated with TNF.....	179
Figure 5.9: Expression of ADAMTS-15 mRNA in PC3, LNCaP and BPH45 cells treated with TNF.....	181
Figure 5.10: Expression of TIMP-3 mRNA in PC3, LNCaP and BPH45 cells treated with TNF.....	183
<u>Chapter 6</u>	
Table 6.1: P-values of proliferation assays done using the MTT method comparing ADAMTS-1 and ADAMTS-15 knock-down with non-targeting knock-down PC3 cells.....	204
Figure 6.1: PC3 cells transfected with siGLO Red using Metafectene Pro, Dharmafect 2 and calcium phosphate transfection reagents.....	194
Figure 6.2: Transient transfection of PC3 cells with siRNA against ADAMTS-1 and ADAMTS-15.....	196
Figure 6.3: Expression levels of ADAMTS-1 mRNA in PC3 stable knock-down clones relative to a WT PC3 cell clone.....	199
Figure 6.4: Cell proliferation assay comparing rate of proliferation in ADAMTS-1 knock-down, ADAMTS-15 knock-down and non-targeting knock-down PC3 cells using the haemocytometer count method.....	201
Figure 6.5: Cell proliferation assay comparing rate of proliferation in ADAMTS-1 knock-down, ADAMTS-15 knock-down and non-targeting knock-down PC3 cells using the MTT method.....	203
Figure 6.6: Cell migration assay comparing rate of migration in ADAMTS-1 knock-down, ADAMTS-15 knock-down and non-targeting knock-down PC3 cells using the scratch method.....	207

Figure 6.7: Cell migration assays comparing rate of migration in ADAMTS-1 knock-down, ADAMTS-15 knock-down and non-targeting knock-down PC3 cells using the modified Boyden chamber method.....	209
Figure 6.8: Counting invading cells after 48 hrs using the fluorescence method at x 40 magnification.....	213
Figure 6.9: Counting invading PC3 cells after 24 hrs using the H&E staining method.....	214
Figure 6.10: Modified Boyden chamber invasion assay comparing the fluorescence counting method with the H&E staining method.....	215
Figure 6.11: Invasion assays comparing invasive potential of ADAMTS-1 knock-down, ADAMTS-15 knock-down and non-targeting knock-down (NTC) PC3 cells using the modified Boyden chamber method.....	215
<u>Chapter 7</u>	
Figure 7.1: Domain structure of ADAMTS-15 and similarity of predicted cleavage products with ADAMTS-1.....	228
Figure 7.2: Protein sequence alignment of the C-terminal half of ADAMTS-15 and ADAMTS-1 showing the similarity between the predicted C-terminal cleavage product and the anti-angiogenic C-Terminal fragment of ADAMTS-1.....	237

“Mankind's three most implacable enemies are Heart Disease, Pneumonia, Cancer. And the most baffling of these is Cancer, which is rapidly overtaking the other two for the rank of World's Worst Disease. Mankind's war of defense on Cancer has only recently begun.”

Time Magazine Editorial, January 12, 1931

“History shows that the progress of the past 50 years has resulted mainly from the slow painstaking attack by pathologists and clinicians, on the problems as presented in the cancer patient, and experience indicates that future progress will be along the same tedious paths.”

James Ewing, 1937

“What it is that makes apparently normal tissue begin to grow abnormally and extend beyond its normal boundaries is, as yet, incompletely understood.”

Anonymous, circa 1959

“Between 1950 and 2000, science has lowered the death rate from heart attacks and strokes. We're making great progress but not in cancer. We have a problem.”

Donald Coffey, October 6, 2009

CHAPTER 1

INTRODUCTION

CHAPTER 1:

INTRODUCTION

Prostate cancer is a disease of the prostate gland in which the epithelial cells lining the acini of the glandular tissue undergo malignant transformation. The reason for this transformation is not clearly understood. Prostate cancer is the most common cancer in men in the western world, and third leading cause of cancer mortality in men, surpassed by lung and colorectal cancer (Jemal 2011). Approximately 30% of men diagnosed with prostate cancer will die of the disease (Aus 2005), usually as a result of metastases (Khafagy 2007). The importance of prostate cancer to public health warrants further study into the mechanisms of pathogenesis and disease progression.

1.1 Epidemiology of Prostate Cancer

Prostate cancer affects men worldwide. Data from 2004 shows an incidence of approximately 90 per 100,000 and a mortality of 26 per 100,000 for the UK (Collin 2008). Comparative figures from the USA show an incidence of 160 per 100,000 and mortality of 19 per 100,000. Incidence and mortality varies in different populations around the globe, with the highest mortality reported in the West Indies, and the lowest in the Far East (Jemal 2011). Within the USA, African American men have the highest incidence of prostate cancer, and Asian men the least (Williams 2009). A similar pattern of variation in incidence between ethnic groups exists in the UK (Chinegwundoh 2006; Ben-Shlomo 2008). The incidence of prostate cancer increases with age. A study involving 8887 men with prostate cancer in an unscreened population found that the median age at diagnosis was 75 years (range 40-96) (Aus 2005). 12% were aged < 65 years, 37% aged 65-74 years and 51% aged \geq 75 years. In populations where serum PSA testing is used for screening, prostate cancer is detected earlier, with an average

age of 63 years at the time of diagnosis (Hugosson 2004). Comparing data from the USA (screened population) with the UK (unscreened population), peak incidence was between ages of 55-64 for USA and age over 85 for UK (Collin 2008), though there is ongoing concern about over-diagnosis and overtreatment of prostate cancer in screened populations. Autopsy studies of men dying from other causes have shown the presence of latent prostate cancer as early as the third decade in men living in USA and Spain (Haas 2008). Regardless of geographical location, the prevalence of latent prostate cancer rises with age, with up to 80% of men older than 80 years having foci of cancer in the prostate at autopsy (Breslow 1977).

1.2 Aetiology and Predisposing Factors

A number of causes have been postulated and investigated including hereditary factors, diet and obesity. The relative risk of developing prostate cancer is two-fold if one brother is affected at age >70 or father <70, 2.5 if one brother is affected at age <70 years, and three-fold if two relatives are affected at age >70 years (Bratt 2007). The risk is even higher for men with two or more affected relatives aged <70 (relative risk of four), and men with three or more affected relatives aged <70 (relative risk of five) (Bratt 2007). A number of susceptibility genes have been identified and investigated in hereditary prostate cancer, including HPC1 on chromosome 1q24-25, PCaP on chromosome 1q42-43, HPCX on chromosome Xq27-28, CAPB on chromosome 1p36, HPC2/ELAC2 on chromosome 17p12, and HPC20 on chromosome 20q13 (Bratt 2002). In addition, a higher frequency of somatic mutations in a number of genes have been identified in prostate cancer patients. The length of the CAG (Cytosine-Adenosine-Guanine) repeat of the AR gene is inversely related to the risk of developing prostate cancer (Bott 2005). Other somatic mutations identified are losses in chromosome

regions 3p, 6q, 7q, 8p, 9p, 10q, 13q, 16q, 17q and 18q and gains in 7p, 7q, 8q and Xq (Bott 2005). A combined genome-wide linkage scan of 1,233 families with a high incidence of prostate cancer by Xu et al identified chromosomes 5q12, 8p21, 15q11, 17q21 and 22q12 as regions harbouring putative susceptibility genes (Xu 2005). Genome-wide association studies by Eeles et al have recently identified a number of single nucleotide polymorphisms (SNPs) associated with hereditary and early onset prostate cancer from 3,268 patients, and have proposed some candidate affected genes (in parenthesis). SNPs were identified on chromosome 3 (CHMP2B, POU1F1), chromosome 6 (SLC22A3, SLC22A2, LPAL2, LPA), chromosome 7 (LMTK2, BHLHB8), chromosome 10 (MSMB), chromosome 11, chromosome 19 (KLK2, KLK3) and the X chromosome (NUDT10, NUDT11, GSPT2, MAGED1/4B/4, CTD-2267G17.3, XAGE2/1C/1D/5/3, SSX8/7/2/2B, SPANXN5, TMEM29B/29) (Eeles 2008). Further analyses identified seven more SNPs at chromosomes 2p21 (THADA), 2q31 (ITGA6), 4q22 (PDLIM5) 4q24 (TET2) 8p21 (NKX3.1) 11p15 (IGF2, IGF2AS, INS, TH), and 22q13 (TTLL1, BIK, MCAT, PACSIN2) (Eeles 2009).

A diet high in animal fat and red meat has been associated with an increased risk of prostate cancer (Meyer 1999). High dietary calcium intake has also been implicated as conferring increased risk (Giovannucci 2006). The anti-oxidant lycopene, contained in tomatoes has been shown to have a protective effect (Etminan 2004), as has cruciferous vegetables (Cohen 2000). The effect of sexual activity, previous vasectomy, alcohol consumption, exposure to ultraviolet radiation and occupation on risk of developing prostate cancer have been investigated, but no conclusive evidence supports a role for these (Kolonel 2004). Dietary selenium, previously thought to have a protective effect from prostate cancer (Clark 1998), has been shown in larger studies to have no effect on prostate cancer risk (Lippman 2009). The role of prostatic inflammation as an

aetiological factor is still under investigation (De Marzo 2007), but epidemiological studies have shown a decreased incidence of prostate cancer in long-term non-steroidal drug (NSAID) users (Garcia Rodriguez 2004; Jacobs 2005; Platz 2005).

1.3 The Prostate Gland

1.3.1 Anatomy

The prostate gland is a walnut-sized exocrine gland that is part of the male uro-genital tract. In Caucasian men, the prostate measures approximately 20g in weight with a volume of 21 cc and increases in size with age (Berry 1984; Rhodes 1999). On average the gland is smaller in men of Eastern extraction (Ganpule 2004; Gupta 2005; Kehinde 2005). Some aspects of prostate anatomy and physiology are worth noting, as it helps in understanding the pathophysiology of prostate cancer and the various management strategies.

The anatomy of the prostate has been recently reviewed by Brooks (Brooks 2007). Figure 1.1 shows the anatomic relationships of the prostate. The apex of the prostate lies inferiorly and the base lies superiorly. Superior to the prostate is the bladder and inferior is the urogenital diaphragm made up of fibres of the levator ani muscle and its fascia. The urethra passes from the bladder through the prostate gland before entering the penis to open externally. The prostate is bound laterally by the lateral venous plexus, neurovascular bundles, and the endopelvic fascia. Special effort is made to preserve the neuro-vascular bundles during a radical prostatectomy in order to maintain potency (Walsh 1983). Superior-posterior to the prostate on either side are the seminal vesicles and vas deferens. These merge to form the ejaculatory ducts that enter the prostate at the base, coursing through the substance of the prostate and opening into the distal prostatic urethra. The prostate is attached to the pubic bone anteriorly by the pubo-prostatic

ligaments. Blood supply to the prostate is from the inferior vesical artery, which divides into urethral and capsular branches. Venous drainage occurs via the periprostatic plexus of veins into the hypogastric vein. Lymphatic vessels from the prostate drain into the obturator and internal iliac lymph nodes on either side and into the para-aortic lymph nodes. These lymph nodes become enlarged when they become infiltrated with cancer cells (Long 1999). The prostate is innervated by the cavernous nerves which supplies sympathetic and parasympathetic innervation. Sympathetic nerve fibres supply the smooth muscle and stroma, while parasympathetic nerve fibres supply the acini.

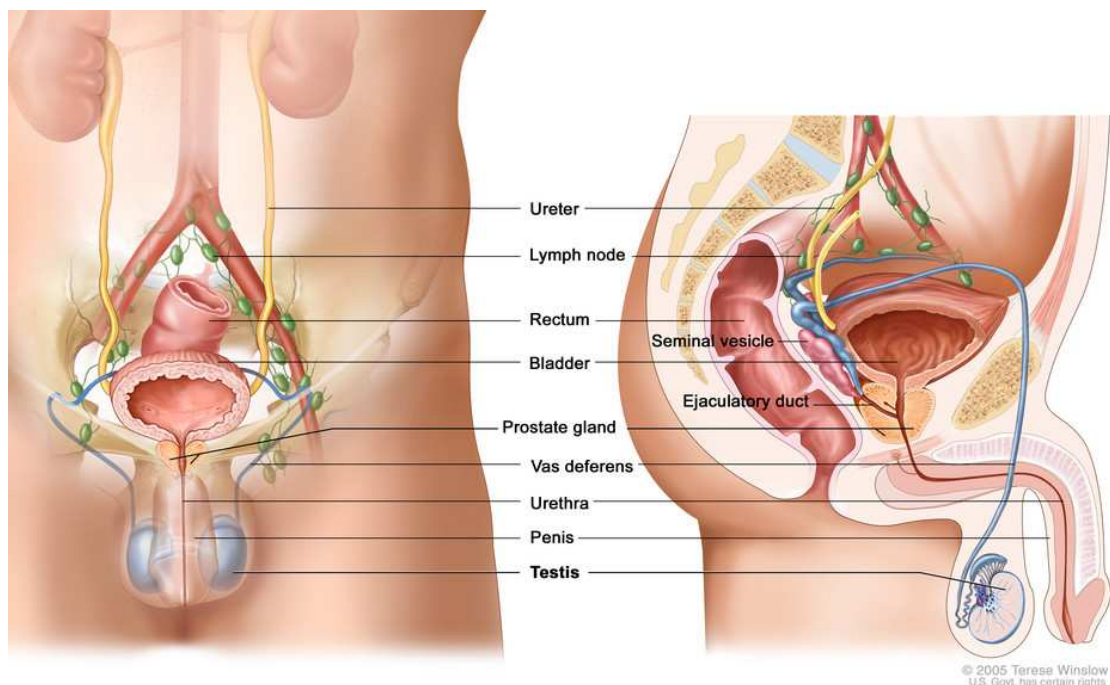


Figure 1.1: Anatomy of the male genito-urinary system. Front and side views show the anatomic relationship between the prostate gland and surrounding organs. (Image obtained from the National Cancer Institute website, www.cancer.gov, and used with the permission of the copyright holder).

The prostate gland is bound externally by a fibrous capsule made up of collagen and smooth muscle. Extension of tumour beyond the capsule reduces the chance of complete tumour resection at prostatectomy (Ayala 1989). Continuous with the capsule

is the fibromuscular stroma. The stroma encircles and invests the glandular components of the prostate.

The prostate gland can be divided into four zones. The transitional zone, which surrounds the prostatic urethra, the central zone, through which the ejaculatory ducts traverse, the peripheral zone, which is the largest zone and forms the posterior and lateral parts of the gland, and the anterior fibromuscular stroma (Figure 1.2) (McNeal 1972; McNeal 1981).

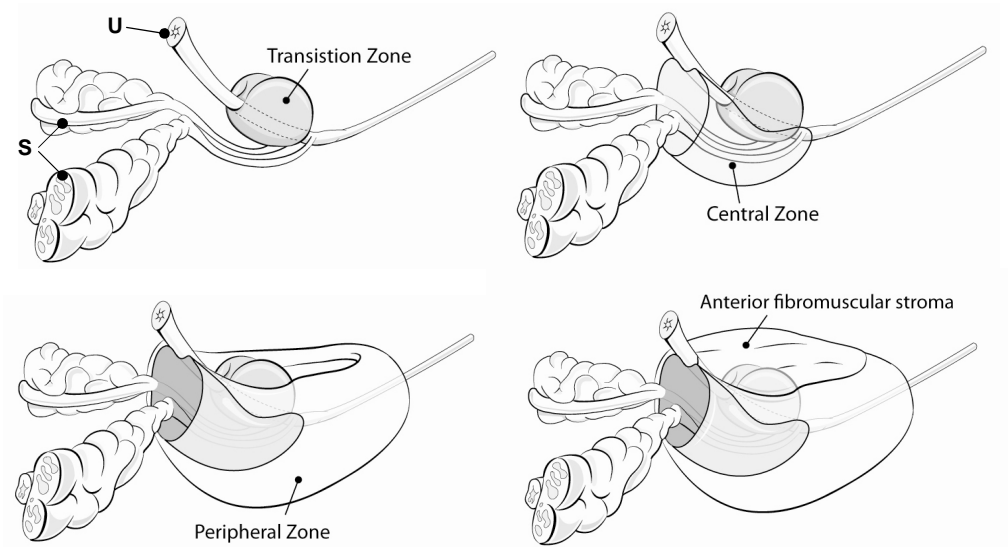


Figure 1.2: Zonal anatomy of the prostate gland as described by J.E. McNeal. Schematic representation of the zones of the prostate showing the anatomic relationship of the zones to the urethra (U), and seminal vesicles (S). The drawings were modified and used with permission from Wolters Kluwer Health Publishing.

About 30% of the prostate is stromal tissue and 70% is glandular tissue (McNeal 1988). The prostatic glands have a tubulo-alvoelar structure lined with simple cuboidal or columnar epithelium. The glandular acini are surrounded by a thin layer of stromal smooth muscle and connective tissue. The prostatic secretions drain into the prostatic urethra via the prostatic sinuses.

1.3.2 Prostate Cells

At the microscopic level, prostate tissue is comprised of epithelial and stromal compartments, separated by the basement membrane (Figure 1.3). Each compartment contains distinct cell types, surrounded by ECM.

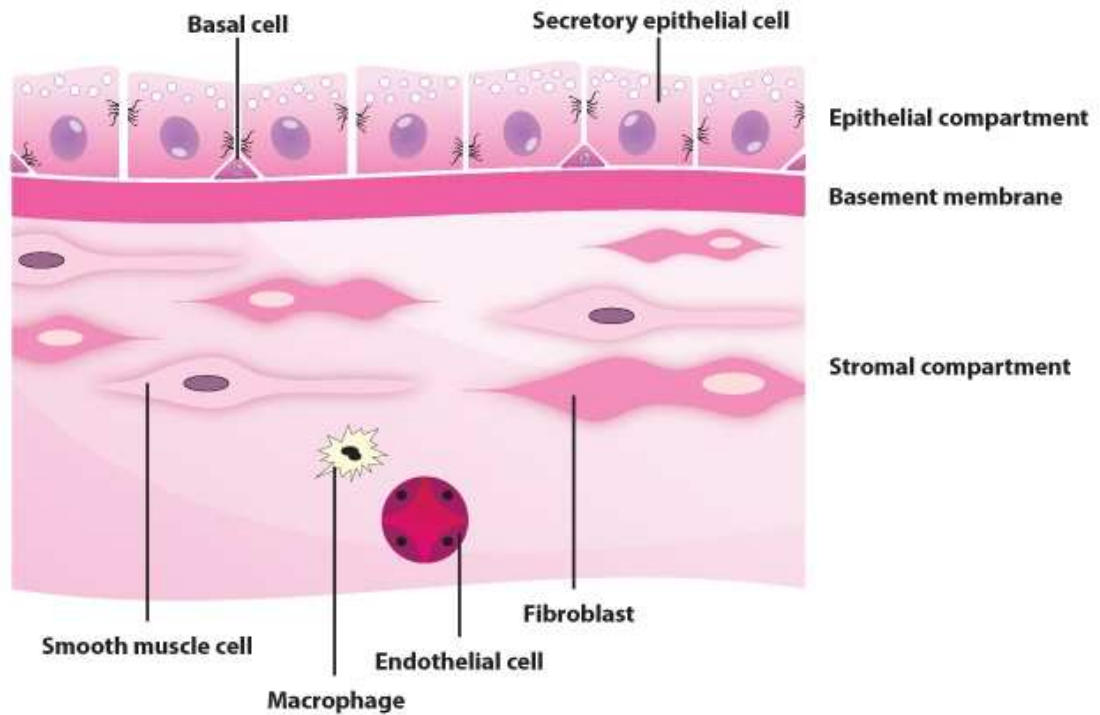


Figure 1.3: Cells of the prostate gland. Schematic representation of the cellular environment of the prostate showing cells of the epithelial and stromal compartments.

1.3.2.1 Epithelial Cells

Prostate epithelial cells are of three types, secretory epithelial cells, basal cells and neuroendocrine cells. The secretory epithelial cells are the most abundant (Peehl 2005). These cells are tall columnar epithelial cells that are terminally differentiated. They originate from the basal cells and become differentiated, expressing cytokeratin 8 and 18, unlike the basal cells which express cytokeratins 5 and 14 (Brawer 1985). They contain abundant granules of secretory vacuoles containing PSA, acid phosphatase and aminopeptidases. The apical cell membrane at the lumen possesses microvilli and form the lining of the acinus. The secretory granules migrate to the apex of the cells where

they are secreted into the lumen of the acini which drain into the prostatic ducts, ending up in the urethra. The cells are attached to the basement membrane and adjacent cells by integrin receptors. Secretory cells express AR and are normally androgen-dependent for growth and survival (Leav 1996). Androgen ablation leads to a 90% decrease in the number of these cells and the remaining cells are shrunken in size (Tetu 1991).

The basal cells are small cells that rest on the basement membrane, wedged between adjacent columnar secretory cells. They proliferate and replenish the epithelial cells (McNeal 1995; Kyprianou 1996). Basal cells express AR mRNA but little or no protein (Iwamura 1994; Leav 1996). Prostate stem cells have been reported to lie in the basal layer (Schalken 2003). Evidence for the existence of prostatic stem cells is supported by the presence of cells highly expressing $\alpha_2\beta_1$ integrins (Collins 2001) and telomerase (Soda 2000). Prostatic stem cells have the potential to differentiate into mature epithelial cells, and are thought to be the origin of malignant clones of cells that develop into cancerous lesions (Collins 2006).

Neuroendocrine cells make up a small percentage of the epithelial component (Bonkhoff 1998). They release neuropeptides and cytokines that regulate the growth and differentiation of the surrounding epithelial cells in a paracrine fashion (Abrahamsson 1999).

1.3.2.2 Stromal Cells

The stromal component of the prostate surrounds the glandular acini and composed of different cell types including smooth muscle cells, fibroblasts, endothelial cells, and inflammatory cells. Smooth muscle cells make up about 50% of the mass of the stroma (Bartsch 1979), and contract under sympathetic adrenergic stimulation during ejaculation to expel prostatic fluid from the acini and ducts into the urethra (Furuya 1982). Fibroblasts produce numerous growth factors including fibroblast growth factor

(FGF), epidermal growth factor (EGF), transforming growth factor-alpha (TGF- α) and -beta (TGF- β) (Hellawell 2002). These growth factors act in a paracrine fashion to regulate growth and development of normal and neoplastic prostate epithelium (Steiner 1993). Epithelial-stromal interactions are required for normal development of both the stromal and epithelial components of the prostate (Cunha 2004).

1.3.3 Extracellular Matrix of the Prostate

The ECM is the acellular, complex network of proteins, glycoproteins and proteoglycans that form the basement membrane on which epithelial cells lie and surrounds the cells in the stromal component. The known components of the ECM include collagens, chondroitin sulphate proteoglycans like aggrecan and versican, heparan sulphate proteoglycans, glycoproteins like elastin, laminin, fibronectin and thrombospondin (Kalluri 2003; Rowe 2009). The ECM components form a structural scaffold for the cells and confers tensile strength and compressive resistance to tissue (Heinegard 2009). In addition to structural functions, the ECM molecules also have several other functional roles. Some of these molecules possess peptide domains that regulate cell functions, and growth factors sequestered by ECM molecules are released during ECM proteolysis (Ruoslahti 1991; Schultz 2009).

The ratio of these ECM components varies between different tissue types. In the human prostate, CSPGs of different sizes have been identified (Goulas 2000). Immunohistochemical staining of prostate tissue has identified CSPGs, type IV collagen, perlecan and laminin distributed evenly in the stromal component, however there was increased peri-acinar staining of CSPGs, suggesting that CSPGs could be playing a role in basement membrane structure and function (Cardoso 2004). Syndecan-1, a HSPG, is expressed by epithelial basal and secretory cells, and is associated with a higher risk of disease progression (Chen 2004; Shariat 2008). Versican and decorin are

secreted by human prostate fibroblasts (Sakko 2003). Versican has been identified as the major component of prostate ECM (Ricciardelli 1998; Ricciardelli 1999). Versican modulates the attachment of prostate cancer cells to ECM components, and promotes cell migration, possibly by binding to the RGD peptide in ECM molecules like fibronectin to which cellular integrins attach (Sakko 2003). Versican is also reported to protect cells from oxidative stress and apoptosis (Wu 2005). Versican expression in prostate fibroblasts is up-regulated by TGF- β (Sakko 2001). Interestingly, TGF- β down-regulates the expression of the proteoglycanases ADAMTS-1 and -15 in prostate fibroblasts and up-regulates the expression and activity of the metalloproteinase inhibitor, TIMP-3 (Cross 2005), suggesting that versican accumulation may be dependent on depletion of ADAMTS-1 and -15 in the ECM.

1.3.4 Prostatic Secretions

Prostatic secretions make up approximately 0.5ml of the human ejaculate (Tauber 1975). Just over 1000 distinct proteins have been detected in 2-dimensional electrophoresis of prostatic fluid (Guevara 1985). The three main proteins contained in prostatic fluid are prostatic acid phosphatase (PAP), prostate specific antigen (PSA) and beta-microseminoprotein (β -MSP) (Lilja 1988). Human PAP is a non-specific phosphomonoesterase secreted as a dimer of molecular mass of 100kDa (Ostrowski 1994). PSA (human kallikrein 3) is a serine proteinase that is secreted as a 34kDa glycoprotein that keeps liquefies semen post-ejaculation by cleaving seminogelins to facilitate sperm motility (Balk 2003). Beta-microseminoprotein is a 94kDa protein that binds human immunoglobulin-gamma and protects sperm from being destroyed in the female reproductive tract (Kamada 1998). Other proteins that have been isolated from the prostate include the spermadhesins AQN 2 and AWN, PSP I and PSP II (Manaskova 2002). Citric acid, lactate dehydrogenase and zinc are also present in prostatic fluid

(Grayhack 1965). The pH of prostatic fluid ranges from 6.2 – 8, and is regulated by the concentration of citric acid (Kavanagh 1985).

1.3.5 Androgen Regulation of the Prostate

The prostate depends on androgens for normal development and function (Sandberg 1980; Nef 2000). Eunuchs, castrated at an early age do not have fully developed glands, and withdrawal of androgens leads to atrophy of the prostate (Wu 1991; Civantos 1995). Androgens regulate the secretory function of prostate epithelial cells. Growth and proliferation is mediated by the prostatic stromal cells, which secrete growth factors in response to androgen stimulation (Steiner 1993; Hellowell 2002). The most abundant androgen in humans is testosterone, with the testes producing up to 95% of circulating androgen, with the remaining 5% from the adrenal (Taplin 2001). Androgen production and secretion is regulated by the hypothalamus and pituitary gland by a negative feedback system (Figure 1.4). The hypothalamus releases luteinising hormone releasing hormone (LHRH), which stimulates the anterior pituitary gland to release luteinizing hormone (LH). LH stimulates the Leydig cells of the testes to secrete testosterone. The hypothalamus also secretes corticotrophin releasing hormone (CRH), which stimulates the anterior pituitary to release adrenocorticotrophic hormone (ACTH). ACTH stimulates the release of androstenedione and dihydroepiandrosterone from the adrenal cortex (Cunha 2004). Testosterone from the circulation is converted in the prostate by 5- α -reductase to DHT, the androgen which is most active in prostate tissue (Steers 2001; Zhu 2003). Serum level of DHT in men diminishes following prostatectomy (Miller 1998; Olsson 2010), suggesting that prostate tissue is the major contributor of DHT to serum. Serum levels of FSH and LH are increased following prostatectomy, indicating that prostatectomy leads to alterations to the negative feedback mechanism on the hypothalamo-pituitary-gonadal axis.

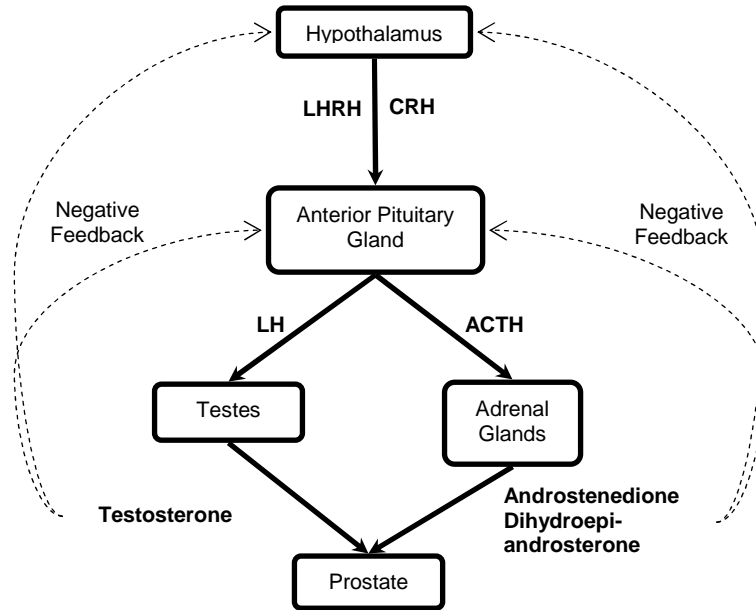


Figure 1.4: Production and regulation of androgens. The hypothalamus produces LHRH which stimulates the anterior pituitary gland to secrete LH. LH stimulates the testes to produce testosterone. The hypothalamus also produces CRH which stimulates the anterior pituitary gland to produce ACTH. ACTH stimulation causes the adrenal glands to secrete androstenedione and dihydroepiandrosterone. The system is regulated by negative feedback loops to maintain homeostasis.

1.4 Pathology of Prostate Cancer

1.4.1 Pathogenesis of Prostate Cancer

Prostate cancer develops from the epithelial component of the gland. It is not certain what the initiating events may be, but the transformation to malignancy is likely to be multifactorial, involving several steps. Prostatic intraepithelial neoplasia (PIN) is proposed to be the precursor lesion of prostate cancer (Graham 1992). As with prostate cancer, the incidence of PIN increases with age (Sakr 1993). The frequency of PIN is higher in prostates with cancer, and the peripheral zone, where most cancers occur harbours most foci of PIN (Qian 1997). PIN is characterised by a progressive loss of

markers of secretory differentiation, hyperplasia, increase in nuclear size, prominent nucleoli, hyperchromatism, changes in ploidy, and progressive disruption of the basal cell layer with an intact basement membrane (Bostwick 1987; Montironi 1990; Amin 1993; Crissman 1993). There is a progression from low grade to high grade PIN, then to carcinoma in-situ (Bostwick 1987; Montironi 1990). The malignant cells in CIS foci degrade the basement membrane and invade the stroma, forming a localised tumour. Cancer cells from localised tumours invade surrounding tissues and eventually metastasize via vascular and lymphatic channels (Ware 1987; Arya 2006).



Figure 1.5: Progression of prostate cancer. Proposed sequence of changes from normal epithelium and ending with metastatic cancer cells at distant sites.

1.4.2 Grading of Prostate Cancer

The Gleason grading system was described by Gleason in 1966 (Gleason 1966), and is accepted as the standard for describing the degree of differentiation of prostate adenocarcinoma (Murphy 1994). The system classifies the histopathologic features from 1 to 5, with 1 being well differentiated and 5 poorly differentiated (Bailar 1966) (Bailar 1966) (Figure 1.6). The Gleason score is a derivation of the Gleason grade and is a sum of the two most predominant grades. Thus, the Gleason score could range from 2 to 10. Grades 2 to 5 are classified as low grade, 6 to 7 medium grade and 8 to 10 high grade prostate cancer (Epstein 1996). The Gleason score remains the best prognostic indicator in clinical use (Albertsen 1998; Buhmeida 2006).

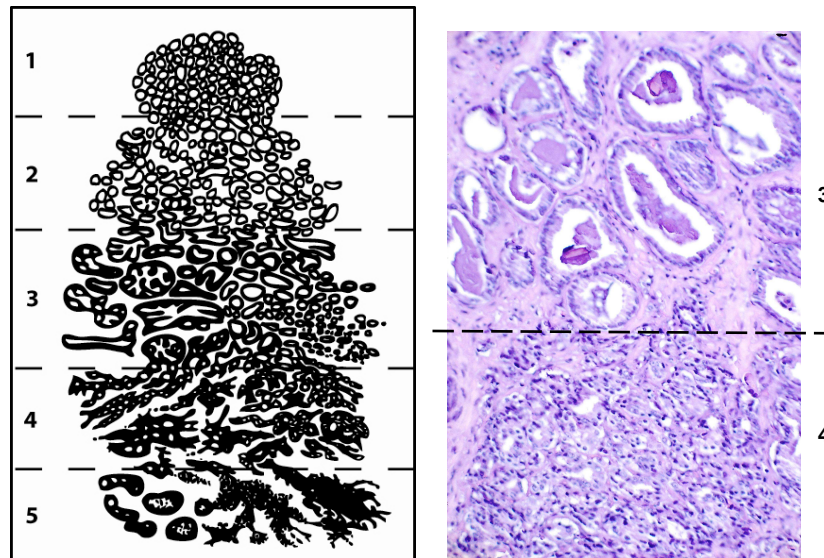


Figure 1.6: The Gleason grading system. On the left is the schematic template devised by D.F. Gleason showing changes in glandular morphology and tissue architecture from well differentiated Grade 1 progressing through to poorly differentiated Grade 5. On the right is a Haematoxylin/Eosin stained histological slide at x 300 magnification. The top half of the slide is moderately differentiated grade 3 and the bottom half is poorly differentiated grade 4. (Image on left was adapted from the original drawing by D.F. Gleason and used with permission from Blackwell Publishing Inc. Image on right was used courtesy of Otis Brawley and obtained from the National Cancer Institute website, www.cancer.gov).

1.4.3 Staging of Prostate Cancer

Prostate cancer is staged according to the universal TNM (Tumour, Node, Metastases) staging system of the International Union Against Cancer (Sobin 1988; Schroder 1992). This system takes into account the extent of local spread of the tumour (T) the presence of lymph node infiltration (N) and the presence of metastases to distant organs (M) (Table 1.1). Localised tumours are confined within the capsule of the gland (Figure 1.7). Prostate cancer can spread locally (Figure 1.8) to infiltrate surrounding tissue including

the pubic bone anteriorly, the bladder superiorly, the seminal vesicles supero-posteriorly, or the rectum posteriorly. Local growth can also obstruct the distal ureters or cause compression of the urethra as it passes through the prostate causing bladder outflow obstruction (Mazur 1991; Paul 1994). Lymph node infiltration usually occurs in stepwise fashion, first involving the iliac lymph node chain, progressing to the para-aortic nodes and mediastinal nodes, and in advanced disease, inguinal, axillary and cervical nodes could be involved (Long 1999). Prostate cancer has a predilection to metastasize to bone (Figure 1.9). Bone is the most common site of metastasis and occurs in up to 95% of prostate cancer patients (Bubendorf 2000). Bone metastases cause severe morbidity in prostate cancer patients due to pain, pathological fractures and spinal cord compression (Osborn 1995; Khafagy 2007).

Tumour	Tx	<i>Primary tumour can not be assessed</i>
	T0	<i>No evidence of primary tumour</i>
	T1	<i>Tumour clinically inapparent, not palpable, not visible by imaging</i>
	T2	<i>Tumour confined to prostate, palpable or visible on imaging</i>
	T3	<i>Locally advanced tumour</i>
	T4	<i>Tumour fixed or invades adjacent structures i.e. bladder, rectum or pelvic wall</i>
Nodes	Nx	<i>Regional lymph nodes can not be assessed</i>
	N0	<i>No regional lymph node metastases</i>
	N1	<i>Regional lymph node metastases</i>
Metastasis	Mx	<i>Presence of distant metastases can not be assessed</i>
	M0	<i>No distant metastases</i>
	M1	<i>Distant metastases present in non-regional lymph nodes, bones or other sites</i>

Table 1.1: Summary of the TNM staging system for prostate cancer.



Figure 1.7: Magnetic resonance imaging (MRI) of the pelvis of a prostate cancer patient. Image shows a localised tumour the prostate gland (Jones, H.E.). MRI can be used to detect extra-capsular extension of tumour or pelvic lymph node invasion.

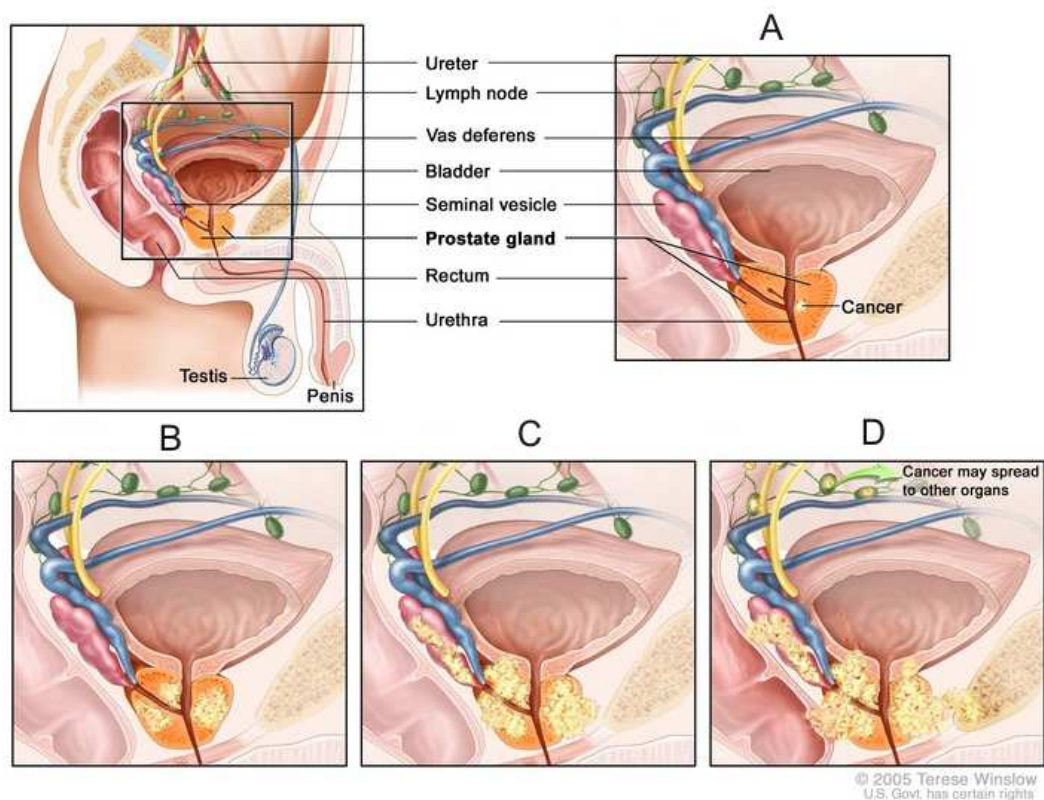


Figure 1.8: Local progression of prostate cancer. The tumour can progress from a T1 tumour in A to a T2 tumour in B, invasion of the seminal vesicles (T3) in C, and eventually invasion of the rectum, pubic bone, and pelvic lymph nodes (T4, N1) in D.

(Image obtained from the National Cancer Institute website, www.cancer.gov, adapted and used with the permission of the copyright holder).

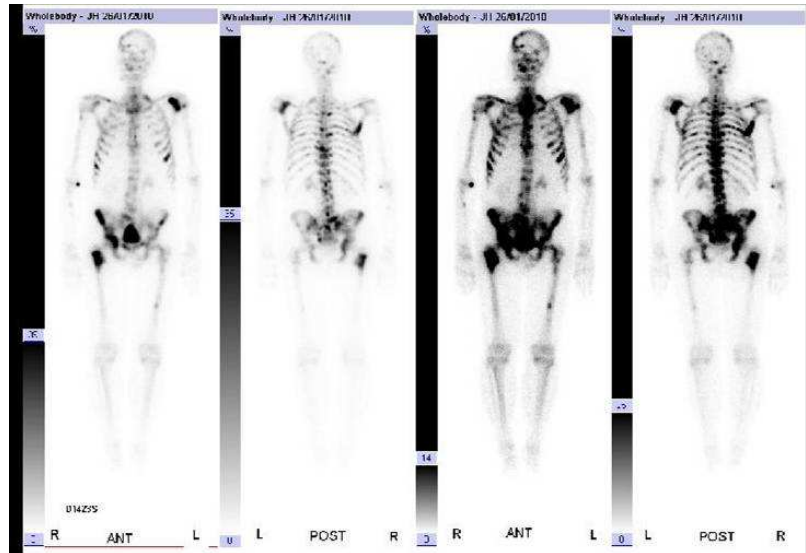


Figure 1.9: Radio-nuclide bone scintigraph of a prostate cancer patient. The disease has progressed, showing evidence of multiple bone metastases. There are multiple ‘hot spots’ in the skull, right humeral head, ribs, vertebrae, pelvis, right femoral head and left femoral mid-shaft.

1.4.4 Role of the Androgen Receptor in Prostate Cancer

Androgen-regulated gene expression is mediated via the action of nuclear receptors (Lee, D.K. 2003). The AR is classified as an N3C4 nuclear receptor (Robinson-Rechavi 2003; Robinson-Rechavi 2003). The AR gene is located on the long arm of the X chromosome at Xq11-12 (Lubahn 1988). The protein has approximately 900 a.a. residues (Trapman 1997), and has a relative mass of 99-110kDa depending on the degree of phosphorylation (Trapman 1988). There are four domains, the amino-terminal domain (NTD), which interacts with co-regulator proteins, the DNA binding domain (DBD), which binds to DNA after activation, a hinge region (HR), and the ligand

binding domain (LBD), which binds to androgens and AR antagonists (Jenster 1992). The NTD has a polymorphic CAG repeat segment, the length of which is thought to inversely correlate with the risk of prostate cancer (Bott 2005). The AR could have up to 930 a.a. residues depending on the length of the CAG repeat segment (Trapman 1997).

Activation of the AR causes a conformational change in the receptor, dissociation from heat shock proteins (HSPs) and translocation of the receptor from the cytoplasm to the nucleus (Lee, D.K. 2003). The activated AR binds to AREs located in proximity to androgen-regulated genes (Brinkmann 1999; Claessens 2004) and influences gene transcription either by up-regulation or down-regulation of the target gene. AREs are 15-base pair (bp) DNA sequences comprising two six-bp half sites separated by a three-bp spacer. The sequence 5'-GGA/TACAnnnTGTTCT-3' has been described as the consensus ARE (Roche 1992).

In addition to growth stimulation via the action of growth factors (Steiner 1993), androgens protect prostate cancer cells from apoptosis (Coffey 2002), induce invasion by prostate cancer cells (Chuan 2006), and also favour angiogenesis within the prostate stroma (Stewart 2001; Colombel 2005). Androgen deprivation therapy (ADT) in the form of surgical or medical castration is used in the management of locally advanced, metastatic, or relapsing disease (Soloway 1991). Androgen deprivation leads to reduction in the size of prostate tumours, and the size and number of metastatic deposits (Huggins 1942). ADT reduces serum androgen concentrations to undetectable levels (Seidenfeld 2000; Anderson 2008), and slows the progression of prostate cancer. High expression levels of AR in cancerous prostates is associated with more aggressive disease (Li 2004). Mutations of the AR are seen in as many as 50% of advanced prostate cancers (Taplin 1995; Marcelli 2000).

Translocation of the androgen-regulated TMPRSS2 (Transmembrane protease serine 2 or epitheliasin) promoter to ETS (E twenty-six) transcription factor genes, more commonly ERG (ETS related gene), has been identified in up to 79 % of prostate cancer specimens (Tomlins 2005) and has been associated with aggressive disease (Wang 2006). The TMPRSS/ERG fusion leads to androgen regulated over-expression of the ETS oncoproteins, favouring tumour initiation and progression (Narod 2008; Tomlins 2009).

Androgens have been reported to down-regulate the expression of E-cadherin and up-regulate N-cadherin in prostate cancer cells (Zhu 2010), changes which are characteristic of epithelial-mesenchymal transition (EMT). EMT is a process by which differentiated epithelial cells de-differentiate and assume a mesenchymal phenotype. Markers of epithelial cells for example E-cadherin and β -catenin are lost, and mesenchymal cell markers for example N-cadherin and vimentin are expressed (Thiery 2003). This change is similar to a process seen during embryonic development which allows endodermal cells to migrate during organ formation. EMT is frequently found in cells at the invasive front of solid tumours and in metastatic deposits and has therefore been implicated in increased cancer cell motility, tumour progression and metastasis (Yilmaz 2010). The expression level of the androgen receptor in prostate cancer cells appears to be critical in androgen-induced EMT. Paradoxically, cells expressing low levels of AR were more susceptible to EMT than cells expressing high levels of AR (Zhu 2010).

AR signalling is evident in hormone-resistant prostate cancer (HRPC), despite castrate levels of serum testosterone (Mohler 2004), and AR signalling in HRPC promotes cancer cell proliferation (Zegarra-Moro 2002). These findings implicate the AR in the

pathogenesis and progression of prostate cancer. The exact mechanism of AR signalling in HRPC progression is not fully understood (Schroder 2008; Yuan 2009).

1.5 Management of Prostate Cancer

Management options for prostate cancer are guided by the stage and grade of the disease. In clinical practice, the extent of disease could be categorised at the time of diagnosis as localised (T1-T2, N0, M0), locally advanced (T3-T4, any N, M0) or metastatic (any T, any N, M1) disease. The choice of whether to treat and what treatment is best has to be made with the patient, taking into account the best clinical evidence available at the time (Patel 2003). Current consensus guidelines for prostate cancer management have been published by the European Association of Urology (EAU) (Heidenreich 2008) and the National Comprehensive Cancer Network (NCCN) in North America (Mohler 2010). The treatment options currently recommended are summarised in Table 1.2.

Stage	Management Options
Localised disease (T1-T2, N0, M0)	<i>Active surveillance, Radical radiotherapy, Radical prostatectomy</i>
Locally advanced disease (T3-T4, any N, M0)	<i>Radical prostatectomy (selected T3, N0), Radical radiotherapy (T3, N0), Androgen deprivation therapy</i>
Metastatic disease (Any T, any N, M1)	<i>Androgen deprivation therapy, Palliative radiotherapy</i>
Hormone-refractory disease (Any T, any N, M1)	<i>Chemotherapy</i>

Table 1.2: Established management options for patients with prostate cancer.

1.6 The Role of Proteinases in Prostate Cancer Tumourigenesis, Progression and Management

Proteinases (or peptidases) are a group of over 600 enzymes in humans whose action is to cleave peptide bonds in proteins. The genes that code for proteinases or their

homologues in humans account for approximately 2% of the human genome (Rawlings 2006). The International Union of Biochemistry and Molecular Biology has divided proteinases into 2 groups; Endopeptidases (or proteinases), which cleave peptide bonds at specific points within the protein and exopeptidases which remove amino acids sequentially from either the N terminus (aminopeptidases) or C terminus (carboxypeptidases) of the protein. The MEROPS classification (www.merops.sanger.ac.uk), divides the proteinases into families according to their structure and evolutionary relationships (Rawlings 2006). Another useful classification system is to group the proteinases according to the residue or moiety at the centre of the active catalytic site e.g. cysteine proteinases, serine proteinases, aspartic proteinases, metalloproteinases etc. (Table 1.3).

Metalloproteinases	Serine Proteinases	Cysteine Proteinases	Aspartic Proteinases
MMPs ADAMs ADAMTSs PSMA Neprilysin	PSA uPA Thrombin Prostasin	Caspases Cathepsins Calpains	Pepsin Renin Cathepsin D

Table 1.3: Classification of selected proteinases according to the nucleophilic amino acid residue at the catalytic site.

In humans, proteinases serve various roles and are involved in numerous biological processes including digestion, coagulation, immunity, endocrine function, blood pressure regulation and maintenance of tissue architecture. Their activity is regulated at the levels of transcription and translation and by the activity of proteinase inhibitors, over 100 of which are encoded in the human genome (Rawlings 2006).

Proteinases are involved in complex activation pathways and cascades. The most extensively characterised of these is the blood coagulation cascade. Timely blood

coagulation is essential for maintaining intravascular fluid volume. The successful formation of a fibrin clot is dependent on sequential activation of clotting factors, most of which are serine proteinases, from the inactive pro-enzyme by other proteinases (Davie 2003). Other proteinase activating cascades are the complement system for maintaining innate immunity, which comprises mainly serine proteinases (Forneris 2012), and the apoptosis pathway, which involves serial activation of caspases to achieve programmed cell death (Wang, Z.B. 2005).

The activity of proteinases in the ECM makes them good candidates for research into tumourigenesis, tumour progression and tumour metastasis. Riddick et al have compared the expression of degradome components in benign and malignant prostate tissue and analysed the correlation with Gleason score (Riddick 2005). The results showed that some proteinases are dysregulated in prostate cancer and correlate positively or negatively with Gleason grade (Table 1.4). This suggests that these proteinases may be playing a role in tumour progression.

Up-regulated (Correlation with Gleason Score)	Down-regulated (Correlation with Gleason Score)
MMP10(+), MMP15(+), MMP24(+), MMP25(=), MMP26(+), Hepsin(+), MTSP1(+), uPA(=), uPAR(+), PAI1(+)	MMP2(-), MMP23(-), Maspin(-), TIMP3(-), TIMP4(-), RECK(-), PAI2(=)

Table 1.4: Expression of proteinases, their receptors and inhibitors in prostate cancer and correlation with Gleason score. MTSP1- Matriptase, uPA- Urokinase type plasminogen activator, uPAR- Urokinase type plasminogen activator receptor, PAI- Plasminogen activator inhibitor, TIMP- Tissue inhibitor of metalloproteinases, RECK- Reversion-inducing cysteine-rich protein with Kazal motifs . + indicates positive correlation, - indicates negative correlation, = indicates no correlation.

The studies on the role of proteinases in prostate cancer have generally investigated the effect of proteinase activity on tumourigenesis, tumour growth, cell motility and invasiveness, angiogenesis, metastasis and clinical management (Table 1.5).

Biological Activity	Proteases Implicated	References
Tumourigenesis	+ Cathepsins - Caspases	<i>Nagler 2004</i> <i>Earnshaw 1999, Jiang 2001</i>
Tumour Growth & Proliferation	+ MMP-7 + MMP-9 + uPA + PSA - Neprilysin	<i>Miyamoto 2004</i> <i>Fowlkes1994, Manes 1999</i> <i>Angelloz-Nicoud 1995</i> <i>Lee 1994</i> <i>Osman 2006, Horiguchi 2007</i>
Migration	+ Calpains + Thrombin	<i>Rios-Doria 2003</i> <i>Black 2007, Loberg 2007</i>
Invasion	+ MMP-9 + MMP-14 + uPA - Prostatin - PSMA	<i>Aalinkeel 2004</i> <i>Udayakumar 2003</i> <i>Pulukuri 2005</i> <i>Chen 2001</i> <i>Ghosh 2005</i>
Angiogenesis	+ Thrombin + ADAM-17 - ADAMTS-1 - ADAMTS-8 - Neprilysin	<i>Kaushal 2006</i> <i>Black 1997, Fajardo 1992</i> <i>Vazquez 1999, Luque 2003,</i> <i>Kuno 2004</i> <i>Vazquez 1999</i> <i>Horiguchi 2007</i>
Metastasis	+ MMPs + PSA + uPA - PAI	<i>Nemeth 2002</i> <i>Romanov 2004</i> <i>Lee 2004, Kerchhiemer 1985,</i> <i>Hiernet 1988</i> <i>Soff 1995</i>

Table 1.5: Summary some known and putative biological activities of proteinases in prostate cancer. (+) indicates a positive effect, (-) indicates a negative effect.

1.6.1 Tumourigenesis

The factors that initiate the transformation of normal cells to malignant cells are not fully understood. However, the outcome is always an increase in the ratio of cell

proliferation relative to cell death. Caspases are members of the cysteine proteinase catalytic class. Caspase-induced apoptosis is effected by a complex cascade, which results in the cleavage of cellular and nuclear proteins that are essential for cell survival (Earnshaw 1999). Caspase-2, 8, 9 and 10 are initiator caspases, because they cleave the precursors of caspase-3, 6 and 7, which are effector caspases. Activation of caspase-3, 7, 8 and 9 has been shown to effect apoptosis in cells (Wolf 1999), with caspase-9 being the initiator caspase for the intrinsic (mitochondrial) apoptotic pathway and caspase-8 the initiator for the extrinsic (death receptor) pathway. Caspase-8 mediated apoptosis can be activated by selenium compounds (Jiang 2001). Caspase inhibitors halt the cleavage of cellular components (Jiang 2001), thereby restricting the process of apoptosis. Apoptosis is the natural process of programmed cell death therefore inhibition of the activity of caspase proteinases could be one of the initiating steps in tumourigenesis, by allowing uncontrolled cell proliferation and the establishment of malignant cell populations.

Lysosomal cysteine proteinases, are so called because of the cysteine residue at the catalytically active site. This group of proteinases could also be involved in the early stages of prostate cancer development. There are high expression levels of cathepsin-X in invasive carcinoma of the prostate (Nagler 2004). Differences in protein expression were analysed in normal, prostatic intraepithelial neoplasias (PIN) and prostate carcinoma tissue. PIN and carcinoma tissue had higher expression of cathepsin-X than normal epithelial tissue, suggesting that cathepsin-X may be involved in the early change from normal to malignant tissue. These findings are not enough evidence that cathepsin-X plays a role in the malignant change of the prostate epithelial cells. Functional studies are required to show if indeed, cathepsin-x plays a role in initiating

the transformation of the epithelial cells, or the increased expression is a consequence of earlier events.

1.6.2 Tumour Cell Growth & Proliferation

The transformation of normal prostate epithelial cells to malignant cells is followed by proliferation of the malignant cell population which may be slow or rapid, depending on the phenotype of the cells. Insulin-like Growth Factors (IGFs) are proteins that have homology to insulin. Availability and activity of these growth factors and their binding proteins, Insulin-like Growth Factor Binding Proteins (IGFBPs), in the prostate are under the influence of proteinases. MMPs are members of the metalloproteinase family. MMP-1, 2, 3, 7 and 9, have been shown to cleave IGFBPs in fibroblasts (Fowlkes 1994; Miyamoto 2004), thereby releasing the growth factor so it is able to bind to its cell surface receptor. MMP-9 has been reported to cleave IGFBP-3 in DU-145 prostate cancer cell lines (Manes 1999). Cleavage of IGFBP-3 caused increased activity of IGF-1 and protected against apoptosis (Miyamoto 2004). These findings indicate that by cleaving IGFBPs, these MMPs increase the bioavailability of IGF, promoting cell growth and proliferation.

Human Kallikrein-3 (hKLK3, PSA) has also been shown to cleave IGFBP-3 *in vitro*, but serum of men with elevated PSA did not have correspondingly high levels of IGFBP-3 fragments (Koistinen 2002). This could be interpreted to mean that even though PSA cleaves IGFBP-3 *in vitro*, serum IGFBP-3 is not cleaved by PSA, perhaps as a result of the presence of PSA inhibitors in serum. However, IGFBP-3 in seminal plasma is cleaved by PSA (Lee 1994), suggesting that the cleavage of IGFBP-3 by PSA is localised to the prostate. Hence proteolytic activity of PSA could also be increasing bioavailability of IGFs in the tumour microenvironment and promoting cell proliferation.

IGFBP-3 is also cleaved by plasmin, a serine proteinase which is itself activated by the cleavage of a precursor protein, plasminogen, by the serine proteinase urokinase-type plasminogen activator (Lee, M. 2004). The activity of uPA has been shown to increase the proliferation rate of PC3 cells *in vitro* (Angelloz-Nicoud 1995) and the addition of a serine proteinase inhibitor, 4-(2-aminoethyl)-benzenesulfonyl fluoride, to the medium inhibited the activity of uPA and led to a decrease in cell proliferation. As previously mentioned cleavage of IGFBP-3 increases the bioavailability of IGFs and promotes cell proliferation. However the use of a broad serine proteinase inhibitor would inhibit other serine proteinases meaning that the effects on cell proliferation might not be specifically attributed to the activity of uPA. Unlike the proteinases already discussed in this section, neprilysin (Neutral Endopeptidase), a cell surface proteinase, is reported to have a negative effect on prostate cancer cell proliferation (Osman 2006). Induction of neprilysin expression in prostate cancer cells *in vivo* caused attenuation of tumour growth, and over-expression of neprilysin also had the effect of decreasing cell viability and proliferation (Horiguchi 2007). The anti-proliferative effect of neprilysin may be as a result of the inactivation of fibroblast growth factor-2 (FGF-2) (Horiguchi 2008).

1.6.3 Tumour Cell Motility, Migration & Invasion

The invasive potential of tumour cells is determined by their ability to migrate outside the confines of the basement membrane and through the surrounding ECM. There is also evidence that tumour cells can migrate, albeit less efficiently, through the ECM in the absence of proteinase activity (Wolf 2003). A number of proteinases have been found to play a role in the motility and invasive potential of prostate cancer cells. Cathepsins B, H, and L are more highly expressed in primary cells cultured from cancerous parts of the prostate compared to cells from adjacent non-cancerous tissue (Friedrich 1999). Cathepsins B and L have also been reported to be expressed in

prostate cancer cell lines (Friedrich 1999; Colella 2002). In the latter study, the cysteine proteinase inhibitor, E-64 (trans-epoxysuccinyl-L-leucyl-amido(4-guanido)-butane), reduced the invasiveness of PC3 and DU145 cells. However, the inhibitory action of E-64 is not specific to cathepsins B and L as it inhibits all papain family members. Transfection of PC3 cells with a plasmid coding for chicken cystatin, an endogenous cysteine proteinase inhibitor, led to decreased invasive potential of the cells (Colella 2003). Collectively, these studies suggest that cysteine proteinases play an active role in prostate cancer cell invasion. Calpains are cysteine proteinases that have been shown to cleave the cytoplasmic domain of E-cadherin (Rios-Doria 2003). E-cadherin is a trans-membrane structural protein which mediates lateral intercellular adhesion in secretory tissues (Geiger 1992). Calpains are over-expressed in localised and metastatic prostate cancer specimens (Rios-Doria 2003), and prostate cancer specimens have been reported to show aberrant or negative staining for E-cadherin (Tomita 2000). Proteolytic cleavage of E-cadherin and subsequent loss of lateral cell-cell adhesion would promote cancer cell motility and invasive potential.

Thrombin is a serine proteinase which is instrumental in blood clotting and is also a growth factor, acting through proteinase activation receptors (PARs). Thrombin cleaves the N-terminus of PARs, which then act as a tethered ligand and activates the receptor (Coughlin 2003). PAR-1, -2 and -4 are over-expressed in malignant prostate cancer tissue and high expression of PAR-1 also predicts biochemical recurrence of prostate cancer (Black 2007). Activation of PAR-1 and -2 enhances migration of LNCaP cells (Black 2007) and stimulation of PC3 cells with thrombin activated PAR-1 and caused cell detachment and increased chemotactic migration (Loberg 2007). These studies suggest that activation of PARs by thrombin increases the potential of prostate cancer cells to migrate.

MMPs are known to degrade ECM components (Lee, M. 2004). The activation of MMPs is dependent on cleavage of the propeptide by other MMPs, cathepsins and plasmin (Lee, M. 2004) (Figure 1.10).

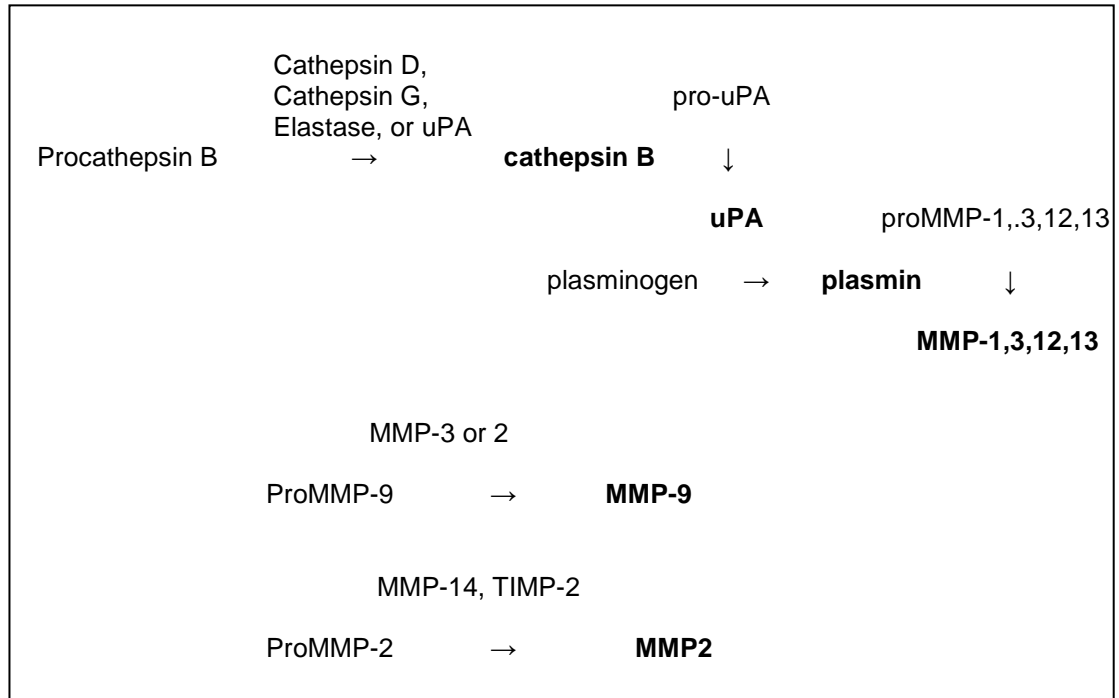


Figure 1.10: Activation cascade of some of the proteolytic enzymes involved in tumour metastasis. The enzymes in bold type degrade the ECM.

This illustrates the point that there is a cascade of events involving a number of proteinases and their inhibitors that regulate ECM turnover. *In vitro*, MMP-9 increases the invasive potential of prostate cancer cell lines (Aalinkeel 2004). The more invasive PC-3 and DU-145 cell lines have higher expression levels of MMP-9 relative to the less invasive LNCaP cells. Over-expression of MMP-9 in LNCaP cells increased their invasive potential and knockdown in PC-3 and DU-145 cells reduced their invasive potential. In another study, inhibition of MMP-14 (MT-1 MMP) expression also decreased the invasive potential of prostate cancer cell lines DU-145, PC-3N and PPC (Udayakumar 2003). MMP-9 and 2 are found to localise at the leading edge of tumour

tissue (Hamacher 2004). This suggests an active role at the tumour edge. Another study showed that there was increased synthesis of collagen in surrounding benign tissue in prostate cancer specimens but decreased collagen content within the cancer focus (Burns-Cox 2001). Increasing collagen production may be a host response to counter the proteolytic activity of the advancing tumour cells.

A Disintegrin and Metalloproteinase (ADAM) and A Disintegrin and Metalloproteinase with Thrombospondin motifs (ADAMTS) are a relatively newly discovered group of metalloproteinases. ADAMs act predominantly as membrane-bound sheddases while some ADAMTSs are proteoglycanases. Expression of ADAM-9, -10, -11, -15 and -17 was detected in prostate cancer lines LNCaP, ALVA-41, DU-145 and PC-3 (McCulloch 2000). ADAM-15 over-expression has been associated with aggressive prostate cancer (Kuefer 2006). ADAMTS expression has also been analysed in prostate cancer cell lines. ADAMTS-1 was expressed in PC-3 and LNCaP, ADAMTS-9 was expressed in DU-145, and ADAMTS-15 was expressed in all three cell lines (Cross 2005). Unlike the more aggressive PC3 and DU145 cell lines, LNCaP cells expressed TIMP-3, the main tissue inhibitor of ADAMTSs, which also inhibits ADAM and MMP activity. Genome-wide cDNA micro-array analysis of prostate cancer tumours identified ADAMTS-1 as one of the genes that are over-expressed in HRPC specimens when compared with hormone-sensitive specimens (Tamura 2007). A sub-group of the ADAMTSs degrade structural components of the ECM (Jones 2005), which suggests that prostate cancer cells expressing these proteinases could be using them to degrade ECM in the TME. Studies into the functional role of the ADAMTS proteinases and their major tissue inhibitor, TIMP-3, in the prostate will shed light on their role in prostate cancer.

The serine proteinase uPA has been implicated in the invasive potential of prostate cancer cells. PC3 cells were compared with PC3CALN, a more aggressive *in vivo* derivative of PC3 cells. PC3CALN cells expressed 3.5 times more uPA than PC3 cells and displayed greater invasive potential, and immunohistochemistry of tumour xenografts demonstrated localisation of uPA to invasive fronts (Gaylis 1989). Supporting these findings, down-regulation of uPA and uPA receptor (uPAR) expression decreased the invasive potential of PC3 cells in a Matrigel invasion assay (Pulukuri 2005). This probably reflects its role in the activation of plasmin, which can then activate MMPs (Figure 1.10), or uPA could be directly acting to facilitate prostate cancer cell invasion.

Prostasin is a serine proteinase that is expressed in normal prostate epithelium as well as in the non-invasive LNCaP prostate cancer cell line (Chen 2001). The more invasive PC3 and DU145 prostate cancer cell lines do not express prostasin, and over-expression of prostasin in PC3 and DU145 cell lines by transfection of prostasin cDNA diminished the invasive potential of these cell lines (Chen 2001). This infers that prostasin has a negative effect on prostate cancer invasion. The mechanism of this action is not yet known.

PSMA, also known as glutamate carboxypeptidase-2 or folate hydrolase, is a transmembrane metallopeptidase. It has been identified as a tumour suppressor in prostate cancer. LNCaP, MDA PCa2b and CWR22RV1 prostate cancer cell lines which express PSMA were less invasive than PC3 and DU145 cell lines which did not express PSMA (Ghosh 2005). Knock-down of PSMA expression in LNCaP cells increased their invasive potential, while over-expression of PSMA in PC3 cells decreased their invasive potential. This suggests that loss of PSMA expression could be an important step in prostate cancer progression, but the mechanism remains unknown.

1.6.4 Angiogenesis

As tumours grow in size, their metabolic demands increase. Blood vessels carry the metabolic substrates necessary for tumour growth and remove toxic metabolic end products. Theoretically, any factors favouring the growth and proliferation of new vessels would favour tumour growth. Studies have implicated some proteinases in either stimulating or inhibiting angiogenesis.

The thrombin receptor, PAR-1, as previously mentioned is over-expressed in advanced prostate cancer specimens compared with specimens with localised disease (Kaushal et al. 2006). Immunohistochemical staining localised the PAR-1 receptors to endothelial cells in vascular networks surrounding prostate cancer cells. Thrombin also increases vascular endothelial growth factor (VEGF) secretion, potentiates the action of VEGF in inducing endothelial cell proliferation, up regulates expression of VEGF receptors and enhances the production of MMP-9 in PC-3 cells (Tsopanoglou 2004). This implies that thrombin regulates both ECM breakdown and angiogenesis. A combination of these two actions will enhance local tumour growth and survival.

ADAM-17 has been identified as the main TNF converting enzyme (TACE), which sheds membrane-bound TNF into its soluble form (Black 1997). TNF has been associated with increased angiogenesis (Fajardo 1992) and so it is possible that TNF produced by tumour associated macrophages (TAMs) could, at a certain critical concentration, be driving angiogenesis in prostate tumours. ADAMTS-1 (METH-1) and ADAMTS-8 (METH-2) inhibit endothelial cell proliferation and VEGF induced angiogenesis (Vazquez 1999). The inhibitory effect is due to the binding and sequestration of VEGF (Luque 2003). The carboxyl-terminal region of ADAMTS-1 which consists of thrombospondin-spacer-thrombospondin (T-S-T) repeats has been found to be responsible for its antiangiogenic activity (Kuno 2004). ADAMTS-1 also

cleaves thrombospondin-1, releasing anti-angiogenic peptides (Lee 2006). Thus angiogenesis can be regulated by the activity of these proteinases which are known to be expressed in prostate cancer (McCulloch 2000; Cross 2005).

Some of the actions of the MMPs lead to a stimulation of angiogenesis, yet others inhibit it. For example, breakdown of the ECM releases ECM-bound growth factors that stimulate angiogenesis (Lee, M. 2004). However breakdown of collagen-18 releases endostatin, which is angio-inhibitory. Thus a balance is maintained between these events, which at different times favours angiogenesis or inhibits it.

In addition to its growth inhibitory action, neprilysin inhibits angiogenesis by reducing the availability of FGF-2 (Horiguchi 2008). Conditioned medium from DU145 cells that were made to over-express neprilysin had decreased concentrations of FGF-2 and stimulated less tubule formation by endothelial cells compared to controls. Tumour xenografts grown *in vivo* from neprilysin over-expressing cells were smaller and less vascular than controls. This evidence points to an anti-tumour role for neprilysin in prostate cancer.

1.6.5 Establishment of Metastasis

Relative to other aspects of tumour progression, few studies have been done to investigate the action of proteinases in metastatic prostate tumours. Prostate cancer metastasises primarily to bone, and bone metastases are a significant cause of mortality in patients with prostate cancer. Because clinical indications for obtaining tissue samples from bone metastases in prostate cancer patients are rare, there is a paucity of metastatic specimens available for study. However, some proteinases have been shown to play a role in metastatic sites.

As well as facilitating tumour cell invasiveness, some MMPs play a role in bone metastases in prostate cancer. In an *in vivo* experiment carried out on nude mice, bone

impregnated with PC-3 cells was subcutaneously implanted. MMP inhibition with the broad-spectrum MMP inhibitor batimastat administered intraperitoneally reduced proliferation of tumour cells, reduced the number of osteoclasts and prevented degradation of marrow trabeculae, but had no effect on angiogenesis or apoptosis (Nemeth 2002). In the *in vitro* arm of the study, MMP inhibition with batimastat prevented Ca^{2+} release from bone fragments co-cultured with PC3 cells. The concentrations of batimastat used had no toxic effects on the cells. Over-expression of the metalloproteinase inhibitors TIMP-1 and TIMP-2 in bone implants led to reduced PC3-induced osteoclast recruitment, osteolysis and bone turnover, suggesting that metalloproteinase activity is involved in one ECM turnover at sites of bone metastasis (Deng 2008).

ADAMTS-1 C-terminal fragments inhibit metastatic potential when over-expressed in Chinese Hamster Ovary (CHO) tumour cells, TA3 mammary carcinoma cells and Lewis lung carcinoma cells (Kuno 2004; Liu 2006). Over-expression of full length ADAMTS-1 inhibited metastases in CHO cells (Kuno 2004), but increased metastases formation by TA3 mammary carcinoma and Lewis lung carcinoma cells (Liu 2006). The ADAMTS-1 gene was one of the genes up-regulated in a genome-wide profiling of 25 CRPC specimens, 12 of which were from metastatic deposits (8 bone, 3 lymph node and 1 liver) (Tamura 2007). It is not known whether ADAMTS-1 up-regulation favours metastasis, or is a host response in an attempt to inhibit the metastatic process.

PSA has been shown to cause preferential adhesion of prostate cancer cells to bone marrow endothelium. Down-regulation of PSA expression in prostate cancer cells by siRNA knock-down led to diminished adhesion of the prostate cancer cells to bone marrow endothelial cells when co-cultured (Romanov 2004). This may explain the

affinity of prostate cancer cells to metastasise to bone, but the mechanism is still not fully understood.

Selective peptide inhibitors of uPA have been reported to inhibit tumour growth and metastasis (Lee, M. 2004). Over-expression of plasminogen activator inhibitor-1 (PAI-1), a natural inhibitor of uPA, caused decreased growth and metastasis of PC3 tumours implanted subcutaneously in athymic mice (Soff 1995). Expression of uPA in metastatic prostate tumours is reported to be 1.5 times greater relative to prostate primary tumours (Kirchheimer 1985), and patients with metastatic prostate cancer have elevated serum uPA levels compared with patients with local disease and healthy controls (Hienert 1988). These studies implicate uPA in the process of prostate cancer metastasis.

1.6.6 Clinical Management

1.6.6.1 Diagnosis and Prognosis

Serum PSA measurement is already established as a useful test to help in diagnosing prostate cancer and monitor disease progression because it is produced almost exclusively by prostate epithelial cells. PSA levels can be elevated in other prostatic conditions and this has led to the search for a more specific biomarker for prostate cancer. Other modalities for diagnostic and prognostic uses of proteinases in cancer are being investigated, such as measuring serum levels of uPA and MMPs either alone or in conjunction with PSA (Matrisian 2003). Proteinase-sensitive magnetic resonance imaging (MRI) contrast agents have been used in experimental settings to detect proteinase expression and activity *in vivo* (Louie 2006). The para-magnetic ion in the contrast agent molecules are bound to and blocked by a substrate that requires cleavage by a specific proteinase in order for the contrast agent to become active. This allows imaging enhancement of sites where the proteinase of interest is active.

1.6.6.2 Prevention and Therapy

Several preventive and therapeutic modalities have been applied in an attempt to modulate the activity of proteinases. Selenium compounds are taken as dietary supplements because of their role in activating caspase-induced apoptosis (Jiang 2001). A meta-analysis of studies on the relationship between selenium intake and prostate cancer concluded that selenium had a protective effect (Etminan 2005). However, more recent evidence from the SELECT trial, a randomised double-blind trial of the effect of selenium and vitamin E supplementation on prostate, lung and colorectal cancer prevention and involving 35,533 men, showed no protective effect with dietary selenium supplementation (Lippman 2009). It is not yet clear why the biological activity of selenium as a caspase activator did not lead to a decreased incidence of prostate cancer.

Cyclooxygenase-2 (COX-2) is over-expressed in prostate cancer (Madaan 2000). COX inhibitors have been shown to reduce MMP production and cell invasiveness in prostate cancer cells *in vitro* (Attiga 2000), and several population-based studies have shown an inverse association of non-steroidal anti-inflammatory drug (NSAID) usage with prostate cancer (Nelson 2000; Leitzmann 2002; Roberts 2002; Garcia Rodriguez 2004; Jacobs 2005; Platz 2005). This suggests that long-term use of NSAIDs may be preventing growth and progression of prostate cancer, possibly by the reduction of MMP production.

Epigallocatechin-3-gallate (EGCG), the major polyphenolic constituent of green tea, has been shown to inhibit MMP-2 and -9 (Adhami 2003), and ADAMTS-1, -4, and -5 (Vankemmelbeke 2003). Green tea is reported to have an inhibitory effect on prostate cancer growth *in vitro* and *in vivo* (Gupta 2001; Adhami 2003). It is not clear whether

the inhibitory effect of green tea on prostate cancer growth and progression is a direct result of inhibition of these proteinases.

Inhibitors of MMPs such as batimastat and marimastat have been used in clinical trials but were shown to produce unacceptable side effects such as joint and muscle pain (Matrisian 2003). Also, results of Phase III clinical trials using marimastat and prinomastat in patients with advanced cancers demonstrated no clinical efficacy (Zucker 2000; Sparano 2004). In another study, batimastat increased metastasis of breast cancer cells to the liver in mice (Kruger 2001). A combination of these findings led to the discontinuation of clinical trials of these MMP inhibitors.

Another aspect of therapy under investigation is the use of viral vectors for gene therapy in prostate cancer. Theoretical models have been described and trials are underway to find the most efficient and safe gene delivery system (Foley 2004). Genes for specific proteinases or their inhibitors could possibly be targeted to up or down-regulate their expression either locally in the prostate, or systemically in cases of widespread metastases. Vectors are being designed that have specific affinity for prostate cells, hence minimising side-effects (Mabjeesh 2002; Song 2008).

1.6.7 Summary of Proteinase Activity in Prostate Cancer

Proteinases play diverse physiological and pathological roles and there is a complex array of enzymatic processes and cascades that regulate the activity of the proteinases, with some proteinases playing dual or auto-regulatory roles depending on the circumstance. Figure 1.11 shows the prostate and bone environment and biological activities regulated by proteinases and inhibitors. The understanding of the function of each of the proteinases and how they interact with each other and with other components of the cellular environment is essential to determining how they can be

exploited as diagnostic, prognostic or therapeutic tools in the management of patients with prostate cancer.

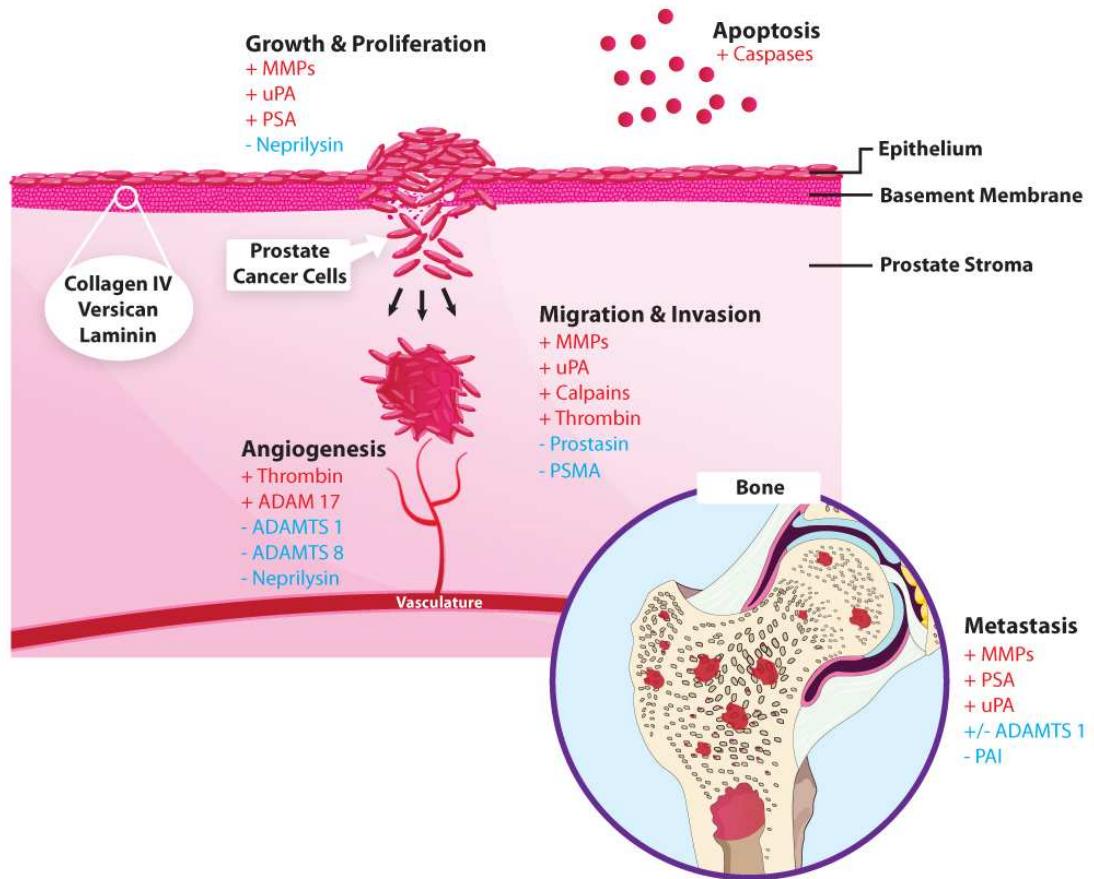


Figure 1.11: Schematic diagram of the prostate and bone micro-environment, showing the proteinases that are playing a role at the different sites.

1.7 The ADAMTS Proteinases

1.7.1 Introduction to the ADAMTS Proteinases

The ADAMTS (A Disintegrin And Metalloproteinase with ThromboSpondin motifs) proteolytic enzymes are a group of metalloproteinases belonging to Family M12 in proteinase Clan MA on the MEROPS database (www.merops.sanger.ac.uk) (Rawlings 2008) and are phylogenetically and structurally related to the MMPs and ADAMs (Huxley-Jones 2007) (Figure 1.12).

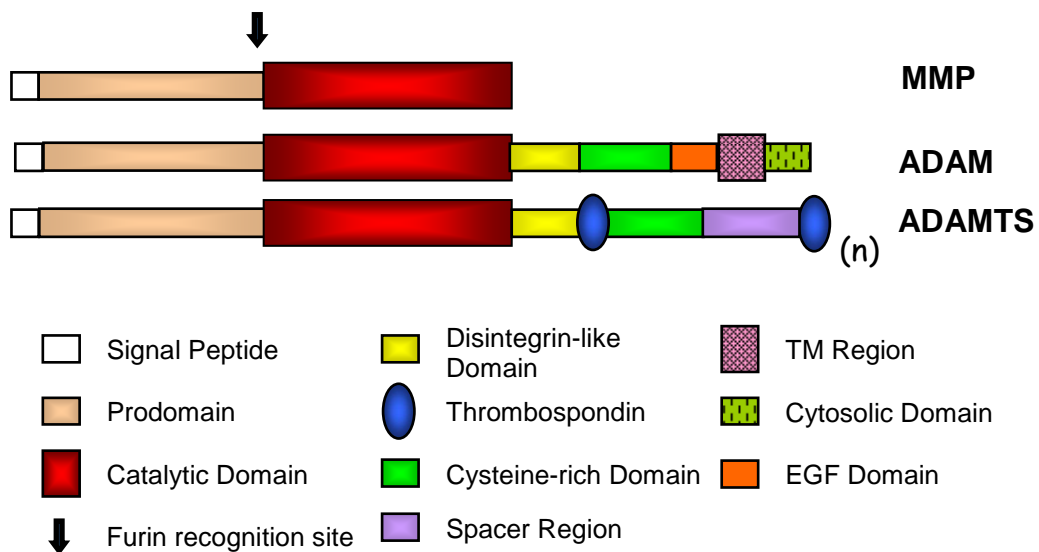


Figure 1.12: Generic domain structure of MMPs, ADAMs and ADAMTSs showing similarities between the groups.

There are 19 ADAMTS proteins coded in the human genome and they play diverse roles in the tissues in which they are expressed (Jones 2005; Porter 2005). ADAMTS-1 was the first to be isolated. In 1997, Kuno et al reported the isolation of a metalloproteinase with thrombospondin motifs from a cachexia inducing adenocarcinoma in mice (Kuno 1997). ADAMTS-1 is essential for normal development of the urogenital tract in mice (Shindo 2000) and for ovulation (Russell 2003). ADAMTS-1 and -8 have anti-angiogenic properties (Vazquez 1999). Anti-angiogenic properties have also recently been described for ADAMTS-2 (Dubail 2010). ADAMTS-1, -4, -5 and -9 have been shown to cleave aggrecan and versican, structural components of the ECM (Kuno 2000; Sandy 2001; Russell 2003; Vankemmelbeke 2003). ADAMTS-5 has been implicated in cartilage breakdown in arthritis (Glasson 2005; Stanton 2005). ADAMTS-2, -3 and -14 are pro-collagen N-peptidases, processing

pro-collagen into the mature form (Colige 2002). Mutations in the *ADAMTS2* gene leads to development of Ehlers-Danlos syndrome type VII C (Colige 1999; Colige 2004). ADAMTS-13 has been identified as the von Willebrand factor cleaving proteinase, processing the von Willebrand factor precursor into the active form for participation in the blood coagulation cascade (Fujikawa 2001; Soejima 2001; Zheng 2001). Functions and substrates have not yet been assigned to ADAMTS-6, -7, -10, -12, -16, -17, -18 and -19. For this reason, these ADAMTSs are sometimes referred to as orphan ADAMTSs. However, ADAMTS-12 has been shown to have proteolytic activity (Cal 2001), and ADAMTS-16 mRNA expression is up-regulated in osteoarthritic cartilage compared to normal cartilage (Kevorkian 2004).

ADAMTS proteins can be divided into sub-groups based on evolutionary relationships (Nicholson 2005) (Figure 1.13). An important feature to note is that the evolutionary sub-grouping closely matches the biological functions of the ADAMTSs. ADAMTS-1, -4, -5, -8 and -15 evolved from a common ancestral protein in invertebrates. The *Ciona intestinalis* ADAMTSf gene has been shown to be orthologous with this sub-group of ADAMTSs (Huxley-Jones 2007). It appears that the human ADAMTS orthologues evolved through a series of gene duplication events, and the differences in protein domain structure are likely to be as a result of gains and losses of introns (Nicholson 2005). The similarity in structure of the ADAMTS members in each sub-group raises the possibility of functional redundancy. However this has not been demonstrated experimentally. ADAMTS-4 and -5 have been demonstrated to be aggrecanases and implicated in cartilage degradation in arthritis but the relative roles of the two enzymes in arthritis have not been resolved completely (Verma 2011). *Adamts5*, but not *ADAMTS4* or *ADAMTS1* knock-out mice were protected from arthritis (Glasson 2004; Glasson 2005; Little 2005; Stanton 2005), indicating that ADAMTS-4 and ADAMTS-1

do not play redundant roles with ADAMTS-5 in the pathogenesis of arthritis. Temporo-spatial differences in expression of ADAMTSs (Cal 2002) also makes it unlikely that they play redundant roles in humans, as they are differentially expressed in tissues during the process of human growth and development.

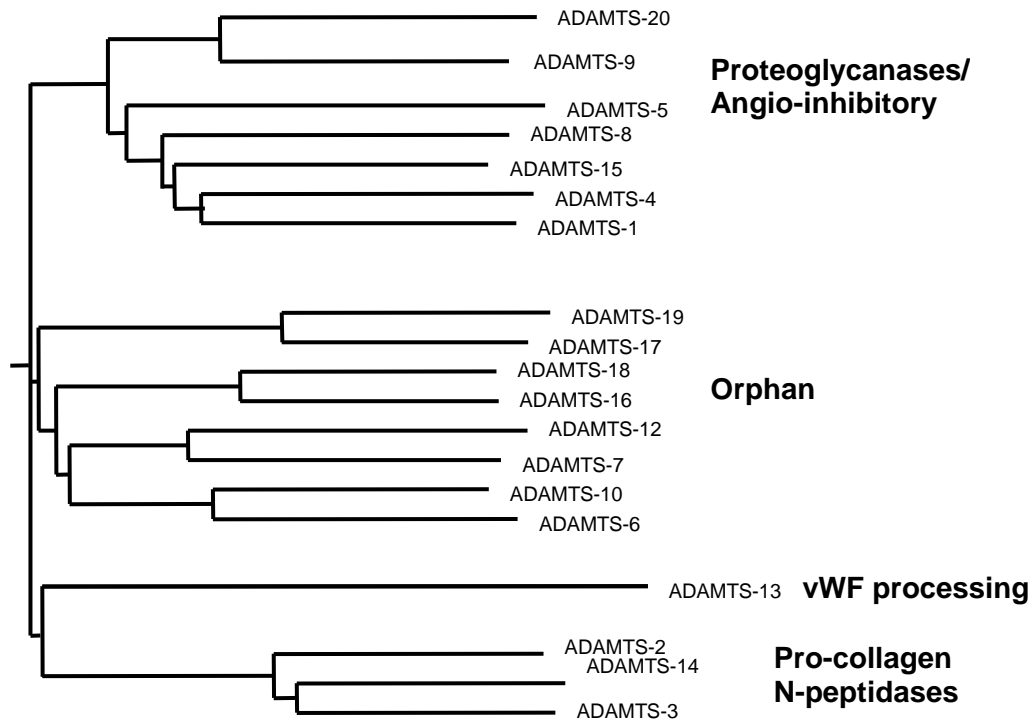


Figure 1.13: Phylogenetic tree of the ADAMTS proteins.

1.7.2 ADAMTSs in Cancer

ADAMTSs have been implicated in malignant processes in several organs. Because of their multi-domain structure and the potential for pro or anti-tumour activity, the role of ADAMTSs in human cancer has attracted interest.

1.7.2.1 Prostate Cancer

ADAMTS-1, -9 and -15 mRNA expression has been detected in prostate cancer cells (Cross 2005). In addition to ADAMTS-1, -9 and -15, ADAMTS-4 and -5 mRNA expression was detected in prostate stromal cells. ADAMTS-1 and -15 were the most

abundantly expressed in the prostate cancer cells. Expression of the ADAMTS inhibitor TIMP-3 was comparatively low in the cells with greater metastatic potential. ADAMTS-15 was the only one of the ADAMTSs that was expressed in all the prostate cancer and stromal cells investigated. Over-expression of ADAMTS-1 has been identified in CRPC tissue (Tamura 2007), suggesting a role for ADAMTS-1 progression of prostate cancer.

1.7.2.2 Breast Cancer

Expression of ADAMTSs has been analysed in breast cancer tissue. Comparing mRNA expression of ADAMTSs in malignant tissue, adjacent normal tissue and cell lines by real-time RT-PCR, ADAMTS-1, -3, -5, -8, -9, -10, and -18 were consistently down-regulated, while ADAMTS-4, -6, -14, and -20 were up-regulated (Porter 2004). High ADAMTS-8 and low ADAMTS-15 expression in malignant breast tumours correlated with worse patient prognosis (Porter 2006), suggesting that ADAMTS-15 may be playing a protective role in breast cancer patients.

1.7.2.3 Glioblastoma

Glioblastoma is a highly invasive form of brain cancer. Comparing expression of ADAMTSs in malignant and adjacent benign tissue using realtime RT-PCR and immunohistochemistry showed that ADAMTS-4 and -5 were over-expressed in tumours and ADAMTS-8 was down-regulated (Nakada 2005; Dunn 2006; Held-Feindt 2006). Over-expression of ADAMTS-5 in a glioblastoma cell line increased invasive potential. The increased invasiveness is thought to be a result of increased cleavage of brevican, a major proteoglycan in brain ECM.

1.7.2.4 Head and Neck Cancer

Head and neck squamous cell cancers (HNSCC) affect the oral and pharyngeal membranes. Expression profiles of ADAMTS mRNA in localised and metastatic HNSCC compared with normal pharyngeal mucosa has revealed dysregulation of ADAMTSs (Demircan 2009). ADAMTS-1, -4, -5, -8, -9 and -15 were down-regulated in approximately 50% of primary tumours compared to normal tissue. Comparing primary tumours with their corresponding metastatic tumours, ADAMTS-1, -4, -5 and -15 were up-regulated, ADAMTS-9 was down-regulated. ADAMTS-8 mRNA expression was similar between metastatic tumours and their parent tumours. These findings suggest that a sub-population of cancer cells with the optimal expression profile are able to metastasize, resulting in differences in ADAMTS expression between parent and metastatic tumours. An alternative explanation is that the cancer cells are able to alter expression profiles of pro and anti-metastatic proteins at each stage of tumour progression.

1.7.2.5 Non-Small Cell Lung Carcinoma

Non-small cell lung carcinoma (NSCLC) is a variant of lung cancer. Using real-time RT-PCR and immunohistochemistry, lower expression of ADAMTS-1 and -8 was found in NSCLC tissue compared with adjacent normal tissue (Dunn 2004; Rocks 2006). Abnormal hypermethylation of the *ADAMTS8* gene was found in the majority of the tumours suggesting epigenetic silencing of *ADAMTS8* in NSCLC cells.

1.7.2.6 Adenocarcinoma of the Colon

ADAMTS-1 has been detected in cachexia inducing colorectal cancer cells (Kuno 1997). Subsequent studies have shown that the *ADAMTS1* gene is hypermethylated in colon cancer cells (Lind, G.E. 2006), and that *ADAMTS1* methylation status could be

used to differentiate normal colorectal mucosa, benign tumours and malignant tumours (Ahlquist 2008). Mutations and epigenetic silencing of the *ADAMTS15* gene have been identified in colorectal cancer (Sjoblom 2006; Vilorio 2009). Over-expression of ADAMTS-15 in colorectal cancer cells reduces invasive potential (Vilorio 2009), suggesting an anti-tumour role for ADAMTS-15.

1.7.2.7 Pancreatic Carcinoma

Pancreatic carcinoma is a tumour with a very poor prognosis. ADAMTS-1 mRNA expression profiles in malignant pancreatic tissue compared with adjacent normal tissue showed that ADAMTS-1 was down-regulated in malignant tissue samples (Masui 2001). The malignant tumours that had higher expression of ADAMTS-1 also had an increased incidence of lymph node metastasis and retroperitoneal invasion. CD34 staining of the tissue samples did not show any correlation between ADAMTS-1 expression and microvascular density.

1.7.2.8 Hepatocellular Carcinoma

Hepatocellular carcinoma (HCC) is the most common cancer in the developing world, and is associated with Hep-B infection (Michielsen 2005). Expression of ADAMTS-1 mRNA was compared between malignant and adjacent cirrhotic liver tissue (Masui 2001). Expression was lower in the malignant tissue samples. Staining for CD34 did not show any correlation between ADAMTS-1 expression and microvascular density.

1.7.2.9 Chondrosarcoma

Chondrosarcoma is a common malignant primary cartilage tumour. Expression of ADAMTS-4 and -5 were analysed by immunohistochemistry and staining scores

correlated with histological grade (Sugita 2004). Expression of both ADAMTS-4 and -5 correlated with histological grade of osteosarcomas, with higher expression levels found in grade 2 and 3 tumours compared with grade 1. Expression of the metalloproteinase inhibitors TIMP-1, -2 and -3 were also found to correlate with histological grades. Put together, this suggests that there is a high rate of ECM turnover in the more aggressive tumours. Expression of ADAMTS-9 has also been detected in chondrosarcoma cells (Demircan 2005), where expression was up-regulated by TNF and IL-1 β .

1.7.2.10 Summary of ADAMTS Roles in Cancer

The expression profiles of ADAMTS proteinases in these various human tumours suggests that they may be playing a role in the pathophysiology of these tumours. It appears that the expression and role played by individual ADAMTSs varies in different tumour sites, as summarised in Table 1.6. The activity of ADAMTSs may be attributed to their multi-domain structure and the degree of processing, and the relative abundance of the resulting fragments at the tumour sites. Specifically in prostate cancer cells, the expression profile of ADAMTS-1 and -15 suggest that they may be the most important members of this group in prostate cancer biology and may be playing a role in progression of prostate cancer.

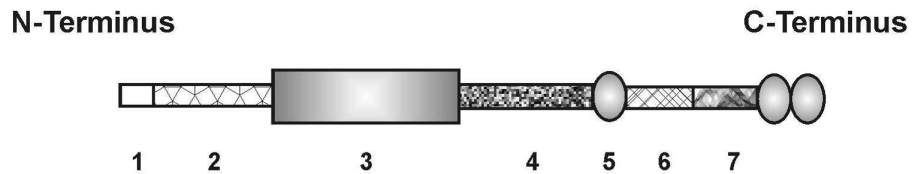
Organ	Up-Regulated	Down-Regulated
Brain	-4, -5	-8
Lung	-	-1, -8
Breast	-4, -6, -14, -20	-1, -3, -5, -8, -9, -10, -18
Pancreas	-	-1
Liver	-	-1
Bone	-4, -5	-
Prostate	? -1, -15	-

Table 1.6: Table summarising the expression of ADAMTS proteins in human cancer tissue and cells compared with non-malignant tissue.

1.7.3 Structure of ADAMTS-1 & -15

The *ADAMTS1* gene codes for a 967 aa protein with a relative molecular mass of 105kDa. The *ADAMTS15* gene codes for a similarly sized 950 aa protein with a relative molecular mass of 103kDa. ADAMTS-1 and -15 share a similar generic structure with other ADAMTS proteins and both belong to the sub-group comprising ADAMTS-1, -4, -5, -8 and -15. The ADAMTSs possess a multi-domain structure, with each domain potentially conferring different properties to the molecule. Each ADAMTS protein consists of a signal peptide and a propeptide domain, a catalytic domain containing a zinc-binding motif, a disintegrin-like domain, and thrombospondin motifs separated by a cysteine-rich spacer region (Vankemmelbeke MN 2001; Jones 2005; Porter 2005).

ADAMTS-1 and -15 share similar structure and sequence homology (Cal 2002), with the same number and configuration of the thrombospondin motifs (Figure 1.14).



1-Signal peptide, 2-Propeptide domain, 3-Proteolytic domain, 4-Disintegrin-like domain, 5-Thrombospondin domain, 6-Cysteine-rich domain, 7-Spacer region

Figure 1.14: Generic structure of ADAMTS-1 and -15. Each ADAMTS protein has a central thrombospondin-like domain. The configuration of the rest of the C-terminal thrombospondin-like domains differs between the members of the group, but is identical for ADAMTS-1 and -15.

Comparison of the domains of ADAMTS-1 and -15 (Table 1.7) shows the similarity between the structure of the two proteins, with potential implications of similar roles for the two proteins.

Domain	Domain Position (Amino Acid Length)	
	ADAMTS-1 (967)	ADAMTS-15 (950)
Signal Peptide	1-49 (49)	1-17(17)
Propeptide	50-252 (203)	18-212 (195)
Catalytic	253-467 (215)	213-427 (215)
Disintegrin-like	468-559 (92)	428-515 (88)
Thrombospondin 1	560-614 (55)	516-571 (56)
Cysteine-rich	615-724 (110)	572-700 (129)
Spacer	725-849 (125)	701-838 (138)
Thrombospondin 2	850-905 (56)	839-895 (57)
Thrombospondin 3	906-967 (62)	896-950 (55)

Table 1.7: Similarities between the ADAMTS-1 and -15 domain length and configuration. Protein sequence data obtained from the Uniprot Database (<http://www.expasy.org/uniprot/>).

A recent study reported for the first time the crystal structure of ADAMTS-1 (Gerhardt 2007). This has further clarified the domain structure of the ADAMTSs. From the N-terminal end, the signal peptide consists of a variable length aa sequence which is cleaved soon after translation in the endoplasmic reticulum (Porter 2005). The propeptide domain may be important for correct protein folding (Cao 2000). Cleavage of the propeptide by proprotein convertases like furin in the golgi apparatus is believed to be essential for activation of the proteolytic domain (Bergeron 2000; Wang 2004). Some recent reports have indicated that the propeptide domain may be retained and cleaved extracellularly after secretion (Longpre 2009). Extracellular activation has not been reported for ADAMTS-1 or -15. The proteolytic domain contains the catalytic zinc pocket which is responsible for the proteolytic properties of the ADAMTSs. MMPs have a cysteine residue within the PRCGVDP motif in the propeptide domain interacting with the zinc pocket of the proteolytic domain, preventing proteolysis (Van Wart 1990). Thus cleavage of the propeptide domain frees the zinc ion to initiate the hydrolytic reaction characteristic of metalloproteinases (the cysteine switch). ADAMTS-1, and -15 have a similar cysteine-containing motif in the prodomain (Cal 2002). On the C-terminal end of the proteolytic domain is a disintegrin-like domain. The structure of the disintegrin domain of ADAMTS-1 was analysed by Gerhardt et al, who concluded that based on the protein fold, the disintegrin domain is actually a cysteine-rich domain, which fails to superimpose on the crystal structures of the disintegrin domains of ADAM-10, VAP-1 or trimestatin and (Gerhardt 2007), which are well characterised disintegrins. It is not yet known if this holds true for the other ADAMTSs. The rest of the C-terminal end of ADAMTS-1 and -15 consists of a central thrombospondin type-1 motif, a cysteine-rich spacer region and two additional

thrombospondin motifs. The number and configuration of the thrombospondin motifs and spacer regions are different in other members of the group. ADAMTS-1 and -15 do not possess PLAC (Protease and Lacunin), CUB (Complement-Uegf-BMP-1) and mucin domains found in some other ADAMTS proteins.

Unlike the ADAMs, the ADAMTSs do not possess a trans-membrane domain. They are therefore secreted from the cell into the ECM where they are sequestered by heparan sulphate proteoglycans (Kuno 1998; Gao 2004).

1.7.4 Functions of ADAMTS-1 & -15

ADAMTS-1 has been extensively studied, and its biological functions are better understood than ADAMTS-15. Following its discovery as an inflammation-associated protein (Kuno 1997), ADAMTS-1 has been shown to be catalytically active and capable of cleaving several ECM components (Kuno 1999).

The mouse *Adamts1* gene promoter has been reported to have transcription factor binding sites for nuclear factor-1-like factor (NF1-like factor), specificity protein-1/specificity protein-3 (Sp-1/Sp-3), CCAAT enhancer binding protein beta (C/EBP β), and GA binding protein (GABP) but no androgen or progesterone response elements (Doyle 2004). These transcription factor binding sites were found to be highly conserved between the mouse, rat and human orthologues of the *ADAMTS1* gene. Selective deletion of each of these binding sites reduced ADAMTS-1 transcription, indicating that basal transcription of ADAMTS-1 was maintained by a combination of activity from each of these binding sites (Doyle 2004). Binding sites have also been reported for hypoxia-inducible factor-1 (HIF-1) (Hatipoglu 2009). *ADAMTS1* gene transcription is up-regulated by progesterone in ovarian granulosa cells via interaction of ligand-activated progesterone receptor (PR) with Sp1/Sp3 and binding of the PR-Sp1/Sp3

complex with the Sp1/Sp3 transcription factor binding sites (Doyle 2004), and by hypoxia in endothelial cells via binding of HIF-1 to response elements in the promoter by a phosphatidylinositol 3-kinase dependent process (Hatipoglu 2009). IL-1 β and TNF have also been reported to induce *ADAMTS1* transcription by mechanisms that are yet to be elucidated (Bevitt 2003; Cross 2006; Ng 2006).

After co-translational cleavage of the signal peptide, the mature ADAMTS-1 protein is sequentially cleaved into two active forms (Rodriguez-Manzaneque 2000). The first cleavage is mediated by furin and removes the propeptide (Longpre 2004), leaving an 87kDa form with an activated catalytic site. This 87kDa form is secreted from the cell and sequestered in the ECM by binding to heparan sulphate proteoglycans (Kuno 1998). The 87kDa form is further processed by autolytic cleavage or by MMP-2, -8, and -15 at the spacer region to yield a 65kDa catalytic fragment and a 22kDa C-terminal fragment containing the two C-terminal thrombospondin (TSP) motifs (Rodriguez-Manzaneque 2000).

The catalytic activity of ADAMTS-1 is evident by the number of substrates that have been identified. These include the proteoglycans aggrecan (Kuno 2000; Rodriguez-Manzaneque 2002; Vankemmelbeke 2003), versican (Sandy 2001; Russell 2003) and syndecan (Rodriguez-Manzaneque 2009). ADAMTS-1 has also been shown to cleave thrombospondin-1 and -2 (Lee 2006), tissue factor pathway inhibitor-2 (Torres-Collado 2006) and gelatin (Lind, T. 2006). Type I collagen degradation is enhanced by ADAMTS-1 expression (Rehn 2007), but it is not clear whether ADAMTS-1 cleaves type-I collagen directly.

Studies of ADAMTS-1 knock-out mice showed a number of defects including malformations of the kidneys, adrenal glands, uterus and ovaries with impaired ovulation in females (Shindo 2000; Mittaz 2004). These findings suggest altered ECM

turnover. However ADAMTS-1 knock-out mice do not exhibit any changes in cartilage turnover, possibly because ADAMTS-1 does not play a major role in the pathogenesis of arthritis or due to redundancy of function between the ADAMTS proteoglycanases (Little 2005).

ADAMTS-1 has multiple functions as a result of its multi-domain structure.

In addition to its proteolytic activity which is mediated by the catalytic domain, the C-terminal TSP motifs are responsible for anti-angiogenic properties (Iruela-Arispe 2003).

ADAMTS-1 inhibits bFGF and VEGF induced angiogenesis (Vazquez 1999). VEGF is sequestered by binding to the TSP domains of ADAMTS-1 and is thus prevented from activating VEGFR2 on endothelial cells (Luque 2003). In addition, cleavage of TSP-1 by ADAMTS-1 releases anti-angiogenic fragments (Lee 2006). ADAMTS-1 is down-regulated in proliferating endothelial cells compared to tubular cells (Glienke 2000).

Two separate studies (Kuno 2004; Liu 2006) have demonstrated that while the full-length ADAMTS-1 had pro-metastatic activity, the TSP-spacer-TSP segment of the C-terminal region inhibited angiogenesis and the establishment of metastases. This shows that the degree of processing of ADAMTS-1 determines the predominant effect of ADAMTS-1 in the tumour micro-environment (TME). Paradoxically ADAMTS-1 has also been shown have pro-angiogenic effects. ADAMTS-1 was up-regulated in endothelial cells during angiogenesis and ADAMTS-1 knock-down decreased endothelial cell invasion (Su 2008). The up-regulation of ADAMTS-1 was temporal and peaked at 4-10 hrs after seeding on a 3D matrix. This possibly indicates that ADAMTS-1 is required for ECM degradation in the early stages of capillary sprouting.

The biological functions of ADAMTS-15 have not been reported. By sequence homology, ADAMTS-15 is expected to have similar activity to ADAMTS-1 (Cal 2002).

Low tumour expression is associated with poor prognosis in breast cancer patients

(Porter 2006). ADAMTS-15 expression is also reported to have anti-tumour effects in colorectal cancer (Viloria 2009). The actual role of ADAMTS-15 is not clear, but the multiple domains could be playing different roles, as is the case with ADAMTS-1, in which the proteolytic domain is responsible for ECM-degrading activity, while the C-terminal domains are responsible for anti-angiogenic activity. The roles played by these proteinases in prostate cancer development and progression are yet to be identified.

Catalytic activity of ADAMTS-1 is inhibited by tissue inhibitor of metalloproteinases (Rodriguez-Manzaneque 2002). Tissue inhibitor of metalloproteinases-3 (TIMP-3) is the most important tissue inhibitor of the ADAMTSs in tissues, although TIMP-2 has less potent inhibitory activity (Hashimoto 2001; Rodriguez-Manzaneque 2002). TIMPs are 25-31kDa proteins with a wedge-shaped crystal structure (Fernandez-Catalan 1998). They possess an approximately 125a.a. N-terminal domain and a smaller 65 a.a. C-terminal domain (Williamson 1990). TIMPs inhibit metalloproteinases by tight binding to the catalytic pocket, preventing binding of the substrate to the catalytic site (Brew 2000). TIMP-3, like ADAMTS-1 is secreted into the ECM where it is sequestered by heparan sulphate proteoglycans (Yu 2000). Mutations in *TIMP3* gene lead to a condition called Sorsby fundus dystrophy characterised by accumulation of ECM components in the retina (Weber 1994). Aggrecanase activity of ADAMTS-1 is also inhibited by catechin gallate esters, which are constituents of green tea. Epigallocatechin gallate and epicatechin gallate selectively inhibit aggrecanase activity of ADAMTS-1, -4 and -5 (Vankemmelbeke 2003). Oral intake of green tea extract inhibited collagen-induced arthritis in mice (Haqqi 1999). The exact mechanism of inhibition of ADAMTSs by catechin gallate esters is yet to be elucidated.

1.8 Inflammation in Prostate Cancer

1.8.1 Immune Cells and Cytokines

Immune cells are present in normal prostate epithelial and stromal tissue (McClinton 1990; Elsasser-Beile 2000; Bostwick 2003). These are mostly T-cells, and are more numerous in the stromal component of the gland. The epithelial T-cells are predominantly CD8+ cytotoxic cells and the stromal T-cells are predominantly CD4+ helper cells (Bostwick 2003). Lymphocytes from prostate cancer tumours have been shown to express higher levels of IL-10 and IFN- γ than circulating lymphocytes of the same patient (Elsasser-Beile 2000). The pro-inflammatory enzyme, cyclooxygenase-2 (COX-2), is over-expressed in prostate cancer tissue and correlates with areas inflammation and angiogenesis (Wang, W. 2005). Prostate cancer cells secrete a number of cytokines into the TME. TNF, IL-1 and IL-6 are secreted in response to inflammation (Wong 2009). IL-6 promotes cell proliferation, and is up-regulated by androgen (Okamoto 1997; Lee, S.O. 2003). Constitutive expression of IL-8 by prostate cancer cells stimulates cell proliferation (Moore 1999). IL-4 has been shown to activate the AR in a ligand-independent manner, and potentiates the growth stimulatory effect of DHT (Lee, S.O. 2003; Lee 2008).

Macrophages, lymphocytes and neutrophils infiltrate tumour sites in response to chemokines and cytokines produced by tumour cells (Coussens and Werb 2002; Pollard 2004), and the hypoxic environment within the tumour (Lewis 2006). TAMs release numerous cytokines into the TME as part of the inflammatory reaction to the presence of the tumour (Dranoff 2004). TAMs are thought to favour tumour progression as a result of the release of pro-tumour and angiogenic cytokines and proteinases including TNF and MMPs (Lin and Pollard 2004; Pollard 2004). Clinical studies have reported that patients with advanced prostate cancer have elevated serum levels of TNF, IL-4,

IL-6 and IL-10 (Twillie 1995; Adler 1999; Drachenberg 1999; Wise 2000; Michalaki 2004). TNF is also over-expressed in prostatic fluid of prostate cancer patients (Fujita 2008).

TNF is thought to induce cachexia in cancer patients (Tracey 1992). Prostate cancer patients with elevated serum TNF have been shown to have lower haemoglobin and serum albumin levels, poorer performance status and poorer prognosis compared to patients with low or absent serum TNF (Nakashima 1998). The role of TNF in prostate cancer progression therefore can not be ignored.

1.8.2 TNF Receptor Signalling

TNF is a multifunctional cytokine that plays a role in systemic inflammatory response, apoptosis, angiogenesis, lipid metabolism and insulin resistance (Beutler 1986; Locksley 2001; Balkwill 2006; Bastard 2006). TNF is produced as a 26kDa membrane-bound protein and is cleaved into a 17kDa soluble form by ADAM-17 (TNF-alpha converting enzyme, TACE) (Black 1997). TNF acts via binding to TNF receptor 1 (TNFR1) and TNF receptor 2 (TNFR2). TNFR1 is present on cells in most tissue sites, while TNFR2 is predominantly expressed in leucocytes. TNF signal transduction is a complex process involving many proteins (Camussi 1991; Englaro 1999; Baud 2001; He 2002; Kawasaki 2002). Activation of TNFR1 by TNF leads to intracellular trimerisation of the receptor and association with TNF receptor-associated death domain (TRADD). TRADD activates the fas-associated death domain (FADD), RIP-associated ICH-1/CED-3-homologous protein with a death domain (RAIDD), MAPK-activating death domain (MADD) and receptor-interacting protein (RIP), leading to activation of caspase-8 and the initiation of the apoptosis cascade. Activation of TNFR2 leads to the association of TNF receptor-associated factor 2 (TRAF2) with TRADD, which then forms a complex with MADD and RIP. The TRAF2-MADD-RIP complex associates

with NFκB-inducing kinase (NIK) and phosphorylates IκK, leading to the translocation of NFκB into the nucleus. The TNFR1-TRADD-TRAF2-MADD-RIP complex also activates MAPK which in turn activates AP1. The NFκB and AP1 transcription factors are responsible for the regulating numerous growth and stress-related genes, including proteinases involved in ECM turnover.

1.9 ADAMTS Expression in Inflammatory Disease

Some cachexia-inducing tumours are known to express high levels of ADAMTS-1 (Kuno 1997). ADAMTS-1 is highly expressed in inflamed tissue (Kuno 1997). ADAMTS-1 and -4 are up-regulated in inflamed atheromatous plaques (Sandy 2001; Jonsson-Rylander 2005). ADAMTS-5 aggrecanase activity is essential for disease progression in murine models of arthritis (Glasson 2005; Stanton 2005). Regulation of ADAMTS-1, -4, -5, -6 and -9 expression by pro-inflammatory cytokines has also been reported (Bevitt 2003; Norata 2004; Demircan 2005; Ng 2006). These studies indicate that ADAMTSs may be playing an active role at sites of inflammation. Dysregulation of proteinases by TNF and other cytokines could alter the homeostatic balance between proteinases and their natural inhibitors in the TME.

1.10 Aims and Hypotheses

ADAMTS-1, -9 and -15 mRNA expression has been detected in prostate cancer cells (Cross 2005). ADAMTS-1 and -15 were the most abundantly expressed, and ADAMTS-15 was the only member of the group that was expressed in all the cancer and stromal cells analysed. ADAMTS-1 over-expression has been reported in metastatic CRPC tumours compared with primary tumours (Tamura 2007), suggesting a role for ADAMTS-1 progression of prostate cancer.

The predominant role of ADAMTS-1 in the literature suggests that it plays an active role in remodelling of the ECM. Degradation of the ECM could result in the release of growth factors sequestered in the ECM, favouring cancer cell proliferation. Break-down of the natural tissue barriers constituted by the ECM and basement membranes could also allow local spread and metastasis of cancer cells. There is little information in the literature on the function of ADAMTS-15. High tumour expression of ADAMTS-15 in breast cancer patients correlates with better prognosis, which suggests that ADAMTS-15 could have anti-tumour activity. The role of AR signalling in the development and progression of prostate cancer has been discussed in Section 1.4.1, and the local and systemic inflammatory response in cancer in Section 1.8.

1.10.1 Aims

The aims of this study were three-fold. Firstly, to determine whether prostate cancer and stromal cells were proteolytically active. Secondly, to evaluate the effect of two signalling pathways that affect prostate cancer development and progression, androgen signalling and inflammation, on the expression of ADAMTS-1, -15 and TIMP-3 in prostate cancer cells. Thirdly, to analyse the functional roles of ADAMTS-1 and -15 in prostate cancer cell proliferation, migration and invasion.

1.10.2 Hypotheses

The following hypotheses were tested:

1. Prostate cancer and stromal cells are proteolytically active.
2. The expression of ADAMTS-1, -15 and TIMP-3 is regulated by androgen in androgen-sensitive LNCaP cells.

3. The expression of ADAMTS-1, -15 and TIMP-3 is regulated by TNF in PC3, LNCaP and prostatic stromal cells.

4. Knock-down of ADAMTS-1 expression decreases the proliferation, migration and invasive potential of PC3 cells.

5. Knock-down of ADAMTS-15 expression increases the proliferation, migration and invasive potential of PC3 cells.

CHAPTER 2

MATERIALS & METHODS

CHAPTER 2:

MATERIALS AND METHODS

2.1 Cell Lines and Culture

The PC3 and LNCaP cell lines used in this study were obtained from ATCC. PC3 cells were originally isolated from bone metastases in a patient with prostate cancer and are not androgen responsive due to non-expression of the AR (Kaighn 1979). LNCaP cells were originally isolated from lymph node metastases (Horoszewicz 1983). LNCaP cells express the AR and are androgen responsive (Horoszewicz 1983). C4-2b4 and PCAF (prostate carcinoma associated fibroblasts) cells were a gift from Dr Colby Eaton at the University of Sheffield. The C4-2b4 cell line is a derivative of LNCaP cells, obtained by repeated passage in castrated male mice (Thalmann 2000), and PCAF cells were isolated from peri-tumoural prostatic stroma (Olumi 1999). BPH45 cells are prostate fibroblasts that were generated in our laboratory by Dr. Colby Eaton (Klingler 1999). The breast cancer cell line MDA-G8, is a derivative of the MDA MB-436 breast cancer cell line (Cailleau 1978; Ottewell 2008) and was a gift from Dr. Ingunn Holen. The U373 astrocytoma cell line (Ponten 1968) was a gift from Prof. Nicola Woodroffe. The PNT1 and PNT2 non-tumourigenic prostatic epithelial cell lines (Berthon 1995) were not used in this study. They were immortalised using the Simian Virus-40 (SV40) viral vector which up-regulates ADAMTS-1 expression (Freimann 2005). As a result of this, the PNT1 and PNT2 cell lines were not considered to be true 'normal' prostatic epithelial cell lines for the purpose of this study. Prostatic stromal cells (BPH45), prostate carcinoma associated fibroblasts (PCAF), the prostate carcinoma cell lines (PC3, LNCaP, and C4-2b4), astrocytoma cell line (U373) and the breast carcinoma cell line (MDA-G8) were routinely cultured in DMEM (Gibco, Invitrogen) supplemented

with 10% (v/v) FCS (Invitrogen), 100units/ml penicillin (Invitrogen), 100µg/ml streptomycin (Invitrogen) and 0.25µg/ml amphotericin B (Invitrogen), unless otherwise stated. FCS is added to cell culture medium as a supplement to serve as a source of protein, growth factors, hormones, lipids and minerals (Freshney 2005). The cells were grown in a humidified incubator at 37°C in a 5% CO₂ atmosphere unless stated otherwise. Plated cells were detached when required by aspirating and discarding spent medium, gently washing twice with PBS and adding 1 X trypsin-EDTA solution (0.25% (w/v) trypsin, 0.1% EDTA, pH 7.2-8.0) (Sigma). Enough trypsin-EDTA was added to completely cover the cell layer (2ml for a T75 tissue culture flask) for 5 minutes at ambient temperature. After cell detachment, an equivalent amount of complete medium was added to inactivate the trypsin and the cells were used as required.

2.2 RNA Extraction

For RNA extraction, cells were lysed with Tri Reagent (Sigma), based on the method described by Chomczynski (Chomczynski 1987). The cell lysates were stored at -80°C until ready for RNA extraction. The protocol provided by Sigma with the Tri Reagent was used for RNA extraction. Ninety-nine percent Chloroform (Sigma) was added to the cell lysate at 0.2mls/ml Tri reagent used. The mixture was agitated in a tube by hand and then left to stand at ambient temperature for 3 minutes. The tubes were centrifuged at 12,000 x g for 15 minutes at 4°C. The aqueous phase at the top was carefully removed with a pipette and placed in a fresh tube. Ninety-nine Isopropanol (Sigma) was added at a volume of 0.5ml/ml Tri reagent used at the start and the tubes were incubated at ambient temperature for 10 minutes. The tubes were centrifuged at 12,000 x g for 10 minutes at 4°C. The supernatant was removed with a pipette, leaving the RNA pellet at the bottom of the tube. The RNA pellet in the tube was washed by adding 75% (v/v)

Ethanol (Sigma) at a volume of 1ml/ml of Tri reagent used at the start. The tube was vortexed and centrifuged at 7,500 x g for 5 minutes at 4°C. The ethanol wash solution was removed with a pipette leaving the RNA pellet at the bottom of the tube. The RNA pellet was air-dried and then re-dissolved in 10-20 µl of Diethyl pyrocarbonate (DEPC) (Ambion, Applied Biosystems) treated water. The RNA solution was stored at -80°C until ready for cDNA synthesis. RNA purity was determined using the A_{260}/A_{280} ratio, with an acceptable ratio being > 1.8 (Glasel 1995).

2.3 cDNA Synthesis

cDNA was synthesised from previously extracted RNA using Superscript II –Reverse Transcriptase (Invitrogen) according to the supplier's protocol. Twenty microlitres reactions were set up in 200µl thin-walled PCR tubes. Each reaction tube contained 4µl of 5x 1st strand buffer (250mM Tris-HCl, 375mM KCl, 15mM MgCl₂, pH 8.3), 2µl of 0.1M dithiothreitol (DTT) solution, 0.5µl of 10mM deoxyribonucleotide triphosphate (dNTP) (Bioline), 0.5µl of 50µM Random Hexamers (Invitrogen) and 0.5µl (20 units) of RNase Inhibitor (Invitrogen), 10.5µl of DEPC-treated water, 1µl (200 units) of reverse transcriptase and 1µl of the RNA extract. Negative controls contained all the reaction components except reverse transcriptase. Reactions were run on a Gene Amp PCR System 9700 (Applied Biosystems). The thermal cycler was set at 25°C for 2 minutes, 42°C for 50 minutes, 70°C for 15 minutes and then cooled to 4°C. cDNA was stored at -20°C until ready for use in real-time RT-PCR reactions.

2.4 Real-time RT-PCR

Relative quantification of gene expression was undertaken by realtime RT-PCR according to the principles and protocol described in the Applied Biosystems User

Bulletin #2: ABI Prism 770 Sequence Detection System, 2001. Real-time RT-PCR was run in 10µl reactions in duplicate using 384-well plates on the ABI Prism 7900HT sequence detector using SDS 2.1 software (Applied Biosystems). For reactions using SYBR-Green, each well contained 5µl of SYBR-Green master mix (Applied Biosystems) 1µl each of forward and reverse primers (Table 2.1) 1µl of DEPC-treated water and 2µl of cDNA to be analysed. For reactions using Taqman assays, 5µl of Taqman master mix (Applied Biosystems) 0.5µl of Taqman gene expression assay (Table 2.2), 2.5µl of DEPC-treated water and 2µl of cDNA for analysis. Sequence detection was either with SYBR-Green or Taqman primer-probes with a FAM reporter and a non-fluorescent quencher. The thermal cycle was 95°C for 5 minutes, then 40 cycles of 95°C for 15s and 60°C for 1 minute. Glyceraldehyde-3-phosphate dehydrogenase (GAPDH) or RNA polymerase II (RNAP) was used as the endogenous control to normalise between samples (Janssens 2004; Radonic 2004). Relative expression levels were determined using the $2^{-\Delta\Delta C_T}$ method (Livak 2001), where $\Delta\Delta C_T$

=

$$(C_T \text{Target Gene} - C_T \text{Endogenous Control})_{\text{Treated}} - (C_T \text{Target Gene} - C_T \text{Endogenous Control})_{\text{Control}}$$

<i>Gene/ Accession No</i>	<i>Fwd/ Rev</i>	<i>5' Position</i>	<i>Sequence</i>	<i>Product size</i>
ADAMTS-1/ AF170084	F	945	GCACTGCAAGGCGTAGGAC	90 b.p.
	R	1034	AAGCATGGTTTCCACATAGCG	
ADAMTS-15/ AJ315733	F	941	TCCTCTTCACCAGGCAGGAC	81 b.p.
	R	1021	GGTCACACATGGTACCCACATCA	
ADAMTS-20/ AF488804	F	3458	AGATGGCACAATGGCGACAT	100 b.p.
	R	3557	CTATCAAGAGCATCACGACAGCTT	
TIMP-3/ X76227	F	329	TCCGAGAGTCTCTGTGGCCTTA	106 b.p.
	R	424	GCACAGCCCCGTGTACATCT	
GAPDH/ NM_002046	F	7	GCTCCTCCTGTTCGACAGTCA	80 b.p.
	R	86	AACTTCCCCATGGTGTCTGA	

Table 2.1: Gene, primer and amplicon data for primer products supplied by Applied Biosystems which were used in experiments with SYBR-Green as the reporter dye.

<i>Gene/ Accession No</i>	<i>Assay ID</i>	<i>5' Position</i>	<i>Reporter</i>	<i>Quencher</i>	<i>Amplicon Length</i>
ADAMTS-1/ NM_006988	Hs00199608_m1	1151	FAM	Non-Fluorescent	68 b.p.
ADAMTS-15/ NM_139055	Hs00373520_m1	1512	FAM	Non-Fluorescent	60 b.p.
ADAMTS-20/ NM_175851	Hs00228033_m1	2712	FAM	Non-Fluorescent	107 b.p.
TIMP-3/ NM_000362	Hs00165949_m1	1280	FAM	Non-Fluorescent	59 b.p.
PSA/ NM_001030047	Hs00426859_g1	170	FAM	Non-Fluorescent	153 b.p.
GAPDH/ NM_002046	Hs99999905_m1	71	FAM	Non-Fluorescent	122 b.p.
RNAP II/ NM_000937.3	Hs00172187_m1	481	FAM	Non-Fluorescent	61 b.p.

Table 2.2: Gene, assay, probe, reporter and amplicon data for Taqman primer products supplied by Applied Biosystems.

2.5 Protein Extraction from Cultured Cells

2.5.1 Extraction using Mammalian Cell Lysis Kit (RIPA Buffer)

The reagents in the Mammalian cell lysis kit (Sigma) are similar to the radioimmunoprecipitation assay (RIPA) buffer (Escribano 1987). Reagents in the kit were stored at -20°C and brought to 4°C prior to use. To make up 1ml of lysis buffer 200µl each of 5x Tris-EDTA buffer, 5x NaCl, 5x SDS, 5x Deoxycholic acid and 5x Igepal CA-630 (Nonyl phenoxy polyethoxy ethanol) were mixed with 10µl proteinase inhibitor cocktail containing 4-(2-aminoethyl)benzenesulfonyl fluoride (AEBSF), pepstatin A, bestatin, leupeptin, aprotinin, and trans-epoxysuccinyl-L-leucyl-amido(4-guanido)-butane (E-64). Cell lysis was performed according to the supplier's protocol. Medium was removed from the cells to be lysed the cells were gently washed with PBS. The lysis buffer was applied to the cells (1ml/10⁶ cells) and placed on a rotating platform in a cold room at 4°C for 1 hour. A cell scraper was used to detach any cells still attached. The cell lysate was triturated with a 1ml pipette to aid cell membrane disruption. The lysate was centrifuged at 12,000 x g for 10 minutes at 4°C. The supernatant was removed with a pipette and saved while the pellet containing cell debris was discarded. The protein solution was stored at -40°C until ready for protein quantification.

2.5.2 Extraction using Triton X-100

The non-ionic detergent, Triton X-100 (Sigma), (Le Maire 1983) was diluted to 0.1% (v/v) in TBS and stored at 4°C. Prior to use, 10µl of proteinase inhibitor cocktail described above was added per 1ml of 0.1% (v/v) Triton. Cell lysis was carried out as described above for the Mammalian cell lysis kit.

2.6 Protein Quantification

Protein quantification for the cell lysate solutions was done using the Bicinchonic acid (BCA) method (Smith 1985) with the Micro BCA assay kit (Pierce, Perbio). The protocol provided with the product was followed. Dilutions of bovine serum albumin (BSA) of known concentrations were used as standards. The micro-plate procedure was used. 150µl of standard and unknown samples were pipetted into a 96-well polystyrene plate in duplicate. BCA working reagent was prepared by mixing reagents MA, MB and MC in a ratio of 25:24:1 ie 25 parts MA + 24 parts MB + 1 part MC. 150µl of working reagent was added to each standard and unknown sample. The samples were incubated at 37°C for 1 hour and then absorbance was read at 562 nm on a Spectramax M5e plate reader (Molecular Devices) running on Softmax Pro version 5.2 software (Molecular Devices). A standard curve was generated and the concentration of the unknown samples was plotted from the curve.

2.7 Immunoprecipitation using Protein A-Agarose

Immunoprecipitation using protein A entails incubating a solution containing a protein of interest with an antibody raised against the protein of interest and precipitating with agarose beads covalently linked to protein A. Protein A binds strongly to rabbit immunoglobulin G (Lubahn) antibodies (Langone 1982; Lindmark 1983). Centrifuging separates the beads which have been bound to the protein of interest via the antibody (Figure 2.1). The protein of interest can then be released by heat, which denatures the proteins and reverses the non-covalent protein-antibody interactions, but not the agarose-protein A covalent bond. The protocol for immunoprecipitation was obtained from the Technical Appendix Section of the Sigma 2007 Antibody Catalogue. Protein A-agarose beads (Sigma) were rehydrated for 1 hour from the lyophilised form with

distilled water. Two millilitres of the rehydrated beads were washed five times in 50ml of TBS then re-suspended in 4ml of TBS to give a 50% (v/v) slurry. The slurry was stored at 4°C. Anti-ADAMTS-15 antibody (Abcam ab28516, See Section 2.10.2) of known concentration was added to the specified amount of cell lysate or medium and incubated for 1 hour at 4°C on a rotating platform to provide gentle mixing. Thirty microlitres of the 50% (v/v) bead slurry was added to the tube and incubated for another hour. Immunoprecipitated complexes were collected by centrifuging at 3000 x g for 2 minutes at 4°C. The supernatant was discarded and the pellet was washed by re-suspending in ice-cold TBS and centrifuging at 3,000 x g for 2 minutes at 4°C. The wash was repeated three times. After the last wash, a syringe with a 26-polystyrene needle was used to completely remove all the wash solution. Thirty microlitres of Laemmli sample buffer (Section 2.9.3) was added to the beads and the samples heated to 95°C. After heating, the samples were centrifuged at 12,000 x g for 30 seconds at ambient temperature. The supernatant was used for SDS polyacrylamide gel electrophoresis (SDS-PAGE).

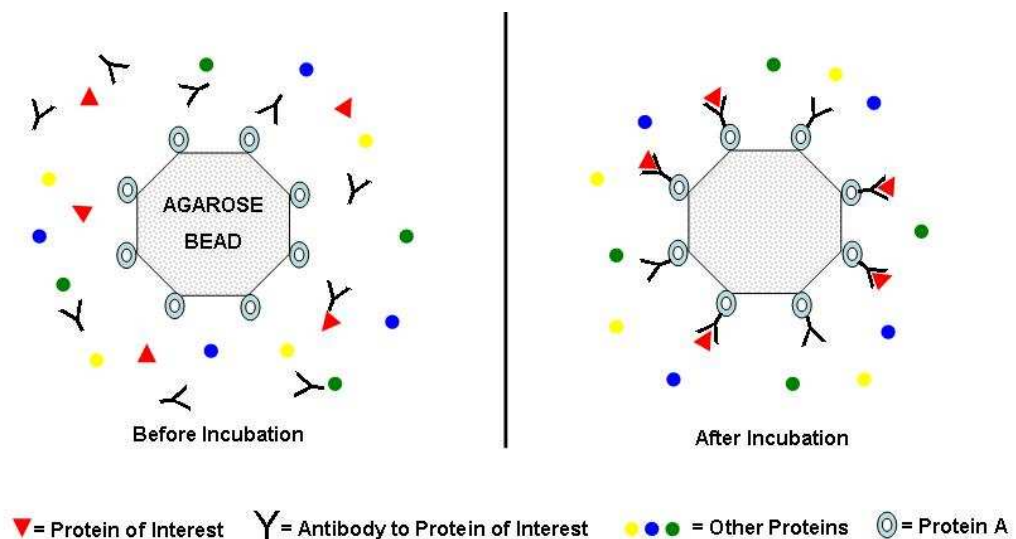


Figure 2.1: Performing immunoprecipitation using protein A-agarose beads. Protein A is covalently bonded to the agarose beads, and protein A has a strong affinity for rabbit

IgG. After incubation, the protein of interest is bound to the agarose beads via the protein A/antibody complex, while other proteins remain in solution. Centrifuging the mixture will result in the protein of interest being pulled down. The protein is released from the complex by heating.

2.8 Precipitation using Heparin-Agarose

Heparin-agarose beads are agarose beads with heparin molecules covalently bonded. Proteins with binding affinity for heparin can be separated from a milieu of proteins by incubating with heparin-agarose beads or by running the protein solution through a heparin-agarose column (Sanz 1993; Ticha 1994; Kraus 2001; Manaskova 2002). ADAMTSs are known to bind to heparan sulphate in the ECM (Kuno 1998; Gao 2004). Heparin-agarose beads (Sigma) were used to pull out ADAMTS-1 and -15 from cell lysates. The protocol for heparin-agarose precipitation was obtained from the Technical Appendix Section of the Sigma 2007 Antibody Catalogue for immunoprecipitation with a few modifications. Heparin-agarose beads (Sigma) were supplied in a suspension of 0.5M sodium chloride (NaCl) containing 0.02% thimerosal as a preservative. Two millilitres of beads were washed five times in 50ml of TBS then re-suspended in 4ml of TBS to give a 50% (v/v) bead slurry. The slurry was stored at 4°C. 30µl of the 50% (v/v) bead slurry was added to either the cell lysate (containing both the cellular and ECM components), or 3-day conditioned medium and incubated for 1 hour at 4°C on rotating platform to provide gentle mixing. Heparin-agarose beads with bound protein were collected by centrifuging at 3000 x g for 2 minutes at 4°C. The supernatant was discarded and the pellet was washed by re-suspending in ice-cold TBS and centrifuging at 3,000 x g for 2 minutes at 4°C. The wash was repeated three times. After the last wash, a syringe with a 26-gauge needle was used to completely remove all the wash

solution. Thirty microlitres of Laemmli sample buffer was added to the beads and the samples were heated to 95°C. After heating, the samples were centrifuged at 12,000 x g for 30s at ambient temperature. The supernatant was used for SDS polyacrylamide gel electrophoresis (SDS-PAGE).

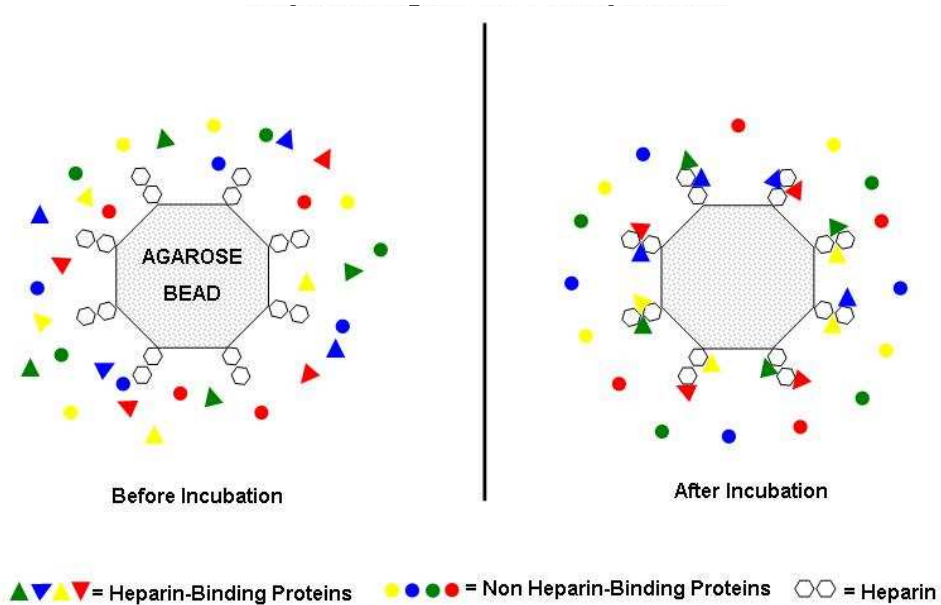


Figure 2.2: Performing precipitation using heparin-agarose beads. Heparin is covalently bound to the agarose beads. Proteins with affinity for heparin will bind to the agarose beads via heparin during incubation, while non heparin-binding proteins remain in solution. After incubation, the heparin-bound proteins are pulled down with the heparin-agarose beads by centrifugation. The precipitated proteins are released from the beads by heating.

2.9 SDS-PAGE

Sodium dodecyl sulphate polyacrylamide gel electrophoresis (SDS-PAGE) was used to separate proteins according to their molecular weight (Raymond 1959; Chrambach 1971). The steps were as follows

2.9.1 Resolving Gel Preparation

SDS-PAGE was undertaken using 10% (v/v) polyacrylamide gels. To make the resolving gels, 2.5mls of 40% (w/v) acrylamide (Bio-Rad), 2.5mls of resolving gel buffer (1.5M Tris HCl, pH 8.8) (Bio-Rad), 4.83mls of distilled water, 0.1mls of 10% (w/v) SDS (Bio-Rad), 0.05mls of 10% (w/v) ammonium persulphate (APS) (Bio-Rad), and 6 μ l of tetramethylethylenediamine (TEMED) (Bio-Rad) were mixed in a 50ml tube. The mixture was quickly loaded into a glass spacer assembly (Bio-Rad). This volume of resolving gel mix was enough to make two gels. Five hundred microlitres of 99.9% butan-2-ol (Sigma) was gently added into the glass spacer above the mixture to flatten the meniscus and prevent oxygen from the air from inhibiting the free radical-mediated polymerisation reaction. The mixture was left to polymerise at ambient temperature. When the resolving gels were polymerised, the glass spacer assembly was tilted sideways to pour out the butan-2-ol. The meniscus was washed twice with distilled water and carefully blotted dry with filter paper.

2.9.2 Stacking Gel Preparation

To make the stacking gel, 0.36mls of 40% (w/v) acrylamide, 1.2mls of stacking gel buffer (0.5M Tris HCl, pH 6.8) (Bio-Rad), 3.14mls of distilled water, 48 μ l of 10% (w/v) SDS, 0.048mls of 10% (w/v) APS and 0.0048mls of TEMED were mixed in a 15ml tube. The mixture was quickly loaded into the glass spacer assembly above the solid resolving gel. This volume of stacking gel mix was enough to make two gels. A ten-well gel comb was inserted into the stacking gel mix in the glass plate assembly and then the gel was left to polymerise.

2.9.3 Sample Preparation

Protein concentration in the samples was determined as described in Section 2.6. Optimal loading volume for the wells in the stacking gel was 10-15 μ l. Therefore, after

the desired protein quantity to be loaded was decided, protein samples were diluted in 1% (v/v) SDS to make up a volume of 10 μ l if necessary. Sample preparation was done according to the method described by Laemmli (Laemmli 1970) with minor modifications. Five microlitres of sample buffer (0.125M tris base, 10% (w/v) SDS, 20% (v/v) glycerol, 0.01% (w/v) bromophenol blue, 2.5% (w/v) dithiothreitol) was added to the sample if reducing conditions were required. If non-reducing conditions were required, sample buffer without the reducing agent, dithiothreitol (DTT) (Cleland 1964) was used. The samples were heated at 95°C for 5 minutes in 500 μ l tubes. A hole was made at the top of each tube with a needle to prevent pressure build-up within the tube. If the sample volume was more than 20 μ l, the cap of the tube was left open to allow evaporation down to the required volume. After heating, the samples were cooled to ambient temperature.

2.9.4 Electrophoresis

The glass spacer plate was assembled into a tank (Bio-Rad). Fifty microlitres of electrophoresis buffer (25mM Tris base, 0.192M glycine, 0.1% (w/v) SDS, pH 8.3) was used to test for any leakage from the inner chamber. The inner chamber was then filled with electrophoresis buffer. The comb was carefully removed and protein samples were loaded into the wells of the stacking gel using a long-tipped sample loading pipette tip (Alpha Laboratories) in the desired lane order. All-Blue or Dual-Colour protein standard ladders (Bio-Rad) were loaded in one of the wells to make it possible to estimate protein size from the bands produced from electrophoresis. The outer chamber was half-filled with electrophoresis buffer; the tank was covered and then connected to a Bio-Rad Power-Pac 300 current source. Electrophoresis was done at 200V until the bromophenol blue reached the bottom of the gel. Overheating of the gel was prevented by placing the electrophoresis tank on ice.

2.10 Western-Blotting

Western blotting was undertaken as described by Towbin et al (Towbin 1979) with minor modifications. The aim of the western blot technique is to transfer proteins that were separated on the electrophoresis gel onto a solid membrane in order to allow immuno-probing.

2.10.1 Protein Transfer

After electrophoresis was completed, a blotting sandwich was assembled in a blotting cassette. Polyvinylidene difluoride (PVDF) membrane (Immobilon, Millipore) was soaked in methanol for 5 minutes and then in transfer buffer (60mM tris base, 40mM CAPS, 15% (v/v) methanol, pH 11). Scourer pads, cellulose blotting paper (Sigma) and the gel were also soaked in transfer buffer for 10 minutes. The blotting sandwich was assembled in the cassette, clear side down in the following order: scourer pad, cellulose blotting paper (Sigma), PVDF membrane, gel, blotting paper, and scourer pad. The cassettes were placed in a vertical tank with the clear side facing the anode. The tank was filled with ice-cold sample buffer and the tank was placed on ice. The proteins were transferred from the gel to the PVDF membrane by electro-blotting at a constant current of 400mA for 30 minutes (Matsudaira 1987).

2.10.2 Immuno-probing

After electro-blot transfer of the proteins to the PVDF membrane, the membrane was blocked for 1 hour in blocking buffer (1% (w/v) casein, 0.05% (v/v) Tween-20, 20mM Tris, 0.5M NaCl, pH 7.4) (Bio-Rad). Primary immuno-detection of ADAMTS-1 was done with either rabbit polyclonal C-terminal antibody (Abcam, ab39194) or mouse monoclonal proteolytic domain antibody (R&D Systems, MAB2197). Dilutions used were 1:1000 (1µg/ml) for the polyclonal antibody, or 1:500 (1µg/ml) for the monoclonal antibody. Recombinant human ADAMTS-1 (R&D Systems, 2197-AD) was

used as a positive control for the MAB2197 antibody in western blot experiments. This recombinant protein consisted of amino acids Arg²⁵⁸ – Phe⁸⁴⁹ which contains the proteolytic and disintegrin domains, the first thrombospondin motif, the cysteine-rich domain and spacer region, with a predicted mass of 66kDa on western blotting.

Primary immunodetection of ADAMTS-15 was done with either rabbit polyclonal cysteine-rich domain antibody (Abcam, ab28516) or rabbit polyclonal propeptide antibody (Abcam, ab45047). The antibodies were used in a dilution of 1:1000 (1µg/ml) and 1:5,000 (200ng/ml) respectively according to the supplier's recommendation for western blotting. The cysteine-rich ADAMTS-15 antibody was raised against a peptide sequence 'HSTNRLTLAVAW', corresponding to His⁵⁹² – Trp⁶⁰³ in the cysteine-rich domain. This peptide was custom-synthesised (Bachem), with an approximate mass of 1.3kDa. The peptide was used in a 1000-molar excess to pre-adsorb the antibody as a negative control. The pre-adsorption protocol was obtained from the Millipore Technical Library (www.millipore.com/userguides/tech1/mcproto016). The peptide was supplied in powder form and was dissolved to a stock concentration of 769nM in blocking buffer. The ab28516 antibody was supplied in a concentration of 1mg/ml (6.67nM), and was diluted 1:1000 in blocking buffer as recommended by the supplier's protocol for western blotting, giving a final working molar concentration of 6.67pM. Antibody-peptide solutions were mixed and incubated for 1 hour at 37°C before use in primary incubation of membranes. GAPDH was detected with a rabbit polyclonal anti-GAPDH antibody (Abcam ab9485) in a dilution of 1:1000 (1µg/ml).

Secondary immuno-detection was done with swine anti-rabbit horseradish peroxidase (HRP) conjugated antibody (P0399) (Dako) for the rabbit primary antibodies, or goat anti-mouse HRP-conjugated antibody (P0447) (Dako) for the mouse primary antibodies in a dilution of 1:3000 (113ng/ml). The stock antibodies were diluted in blocking buffer.

The PVDF membrane was incubated in the primary antibody solution for 12 hours at 4°C. After primary incubation, the membrane was washed three times for 5 minutes each in wash buffer (0.05% (v/v) Tween-20 in TBS) and incubated in secondary antibody for 1 hour at ambient temperature.

2.11 Horseradish Peroxidase (HRP) Detection

The PVDF membranes were washed three times for 5 minutes each in wash buffer after the secondary antibody incubation to remove unbound secondary antibody. HRP detection was done with ECL Plus western blotting detection kit (Amersham, GE Healthcare). The chemiluminescent substrate, Lumigen PS-3 Acridan is cleaved by horseradish peroxidase and acridinium esters react with peroxide in the reagent to emit light as a by-product, which can be detected on x-ray film. Detection solutions A (containing ECL Plus substrate solution with Tris buffer) and B (containing stock acridan solution in dioxane and ethanol) were mixed in a ratio of 40:1. Excess wash buffer was drained off the membrane and the membrane was placed protein-side-up on a flat surface. The protein side of the membrane was covered with detection solution and left to incubate for 5 minutes. Excess detection solution was drained off. The membrane was covered in plastic film and placed in an x-ray cassette. Hyperfilm ECL (Amersham, GE Healthcare) x-ray film was exposed on the membranes in the cassette and developed using developer and fixer solutions (AGFA).

2.12 PVDF Membrane Stripping

When re-probing of PVDF membranes was required, the membranes were stripped to remove bound primary and secondary antibodies from the membrane. This was done by incubating the PVDF membranes in TBST brought to pH 2.0 by titrating with HCl. The

membranes to be stripped were incubated for 6 hours at 4°C with agitation. After incubation, the membrane was washed three times with washing buffer to remove the acidic solution. In order to ensure that the primary antibody from the previous experiment had been completely removed, the membranes were then probed with secondary antibody and HRP detection was done as described above.

2.13 Densitometry

Bands detected on x-ray films from western blotting experiments were semi-quantitatively analysed by densitometry when required using a GS 710 Calibrated Imaging Densitometer (Bio-Rad) running on Quantity One version 4.5.1 software (Bio-Rad). A boundary was drawn around each band for analysis. The adjusted area and density (volume) of the band from each treatment sample was compared with the band from the control sample, measured as ODmm², and was defined by the software as the sum of the intensities of the pixels (in OD) within a volume boundary multiplied by the area of a single pixel (in mm²) minus the background volume.

2.14 Fluorescence Immunocytochemistry

Fluorescence immunocytochemistry was undertaken following the protocol in the Abcam Online Technical Manual (www.abcam.com/technical). Fifty thousand cells were plated in each chamber of 4-chamber cell culture chamber slides (BD Biosciences). Cells were left to incubate for 48 hours. The medium was washed off with TBS and the cells were fixed and permeabilised by adding 200µl of ice-cold acetone (Sigma) to the cells in each chamber for 10 minutes at -20°C. The cells were then washed three times with TBS and incubated with 1% (w/v) bovine serum albumin (BSA) for 1 hour to block non-specific antibody binding, followed by three washes in

TBS for 5 minutes each. The rabbit polyclonal ADAMTS-15 propeptide antibody (Abcam, ab45047) was diluted 1:1,000 (1µg/ml) in 1% (w/v) BSA and 500 µl was added to each chamber. The cells were incubated for 12 hours at 4°C with gentle agitation. The antibody solution was decanted and the cells were washed three times in TBS for 5 minutes each. Secondary antibody incubation was done using Alexa Fluor 594 fluorescent tagged goat anti-rabbit IgG antibody (Molecular Probes, Invitrogen). According to the product information sheet, the Alexa Fluor 594 fluorescent dye has an excitation maximum of approximately 590nm (orange) and a fluorescence emission maximum of approximately 617nm (red). The Alexa Fluor 594-tagged secondary antibody was supplied at a concentration of 2mg/ml and diluted 1:1000 in 1% (w/v) BSA. The cell monolayer was incubated in antibody solution for 1 hour at ambient temperature in the dark. The antibody was decanted and the cells were washed in TBS 3 times in the dark for 5 minutes each. The nuclei of the cells were counter-stained with 1µg/ml DAPI (4', 6-diamidino-2-phenylindole) (Sigma) in TBS. DAPI binds to grooves that lie between the DNA strands in the DNA double-helix (Kapuscinski 1995). DAPI has an excitation maximum of approximately 358nm (ultraviolet) and a fluorescence emission maximum of 461nm (blue) when bound to double-stranded DNA (Manzini 1983; Kapuscinski 1995), making it possible to identify cell nuclei. The chambers were separated from the slides using the instrument provided by the manufacturer. A drop of mounting fluid was used to cover the cells and a glass cover slip placed on top. Images were acquired with a Leica DMI 4000B microscope using LAS AF version 1.6.3 software.

2.15 Regulation of ADAMTS and TIMP-3 mRNA Expression by DHT in LNCaP Cells

The androgen-sensitive LNCaP prostate cancer cell line was used to test the effects of DHT on ADAMTS expression. LNCaP cells were plated into 24-well culture plates at a density of 1×10^4 cells/well for RNA extraction, and in 6-well culture plates at 5×10^4 for protein extraction. Cells were grown for 48 hours in DMEM supplemented with 10% FCS, 100units/ml penicillin, 100 μ g/ml streptomycin and 0.25 μ g/ml amphotericin B, at 37°C in a humidified atmosphere of 5% CO₂. Medium was changed to serum-free DCCM (Biological Industries), supplemented with 2mM L-glutamine, and the cells were allowed to acclimatise to the new medium for 48 hours. This change of medium was done 48 hours before DHT treatments to minimise the effects of a change of medium on the experimental outcome. The medium was then removed and cells were treated in fresh DCCM medium for 24 hours with DHT (Sigma), or with flutamide (Sigma), a non-steroidal AR antagonist (Peets 1974). The treatment doses used were 0.1, 1.0 and 10nM DHT, 1 μ M flutamide, or 10nM DHT + 1 μ M flutamide. DHT and flutamide were dissolved in 0.1% ethanol. The control arm was treated with 0.001% ethanol, as this was the final concentration of ethanol in the treatment arms. For mRNA expression analyses, medium was removed after 24 hours and Tri Reagent (Sigma) was applied to the wells to lyse the cells. The resulting cell lysate was stored at -80°C awaiting RNA extraction. RNA was extracted and cDNA synthesized as previously described in Sections 2.2 and 2.3. For protein expression analyses, cells were treated with DHT and flutamide for 72 hours in 6-well cell culture plates after which medium was removed and the cells gently washed with phosphate buffered saline (PBS). 0.01% (v/v) Triton X-100 in Tris-buffered saline (TBS) was mixed at 4°C in a volume ratio of 100:1 with Proteinase Inhibitor Cocktail (Sigma) as described in Section 2.5.2. Two

hundred microlitres of the mixture was applied to each well for 1 hour at 4°C to lyse the cells. The lysate was centrifuged at 12,000 x g for 10 minutes at 4°C. The supernatant was removed and saved while the pellet containing cell debris was discarded. The supernatant was stored at -40°C awaiting protein quantification and western blotting.

2.16 Identification of Putative AREs

The genomic sequences for *ADAMTS1*, *ADAMTS15*, *TIMP3*, *hKLK3* (Human Kallikrein 3, PSA) and *FOLH1* (Folate Hydrolase 1, PSMA) were obtained from the Ensembl genome database, Release 49 (www.ensembl.org) (Birney 2004). The 5' flanking sequence containing the gene regulatory region, the transcription start point (TSP) and the gene sequence with intron and exon information were identified. Using an *in silico* approach with the online nuclear receptor binding site search tool NUBIScan version 2.0 (www.nubiscan.unibas.ch) (Podvinec 2002), a matrix was created consisting of the following nine ARE half-sites AGAACA, TGTACC, TGTACA, TGTTCT, GGTACA, AGTGCT, TGGTCA, AGTTCT and AGTACG. Each half site has previously been shown to be a functional AR binding site (Monge 2006) (Table 2.3).

Description	ARE Sequence	Specificity for Androgen Receptor
ARE Consensus	5'- <i>GGTACA</i> ggg <i>TGTTCT</i> -3'	Specific
PSA ARE I	5'- <i>AGAACA</i> gca <i>AGTGCT</i> -3'	Specific
Slp HRE	5'- <i>TGGTCA</i> gcc <i>AGTTCT</i> -3'	Specific
C3 (1) ARE	5'- <i>AGTACG</i> tga <i>TGTTCT</i> -3'	Non-specific
GRE Consensus	5'- <i>TGTACA</i> gga <i>TGTTCT</i> -3'	Non-specific
NR3C Consensus ARE	5'- <i>AGAACA</i> nnn <i>TGTACC</i> -3'	Non-specific

Table 2.3: Six HREs that have been experimentally verified and shown to be functional AR binding sites). The 6 bp half-sites from these HRE sequences (***bold italics***) were used to generate the matrix used for the *in silico* searches.

A search strategy was designed to perform a search for putative AREs composed of direct repeats (DRs), inverted repeats (Patel), and everted repeats (ERs) of these half-sites interposed by a non-specific 3 bp sequence, forming a complete 15 bp ARE. A threshold score of 0.8 was set to minimize false-positive predictions. This threshold setting ensured that only putative AREs with quality corresponding to 80-100% similarity with the half-sites in the matrix were detected. The frequency and position of response elements identified in the *ADAMTS1* and *ADAMTS15* promoters and gene sequences which met the search criteria were recorded. For comparison, the promoter region and sequence of the *hKLK3* and *FOLH1* genes were also analyzed using the same strategy. *hKLK3* gene expression is known to be up-regulated by androgen, and the promoter region contains the functional ARE (AGAACA_gcaAGTGCT) at -170 bp from the TSP (Riegman 1991). The expression of the *FOLH1* gene is down-regulated by androgen (Israeli 1994).

2.17 Regulation of ADAMTS-1, -15 and TIMP-3 mRNA Expression by TNF in PC3, LNCaP and Prostate Stromal Cells

PC3, LNCaP and BPH45 cells were plated in 12-well plates at a density of 5×10^4 cells/well for PC3 and LNCaP, and 1×10^5 cells/well for the stromal cells. Cells were grown to 60% confluence. Medium was changed as above. Cells were treated for 24 hours with TNF (Biosource) at concentrations of 10pg/ml (0.571pM), 100pg/ml (5.71pM) or 10ng/ml (571pM). TNF was dissolved in 0.1% (w/v) bovine serum albumin (BSA) in phosphate buffered saline (PBS). The control arm was treated with 0.0001% (w/v) BSA, as this was the final concentration of BSA in the treatment arms. After 24hour of treatment, medium was removed and Tri Reagent (Sigma) was applied

to the wells as described in Section 2.2. The resulting cell lysate was stored at -80°C awaiting RNA extraction. RNA was extracted and cDNA synthesized as previously described (Section 2.3).

2.18 Transfection Protocols

Silencing of gene expression by RNA interference is widely used in the study of gene function and several methods for delivery of siRNA have been described (Sandy 2005). Electroporation, calcium phosphate and lipid-based methods were used in this study.

2.18.1 Electroporation

Electroporation was done using the Nucleofector II (Amaxa, Lonza) and electroporation Kit-V for PC3 cells and Kit-R for LNCaP cells. Cells to be electroporated were trypsinised as described in Section 2.1. Five millilitres of complete medium was used to inactivate the trypsin and the cells were counted using an Improved Neubauer haemocytometer (Hawksley). 1×10^6 PC3 cells or 2×10^6 LNCaP cells were placed in 1.5ml tubes corresponding to the number of transfections to be done. The cells were centrifuged at $800 \times g$ for 1 minute and the supernatant removed. The cells were re-suspended in nucleofector solution for 5 minutes. $0.5 - 5\mu\text{g}$ of DNA or $0.5 - 3\mu\text{g}$ of siRNA was added to each tube and mixed with the cell suspension. The contents of each tube were transferred into separate Amaxa cuvettes, avoiding creation of bubbles while pipetting. Cuvettes were placed in the nucleofector machine and electroporated using program T-13 for PC3 cells and program T-09 for LNCaP cells. The cells were quickly transferred into 6-well plates containing complete medium with no antibiotics, pre-warmed to 37°C . The plastic pipettes provided in the kit were used for transferring the cells in order to minimise damage to the cells. The cells were subsequently incubated in

a humidified incubator at 37°C in a 5% CO₂ atmosphere. Knock-down of target siRNA was analysed by real-time RT-PCR at specified time points after transfection.

2.18.2 Calcium Phosphate

Calcium phosphate transfection was done using a Profection kit (Promega) by the reverse transfection method described in Ambion TechNotes 11(6) 2004. Cells were trypsinised (Section 2.1). Five millilitres of complete medium was added to inactivate the trypsin. The cells were centrifuged 800 x g for 1 minute and the trypsin-containing supernatant was removed. The cells were re-suspended in complete medium without antibiotics and counted using an Improved Neubauer haemocytometer (Hawksley). Wells of a 96-well polystyrene plate were used to prepare the reagents and siRNA for the transfections. For each transfection, 0.4µg of siRNA was added to 1.2µl of 2M calcium chloride (CaCl₂) in 10µl of nuclease free water. Ten microlitres of 2x 4(-2-hydroxyethyl)-1-piperazineethanesulfonic acid (HEPES) buffered saline (HBS) containing 50mM HEPES (pH 7.1), 280mM NaCl, and 1.5mM Na₂HPO₄ was pipetted into a separate well. The siRNA-CaCl₂ mix was added drop-wise into the HBS and the mixture was incubated at ambient temperature for 30 minutes. A 48-well plate was prepared for the final transfection by adding 80µl of complete medium with no antibiotics to each well to be used. The siRNA-CaCl₂-HBS mix was added to the medium in the respective wells. Thirty thousand cells were added to each of the wells containing the siRNA mix and the final volume of each well was made up to 200µl with complete medium containing no antibiotics. The cells were left in the transfection reagent for 16 hours during which time they attached to the bottom of the plate. Medium containing the transfection reagents was removed and replaced with fresh complete medium containing no antibiotics. Knock-down of target siRNA was analysed by real-time RT-PCR at specified time points after transfection.

2.18.3 Lipid-based Methods

2.18.3.1 Metafectene Pro

Metafectene Pro transfection was done by the reverse transfection method described in Ambion TechNotes 11(6) 2004. Cells were trypsinised (Section 2.1) and 5ml of complete medium was added to the tube to inactivate the trypsin. The cells were centrifuged briefly and the trypsin-containing medium was removed. The cells were re-suspended in complete medium without antibiotics and counted using an Improved Neubauer haemocytometer (Hawksley). Wells of a 96-well polystyrene plate were used to prepare the reagents and siRNA for the transfections. In one well, 0.5µg of siRNA was added to 50µl of serum-free medium and in a separate well, 3µl of Metafectene Pro (Biontex) was added to 50µl of serum-free medium. The contents of the first well were added to the second and the siRNA mix was incubated at ambient temperature for 20 minutes. The mix was then placed into the wells of a 48-well plate which was to be used for transfection. Thirty thousand cells were added to each of the wells containing the siRNA mix and final volume of each well was made up to 200µl with complete medium containing no antibiotics. Knock-down of target siRNA was analysed by real-time RT-PCR at specified time points after transfection.

2.18.3.2 Dharmafect 2

Transfection with Dharmafect 2 was also done by the reverse transfection method as described in Ambion TechNotes 11(6) 2004. Cells were trypsinised (Section 2.1) and 5ml of complete medium was added to the tube to inactivate the trypsin. The cells were centrifuged briefly and the trypsin-containing medium was removed. The cells were re-suspended in complete medium without antibiotics and counted using an Improved Neubauer haemocytometer (Hawksley). Wells of a 96-well polystyrene plate were used to prepare the reagents and siRNA for the transfections. In one well, 2.5µg of siRNA

was added to 10 μ l of serum-free medium and in a separate well, 0.4 μ l of Dharmafect 2 (Dharmacon, Thermo Fisher) was added to 19.6 μ l of serum-free medium. The contents of the first well were added to the second and the siRNA mix was incubated at ambient temperature for 20 minutes. The mix was then placed into the wells of a 48-well plate which was to be used for transfection. Thirty thousand cells were added to each of the wells containing the siRNA mix and final volume of each well was made up to 200 μ l with complete medium containing no antibiotics. Knock-down of target siRNA was analysed by real-time RT-PCR at specified time points after transfection.

2.19 Transient Knock-down of ADAMTS-1 and -15

Transient transfection was undertaken using siGENOME SMARTpool siRNA synthesized commercially by Dharmacon. Each SMARTpool siRNA vial contained a pool of four different siRNA sequences directed against the gene of interest. The sequences are listed in Table 2.4. GAPDH was knocked down to serve as a positive control, and a non-targeting siRNA sequence (NTC) bearing no identity to any sequence in the human genome was transfected into cells in a separate set of wells as a negative control. The sequences of the positive and negative control were proprietary. GAPDH and NTC experiments were carried out using siControl GAPD (Cat# D-001140-01-05) and siControl Non-Targeting siRNA (Cat# D-001206-13) respectively. To monitor transfection efficiency, separate cells were transfected with siGLO Red (Cat# D-001630-02-05). Cells were transfected using either electroporation with the Nucleofector II kit (Amaxa, Lonza), calcium phosphate with the Profection kit (Promega), Metafectene Pro (Biontix) or Dharmafect 2 (Dharmacon), as described in Sections 2.18.1. Figure 2.4 shows a schematic representation of the gene knock-down process.

<i>Gene</i>	<i>SMARTpool ID</i>	<i>Sense/ Antisense</i>	<i>Sequence</i>	
<i>ADAMTS1</i>	D-005761-01	Sense	GGAAAUGGAUCUACUUGUAUU	
		Antisense	5'-UACAAGUAGAUCCAUUUCCUU	
	D-005761-03	Sense	GAAGGGA.AAUGGUGUAUCAUU	
		Antisense	5'-UGAUACACCAUUUCCCUUCUU	
	D-005761-04	Sense	GAACCAGGAUUCCCACAUGUU	
		Antisense	5'-CAUGUGGGAAUCCUGGUUCUU	
	D-005761-05	Sense	GCAGUGGUCUAAAGCAUUAUU	
		Antisense	5'-UAAUGCUUUAGACCACUGCUU	
	<i>ADAMTS15</i>	D-005766-01	Sense	GCGCGGACCUGGAACAUAUUU
			Antisense	5'-UAAUGUUC CAGGUCCGCGCUU
D-005766-03		Sense	CUGCGACGCUUCUAUUUU	
		Antisense	5'-AAUAGAAGCAGCGUCGAGUU	
D-005766-04		Sense	CCAAGCGUUUCGUGUCUAUUU	
		Antisense	5'-AUAGACACGAAACGCUUGGUU	
D-005766-05		Sense	GCAAGAAGGUGACUGGACUUU	
		Antisense	5'-AGUCCAGUCACCUUCUUGCUU	

Table 2.4: Sequence data for siGENOME SMARTpool siRNA from Dharmacon showing the sequence ID and the nucleotide sequence for each of the siRNA duplexes. For each gene, four siRNA duplexes were pooled together and supplied in one vial.

2.20 Stable Knock-down of ADAMTS-1

Two shRNA sequences against ADAMTS-1 mRNA were designed using a web design tool on the Ambion website (www.ambion.com), and synthesised by Ambion. They were designated ATS1a and ATS1b (Figure 2.3). The oligonucleotides were annealed and inserted into the p-Silencer CMV vector (Invitrogen) using the manufacturer's

protocol. TOP-10 competent *E.coli* (Promega) were transformed with the vector and incubated in LB broth (Invitrogen) at 37°C for 24hours. Plasmid DNA from the *E.coli* was then extracted with Maxipreps (Qiagen) using the supplier’s protocol. PC3 cells were transfected using either electroporation with the Nucleofector II kit (Amaya, Lonza) or calcium phosphate with the Profection kit (Promega) as described in Sections 2.18.1 and 2.18.2 respectively (Figure 2.4). Successfully transfected cells were selected by growing in complete medium containing 12.5µg/ml puromycin (Invitrogen) for AT51a or complete medium containing 500µg/ml geneticin (neomycin) (Invitrogen) for AT51b. Knock-down levels were analysed by real-time RT-PCR.

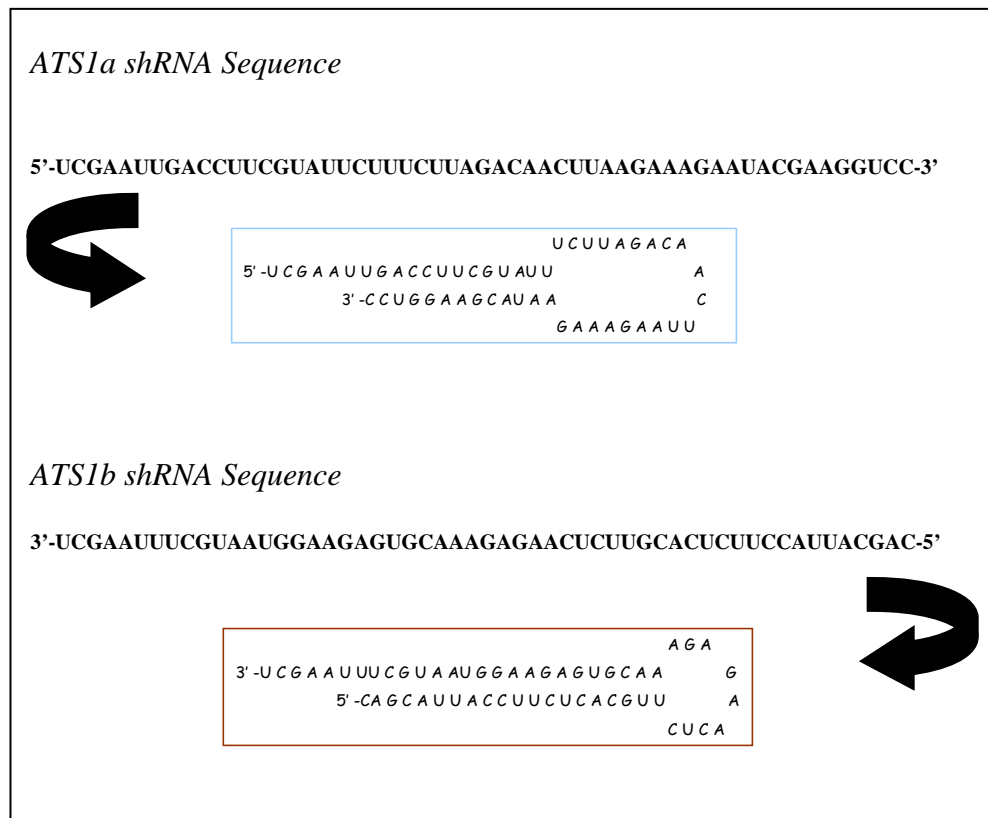


Figure 2.3: shRNA sequences designed for AT51a and AT51b showing expected hairpin structure when folded.

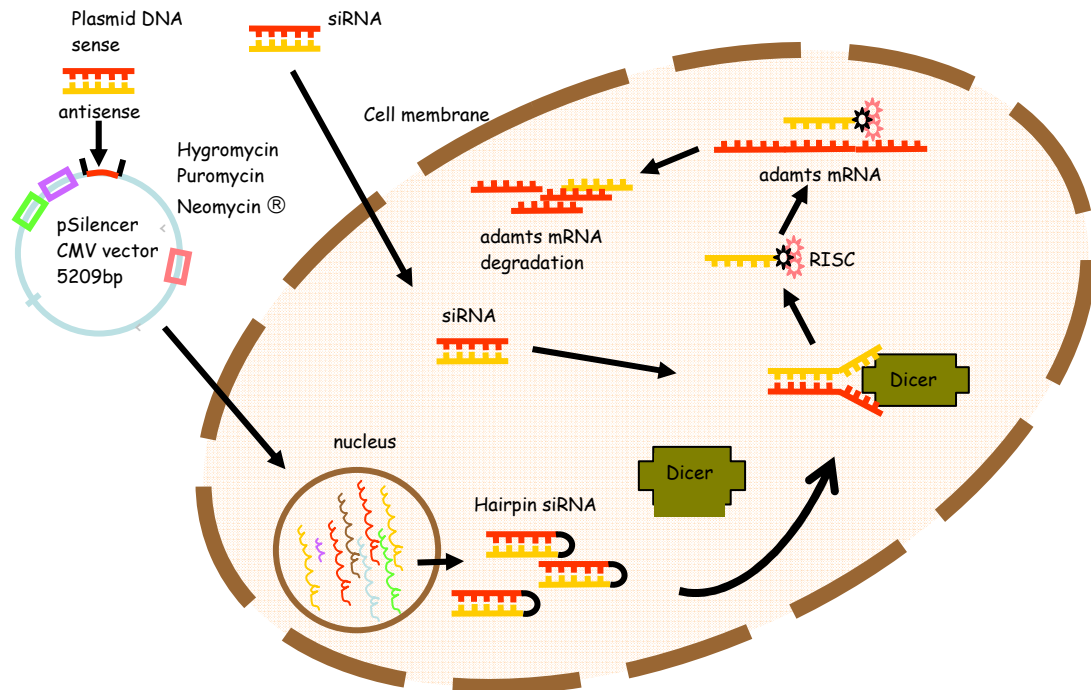


Figure 2.4: Schematic representation of transient and stable knock-down of ADAMTS-1 and ADAMTS-15.

2.21 Proteolysis Assays

Methods to image proteolytic activity were adapted from Sameni et al (Sameni 2003). To create multicellular spheroids, PC3 or stromal cells were grown until confluent then trypsinised. The trypsinised cells were gently transferred using a pipette into a 100mm dish that had its base coated with 1% (w/v) agar. Clumps of cells formed spheroids in 24-48 hours. Quenched fluorescent gelatin, (DQ-Gelatin) (Molecular Probes, Invitrogen) was added to ECM Gel (Sigma) at 4°C in a concentration of 25-40µg/ml. ECM Gel is a solubilised extract from the Engelbreth-Holm-Swarm (EHS) mouse sarcoma which is rich in ECM proteins including laminin, collagen IV, heparan sulphate proteoglycans, enactin and nidogen (Kleinman 1982). DQ-Gelatin consists of molecules of a fluorescent probe and a quencher bound to gelatin. As the gelatin molecule is cleaved, the probe and quencher are separated and fluorescence can be

visualised (Jones, L.J. 1997) (Figure 2.5). Gelatin is a partially denatured form of collagen, and gelatinolytic activity has been used as a measure of proteolytic activity (Fields 1990; Wilson 1993; Ratnikov 2000; Frederiks 2004).

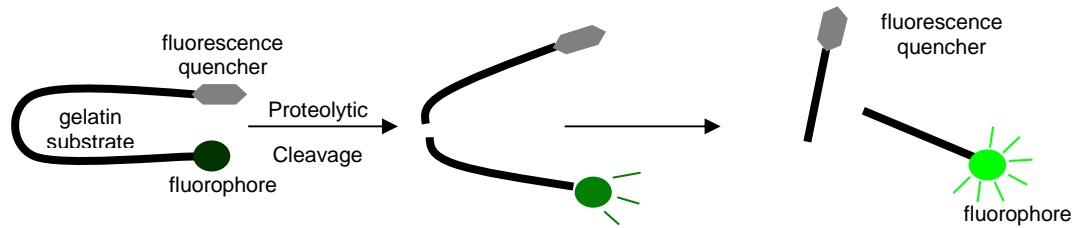


Figure 2.5: Cleavage of quenched fluorescent gelatin by proteolysis. Gelatin molecules in DQ-Gelatin are conjugated to a fluorophore and a fluorescence quencher. Proteolytic cleavage of the gelatin molecule separates the fluorophore from the quencher and fluorescence is emitted.

Spheroids or cells were left to sediment by gravity in a 1.5ml tube, and then pipetted from the bottom of the tube using a Pasteur pipette. ECM gel is in a liquid state between 0-8°C and solidifies at temperatures above 8°C. They were suspended in ECM Gel mix at 4°C and plated onto sterile glass cover slips in 6-well plates. The ECM Gel was left for 10-15 minutes in a tissue culture hood to solidify. Five millilitres of complete or serum-free medium was added to each well. Plates were incubated and photographs were taken at various time points up to 7 days.

2.22 Chemotaxis Assay

Chemotaxis assays were performed using modified Boyden chambers (Boyden 1962; Albini and Benelli 2007). Two hundred thousand PC3 cells were placed in the upper chamber in 200µl of serum-free medium and 500µl of the chemo-attractant to be tested was placed in the lower chamber. The chemo-attractant media were all prepared from

DMEM as follows. Serum-free DMEM, DMEM with 10% (v/v) FCS added (complete medium), or stromal cell-conditioned complete medium conditioned for different durations. The conditioning was done using confluent BPH45 cells in T75 tissue culture flasks. Ten millilitres of complete medium was added and left to condition for 24 hours, 48 hours, 72 hours or 7 days. The medium was then removed and centrifuged at 5,000 x g for 10 minutes to remove cells or debris. The supernatant was placed in a fresh tube and stored at -40°C until ready for use. Chemotaxis assays were performed by incubating the cells at 37°C for 12 hours in the upper compartment of the Boyden chambers with no Matrigel coating on the filters (Figure 2.6). After incubation, the filters were stained with 4% (w/v) crystal violet in ethanol for 1 hour and then counted. The non-migrating cells were first wiped off the top of the filter membrane using moistened cotton buds. The filters were stained for 1 hour and then washed gently with tap water. Four high power fields (hpf) were counted at magnification of x 20 and the mean was calculated.

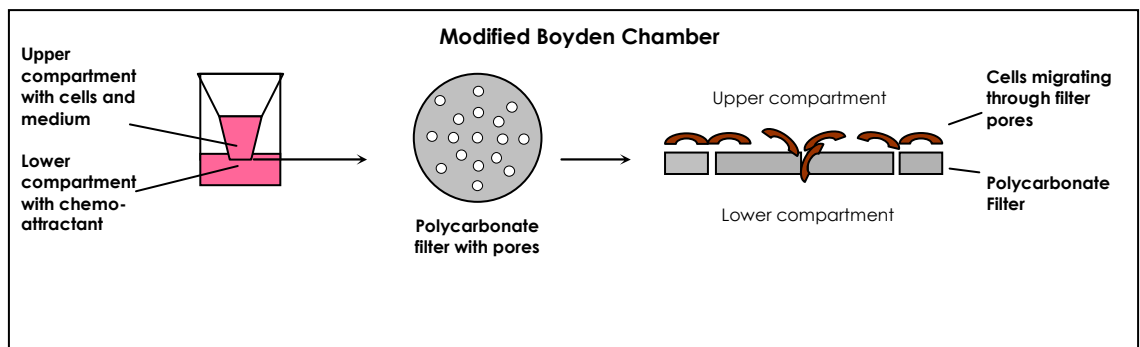


Figure 2.6: Modified Boyden chamber used for chemotaxis assays. PC3 cells were plated in the upper compartment and the test chemo-attractant medium in the lower compartment. There was no Matrigel coating on the filters. Number of cells migrating through the filter to the lower compartment were counted as a measure of the chemo-attractive gradient.

2.23 Proliferation Assays

2.23.1 Haemocytometer Cell Counts

Proliferating cells were counted directly using an Improved Neubauer haemocytometer (Hawksley) to produce a growth curve (Jones, H.E. 1997; Wiepz 2006). Fifty thousand cells/well were placed in 12-well plates in quadruplicate in serum-free medium. At 24, 48, and 60 hours, cells were detached using trypsin-EDTA (Section 2.1), res-suspended in serum-free medium and counted. After each count, the cells were re-plated and incubated until the next time point.

2.23.2 MTT Assay

Cell proliferation was analysed using the *In vitro* Toxicology Assay Kit (Sigma), which is based on the MTT (3-[4,5-dimethylthiazol-2-yl]-2,5-diphenyl tetrazolium bromide) reaction. The assay was done according to the protocol provided by the supplier. Mitochondrial dehydrogenases of viable cells cleave the tetrazolium ring of MTT forming formazan crystals which change the colour of the solution from yellow to purple (Vistica 1991). The intensity of the purple colour is directly proportional to the number of viable cells. Fifty thousand cells were plated in 12-well plates in triplicate. For each experiment, 4 sets of cells were plated, 1 set to be counted on day 0, day 1, day 2 and day 5 of the experiment. The MTT vial provided in the kit was reconstituted with 3mls of DMEM without phenol red. At the designated time point, the cells were removed from the incubator and 100 μ l of the MTT solution was added to 900 μ l of DMEM without phenol red in each well. The cells were returned to the incubator for 2 hours. After the 2 hours incubation, the cells were removed from the incubator and 100 μ l MTT solubilisation solution was added to each well with gentle trituration to dissolve the purple formazan crystals. 200 μ l of formazan solution from each well was transferred into separate wells of a 96-well plate and absorbance was measured using a

Spectramax M5e plate reader (Molecular Devices) running on Softmax Pro version 5.2 software (Molecular Devices). Background absorbance of the plate was measured at 690nm and subtracted from the absorbance of the formazan solution measured at 570nm.

2.24 Migration Assays

For the purpose of this thesis, migration refers to the movement of living cells in contact with a biologic or synthetic scaffold, from one position to another, with no physical barrier between the two positions. Migration assays were performed either with the Boyden chamber or with the scratch assay.

2.24.1 Migration using the Scratch Assay

The scratch assay (O'Toole 1997; Cao 2006; Liang 2007) was used with some modifications. Matrigel (BD Biosciences), similar to ECM gel (Sigma), is a solubilised extract from the Engelbreth-Holm-Swarm (EHS) mouse sarcoma containing laminin, collagen IV, heparan sulphate proteoglycans, enactin and nidogen (Kleinman 1982). Matrigel was diluted in ice-cold serum-free medium to a concentration of 60µg/ml. Twelve-well plates were coated with 500µl of the Matrigel solution and allowed to dry overnight in a tissue culture hood. The excess Matrigel was gently washed off using PBS. One hundred thousand cells were plated in each well to be used and left for 24 – 48 hours to attach. A 200µl plastic pipette tip was used to scratch the bottom of the plate, creating a gap in the cell monolayer. The medium was removed and disrupted cells were gently washed off with PBS. One millilitre of fresh serum-free medium was added to each well. Cytosine arabinoside (Ara-C) (Sigma) was added at a concentration of 500ng/ml to inhibit a cell proliferation during the migration process (Dawson 1986). The plate was placed for 24 hours in a humidified time-lapse microscopy chamber at

37°C in 5% CO₂ for image capture. Images were captured with a Leica DMI 6000B time-lapse microscope running on LAS AF software version 1.7.0 (Leica Microsystems). Distance migrated was calculated by subtracting the width of the start gap from the width of the end gap (Figure 2.7).

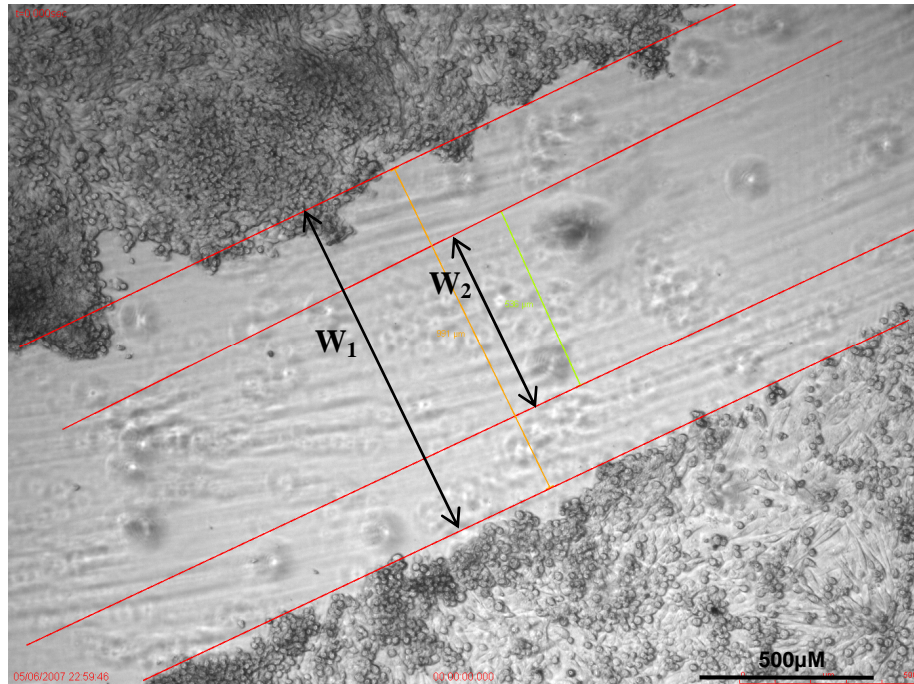


Figure 2.7: Cell migration using the scratch assay. PC3 cells were allowed to grow to confluence and then a scratch created using a sterile plastic 200µl pipette tip. Cytosine arabinoside was added to inhibit cell proliferation during the assay. The width of the gap at the end of the assay was subtracted from the width at the start ($W_1 - W_2$) to give distance migrated.

2.24.2 Migration using the Boyden Chamber Assay

The modified Boyden chamber was adapted for use in migration assays (Boyden 1962; Albini 1987; Taniguchi 1989; Szpaderska 2001; Albini 2007). Transwell permeable polycarbonate 13mm filter wells with 8µm pore size (Corning, Fisher Scientific) were used with no Matrigel coating applied to the filters. Two hundred thousand cells were plated in the upper chamber of the transwell inserts in serum-free medium. Forty-eight

hour conditioned medium from prostatic stromal cells was placed in the lower chamber as a chemo-attractant (Figure 2.6). Previous experiments had confirmed the chemotactic effect of prostatic stromal cell-conditioned medium on PC3 cells (Section 3.5). The chambers were placed in a humidified incubator at 37°C in 5% CO₂ for 6 hours. This duration was determined to be the optimal time for counting migrating PC3 cells using this method in preliminary experiments. The number of cells migrating to the lower surface of the filter was counted by staining the filters with either haematoxylin and eosin (H&E), or with 4% (w/v) crystal violet in 95% ethanol (Sigma). For H&E or crystal violet staining, the non-migrating cells were first wiped off the top of the filter membrane using moistened cotton buds. The filters were stained for 1 hour and then washed gently with tap water. Four high power fields (hpf) were counted at magnification of x 20 and the mean was calculated.

2.25 Invasion Assays

For the purpose of this thesis, invasion refers to the movement of living cells in contact with a biological or synthetic scaffold, from one point to another, with a biological barrier separating the two points. Thus, the cells must penetrate the intervening biological barrier to get from one point to the other. Invasion assays were adapted for modified Boyden chambers (Boyden 1962; Albini 1987; Taniguchi 1989; Szpaderska 2001; Albini 2007). Matrigel (BD Biosciences) supplied at a concentration of 6.5mg/ml was diluted with chilled serum-free medium. The medium had to be chilled as Matrigel solidifies at temperatures above 8°C. Transwell permeable polycarbonate 13mm filter wells with 8µm pore size (Corning, Fisher Scientific) were coated with 5µg or 20µg or no Matrigel. Some filters were also coated on the under-surface with Matrigel containing 50µg/ml of DQ-Gelatin. This is method was developed to enable detection of

invading cells in real-time and was used to determine the optimal time to terminate the assay. Filters were left to dehydrate by air drying in a tissue culture hood overnight. They were then rehydrated in serum-free medium for 1 hour prior to experiments. Two hundred thousand cells were plated in the upper chamber of the transwell inserts in serum-free medium. Forty-eight hour conditioned medium from prostatic stromal cells was placed in the lower chamber as a chemo-attractant (Figure 2.8). Previous experiments had confirmed the chemotactic effect of prostatic stromal cell-conditioned medium on PC3 cells (Section 3.5). The number of invading cells was counted either by staining the filters with either haematoxylin and eosin (H&E), or with 4% (w/v) crystal violet in 95% ethanol. In the wells with the under-coating of DQ-Gelatin in Matrigel, invading cells were detected by counting fluorescent spots as the invading cells proteolytically cleaved the DQ-Gelatin on the under-surface of the filter (Figure 2.8). For H&E or crystal violet staining, the non-invading cells were first wiped off the top of the filter membrane using moistened cotton buds. The filters were stained for 1 hour and then washed gently with tap water. Four high power fields (hpf) were counted at magnification of x 20 and the mean was calculated.

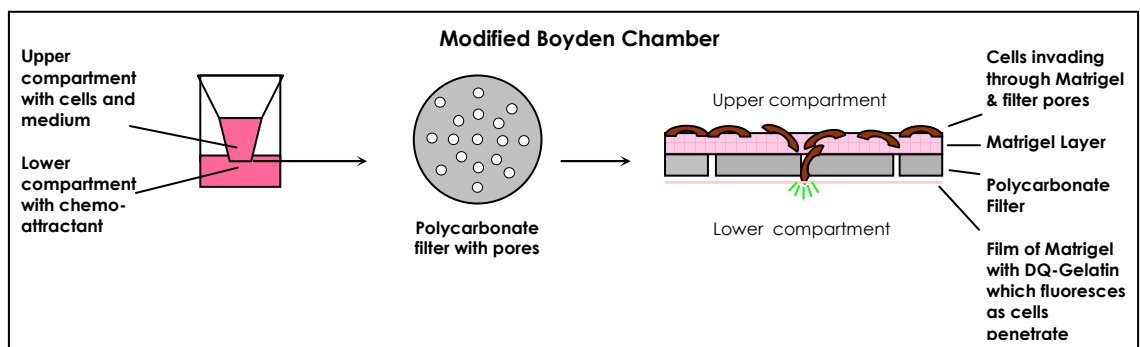


Figure 2.8: Modified Boyden chamber used for invasion assays. Some filters were coated on the under-surface with Matrigel containing DQ-Gelatin. This enabled

counting of invading cells by the fluorescence emitted as they made contact with the DQ-Gelatin on the under-surface.

2.26 Statistical Analysis

Data from preliminary ADAMTS mRNA expression studies using realtime RT-PCR had shown wide variations in expression levels. The D'Agostino-Pearson test for normality did not support a Gaussian distribution of the data. Therefore for mRNA expression experiments, non-parametric statistical tests were used. The Kruskal-Wallis test was used to test for statistically significant differences between the medians of each treatment group. Differences in expression levels were tested for significance with the Dunn's multiple comparison test, which analyzes differences in rank sum between each treatment group and control. The Grubb's test was used to identify and remove outlying samples where appropriate.

Data from chemotaxis, proliferation, migration and invasion assays appeared to be normally distributed. The D'Agostino-Pearson test for normality supported a Gaussian distribution of the data and therefore parametric statistical tests were used. For the chemotaxis assays, analysis of variance (ANOVA) and Dunnett's post test was used to determine if there was variance between the means of the test chemo-attractant groups and if the means differed significantly from the control mean. For the proliferation, migration and invasion experiments, the unpaired t-test was used to analyse for statistically significant differences between the control and knock-down cell groups. All statistical tests were performed on Graphpad Prism 5.0 (GraphPad Software Inc). Statistically significant differences were defined by p values ≤ 0.05 .

CHAPTER 3

IMAGING OF PROTEOLYSIS

CHAPTER 3:

IMAGING PROTEOLYTIC ACTIVITY OF PROSTATE CANCER AND STROMAL CELLS

3.1 Introduction

ECM degradation and remodelling is a hallmark of cancer progression (Rowe 2009). The exact mechanisms of ECM invasion and metastasis are not fully elucidated but ECM proteolysis has been demonstrated around invading cancer cells (Wolf 2009). Stromal cells are reported to be active participants in ECM proteolysis and degradation (Sameni 2003; Sloane 2005; Sloane 2006; Sameni 2009). Gelatinolysis has been used to evaluate proteolytic activity (Fields 1990; Wilson 1993; Ratnikov 2000; Frederiks 2004). ADAMTS-1 is reported to have gelatinolytic activity (Lind, T. 2006), but gelatinolytic activity of ADAMTS-15 has not been determined. The purpose of the experiments described in this chapter was to investigate the gelatinolytic activity of prostate cancer and stromal cells in a 3D culture model. Gelatinolytic activity of the cells would suggest proteolytic ECM degradation by extracellular proteinases possibly including ADAMTS-1.

3.2 Gelatinolytic Activity of Multicellular Tumour Spheroids

Multicellular tumour spheroids were made from PC3 cells (Figure 3.1), LNCaP cells (Figure 3.2) and BPH45 prostate stromal cells (Figure 3.3) and grown in 3D culture in ECM gel containing DQ-Gelatin as described in Section 2.21. Images were captured under a fluorescence microscope at 12, 24, 48 and 60 hours after culture. There was no fluorescence visible at the 12 and 24 hour time points (Figures not shown). Fluorescence became visible after 48 hours in culture and increased in intensity up to the 60 hour time point with no appreciable increase in intensity after 60 hours. The

tumour spheroids produced cellular projections indicating that the cells were invading the ECM gel (Figures 3.1 and 3.3). The LNCaP spheroids did not produce any cellular projections at the 60 hour time point, suggesting that LNCaP cells were slower than PC3 and BPH45 cells to invade the ECM gel. Fluorescence appeared to be most intense over the body of the tumour spheroids, while there was comparatively less intense fluorescence around the invading cells (Figures 3.1B and 3.3B). Fluorescence from BPH45 tumour spheroids was brighter than fluorescence from the PC3 spheroids (Compare Figure 3.1B with Figure 3.3B). Representative images from three separate experiments were shown.

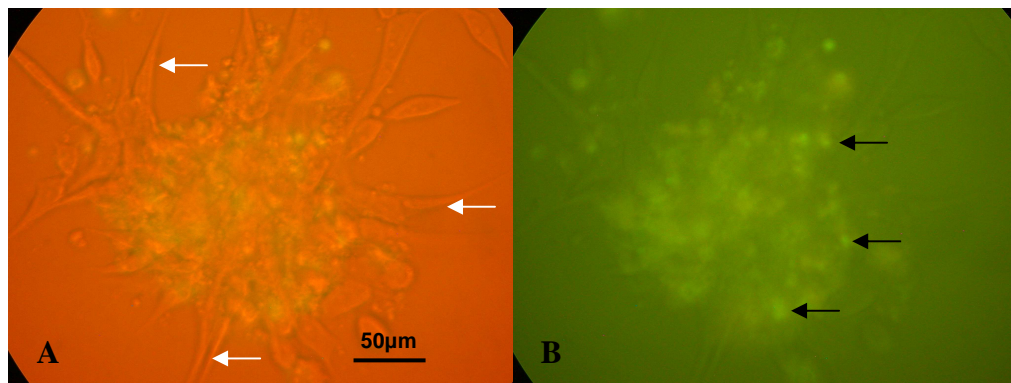


Figure 3.1: PC3 multicellular tumour spheroid grown in 3D culture in ECM gel containing 25mg/ml DQ-Gelatin. Images were captured under a fluorescence microscope after 60 hours in culture. A, in white+blue light and B blue light only. Green fluorescence indicated areas of gelatinolytic activity (black arrows). Cellular projections were seen as the cells in the tumour spheroid began to invade the ECM gel (white arrows). There was no obvious fluorescence at the leading edge of the cellular projections.

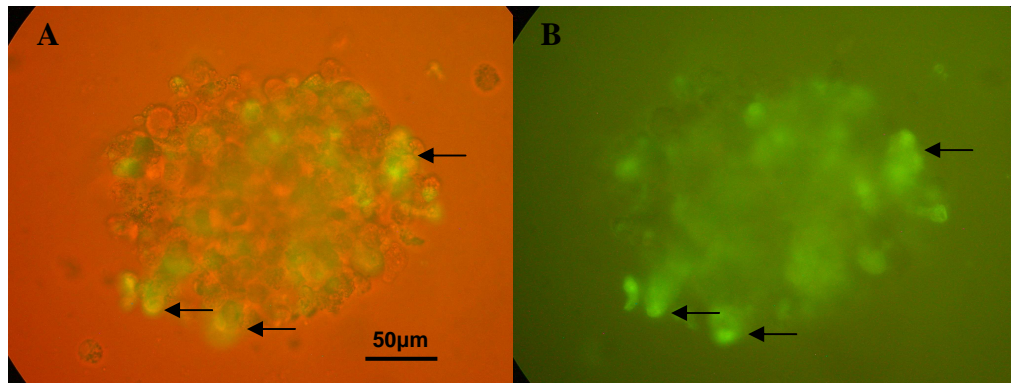


Figure 3.2: LNCaP multicellular tumour spheroid grown in 3D culture in ECM gel containing 25mg/ml DQ-Gelatin. Images were captured under a fluorescence microscope after 60 hours in culture. A, in white+blue light and B, blue light only. Green fluorescence indicated areas of gelatinolytic activity (black arrows). No cellular projections were seen at this time point suggesting that LNCaP tumour spheroids are slower at invading the ECM gel than PC3 tumour spheroids (Figure 3.1).

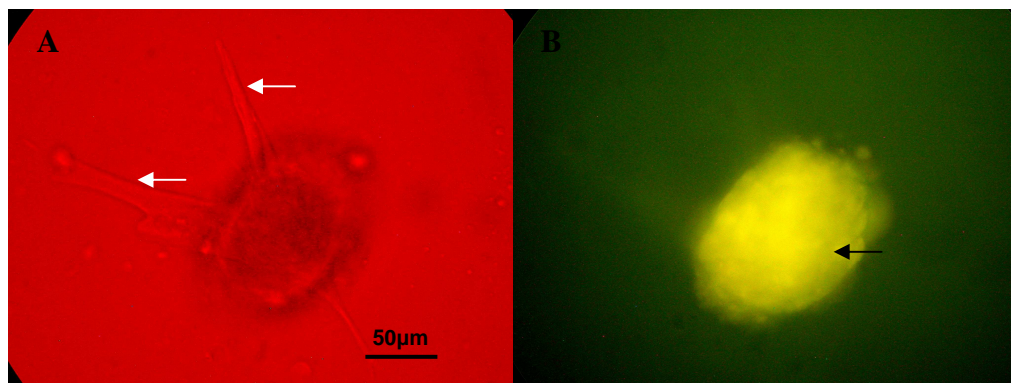


Figure 3.3: BPH45 (stromal cell) multicellular tumour spheroid grown in 3D culture in ECM gel containing 25mg/ml DQ-Gelatin. Images were captured under a fluorescence microscope after 60 hours in culture. A, in white light and B, blue light. Green fluorescence indicated areas of gelatinolytic activity (black arrow). Cellular projections were seen as the cells in the tumour spheroid began to invade the ECM gel (white arrows). There was no obvious fluorescence seen at the leading edge of the cellular

projections, but there was intense fluorescence over the body of the tumour spheroid, which was brighter than fluorescence seen around the PC3 and LNCaP spheroids (Figures 3.1 and 3.2).

3.3 Gelatinolytic Activity of PC3 Cells in Monolayer Culture

PC3 cells were suspended in ECM gel containing DQ-Gelatin and grown in monolayer 3D culture in a tissue culture dish (Section 2.21). The cells settled to the bottom of the dish before the ECM gel was fully set. The cells were observed for fluorescence at 24 hour intervals after culture. Fluorescence became visible after 7 days in culture, in contrast with the multicellular tumour spheroids which were fluorescent after 2 days. Fluorescence was greater around elongated cells compared to rounded cells (Figures 3.4 and 3.5), suggesting that migrating cells in monolayer culture are more proteolytically active than non-migrating cells. Representative images from three different experiments were shown.

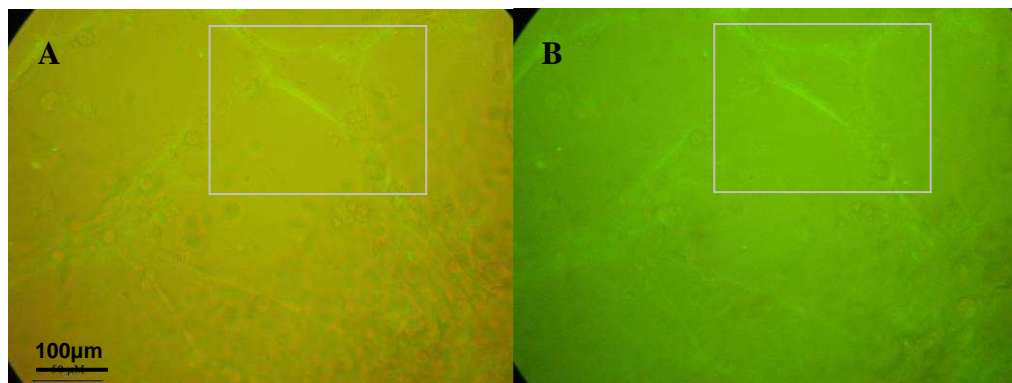


Figure 3.4: PC3 cells in monolayer 3D culture in ECM gel containing 25mg/ml DQ-Gelatin. Images were captured under a fluorescence microscope after 7 days of culture. A, in white+blue light and B, blue light. Green fluorescence indicated areas where gelatinolytic activity was present. The boxed area is showed under higher magnification in Figure 3.5.

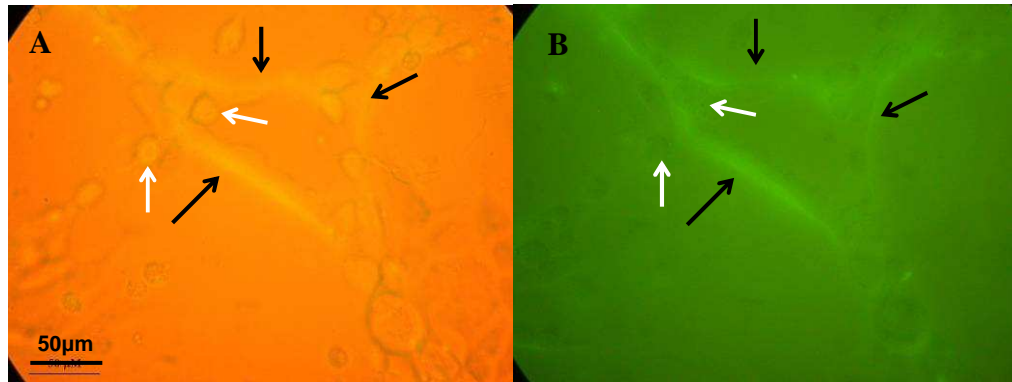


Figure 3.5: PC3 cells in Figure 3.4 (inset boxes) at higher magnification. A, in white+blue light and B, blue light only. Green fluorescence indicated areas of gelatinolytic activity. Elongated cells (black arrows) emitted more fluorescence than round cells (white arrows).

3.4 Co-Culture of PC3 Cells and Prostate Stromal Cells

To determine whether interaction between prostate cancer and stromal cells would affect the pattern of gelatinolytic activity, PC3 multicellular tumour spheroids were co-cultured with BPH45 prostate stromal cells in ECM gel containing DQ-Gelatin. At 7 days, the PC3 tumour spheroids and the stromal cells were well established. The stromal cells were distinguished by their large, elongated shape and characteristic bright-green fluorescence (Figures 3.3, 3.6B and 3.7). PC3 cells migrated out from the PC3 spheroids and formed aggregates around the stromal cells (Figures 3.6 and 3.7). Representative images from three different experiments were shown.

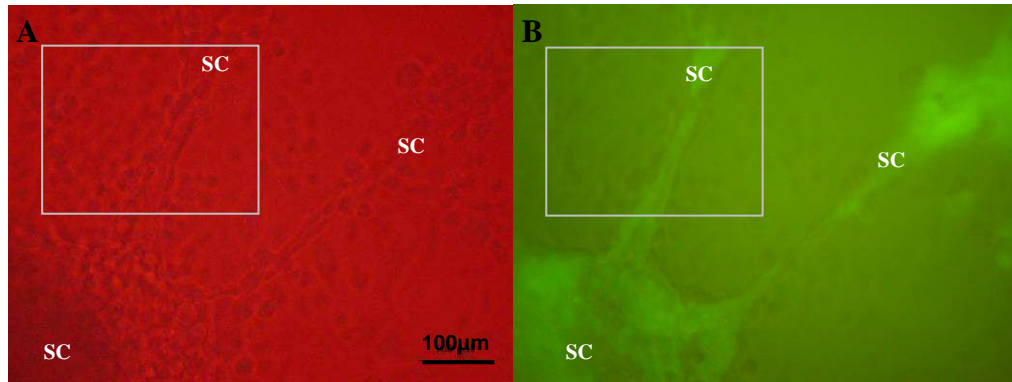


Figure 3.6: PC3 and BPH45 stromal cell co-culture in ECM gel containing 25mg/ml DQ-Gelatin after culture for 7 days. A, in white light and B, in blue light. Areas of green fluorescence indicated proteolytic activity. PC3 cells formed aggregates around the stromal cells (SC).

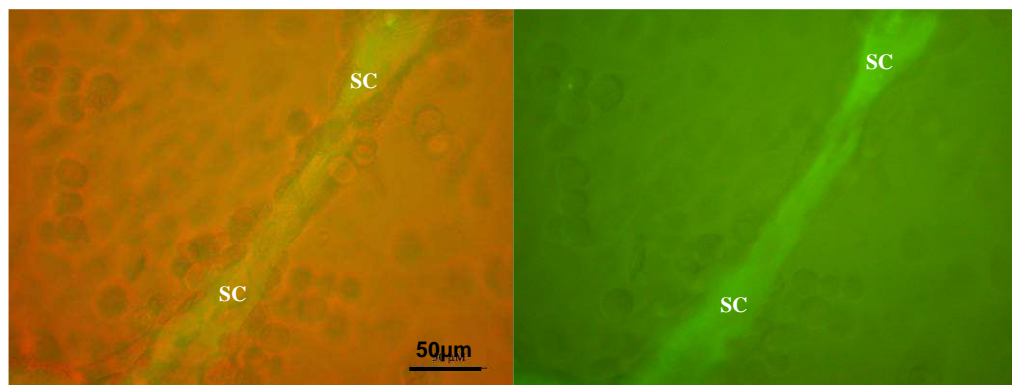


Figure 3.7: PC3 and BPH45 stromal cell co-culture from Figure 3.6 (inset boxes) A, in white+blue light and B, in blue light. PC3 cells (round shaped cells) formed aggregates around the stromal cells (SC). The stromal cells were identifiable by their elongated shape and the characteristic bright green fluorescence (see Figure 3.3A and B).

3.5 Chemotactic effect of Conditioned Medium from Stromal Cells on PC3 Cells

Co-culture of PC3 and stromal cells (Section 3.4) suggested that PC3 cells were attracted to or divided preferentially near to the surrounding stromal cells. To determine whether prostatic stromal cells released factors that produced a chemo-attractive or mitotic gradient which could explain the findings in Section 3.4, PC3 cells were seeded

in the upper compartment of a modified Boyden chamber with conditioned medium from stromal cells in the lower compartment (Section 2.22). DMEM with 10% (v/v) FCS was used as the control chemo-attractant in separate wells. One-way ANOVA was used to test for variance in the means of the groups, and the Bonferroni multiple comparison test was used to compare DMEM + 10% (v/v) FCS with each of the other chemo-attractant media. Similar results were obtained in two separate experiments. There was a significant variance between the means ($p < 0.001$). The chemo-attraction of PC3 cells increased with the duration of conditioning of DMEM in stromal cell culture, with $p < 0.001$ after 48 hours of conditioning (Figure 3.8). The decrease in chemo-attraction between 48 hour and 72 hour conditioning was not statistically significant. Conditioning was extended to 7 days. There was a further increase in the chemo-attractive gradient at 7 days ($p < 0.001$). However at 7 days, there was detachment of cells from the culture flask and the phenol red indicator in the culture medium changed to yellow, indicating a drop in pH of the medium.

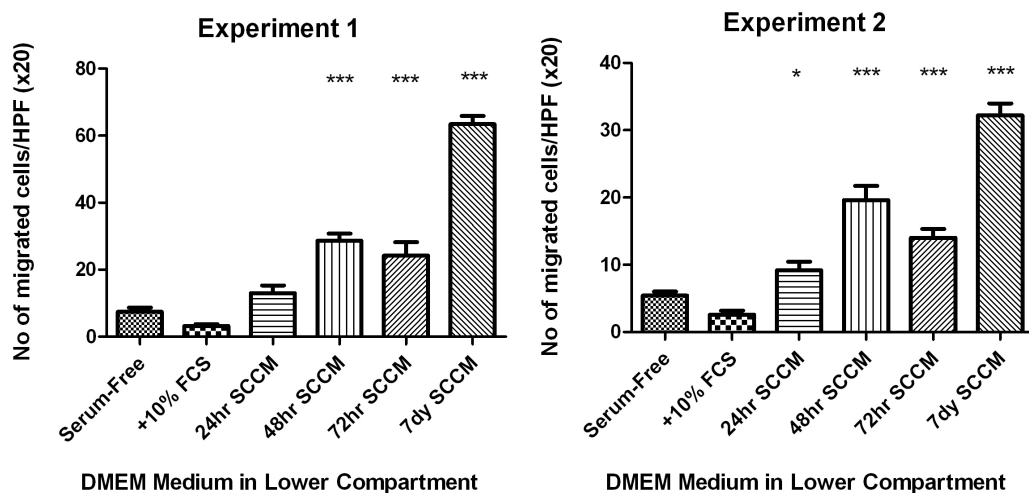


Figure 3.8: Chemotaxis assay showing the chemo-attractive force on PC3 cells by DMEM conditioned with BPH45 stromal cells. PC3 cells were seeded in the upper compartment in serum-free DMEM. DMEM with 10% (v/v) FCS was conditioned for

*the specified durations and used in the lower compartment of a modified Boyden chamber (Figure 2.7). Serum-free DMEM was also used as one of the test chemo-attractants. DMEM + 10% FCS was designated as the control group. Each experiment was done with 4 replicates. Mean (\pm) SEM is shown. SCCM= stromal cell conditioned medium; * = $p < 0.05$, ** = $p < 0.01$, *** = $p < 0.001$.*

3.6 Discussion

This chapter describes demonstrated the proteolytic activity of prostate cancer and stromal cells in 3-D culture and the chemotactic effect of prostatic stromal cells on cancer cells. Prostate cancer and stromal cells proteolytically degraded components of the surrounding ECM, visualised by cleavage of DQ-Gelatin which was added to the ECM gel in which the cells were cultured. Gelatinolysis could be due to the activity of a number of proteinases including MMP-2 (gelatinase A) and MMP-9 (gelatinase B). ADAMTS-1 has also been shown to have gelatinolytic activity (Lind, T. 2006). Proteinase-specific inhibitors were not used, so it is not possible to identify specifically which proteinases were responsible for the gelatinase activity.

In the proteolysis experiments, the stromal tumour spheroids and stromal cells emitted brighter fluorescence than the PC3 and LNCaP cancer spheroids and cells, suggesting that the stromal cells were more proteolytically active. Some reports have suggested that cross-talk between cancer and stromal cells results in stromal cells executing pro-tumour activity, including excessive proteolysis and ECM degradation (Sameni 2003; Sloane 2005; Sloane 2006; Sameni 2009). Experiments in this chapter also imaged the early invasion of the ECM by tumour cells as they migrated out of the multicellular spheroids (Figures 3.1 and 3.3). The invading cellular projections did not emit obvious fluorescence compared to the body of the tumour spheroids. This could be because

invading cells are able to switch between proteolysis dependent and independent states as they migrate (Sahai 2003; Wolf 2003), suggesting that some stages of ECM invasion by cancer cells may not be entirely proteolysis dependent. The multicellular tumour spheroid model could be further developed to give further insights into the interactions between invading tumour cells and the TME during invasion. Imaging of PC3 cells in monolayer 3D culture suggested that elongated cells were more proteolytically active than round cells (Figure 3.5). The experiments were not designed to study cell migration, so it is not possible to conclude that the elongated cells were in the process of migrating, but this may be the case. The images of the proteolysis experiments generally showed limited pericellular detail, which should be taken into account when making inferences on the observations from these experiments.

Co-culture of PC3 and prostatic stromal cells resulted in PC3 cells aggregating around the stromal cells. This could either be due to PC3 cells migrating towards the stromal cells in response to a chemotactic gradient, or the PC3 cells around the stromal cells proliferating at a higher rate than those more distant to the stromal cells. To investigate this phenomenon, chemotaxis assays were performed with PC3 cells using stromal cell-conditioned medium. There was strong evidence of chemo-attraction of PC3 cells by stromal cell-conditioned medium, and the chemo-attractive effect increased with longer duration of conditioning. This infers that there are soluble factors released by prostatic stromal cells that influence the behaviour of cancer cells. Growth factors produced by stromal cells, for example fibroblast growth factor (FGF) (Byrne 1996; Culig 1996) could be responsible for the chemotactic effect. Conditioning up to seven days appeared to have depleted the nutrients in the medium. The increased chemo-attraction seen at the 7-day time point may be due to cell lysis and release of soluble cytoplasmic molecules into the culture medium, It is known that tumour-stromal interaction has an important

influence on tumour progression (Chung 2005; Thalmann 2010), but no experiments in this study were performed to further characterise these interactions.

In conclusion, imaging of proteolytic activity by prostate cancer and stromal cells showed evidence of ECM proteolysis and has demonstrated that prostatic stromal cells play a contributory role in ECM remodelling. There is interaction between cancer and stromal cells via the release of soluble factors into the ECM and also possibly via direct cell to cell contact.

CHAPTER 4

EXPRESSION OF ADAMTS-1, -15 & TIMP-3 IN PROSTATE CELLS

CHAPTER 4:

EXPRESSION OF ADAMTS-1, -15 & TIMP-3 IN PROSTATE CELLS

4.1 Introduction

Work by Cross et al analysed the relative expression of ADAMTS-1, -15 and TIMP-3 in PC3, LNCaP and DU145 prostate cancer cell lines and BPH45 prostate stromal cells (Cross 2005). ADAMTS-1 and -15 were the most abundantly expressed. TIMP-3 expression was relatively higher in BPH45 and LNCaP cells. To confirm these findings and to perform further expression analyses, ADAMTS-1, -15 and TIMP-3 mRNA relative expression was determined by realtime RT-PCR in PC3, LNCaP and C4-2b4 prostate cancer cell lines, and PCAF prostatic fibroblasts (Section 2.1). Expression in U373 astrocytoma and MDA-G8 breast cancer cell lines was also analysed as positive controls. The U373 cell line has been reported to express ADAMTS-1 (Dr Martin Reid, pers commun), and the MDA-G8 cell line has been reported to express ADAMTS-15 (Dr Julia Woodward, pers commun). SDS-PAGE and western blotting were undertaken as described in Sections 2.5 to 2.11 to investigate ADAMTS-1 and -15 protein expression in prostate cancer and stromal cells.

4.2 ADAMTS-1, -15 and TIMP-3 mRNA Expression

The PC3 cell line was arbitrarily chosen as the calibrator sample for mRNA relative expression analyses. ADAMTS-1 expression was detected in all the cell lines (Figure 4.1). Expression was highest in C4-2b4 and PCAF cells and lowest in the U373 and MDA-G8 cell lines.

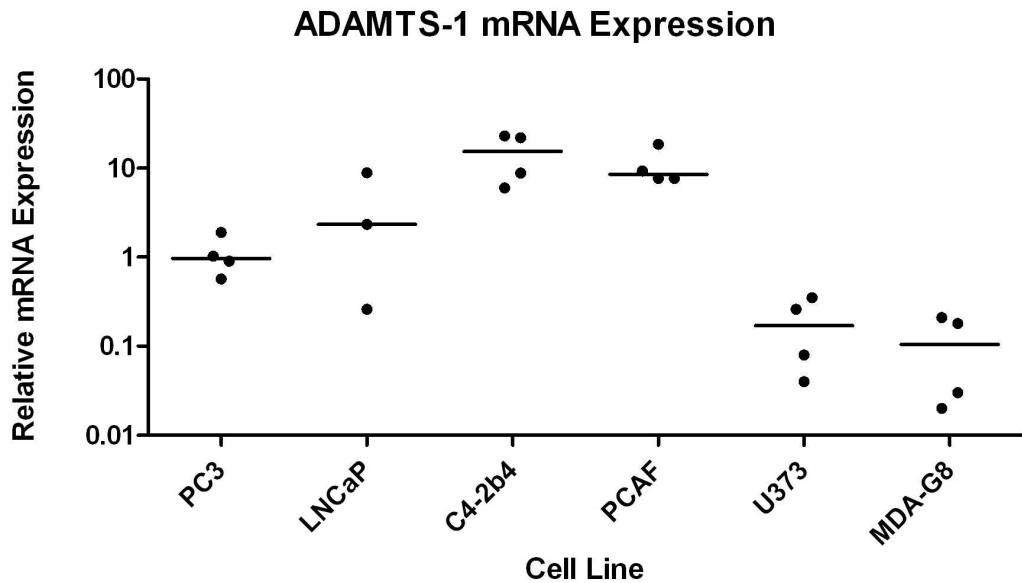


Figure 4.1: ADAMTS-1 mRNA expression levels in LNCaP, C4-2b4, PCAF, U373 and MDA-G8 cell lines relative to PC3 plotted on a log scale. U373 and MDA-G8 are astrocytoma and breast carcinoma cell lines respectively and were used as positive controls. Each data point represents an individual sample of cDNA (n=4). The horizontal bars indicate the value of the median expression level for each cell line.

ADAMTS-15 mRNA expression was also detected in all the cell lines used (Figure 4.2). Expression was highest in the U373 cell line, and lowest in the C4-2b4 cell line. The relative expression levels between the prostate cell lines was in keeping with findings of Cross et al (Cross 2005), who detected highest expression of ADAMTS-15 mRNA in PC3 cells, and lower levels in LNCaP and stromal cells.

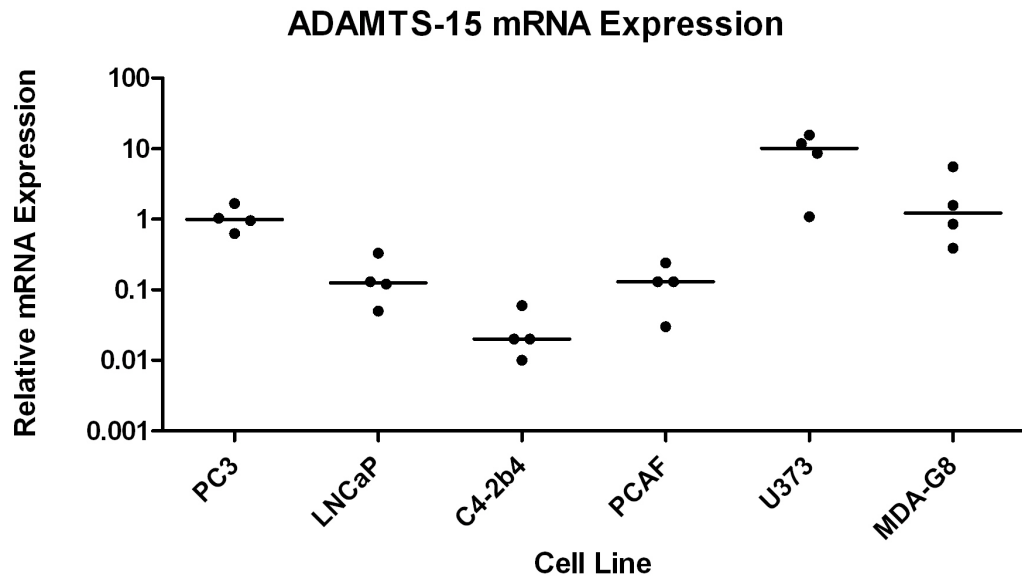


Figure 4.2: ADAMTS-15 mRNA expression levels in LNCaP, C4-2b4, PCAF, U373 and MDA-G8 cell lines relative to PC3 plotted on a log scale. Each data point represents an individual sample of cDNA ($n=4$). The horizontal bars indicate the value of the median expression level for each cell line.

TIMP-3 is the main inhibitor of the ADAMTS proteinases in tissue (Hashimoto 2001; Rodriguez-Manzaneque 2002). Expression levels of TIMP-3 were also analysed (Figure 4.3) to enable comparisons between proteinase and inhibitor expression levels. TIMP-3 expression levels were highest in the PCAF and U373 cell lines, and lowest in the C4-2b4 and MDA-G8 cell lines. The PC3, LNCaP and C4-2b4 prostate cancer cell lines all expressed low levels of TIMP-3 mRNA compared to PCAF cells. This is in keeping with previous reports (Cross 2005) in which prostate stromal cells had higher expression of TIMP-3 than prostate cancer cells.

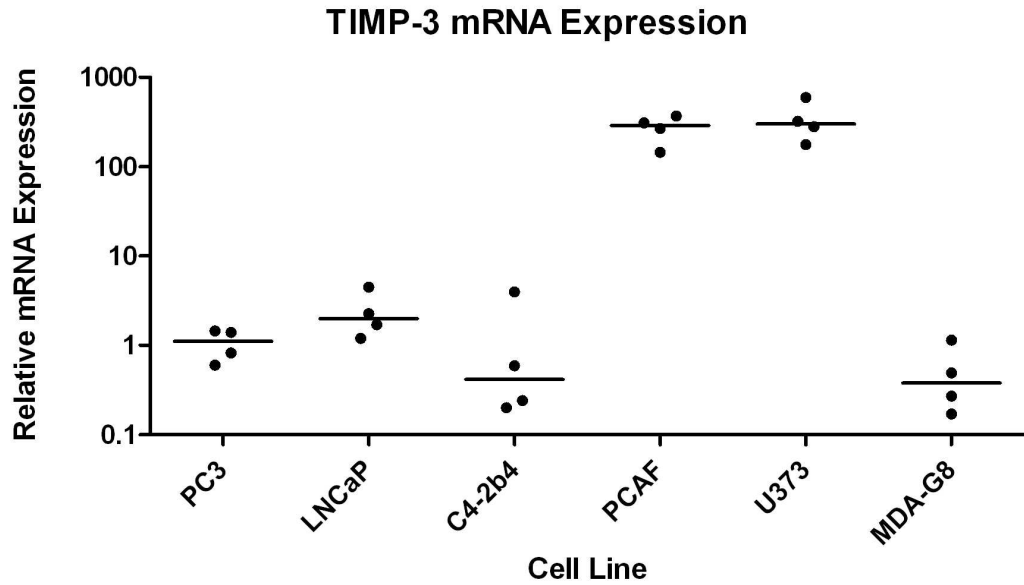


Figure 4.3: TIMP-3 mRNA expression levels in LNCaP, C4-2b4, PCAF, U373 and MDA-G8 cell lines relative to the PC3 cell line plotted on a log scale. Each data point represents an individual sample of cDNA (n=4). The horizontal bars indicate the value of the median expression level for each cell line.

In summary, the results show that relative to PC3 cells. The LNCaP cell line expressed moderate levels of ADAMTS-1, low levels of ADAMTS-15 and high levels of TIMP-3. The C4-2b4 cell line expressed high levels of ADAMTS-1, low levels of ADAMTS-15, and moderate levels of TIMP-3. The PCAF cell line expressed high levels of ADAMTS-1, low levels of ADAMTS-15 and high levels of TIMP-3. This summary is based on an arbitrary definition of low expression being ≤ 0.3 -fold, moderate expression being 0.4-2.9-fold and high expression being ≥ 3 -fold the expression relative to PC3 cells.

4.3 ADAMTS-1 and -15 Protein Expression

At the time of this study, no commercially available antibodies against ADAMTS-1 and -15 had been validated in the published literature. Of the antibodies that were commercially available, two antibodies each were used to probe for ADAMTS-1 and -15. The anti-ADAMTS-1 rabbit polyclonal antibody was directed against the C-terminus while the mouse monoclonal antibody was directed against the proteolytic domain. For ADAMTS-15, one antibody was directed against a peptide sequence 'HSTNRLTLAVAW' located in the cysteine rich region. The other antibody was directed against the pro-peptide domain. Cell lysate solutions and conditioned culture medium were prepared from the cell lines (Section 2.5, 2.7 and 2.8) and used for western blot experiments.

4.3.1 Probing for ADAMTS-1 in Cell Lysate Preparations

Probing for ADAMTS-1 with the C-terminal antibody detected multiple bands ranging from 15-150kDa in size (Figure 4.4). The greatest number of bands was detected in the C4-2b4 cell line which also had relatively high mRNA expression levels. There was a single dark band of approximately 23kDa detected in the U373 lane. MDA-G8, PC3 and LNCaP cell lines had bands ranging from 15kDa to 75kDa. C4-2b4 and PCAF lysates had bands ranging from 15kDa to 150kDa, but the bands were faint in the lane loaded with PCAF. Dilution of the antibody solution to 1:10, 1:100 and 1:1000 caused the intensity of all the bands to be attenuated uniformly and did not identify any bands with greater affinity for the antibody.

Probing for ADAMTS-1 using an Antibody Raised Against the C-terminal Domains

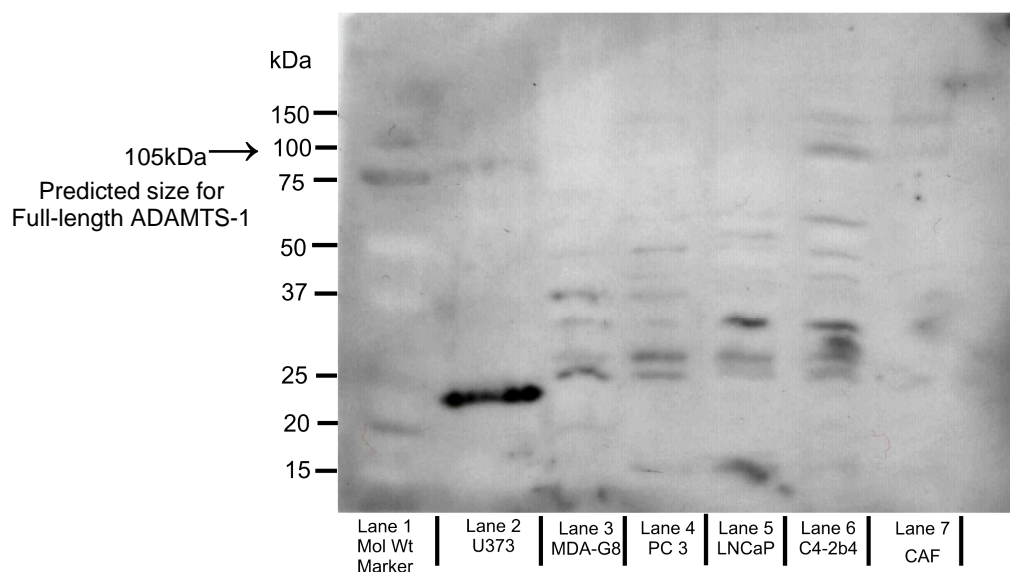


Figure 4.4: Western blotting of cell lysates using a rabbit polyclonal antibody (Abcam, ab39194) raised against the C-terminus of ADAMTS-1. 100µg of cell lysate protein was loaded in each lane. Multiple bands were detected ranging in size from 15kDa to 100kDa. The greatest number of bands was detected in the C4-2b4 cell line. The image is representative of two experiments with similar results.

Probing with the catalytic domain antibody detected bands in PC3, LNCaP and C4-2b4 cell lines ranging from 30-100kDa in size (Figure 4.5). The band with the highest intensity was detected in the C4-2b4 cell line at a size of approximately 70kDa, and fainter bands at 100kDa and 50kDa. The PC3 cell lysate had bands of 100kDa, 70kDa and 50kDa, and the LNCaP cell lysate had bands at 70kDa and 50kDa. The U373 and MDA-G8 samples had faint bands at 50kDa and 30kDa. Ten nanograms of human recombinant ADAMTS-1 proteolytic domain (Section 2.10.2) was also loaded and a band of 50kDa was detected, with a fainter band of size 75kDa (Figure 4.5). The product literature for the recombinant ADAMTS-1 protein had predicted a size of 66kDa on western blot.

Probing for ADAMTS-1 using an Antibody Raised Against the Catalytic Domain

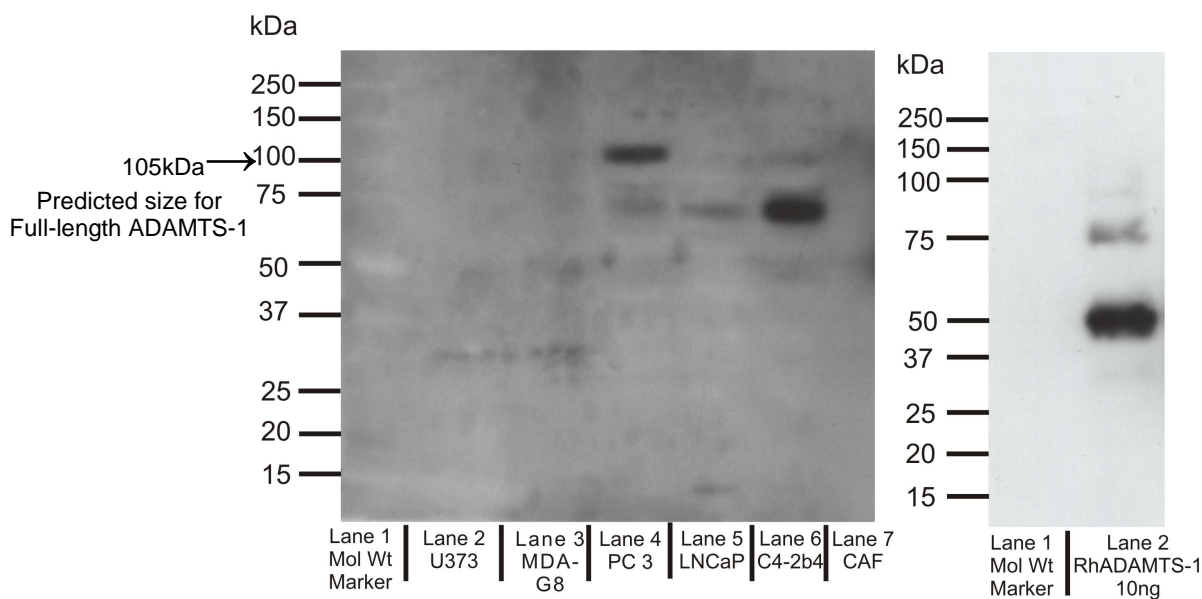


Figure 4.5: Western blotting of cell lysates using a mouse monoclonal antibody (R&D Systems, MAB2197) raised against the catalytic domain of ADAMTS-1. 100 μ g of cell lysate protein was loaded in each lane. Bands were detected ranging from 30kDa to 100kDa in the PC3, LNCaP and C4-2b4 cell lines, with the most intense band in the C4-2b4 cell line. 10ng human recombinant ADAMTS-1 (RhADAMTS-1) was loaded as a positive control. Bands of size 50kDa and 75kDa approximately were detected with higher intensity in the 50kDa band. The image is representative of two experiments with similar results.

Cleavage of full-length ADAMTS-1 yields products of ranging in size from 22kDa to 87kDa (Rodriguez-Manzanaque 2000). The first cleavage removes the propeptide leaving an 87kDa form with an activated catalytic site. The 87kDa form is further cleaved at the spacer region to yield a 65kDa catalytic fragment and a 22kDa C-terminal fragment containing the two C-terminal thrombospondin motifs (Rodriguez-Manzanaque 2000). This did not fully explain the number of bands detected using the

ADAMTS-1 C-terminal antibody (Figure 4.4). The bands detected using the ADAMTS-1 catalytic domain antibody (Figure 4.5) were more in keeping with the sizes of expected ADAMTS-1 cleavage fragments. This suggested that the catalytic domain antibody was the more reliable of the two antibodies and was therefore selected for further experiments.

4.3.2 Test of Validity of the Anti-ADAMTS-1 Antibody Raised Against the Catalytic Domain

Western blotting experiments using the mouse monoclonal anti-ADAMTS-1 catalytic domain antibody (R&D Systems, MAB2197) detected bands in PC3, LNCaP and C4-2b4 cell lysates (Figure 4.5). The bands were of expected sizes for ADAMTS-1 fragments. The intensity of the bands was also greater than those detected with the rabbit polyclonal anti-ADAMTS-1 antibody raised against the C-terminus (Abcam, ab39194). Western blotting experiments were performed to validate the specificity of the catalytic domain antibody. ADAMTS-1 expression in PC3 cells was transiently knocked down by electroporation (Section 2.18.1) using siRNA specific for ADAMTS-1 (Section 2.19). At 48 hours post-transfection, ADAMTS-1 mRNA expression in PC3 prostate cancer cells, analysed by real-time RT-PCR (Sections 2.2, 2.3 and 2.4), was inhibited by 80% (+/- 10%, n=2).

		NTCKd	ATS1Kd	GAPKd
ADAMTS-1 Relative Expression	Experiment 1	1	0.2	1.2
	Experiment 2	1	0.1	0.99
GAPDH Relative Expression	Experiment 1	1	0.73	0.04
	Experiment 2	1	0.85	0.1

Table 4.1: Relative expression of ADAMTS-1 and GAPDH in PC3 cells determined by realtime RT-PCR following knock-down of ADAMTS-1 and GAPDH.

At day 5 post-transfection, cells were lysed and protein samples were prepared as previously described (Section 2.5.2). Protein expression was analyzed by western blotting (Sections 2.9 and 2.10). Fifty kDa bands were detected in all the lanes. Bands from the cells treated with ADAMTS-1 siRNA (Lane 4) was not attenuated (Figure 4.6). To control for errors in sample loading, the membrane was stripped and then re-probed with anti-GAPDH antibody. Thirty-four kDa bands were detected with equal intensity in the NTCKd and ADAMTS-1 knock-down lanes, indicating equal sample loading in these two lanes. The band was attenuated with GAPDH knock-down (Figure 4.6, Lane 6). Similar results were obtained when the experiment was repeated using LNCaP and C4-2b4 cells. ADAMTS-1 knock-down did not lead to attenuation in the intensity of the band in the AT51Kd lane compared to the NKCKd lane as would be expected, therefore the mouse monoclonal anti-ADAMTS-1 catalytic domain antibody (R&D Systems, MAB2197) could not be reliably used to analyse ADAMTS-1 protein expression in these cell lines.

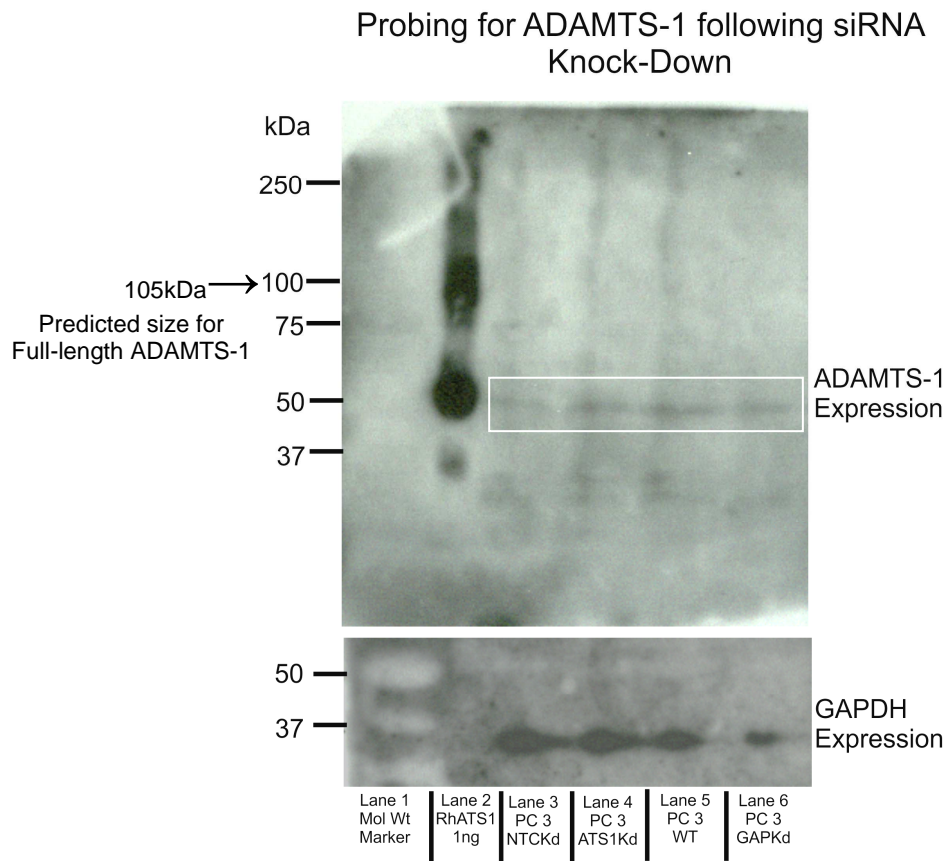


Figure 4.6: Test of specificity of the mouse monoclonal anti-ADAMTS-1 catalytic domain antibody (R&D Systems, MAB2197). ADAMTS-1 expression in PC3 prostate cancer cells was transiently knocked down and western blotting was performed with the cell lysates. 100µg protein was loaded per lane, except Lane 2 which was loaded with 1ng recombinant human ADAMTS-1 (RhATS1). Lane 3 was loaded with cell lysate from non-targeting knock-down cells (NTCKd), Lane 4 was loaded with cell lysate from ADAMTS-1 knock-down cells, Lane 5 with WT PC3 cell lysates and Lane 6 was loaded with cell lysate from GAPDH knock-down cells. The upper panel is an image of the blot after probing with the ADAMTS-1 antibody. A 50kDa band was detected in each lane (white inset box). The band in Lane 4 (ADAMTS-1 knock-down) was not attenuated compared with Lane 3 (control). The lower panel is an image of the same membrane after it had been stripped and re-probed with anti-GAPDH antibody. 34kDa bands were detected in Lanes 3 and 4 of equal intensity, showing that sample loading was equal in

the two lanes. GAPDH knockdown led to attenuation of the band in Lane 6 on the lower panel. These results are representative of two experiments.

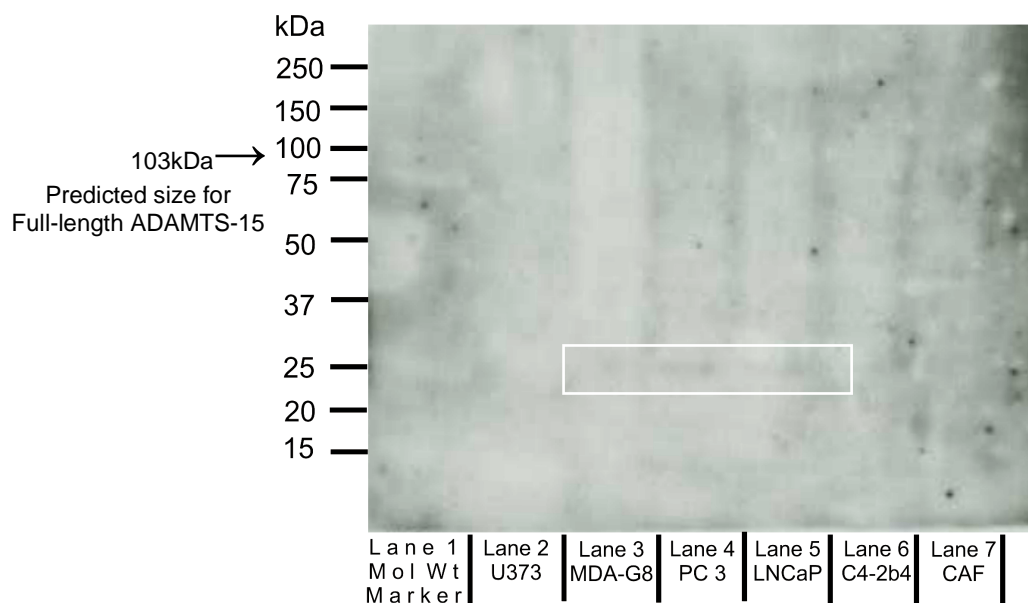
4.3.3 Probing for ADAMTS-15 in Cell lysate and Culture Medium

Cell lysate preparations were probed for ADAMTS-15 using an antibody raised against the cysteine rich domain of ADAMTS-15. This was done by western blotting experiments using cell lysates, and by using samples prepared from immunoprecipitation and heparin-agarose precipitation of cell lysates and culture medium.

4.3.3.1 Probing for ADAMTS-15 in Cell lysates using the ab28516 Antibody

Cell lysate preparations were probed for ADAMTS-15 as described (Section 2.9 and 2.10). An antibody (ab28516) raised against the cysteine rich domain of ADAMTS-15 (amino acids Ser⁵⁷²-Val⁷⁰⁰) was used. The peptide sequence, 'HSTNRLTLAVAW', used as the immunogen was custom-synthesized by Bachem. This peptide was used to pre-adsorb the antibody as described (Section 2.10.2) for use as a negative control in western blot experiments. For all experiments using this antibody, corresponding membranes were probed with non pre-adsorbed antibody solution and with pre-adsorbed antibody solution. Western blotting using this antibody produced very low intensity bands from PC3 and LNCaP cell lysates (Lanes 4 and 5) of approximately 25kDa size (Figure 4.7A). This raised the possibility that ADAMTS-15 was being expressed in very low concentrations in our cell lines. Mature ADAMTS-15 is approximately 100kDa (Cal 2002), and cleavage products of 25kDa have not been reported, but could be a possible explanation for the 25kDa bands.

A Probing for ADAMTS-15 using an Antibody Raised Against the Cysteine-Rich Domain



B Probing for ADAMTS-15 using an Antibody Raised Against the Cysteine-Rich Domain (Pre-Adsorbed)

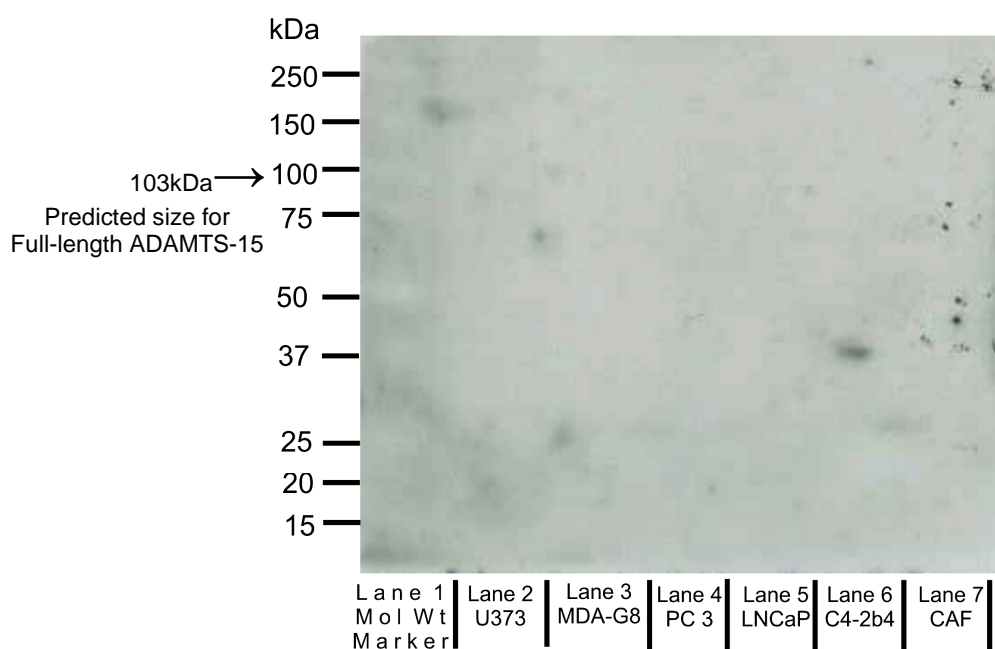


Figure 4.7: Detection of ADAMTS-15 using the rabbit polyclonal cysteine-rich domain antibody (Abcam, ab28516). A, using the non pre-adsorbed antibody, and B, using the pre-adsorbed antibody for primary immuno-probing. 100µg protein each from U373, MDA-G8, PC3, LNCaP, C4-2b4 and PCAF cell lysate were loaded on respective lanes. Low intensity bands were detected in A in Lanes 3 (MDA-G8), 4 (PC3) and 5 (LNCaP)

at approximately 25kDa (white inset box). The images are representative of two separate experiments.

4.3.3.2 Immunoprecipitation and Probing for ADAMTS-15 in Cell Lysates and Culture Medium using the ab28516 Antibody

Low intensity bands were detected using the ADAMTS-15 cysteine-rich domain antibody (Section 4.3.3). This possibly could have been as a result of ADAMTS-15 being present in relatively small concentrations in the lysates being used for the western-blotting experiments. To increase the detection of ADAMTS-15, immunoprecipitation of ADAMTS-15 was done as described in Section 2.7.

Performing western blotting with immunoprecipitate samples, it is expected that bands at 25kDa and 50kDa will be detected, corresponding to the immunoglobulin light and heavy chains respectively. ADAMTS-15 has a predicted relative mass of 100kDa (Cal 2002). The antibody was raised against a 12 aa sequence in the cysteine-rich domain of ADAMTS-15.

Samples obtained by immunoprecipitation were used for western blotting experiments. One nanogram of anti-ADAMTS-15 antibody was added to 1ml of 1mg/ml of cell lysate protein and immunoprecipitation was undertaken as described in Section 2.7. Intense staining was detected ranging in size from 17kDa to 60kDa in all the lanes. The same appearance was seen on the membrane probed with the pre-adsorbed antibody, which served as a negative control (Figure 4.8). Similar pattern and intensity of staining was observed reducing the x-ray film exposure time from ten to two seconds.

Probing for ADAMTS-15 after Immunoprecipitation using an Antibody Raised Against the Cysteine-Rich Domain

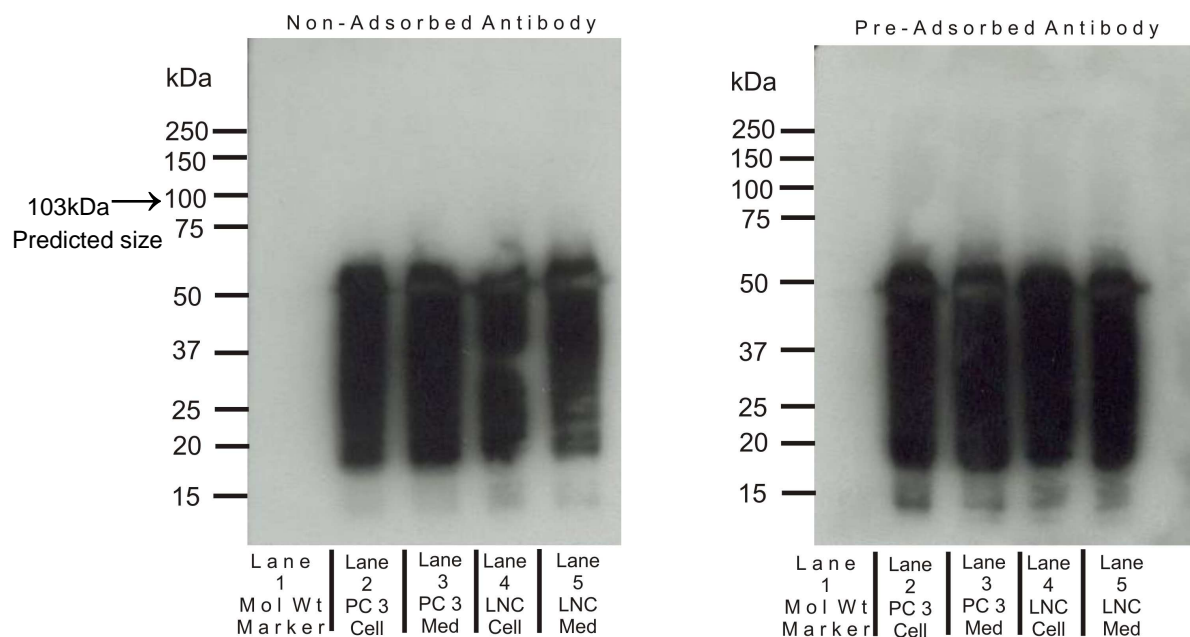


Figure 4.8: Immunoprecipitation and western blotting for ADAMTS-15. Immunoprecipitation was done on 1ml of 1mg/ml cell lysate protein solutions containing both the cellular and ECM components and 10ml of 3-day conditioned medium from PC3 and LNCaP cells. 1ng of antibody and 30 μ l protein A-agarose bead slurry was used for immunoprecipitation. Multiple high-intensity bands of size 20kD-50kDa were detected in all the lanes.

This result was unexpected. The fact that bands were detected on the negative control meant that there was a source of error in the method, or the specificity of the antibody. To find out the source of the error, several control experiments were required. The protein A beads were washed five times in TBS, 1ml beads in 50mls TBS for each wash. This was done to remove any residual unbound protein A from the beads. Western blot experiments were repeated with modifications introduced in a logical manner to detect the source of the unexpected bands.

Firstly, a western blot was done with two membranes (Figure 4.9). The lysates used were identical. Membrane 1 was probed with the anti-ADAMTS-15 antibody as the primary antibody, and the HRP-labelled anti-rabbit antibody as the secondary antibody. Membrane 2 was incubated with TBST primarily, and then secondary incubation with the same HRP-labelled anti-rabbit antibody. The intense bands seen in Figure 4.8 were seen again on both membranes, indicating that the detection did not require the presence of the anti-ADAMTS-15 (primary) antibody and the secondary antibody was binding directly to proteins of size 15-50kDa that were present in relatively large amounts in the samples (Figure 4.9).

Probing of Membranes to Determine Source of Bands Detected following Immunoprecipitation

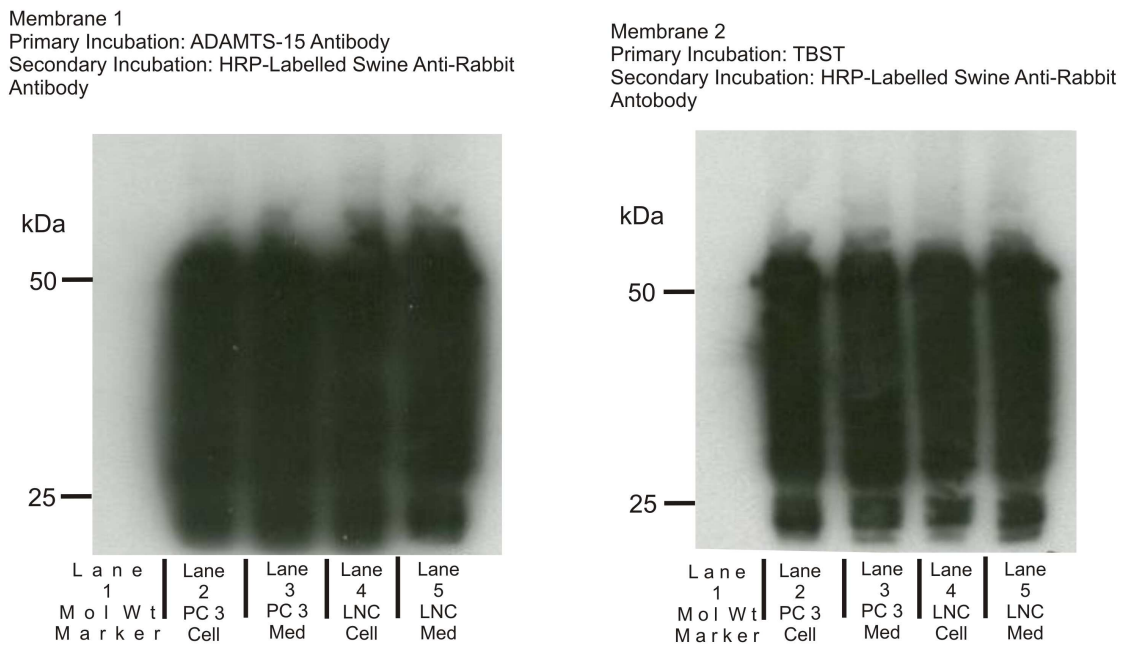


Figure 4.9: PVDF membranes were probed with either anti-ADAMTS-15 primary and HRP-labelled secondary antibodies (Membrane 1), or TBST as primary and HRP-labelled secondary antibody (Membrane 2). The same pattern of multiple bands was seen as in Figure 4.8. The presence of the bands on Membrane 2, which had only TBST for the primary incubation indicated that the HRP-labelled secondary antibody was

binding directly to the proteins in the PVDF membrane and did not require the presence of the primary antibody.

The membranes were stripped as described (Section 2.12) and HRP detection done after incubating for 6 hours in TBST. No bands were detected (Figure not shown), indicating that the detection reagents were not contaminated, and the bands were as a result of detection of a protein present in the loaded samples, possibly the antibody used for immunoprecipitation, or protein A from the beads. The secondary antibody was a swine anti-rabbit IgG antibody, which would have an affinity to bind to protein A.

To determine whether the antibody used for immunoprecipitation was the source of the bands detected in Figure 4.9, serially diluted anti-ADAMTS-15 antibody (1ng, 100pg, 10pg and 1pg) was loaded and used for western blotting. The resulting PVDF membrane was incubated in HRP-labelled anti-rabbit secondary antibody for 1 hour and HRP detection performed. There were no bands detected (Figure not shown), indicating that the immunoprecipitation antibody was not responsible for the intense bands detected on Figures 4.8 and 4.9.

To determine whether the intense bands were coming from the immunoprecipitation beads, a western blot experiment was set up with separate samples as follows; Laemmli sample buffer with 2ng anti-ADAMTS-15 antibody, Laemmli sample buffer with protein A-agarose beads, Laemmli sample buffer with protein A-agarose beads that had been incubated with PC3 cell lysate without any immunoprecipitation antibody, and lastly, Laemmli sample buffer after with protein A-agarose beads that had been incubated with PC3 cell lysate and 1ng of anti-ADAMTS-15 antibody. Each of the samples was heated as described in Section 2.9.3. The samples were loaded and electrophoresis and western blotting performed as previously described (Section 2.9 and

2.10). A duplicate set of samples was used for the negative control (pre-adsorbed antibody). Multiple bands were again seen on both membranes (Figure 4.10, non-pre-adsorbed and pre-adsorbed). The most intense band in each lane was approximately 50kDa. All the lanes with samples that had been in contact with the protein A-agarose beads had the bands, including the sample that had sample buffer heated with beads that had not been in contact with cell lysate or antibody (Figure 4.10 Lane 3 on both blot images). The lanes with 2ng antibody had no bands detected (Figure 4.10, Lane 2 on both blot images). This experiment confirmed that the protein A-agarose beads were the source of the multiple bands seen in the immunoprecipitation western blotting experiments. For this reason, plans further western blotting experiments using protein A immunoprecipitation were abandoned.

Determination of Source of Bands Detected Following Immunoprecipitation

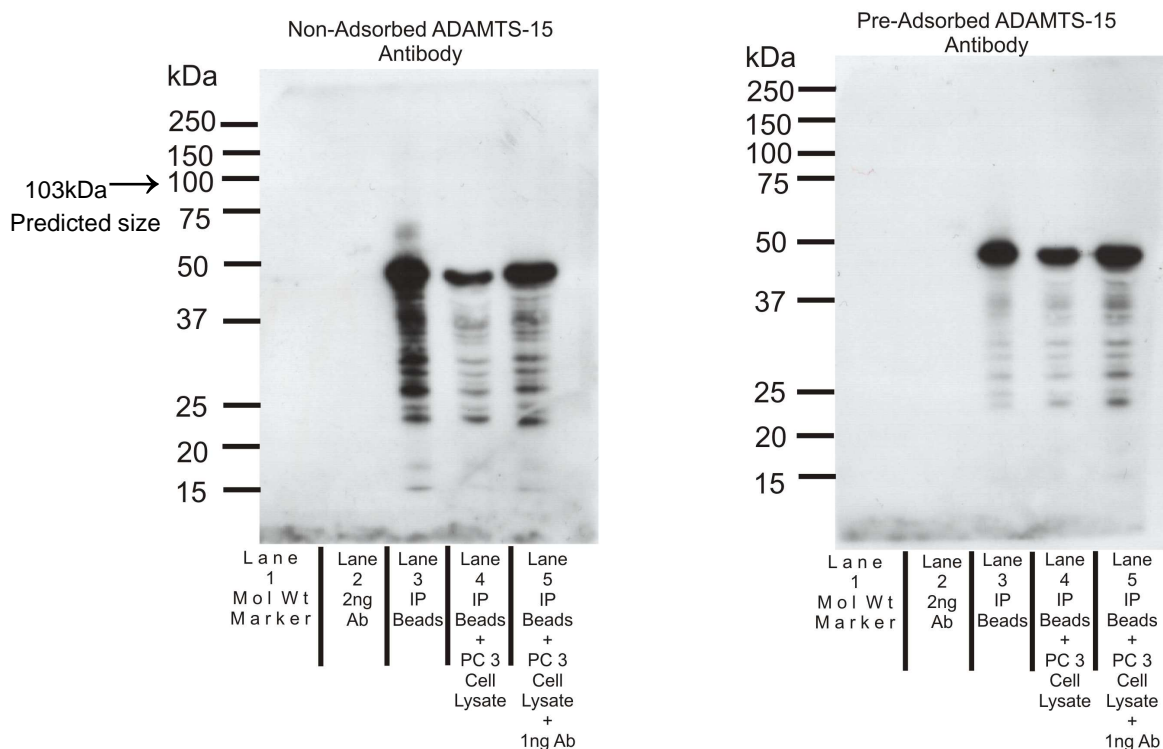


Figure 4.10: Western blot to determine the source of bands detected on lysates after immunoprecipitation. Bands were detected on the negative control membrane (probed

with pre-adsorbed antibody) on the right as well as the membrane on the left which was probed with antibody which was not pre-adsorbed. 2ng of ADAMTS-15 antibody was loaded in Lane 2, which was not detected. All the lanes loaded with lysates that had been in contact with the protein A-agarose beads had multiple bands detected, including Lane 3, which was loaded with Leammli sample buffer which contained protein A beads but contained no lysate protein.

4.3.3.3 Heparin-agarose Precipitation and Probing for ADAMTS-15 in Cell lysates and Culture Medium using the ab28516 Antibody

ADAMTS-1, -4, -5 and -9 are known to bind heparan sulphate in the ECM (Kuno 1998; Somerville 2003; Gao 2004; Zeng 2006). Heparan sulphate and heparin are negatively charged polysaccharides composed of α 1-4 linked repeating disaccharide units containing a uronic acid and an amino sugar that may be repeated to form a structure of varying lengths (Powell 2004). Heparan sulphate is present on cell surfaces and in the ECM where it is covalently bound to several core proteins to form heparan sulphate proteoglycans (Bernfield 1999).

Cell lysates containing the cellular and ECM components from PC3, LNCaP, C4-2b4 prostate cancer cell lines and PCAF stromal cells were incubated with heparin-agarose beads to concentrate ADAMTS-15 from the lysate solutions for detection by western blotting. One millilitre of 2mg/ml lysate solution was incubated with 30 μ l of 50% (v/v) heparin-agarose bead slurry as described in Section 2.8. The anti-ADAMTS-15 antibody raised against the cysteine-rich domain was used for primary incubation.

Western blotting experiments did not detect any bands in the samples prepared from the cell lysates from PC3, LNCaP, C4-2b4 and PCAF cells (Figure not shown).

Medium from PC3 and LNCaP cells was also incubated with heparin-agarose beads to determine whether ADAMTS-15 protein was released into the medium and could be precipitated and detected by western blotting. Ten millilitres of 3-day conditioned medium from confluent PC3 and LNCaP cells was used for incubation with heparin-agarose beads as described in Section 2.8. No bands were detected in any of the lanes.

4.3.3.4 Probing for ADAMTS-15 in Cell lysates using the ab45047 Antibody

Western blotting experiments were performed on cell lysate samples as previously described in Sections 2.9, 2.10 and 2.11. Protein quantification was done using the BCA method as described in Section 2.6. Probing with the anti-ADAMTS-15 antibody (ab45047), raised against the propeptide domain of ADAMTS-15, bands of 50kDa were detected in the lanes with MDA-G8, PC3, LNCaP and C4-2b4 cell lysate (Figure 4.11). The 50kDa band was most intense in the lane loaded with C4-2b4 lysate. Lanes with U373 and PCAF cell lysates produced no bands.

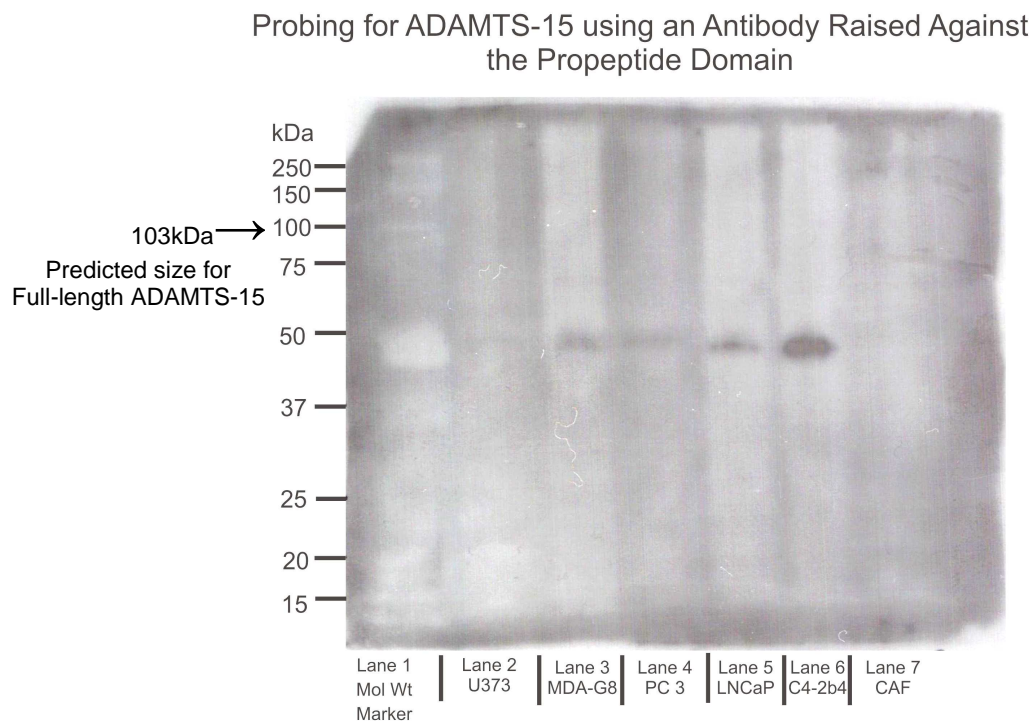


Figure 4.11: Western blotting for ADAMTS-15 protein expression using a rabbit polyclonal propeptide domain antibody (Abcam ab45047). 100µg of cell lysate protein

was loaded in each lane. 50kDa bands were detected in the MDA-G8, PC3, LNCaP and C4-2b4 cell lines, with the most intense band arising from the lane with the C4-2b4 lysate.

4.3.5 Validation of the Anti-ADAMTS-15 Antibody Raised Against the Propeptide Domain

Western blotting experiments using the rabbit polyclonal propeptide domain antibody (Abcam ab45047) detected a 50kDa band in MDA-G8, PC3, LNCaP and C4-2b4 cell lysate (Figure 4.11). To validate the specificity of this antibody to ADAMTS-15, expression of ADAMTS-15 in C4-2b4 cells was transiently knocked down by transfecting the cells with siRNA specific for ADAMTS-15 (Section 2.19) using Dharmafect 2 transfection reagent (Section 2.18.3.2). At 48 hours post-transfection, ADAMTS-15 mRNA expression in C4-2b4 prostate cancer cells, analysed by real-time RT-PCR (Sections 2.2, 2.3 and 2.4), was inhibited by 80% (+/- 10%, n=3). At day 5 post-transfection, cells were lysed and protein samples were prepared as previously described (Section 2.5.2). Protein expression was analyzed by western blotting (Section 2.9 and 2.10). Fifty kDa bands were detected in all the lanes but the band was attenuated in the cells treated with ADAMTS-15 siRNA (Figure 4.12). Densitometric analysis of the 50kDa band showed that its expression was knocked down by over 80%. To control for errors in sample loading, the membrane was stripped and then re-probed with anti-GAPDH antibody. Thirty-four kDa bands were detected with equal intensity in the non-targeting knock-down control (NTCkd) and ADAMTS-15 knock-down (ATS15kd) lanes (Figure 4.12), indicating equal sample loading in these two lanes. The band was absent in the GAPDH knock-down (GAPkd) lane. The detection of down-regulated

expression of the 50kDa band by the antibody in the cells treated with siRNA to the *ADAMTS15* gene verified the specificity of the ab45047 antibody.

Probing for ADAMTS-15 following siRNA Knock-Down

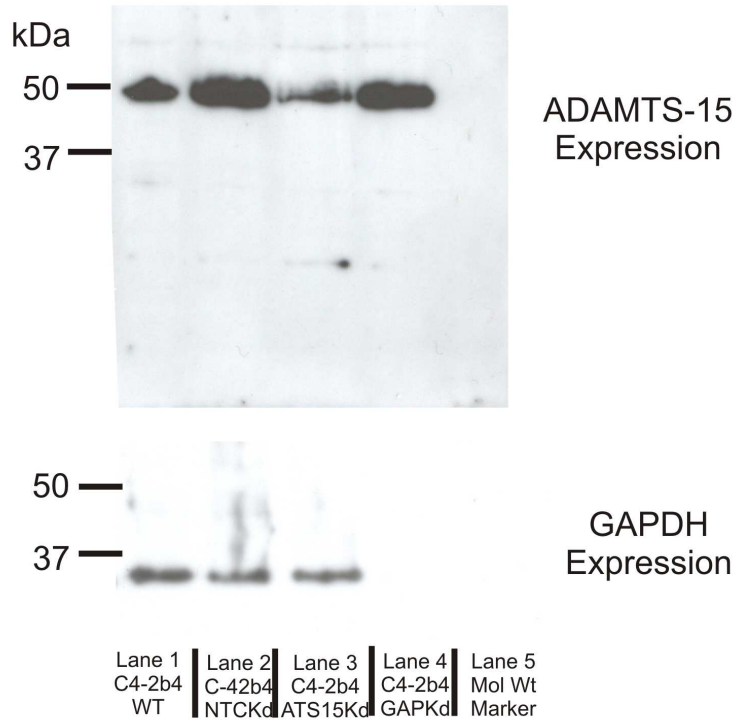


Figure 4.12: Validation of the specificity of the rabbit polyclonal anti-ADAMTS-15 antibody (Abcam ab45047). ADAMTS-15 expression in C4-2b4 prostate cancer cells was transiently knocked down. Western blotting was performed with the cell lysates. 100µg protein was loaded per lane. Lane 1 had the lysate from wild-type C4-2b4 cells (Gerhardt), Lane 2 had the lysate from non-targeting knock-down cells (NTCKd), Lane 3 was from ADAMTS-15 knock-down cells (ATS15kd) and Lane 4 from GAPDH knock-down cells (GAPkd). The upper panel is an image of the blot after probing with the anti-ADAMTS-15 antibody. A 50kDa band was detected in each lane. The band in Lane 3 was attenuated compared with Lane 2, in keeping with ADAMTS-15 knock-down in Lane 3. The lower panel is an image of the same membrane after it had been stripped and re-probed with anti-GAPDH antibody. Lane 4 is attenuated. Bands in Lanes 2 and

3 are of similar intensity, signifying equal sample loading. These results are representative of two experiments.

4.3.6 Heparin-agarose Precipitation and Probing for ADAMTS-15 in Cell lysates and Culture Medium using the ab45047 Antibody

Western blotting experiments using samples prepared from heparin-agarose experiments in Section 4.3.3.3 did not detect any bands when the PVDF membrane was probed with the ab28516 antibody. The ab45047 antibody detected bands when used to probe for ADAMTS-15 in cell lysates, and these bands were shown to be attenuated when ADAMTS-15 was knocked down (Section 4.3.5), thereby validating the specificity of the ab45047. To determine whether ADAMTS-15 could be detected following heparin-agarose precipitation, the experiment in Section 4.3.3.3 was repeated using the ab45047 antibody for immunodetection. Cell lysates containing the cellular and ECM components from PC3, LNCaP, C4-2b4 prostate cancer cell lines and PCAF stromal cells were incubated with heparin-agarose beads to concentrate ADAMTS-15 from the lysate solutions for detection by western blotting. One millilitre of 2mg/ml lysate solution was incubated with 30 μ l of 50% (v/v) heparin-agarose bead slurry as described in Section 2.8. Western blotting experiments did not detect any bands in the samples prepared from the cell lysates from PC3, LNCaP, C4-2b4 and PCAF cells (Figure not shown)

4.4 Fluorescence Immunocytochemistry for Detection of ADAMTS-15 Expression in PC3 Prostate Cancer Cells

ADAMTS-15 expression was transiently knocked down in PC3 cells by electroporation (Section 2.18.1) using siRNA specific for ADAMTS-15 (Section 2.19). At 48 hours

post-transfection, ADAMTS-15 mRNA expression, analysed by real-time RT-PCR (Sections 2.2, 2.3 and 2.4), was inhibited by 90% (+/- 10%, n=3). At day 5 post-transfection, fluorescence immunocytochemistry was used to detect ADAMTS-15 expression in PC3 cells as described in Section 2.14. The rabbit polyclonal anti-ADAMTS-15 antibody (Abcam ab45047) was used as the primary antibody. This antibody was raised against the propeptide domain of ADAMTS-15. Secondary antibody incubation was done using Alexa Fluor 594 goat anti-rabbit fluorescent tagged antibody, which has a fluorescence emission maximum of 617nm (red). GAPDH expression was also knocked down in a separate set of PC3 cells and fluorescence immunocytochemistry done using the same protocol. The nuclei of the cells were counter-stained with DAPI (4', 6-diamidino-2-phenylindole). DAPI has a fluorescence emission maximum of 461nm (blue) when bound to double-stranded DNA (Manzini 1983; Kapuscinski 1995). Fluorescence was compared between ADAMTS knock-down cells and non-targeting knock-down controls. Images were acquired with a Leica DMI 4000B microscope using LAS AF version 1.6.3 software.

ADAMTS-15 expression was detected in the non-targeting knock-down (NTCKd) cells (Figure 4.13) but not in the ADAMTS-15 knock-down (ATS15kd) cells (Figure 4.14). As expected the nuclei emitted blue fluorescence due to the DAPI stain. The red fluorescence signal detected was very weak, and without staining of the cell membranes, detailed localisation of ADAMTS-15 was not possible. However, the areas of red fluorescence relative to the position of the nuclei suggests the staining was in the cytoplasm.

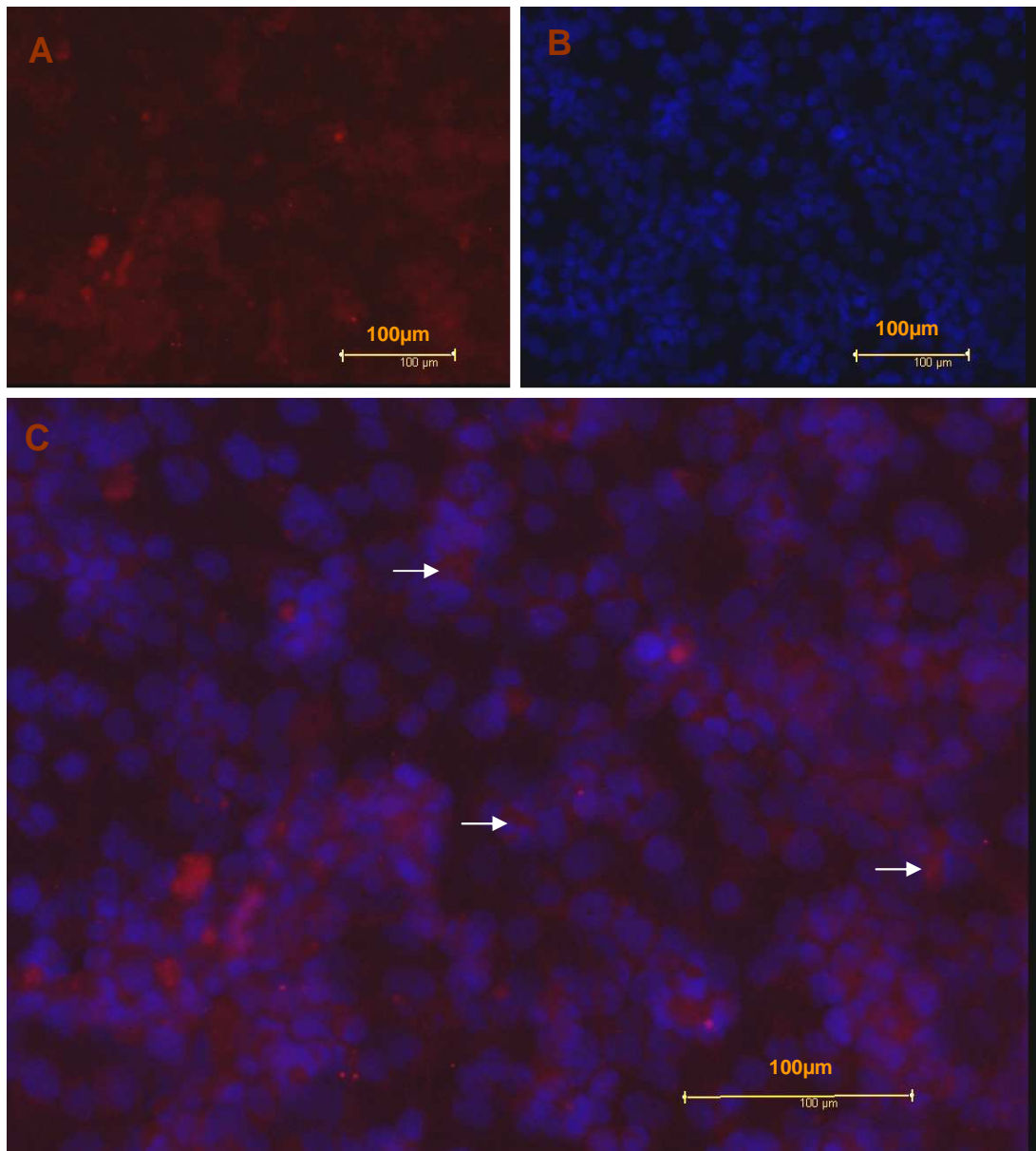


Figure 4.13: Fluorescence immunocytochemistry for detection of ADAMTS-15 expression. Non-targeting knock-down PC3 cells were cultured in monolayer in chamber slides. At day 5 post-transfection, fluorescence immunocytochemistry was undertaken. Rabbit anti-ADAMTS-15 antibody (Abcam ab45047) raised against the propeptide domain was the primary antibody. Secondary antibody incubation was performed using Alexa Fluor 594-tagged goat anti-rabbit antibody, which emits red fluorescence. The nuclei of the cells were counter-stained with DAPI. Weak red fluorescence signal (ADAMTS-15) was detected (A). The nuclei emitted a blue

fluorescence signal (B). The composite image (C) suggested that the red signal was in the cytoplasm (white arrows).

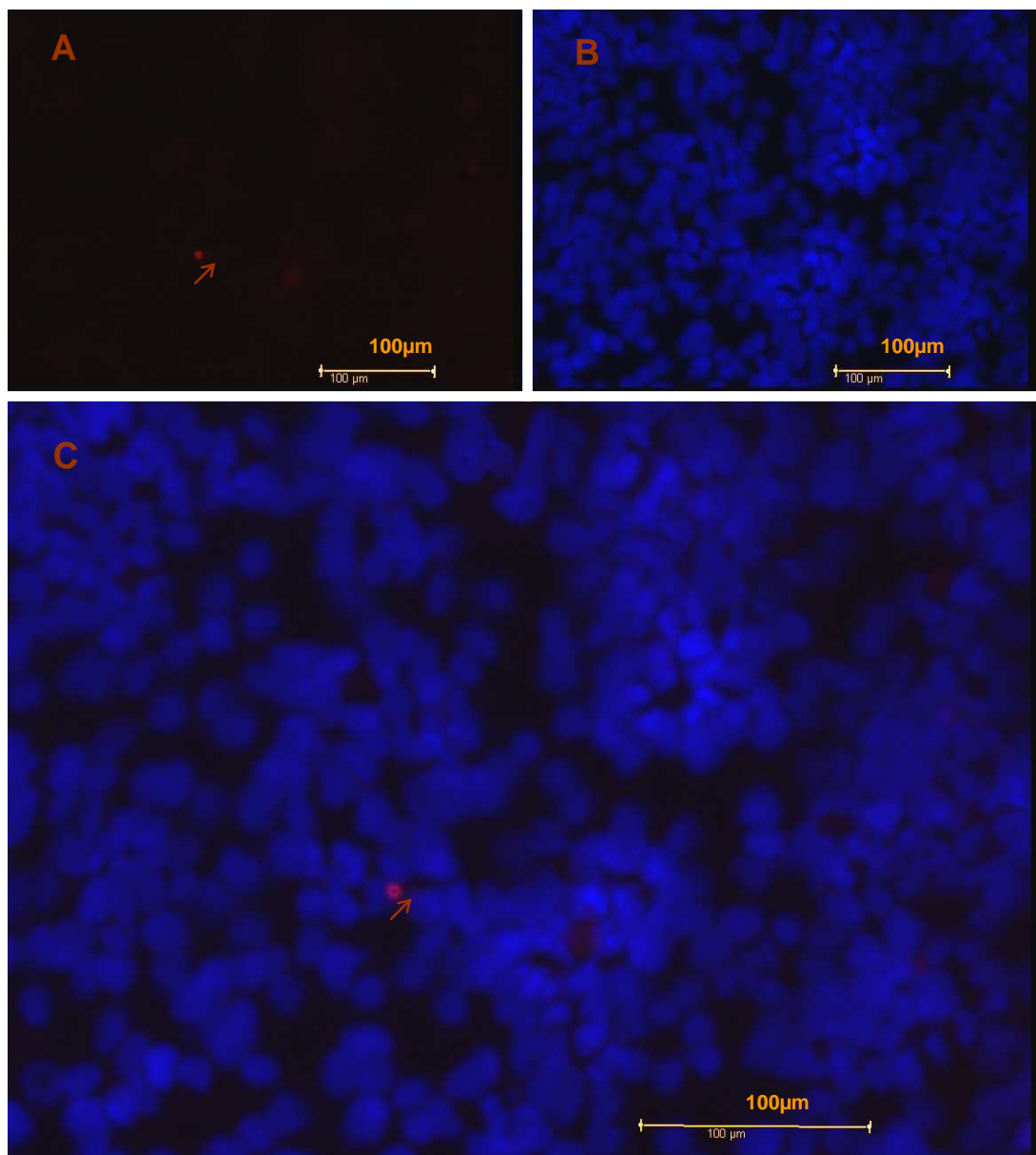


Figure 4.14: Fluorescence immunocytochemistry probing for ADAMTS-15 in ADAMTS-15 knock-down cells. ADAMTS-15 mRNA expression was knocked down by 90% in PC3 cells using siRNA. The cells were cultured in monolayer in chamber slides. At day 5 post-transfection, fluorescence immunocytochemistry was performed using the same methodology as for Figure 4.13. No fluorescence signal was detected in (A). The nuclei emitted a blue fluorescence signal (B). The composite image is shown in (C). Bar at

bottom left of each image denotes 100 μ m. The red dot appearing in image A and also in C (red arrows) is an artefact, as it did not change position when the field of view was changed.

Immunodetection of GAPDH showed that there was red fluorescence emitted by the non-targeting knock-down (NTCKd) cells (Figure 4.15) but no red fluorescence emitted by the GAPDH knock-down (GAPkd) cells (Figure 4.16). DAPI staining emitted blue fluorescence from the nuclei. The red fluorescence signal was weak, but the staining appeared to be outside the nucleus, in keeping with the role of GAPDH in glycolysis (Mazzola 2003).

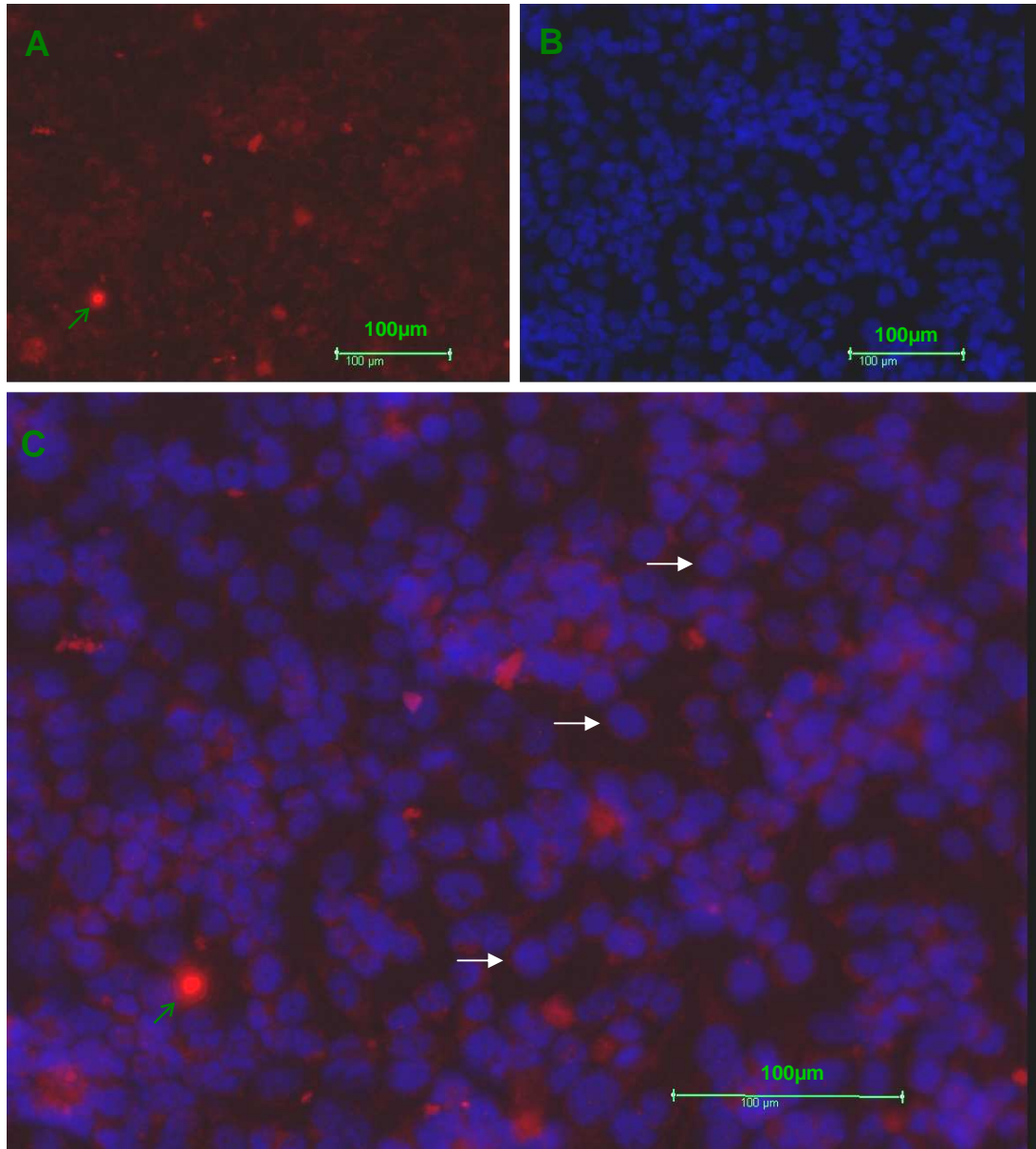


Figure 4.15: Fluorescence immunocytochemistry for detection of GAPDH expression. Non-targeting knock-down PC3 cells were cultured in monolayer in chamber slides. At day 5 post-transfection, fluorescence immunocytochemistry was performed using the same methodology as for Figure 4.13, except rabbit anti-GAPDH antibody (Abcam ab9485) was used for primary immunodetection. Weak red fluorescence signal was detected (A). The nuclei emitted a blue fluorescence signal (B). The composite image (C) suggested that the red signal was outside the nucleus (white arrows). The red dot

appearing in image A and also in C (green arrows) was an artefact, as it did not change position when the field of view was changed.

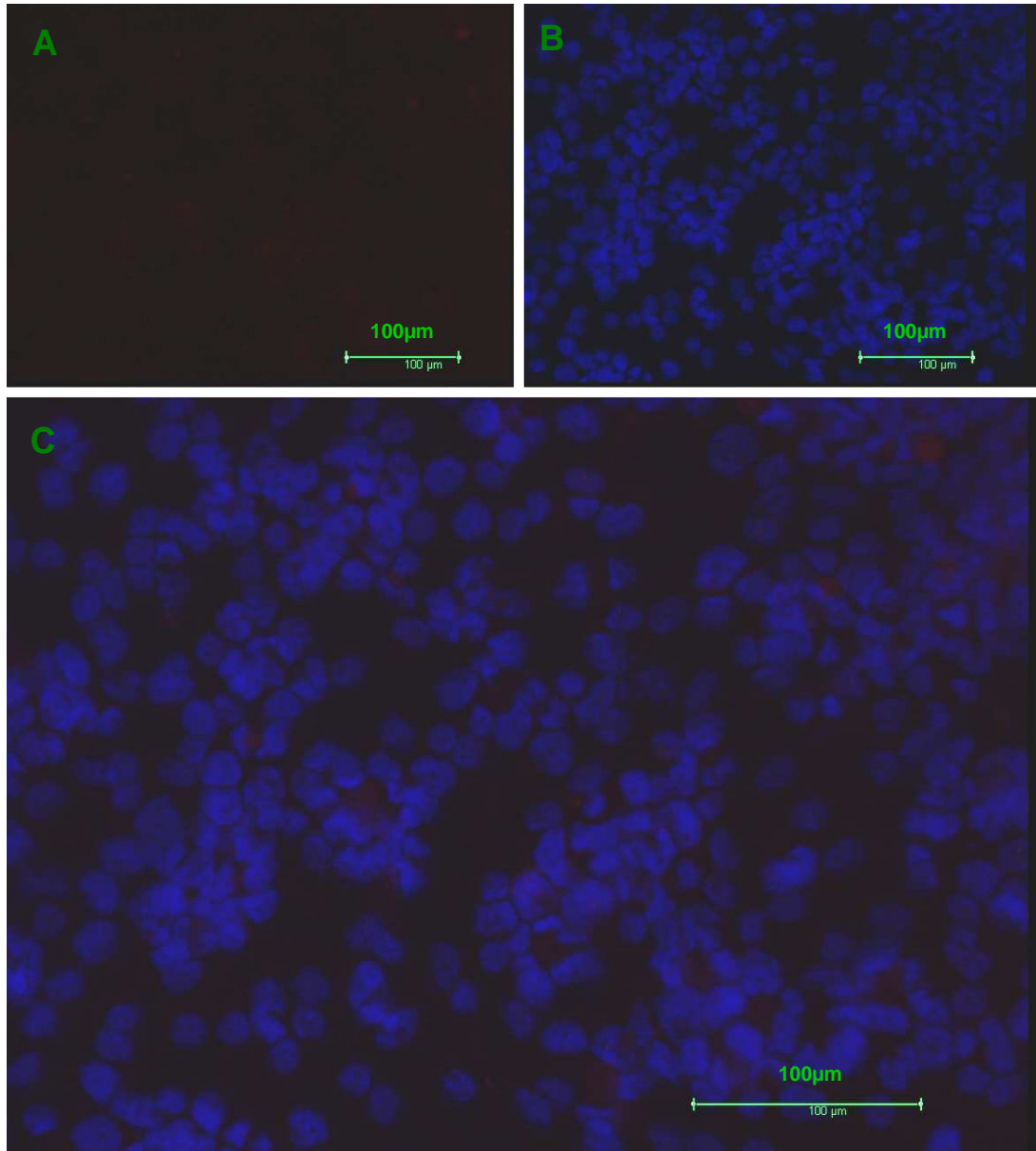


Figure 4.16: Fluorescence immunocytochemistry probing for GAPDH in GAPDH knock-down cells. GAPDH mRNA expression was knocked down by 99% in PC3 cells using siRNA. The cells were cultured in monolayer in chamber slides. At day 5 post-transfection, fluorescence immunocytochemistry was performed using the same methodology as for Figure 4.13, except rabbit anti-GAPDH antibody (Abcam ab9485)

was used for primary immunodetection. No fluorescence signal was detected in (A). The nuclei emitted a blue fluorescence signal (B). The composite image is shown in (C).

4.5 Discussion

This chapter reports the results of experiments analysing the expression of ADAMTS-1 and -15 in prostate cancer and stromal cells using real-time RT-PCR, western blotting and fluorescence immunocytochemistry.

Real-time RT-PCR was used to analyse ADAMTS-1 and -15 expression at transcriptional level in PC3, LNCaP, C4-2b4 and PCAF cells (Section 4.2). Expression levels of TIMP-3, the main inhibitor of the metalloproteinases, was also analysed. For comparison, expression in U373 (astrocytoma) and MDA-G8 (breast cancer) cells were analysed because these cells have been reported to express ADAMTS-1 (Dr Martin Reid, pers commun) and ADAMTS-15 (Dr Julia Woodward, pers commun) respectively. The relative expression method was used, with PC3 cells acting as the calibrator sample in each experiment, ie expression levels were calculated relative to expression in PC3 cells.

The mRNA expression analyses showed variability of expression in some cell lines between experiments, for example ADAMTS-1 expression in LNCaP cells (Figure 4.1) and TIMP-3 expression in C4-2b4 cells (Figure 4.3). Variability in ADAMTS and TIMP gene expression in cell lines between experiments has been previously reported (Giricz 2010; Stokes 2010), with variability of up to 1000-fold. This could partly be explained by the existence of sub-clones within cell line populations. PC3 and LNCaP cell lines are reported to have sub-clones (Festuccia 2000; Wan 2003). This is also supported by findings in this study (Section 6.2.2) which showed that sub-clones of the PC3 cell line had varied expression of ADAMTS-1. This limitation has to be taken into

account when interpreting mRNA expression data from cell lines especially with low experiment numbers.

The results show that in relative terms, the LNCaP cell line expressed moderate levels of ADAMTS-1, low levels of ADAMTS-15 and high levels of TIMP-3. The C4-2b4 cell line expressed high levels of ADAMTS-1, low levels of ADAMTS-15, and moderate levels of TIMP-3. The PCAF cell line expressed high levels of ADAMTS-1, low levels of ADAMTS-15 and high levels of TIMP-3. This is based on an arbitrary definition of low expression being ≤ 0.3 fold, moderate expression being 0.4-2.9 fold and high expression being ≥ 3 fold relative to expression in PC3 cells.

The data showed that there were high expression levels of TIMP-3 in the LNCaP and PCAF cells, indicating that TIMP-3 activity may be attenuating the action of metalloproteinases in these cells. The high expression levels of TIMP-3 in PCAF cells also suggests that stromal cells adjacent to cancer cells may be modulating the activity of cancer cells by secreting a proteinase inhibitor into the TME. Several reports have reported that interactions between cancer and stromal cells can alter tumour characteristics (Chung 2005; Thalmann 2010).

It would have been ideal to analyse expression using normal epithelial prostate cells as the calibrator samples but at the time of these experiment, no normal epithelial cells were available in our laboratory. The PNT1 and PNT2 non-tumourigenic prostatic epithelial cell lines were immortalised using the SV40 transfection vector (Berthon 1995), which is reported to up-regulate ADAMTS-1 expression in human transformed ovarian granulosa cells compared with non-transformed granulosa cells (Freimann 2005). As a result of this, the PNT1 and PNT2 cell lines were not considered to be true 'normal' prostatic epithelial cell lines for the purpose of this study.

The mRNA expression data confirmed that ADAMTS-1, -15 and TIMP-3 were expressed in prostate cancer and stromal cell as was previously reported by Cross et al (Cross 2005), with similar expression patterns. Relative expression levels of ADAMTS-1 and -15 in PC3, LNCaP and PCAF stromal cells show a similar pattern with the work of Cross et al. However, Cross et al found undetectable levels of TIMP-3 in PC3, whereas data from my experiments showed that TIMP-3 expression was detected and was approximately 3-fold higher in LNCaP cells compared to PC3 cells. The Ct values (the cycle number during the PCR reaction at which fluorescence level generated by the amplification of the gene of interest exceeds the background fluorescence) for TIMP-3 in PC3 cells usually ranged from 32-35, compared with 16-18 for GAPDH. This indicates very low transcript levels of TIMP-3. Expression of TIMP-3 in BPH stromal cells reported by Cross et al was approximately 100 fold relative to LNCaP cells. In my experiments, TIMP-3 expression was also 100 fold in PCAF stromal cells relative to LNCaP. The data are not directly comparable because of the fact that transcript levels have been analysed using the relative expression method, but the pattern of mRNA expression is similar for the two studies.

Semi-quantitative analysis of ADAMTS-1 and -15 by western blotting was challenging for a number of reasons. The main reason was that at the time of these experiments, there were no commercially available antibodies against ADAMTS-1 and -15 that had been validated in published reports (to my knowledge). Antibodies are useful tools for laboratory research, but the lack of specificity of commercially available antibodies continues to be a source of concern (Bordeaux 2010). The utility of two anti-ADAMTS-1 and two anti-ADAMTS-15 antibodies were evaluated.

The first anti-ADAMTS-1 antibody (Abcam, ab39194) was raised against the C-terminal domains of ADAMTS-1. The product literature did not indicate specifically the

size or sequence of the antigen used for antibody synthesis. The western blot experiments which were performed using this antibody detected multiple bands of varying sizes (Figure 4.4). This image was difficult to evaluate. It is possible that the antibody was reacting non-specifically to other proteins in the lysate. However it is known that fragments of 87kDa, 65kDa and 22kDa are sequentially cleaved from full length ADAMTS-1 (Rodriguez-Manzaneque 2000), and it is possible that the multiple bands detected were C-terminal fragments of varying lengths. Alternatively, the cells could have been producing splice-variants of ADAMTS-1, although this has not been reported previously. Because of the multiplicity of bands detected, it would have been difficult to assess the effect of ADAMTS-1 knock down in subsequent experiments using this antibody. The second anti-ADAMTS-1 antibody (R&D Systems, MAB2197) used was raised against the catalytic domain (amino acids Arg²⁵⁸ – Phe⁸⁴⁹). This antibody detected bands of size 75kDa-100kDa (Figure 4.5). This variation in size could be as a result of splice variants of ADAMTS-1 or post-translational processing (Rodriguez-Manzaneque 2000) as mentioned earlier. Validation of this antibody using ADAMTS-1 knock-down cells showed that mRNA knock-down did not attenuate the intensity of the bands on western-blot (Figure 4.6). Importantly, the bands detected in Figure 4.6 were of 50kDa size. No bands of 75kDa or 100 kDa were detected in the lanes with PC3 cell lysate blots but were present in the lane with recombinant human ADAMTS-1. Again, this could be as a result of post translational processing of full-length ADAMTS-1 from 105kDa to smaller fragments of 50kDa, but could also be due to non-specific antibody binding to another protein of 50kDa.

Western blotting for detection of ADAMTS-15 was done with two antibodies. The first antibody (Abcam, ab28516) was raised against a peptide sequence 'HSTNRLTLAVAW', corresponding to His⁵⁹² – Trp⁶⁰³ in the cysteine-rich domain. This

antibody detected faint bands of 25kDa in PC3 and LNCaP cells (Figure 4.7). Immunoprecipitation was used in an attempt to increase the concentration of ADAMTS-15 protein in the samples. This created a problem because multiple high intensity bands were detected of size ranging from 15kDa to 50kDa (Figure 4.8). A number of control experiments were performed to detect the source of the bands. The results showed that the protein A-agarose beads were the source of the protein being detected. Protein A has a mass of 40-60kDa and binds strongly to IgG (Lindmark 1983). The unknown protein was binding directly with the HRP-labelled IgG secondary antibody (Figure 4.9, Membrane 2). Immunoprecipitation had to be abandoned because the dark bands were attributed to release of protein A from the agarose beads into solution, which was contaminating the immunoprecipitation samples. This should not have occurred, as the product information sheet stated that the protein A was covalently bound to the agarose via covalent bonds. However, this process must have been incomplete, with non-specifically adsorbed protein A being released in the detergent-containing buffers used for this experiment

Heparin-agarose precipitation was also undertaken in another attempt to concentrate ADAMTS-15 and enable detection with the ab28516 antibody. Immobilised heparin has been used to separate heparin-binding proteins from solution (Manaskova 2002) and ADAMTS-1, -4, -5 and -9 are known to bind heparin and heparan sulphate (Kuno 1998; Somerville 2003; Gao 2004; Zeng 2006). In the western blot experiments using heparin-agarose precipitation to prepare the samples, no distinct bands were detected. This could possibly be because other heparin-binding proteins were more abundant in the cell lysates and had higher binding affinity to heparin than ADAMTS-15. For example β -microseminoprotein and spermadhesins have been reported to have the greatest affinity for heparin of the heparin-binding proteins in prostate tissue (Manaskova 2002).

Alternatively, ADAMTS-15 may have been undetected because the ab28516 antibody was not binding to ADAMTS-15 with high enough affinity. No control experiments were performed to identify the reason for the absence of bands, and the use of this antibody was discontinued in further experiments.

The second anti-ADAMTS-15 antibody used (ab45047) was raised against the propeptide domain of ADAMTS-15. This antibody detected 50kDa bands on western blots (Figure 4.11). ADAMTS-15 knock-down using siRNA led to attenuation of the intensity of the 50kDa band (Figure 4.12), indicating that this antibody was specifically binding to ADAMTS-15. The full length ADAMTS-15 (including the signal peptide) is predicted to be a 103kDa protein (Cal 2002). The propeptide domain, Gly¹⁸ – Arg²¹² is approximately 21kDa. A 50kDa band suggests that ADAMTS-15 was processed post-translationally, with cleavage yielding a 50kDa propeptide-containing fragment. Alternatively, the cells in the experiments were expressing a 50kDa splice variant of ADAMTS-15. Another possibility is that the 21kDa propeptide could have been dimerised or glycosylated, with a resulting mass of 50kDa. Splice variants and dimerisation of ADAMTS-15 have not been described previously, but the ADAMTS-15 propeptide has a potential glycosylation site at N¹⁴¹ (N-A-S).

With the validation of the ab45047 antibody, heparin-agarose precipitation was repeated and western blotting performed using this antibody. No bands were detected. This suggests that if ADAMTS-15, like some of the other ADAMTSs, is a heparin-binding protein, there were other proteins in the cell lysates that had stronger binding affinity for heparin than ADAMTS-15. Another possibility is that the C-terminal heparin-binding domains have been cleaved off and were precipitated by the heparin-agarose beads but not detected by the propeptide domain antibody, which would be in keeping with reports showing that ADAMTSs bind to heparan sulphate and heparin via the TSP

domains at the C-terminal (Kuno 1998; Somerville 2003; Gao 2004; Zeng 2006). TIMP-3 protein expression was not analysed in this study. Validation of commercially available TIMP-3 antibodies was the subject of a doctorate study by another member of this research group, Miss Olajumoke Adeniji. Her effort was therefore not duplicated. The ab45047 antibody was used in fluorescence immunocytochemistry to probe expression of ADAMTS-15 in ADAMTS-15 knock-down and non-targeting knock-down control cells. ADAMTS-15 expression was detected in the non-targeting knock-down cells but not the ADAMTS-15 knock-down cells (Figures 4.13 and 4.14). This provided further evidence of the validity of the ab45047 antibody.

In conclusion, this chapter describes experimental steps taken to validate antibodies for use in expression studies of ADAMTS-1 and -15. Neither of the two anti-ADAMTS-1 antibodies was found to be reliable in analysis of ADAMTS-1 expression, one of the anti-ADAMTS-15 antibodies was validated and this antibody was used in further experiments requiring analysis of ADAMTS-15 protein expression.

CHAPTER 5

REGULATION OF ADAMTS-1, -15 AND TIMP-3 EXPRESSION IN PROSTATE CELLS BY DIHYDROTESTOSTERONE & TUMOUR NECROSIS FACTOR

CHAPTER 5:

REGULATION OF ADAMTS-1 AND -15 mRNA EXPRESSION IN PROSTATE CELLS BY DHT AND TNF

5.1 Introduction

Prostate epithelial cells depend on androgens for proliferation and differential gene expression (Sandberg 1980). Growth and proliferation is mediated by growth factors which are secreted in response to androgen stimulation (Steiner 1993; Hellowell 2002). Testosterone from the circulation is converted in the prostate by 5- α -reductase to DHT, the androgen which is most active in prostate tissue (Steers 2001; Zhu 2003). ADT in the form of surgical or medical castration is used in the management of locally advanced, metastatic, or relapsing disease. Androgen deprivation leads to reduction in the size of local tumours, and the size and number of metastatic deposits, as well as changes in gene expression (Huggins 1942; Nishi 1996). ADT reduces serum androgen concentration from about 2nM to undetectable levels (de Jong 1991; Anderson 2008), which has an adverse effect on castration-sensitive prostate cancer cell survival.

ADAMTS-1 mRNA has been shown to be up-regulated by DHT in endometrial stromal cells after 24 hour treatments (Wen 2006). *In vitro*, LNCaP cell proliferation is maximally stimulated by DHT at concentrations between 1 and 10nM (Horoszewicz 1983; Lin 1998; Sherwood 1998; Zhu 2003). The dissociation constant of the androgen receptor with DHT in prostate is 0.34nM at 0°C and pH7.5, and by extrapolation approximately 0.15nM at 37°C (Wilson 1976).

LNCaP cells were treated with DHT to analyse the effect of DHT on ADAMTS-1 and -15 expression as described in Section 2.15. To cover the range between castrate levels and maximal DHT stimulation, treatment doses of 0.1, 1.0 and 10nM DHT were used and compared with the control cells which had no DHT. Flutamide is a non-steroidal anti-androgen (Peets 1974). The inhibitory constant of flutamide is approximately

175nM at 4°C and pH7.5 (Kemppainen 1999). Prostate cancer cells have been reported to carry mutations of the AR, which are thought to facilitate the progression to metastasis and castration resistance (Taplin 1995). Non-steroidal anti-androgens have been shown to paradoxically have agonistic activity in LNCaP cells and derivative cell lines as a result of AR mutations (Veldscholte 1990; Culig 1999). To determine the effect of an excess of flutamide, LNCaP cells were also treated with 1µM flutamide, or 10nM DHT + 1µM flutamide. PSA expression was used as a positive control.

Patients with advanced prostate cancer are reported to have elevated serum levels of TNF (Michalaki 2004). As macrophages infiltrate the tumour site, they release cytokines locally as part of the inflammatory reaction to the presence of the tumour (Coussens 2002). This could explain the elevated levels of TNF and IL-6 in patients with advanced prostate cancer (Michalaki 2004). In that study, serum TNF and IL-6 levels were as high as 6.3 and 9.3 pg/ml respectively in patients with metastatic disease, compared with TNF and IL-6 serum levels of 1.1 and 1.3 pg/ml respectively in patients with localised disease. TNF concentrations may be much higher locally at the tumour site. In patients with rheumatoid arthritis (RA), TNF levels are approximately five times higher in synovial fluid than in serum (Steiner 1999). TNF levels in synovial fluid, the local site of inflammation in RA range from 39 – 382pg/ml (Lettesjo 1998; Steiner 1999). ADAMTS-1, -4, -5, -6 and -9 are reported to be regulated by pro-inflammatory cytokines (Bevitt 2003; Demircan 2005; Ng 2006). TNF induces cancer cachexia (Tracey 1992), an activity that is mediated by TNF receptor type I (TNFR1) activation (Llovera 1998). ADAMTS-1 is highly expressed in some cachexia-inducing tumours (Kuno 1997). TNF and other cytokines could have an effect on prostate cancer progression by modulating the expression of ECM proteinases, and altering the homeostatic balance between proteinases and their natural inhibitors.

To cover the range of TNF concentrations detected in serum and tissue in physiological and pathological states, PC3, LNCaP and BPH45 prostatic stromal cells were treated with TNF at concentrations of 10pg/ml (0.571pM), 100pg/ml (5.71pM), 10ng/ml (571pM) or control (solvent only) as described in Section 2.17. The dissociation constant of TNF with TNFR1 and TNFR2 is 19pM and 420pM respectively at 37° and pH7.5 (Grell 1998).

5.2 Regulation of PSA, ADAMTS-1, ADAMTS-15 and TIMP-3 mRNA expression by DHT and Flutamide

The effect of DHT and flutamide on PSA, ADAMTS-1 and -15 mRNA expression was analysed. Changes in expression of the metalloproteinase inhibitor, TIMP-3, was also analysed.

5.2.1 Regulation of PSA Expression by DHT

PSA mRNA expression in LNCaP cells was up regulated when the cells were treated with increasing concentrations of DHT (Figure 5.1), with median up-regulation of 1.5, 6.9 and 16-fold when treated with 0.1, 1.0 and 10nM DHT respectively. There was significant variance in the medians using the Kruskal-Wallis test ($p = 0.0076$). Using Dunn's multiple comparison test, there was a significant difference in PSA mRNA expression between control and 10nM DHT treatment ($p < 0.01$), but not DHT 0.1nM or DHT 1nM treatment ($p > 0.05$). Flutamide 1 μ M treatment did not regulate PSA expression compared with control ($p > 0.05$), which suggests that flutamide did not have AR agonist activity at 1 μ M. Comparing DHT 10nM treatment and DHT 10nM + Flutamide 1 μ M treatment showed no significant difference ($p > 0.05$), indicating that Flutamide did not inhibit the effect of DHT 10nM (Figure 5.1).

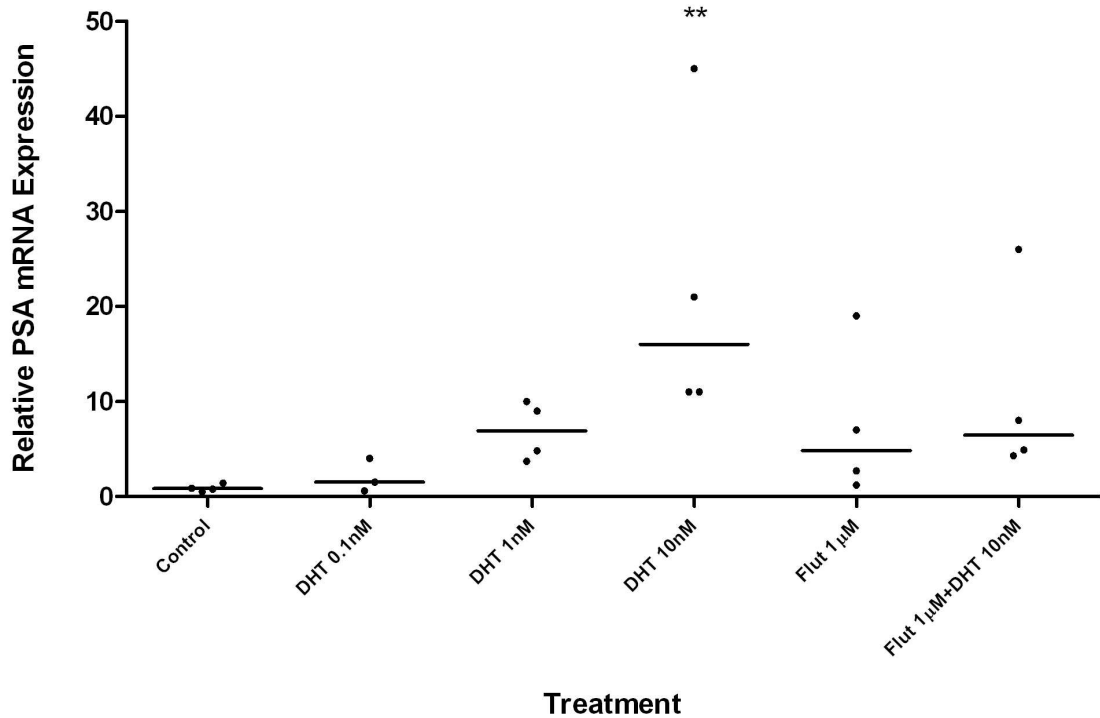


Figure 5.1: Relative expression of PSA mRNA in LNCaP cells treated with DHT and the non-steroidal androgen antagonist flutamide. Cells were treated for 24 hours with the specified doses of DHT or flutamide, lysed and cDNA was synthesized for analysis by real-time RT-PCR. Each data point represents an individual sample of cDNA. The horizontal bars denote the median expression level for each treatment group. Expression levels in treated cells shown as fold changes relative to controls. Results were collated from 4 separate experiments (n=4) showing the expression level of PSA mRNA in the treated cells relative to expression in untreated cells (control). The Kruskal-Wallis test for variance of the medians and Dunn's multi-comparison test was used to analyse for differences between the groups. Asterisks at the top denote treatment groups in which difference in expression levels relative to control were statistically significant (**=p<0.01).

5.2.2 Regulation of ADAMTS-1 mRNA Expression by DHT

DHT treatment did not significantly regulate expression of ADAMTS-1 mRNA at any of the concentrations used (Figure 5.2). The Kruskal-Wallis test demonstrated that the medians had no significant variance ($p = 0.2172$). Dunn's multiple comparison test was used to analyze differences in rank sum between each treatment group and control. ADAMTS-1 mRNA expression was not significantly regulated with any of the treatments used.

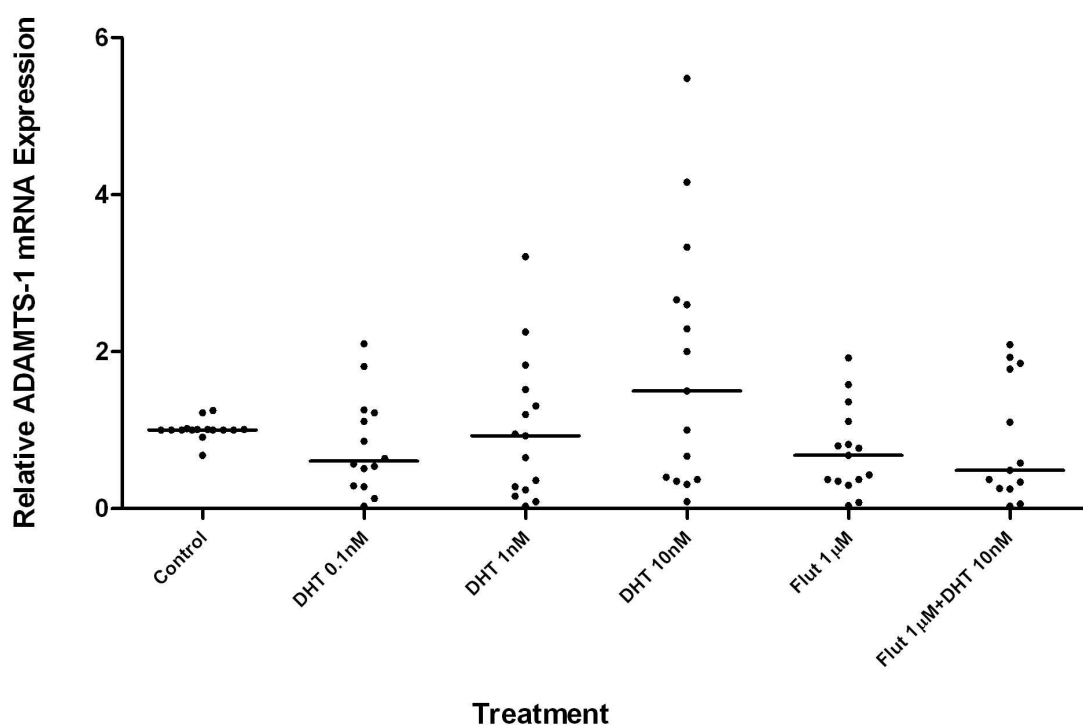


Figure 5.2: Expression of ADAMTS-1 mRNA in LNCaP cells treated with DHT and the non-steroidal androgen antagonist flutamide. Experimental conditions were the same as described in Figure 5.1. Results were collated from 15 separate experiments ($n=15$) showing the expression level of ADAMTS-1 mRNA in the treated cells relative to expression in untreated cells (control). The Kruskal-Wallis test for variance of the

medians and Dunn's multi-comparison test were used to analyse for differences in expression between the groups.

5.2.3 Regulation of ADAMTS-15 mRNA and Protein Expression by DHT

DHT treatment down-regulated the expression of ADAMTS-15 mRNA by 40% and by 70% with treatments of 0.1nM and 1nM DHT respectively (Figure 5.3). The Kruskal-Wallis test demonstrated that the medians had a significantly different variance ($p = 0.0022$). Dunn's multiple comparison test was used to analyze differences in rank sum between each treatment group and control. ADAMTS-15 mRNA expression was significantly down-regulated with treatments of 0.1nM DHT ($p < 0.05$), 1nM DHT ($p < 0.001$), 1 μ M flutamide ($p < 0.01$) and 10nM DHT with 1 μ M flutamide ($p < 0.05$). Comparing the 10nM DHT treatment group with the 10nM DHT plus 1 μ M flutamide treatment group showed no significant difference in ADAMTS-15 expression. Grubb's test was applied to the 10nM DHT treatment group to identify and remove an outlying sample, after which the difference in the median ADAMTS-15 mRNA expression between control and the 10nM DHT group was significant ($p < 0.05$).

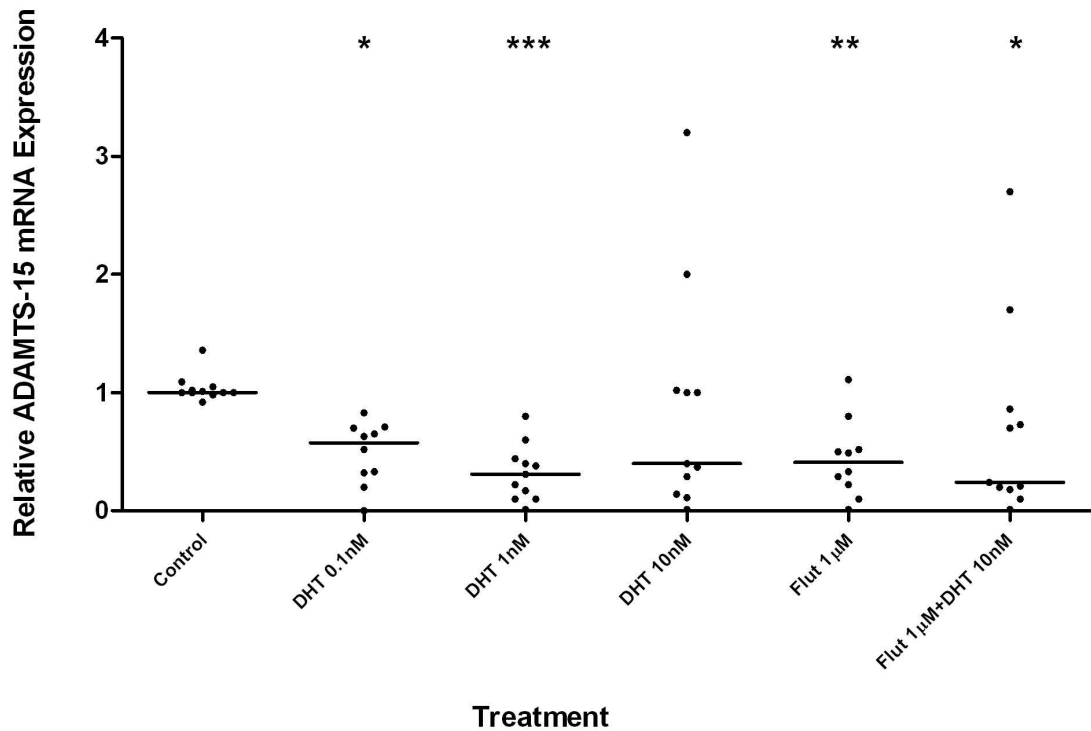


Figure 5.3: Expression of ADAMTS-15 mRNA in LNCaP cells treated with DHT and the non-steroidal androgen antagonist flutamide. Experimental conditions were the same as described in Figure 5.1. Results collated from 11 separate experiments ($n=11$) showing the expression level of ADAMTS-15 mRNA in the treated cells relative to expression in untreated cells (control). The Kruskal-Wallis test for variance of the medians and Dunn's multi-comparison test were used to analyse for differences between the groups. Asterisks were used to denote treatment groups in which difference in expression levels relative to control were statistically significant ($p < 0.05$ *, $p < 0.01$ **, $p < 0.001$ ***).

To analyze the effect of DHT stimulation on ADAMTS-15 protein expression, LNCaP cells were treated with DHT with and without flutamide for 72 hours as described in Section 2.15. Western blotting was done using the ab45047 anti-ADAMTS-15 antibody which was validated previously (Section 4.3.5). 50kDa bands were detected in all the

lanes (Figure 5.4). To determine if there were differences in intensity of the bands, they were analyzed by densitometry as described previously (Section 2.13). In keeping with the mRNA data, ADAMTS-15 protein was down-regulated by DHT. Densitometric analysis showed that down-regulation by DHT was in a dose-dependent manner (Table 5.1). This effect was not inhibited by flutamide. In fact, as had been observed at the mRNA level, treatment with flutamide treatment alone also caused down-regulation of ADAMTS-15 protein.

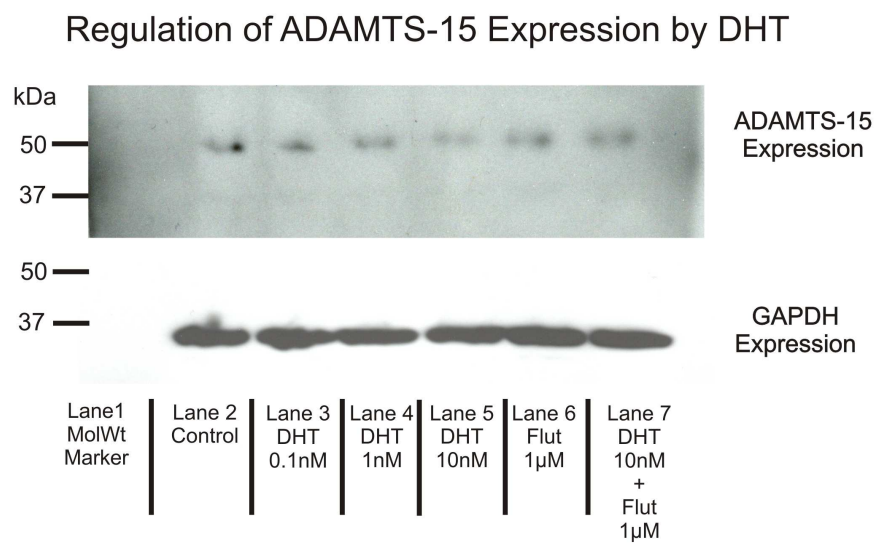


Figure 5.4: Expression of ADAMTS-15 protein in LNCaP cells treated with DHT. Western blotting was used to detect ADAMTS-15 expression in LNCaP cells treated for 72hours with control, 0.1nM DHT, 1nM DHT, 10nM DHT, 1μM flutamide and 10nM DHT plus flutamide. Cellular protein and surrounding ECM were solubilised with Triton X-100 and protein was quantified with the MicroBCA assay. 100μg of protein was loaded in each lane. Bands of 50kDa were detected (Upper Panel). The PVDF membrane was stripped and re-probed with anti-GAPDH antibody (Lower Panel) as a control for equal sample loading. The experiment is representative of two, with similar results.

		Lane 1 Control	Lane 2 DHT 0.1nM	Lane 3 DHT 1nM	Lane 4 DHT 10nM	Lane 5 Flutamide 1µM	Lane 6 DHT10nM + Flutamide 1µM
Experiment 1	Adjusted Densitometric Volume (ODmm ²)	0.2025	0.1238	0.0905	0.0483	0.0659	0.055
	Adjusted volume relative to control	1	0.6	0.4	0.2	0.3	0.3
Experiment 2	Adjusted Densitometric Volume (ODmm ²)	0.2038	0.2231	0.0217	0.0022	0.05	0.0093
	Adjusted volume relative to control	1	1.1	0.1	0.01	0.2	0.05

Table 5.1: Densitometric analysis of 50kDa bands detected on western blots. The bands detected in each lane were analysed by densitometry for differences in intensity. The adjusted volume of the bands were quantified and compared with control. Results from two separate experiments are shown, the western blot for one of which is shown in Figure 5.4.

5.2.4 Regulation of TIMP-3 mRNA Expression by DHT

There was a dose dependent down-regulation of TIMP-3 mRNA expression by DHT which was not reversed with flutamide (Figure 5.5). The Kruskal-Wallis test demonstrated that the medians had a significantly different variance ($p < 0.0001$). Dunn's multiple comparison test was used to analyze differences in rank sum between each treatment group and control. Median expression of TIMP-3 was down-regulated by 50% with treatment of 1nM DHT ($p < 0.05$), 60% with treatment of 10nM DHT ($p < 0.001$), 60% with treatment of 1µM flutamide ($p < 0.01$) and 80% with treatment of 10nM DHT plus 1µM flutamide ($p < 0.001$). Flutamide did not inhibit the effect of DHT. Comparing the 10nM DHT treatment group with the 10nM DHT plus 1µM flutamide treatment group showed no significant difference in TIMP-3 expression. Flutamide again had a similar effect as DHT by down-regulating TIMP-3 expression.

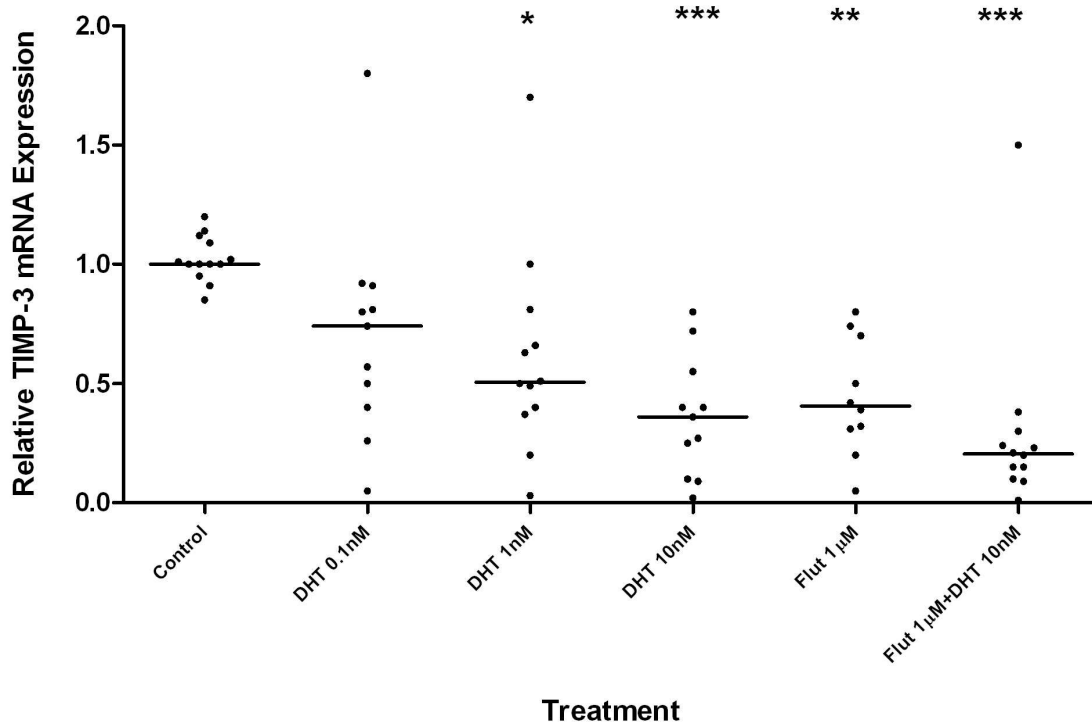


Figure 5.5: Expression of TIMP-3 mRNA in LNCaP cells treated with DHT and the non-steroidal androgen antagonist flutamide. Experimental conditions were the same as described in Figure 5.1. Results were collated from 12 separate experiments ($n=12$). The Kruskal-Wallis test for variance of the medians and Dunn's multi-comparison test were used to analyse for differences between the groups. Asterisks were used to denote treatment groups in which difference in expression levels relative to control were statistically significant ($p<0.05$ *, $p<0.01$ **, $p<0.001$ ***).

5.3 Putative AREs in the ADAMTS1 and ADAMTS15 Genes

AREs are 15-base pair (bp) DNA sequences comprising two six-bp half sites separated by a three-bp spacer. The sequence 5'-GGA/TACAnnnTGTTCT-3' has been described as the consensus ARE (Roche 1992), but there is considerable variation in the sequence and configuration of AREs located in association with androgen responsive genes (Monge 2006).

Expression of ADAMTS-15 was down-regulated by DHT (Section 5.2.3), but the *ADAMTS15* gene has not been previously described as an androgen-regulated gene. The *ADAMTS1* and *ADAMTS15* gene promoters and gene sequences were screened to identify putative AREs using the online nuclear receptor binding site search tool, NUBIScan as described in Section 2.16.

One ARE was identified in the *ADAMTS15* promoter and 12 AREs in the gene sequence. ADAMTS-1 mRNA expression was not regulated by DHT in previous experiments (Section 5.2.2). The *ADAMTS1* gene had no putative AREs in the promoter region and only two in the gene sequence. Tables 5.2 and 5.3 give the position, orientation, sequence and score for the putative AREs identified.

Schematic representations of the *ADAMTS1* and *ADAMTS15* genes in Figure 5.6 and 5.7 shows the relative positions of the putative AREs identified.

	Position (Strand)	Repeat Orientation	ARE Sequence	Score
Promoter	-	-	-	-
Sequence	4933(-)	DR	GGTGCTacaTGTGCT	0.82
	7676(+)	DR	TGGTCAatcaTGTTCT	0.81

Table 5.2: Positions, orientation, sequence and similarity score of the AREs detected in the *ADAMTS1* Gene. For the repeat orientation, DR denotes direct repeat.

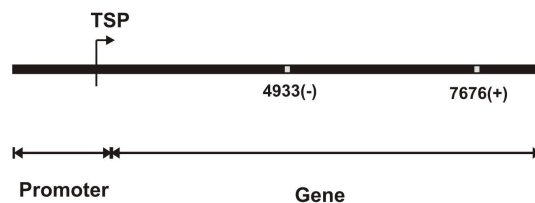


Figure 5.6: Putative AREs identified in the *ADAMTS1* gene. The transcription start point (TSP) denotes the end of the promoter and the start of the gene sequence. 2 AREs

was identified in the gene sequence. The positions (bp) of the AREs relative to the TSP are indicated; (+) and (-) denote sense and antisense strands respectively.

	Position (Strand)	Repeat Orientation	ARE Sequence	Score
Promoter	-2319(+)	ER	GGAACAtaaGGTGCG	0.81
Sequence	914(+)	DR	AGCACCCcgAGTACT	0.81
	914(+)	ER	AGCACCCcgAGTACT	0.88
	914(+)	IR	AGCACCCcgAGTACT	0.81
	928(-)	DR	AGTACTcggGGTGCT	0.88
	2357(+)	ER	GGCACAgctAGTCCC	0.81
	6884(-)	DR	AGTGCTctgAGTGCA	0.87
	6893(-)	DR	AGTGCCgagAGTGCT	0.84
	7038(+)	IR	TGTGCTgccTGGACT	0.86
	12880(-)	DR	TGTCCCcacAGTGCC	0.81
	16123(+)	DR	TGAACCggtAGTTCA	0.82
	16123(-)	ER	TGAACCggtAGTTCA	0.89
	19163(+)	IR	AGCACTctcTGAAct	0.81
19177(-)	DR	AGTTCAgagAGTGCT	0.90	
24790(+)	IR	AGTGCAactTGCACC	0.84	

Table 5.3: Positions, orientation, sequence and similarity score of the AREs detected in the ADAMTS15 Gene. For the orientation, DR, ER, and IR denote direct repeat, everted repeat and inverted repeat respectively.

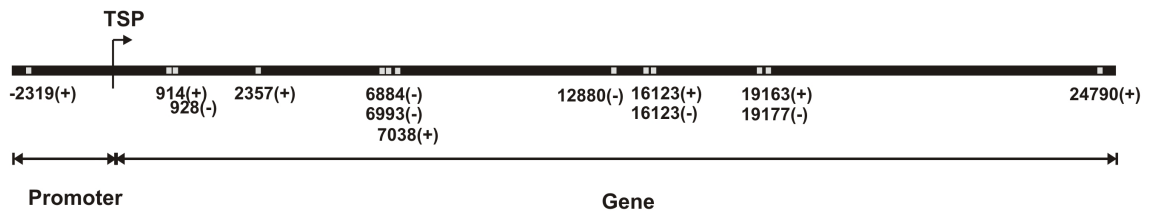


Figure 5.7: Putative AREs identified in the ADAMTS15 gene. The transcription start point (TSP) denotes the end of the promoter and the start of the gene sequence. 1 ARE was identified in the promoter and 12 in the gene sequence. The positions (bp) of the AREs relative to the TSP are indicated; (+) and (-) denote sense and antisense strands respectively.

The same search was performed on the *TIMP3* gene, which was also down-regulated by DHT (Section 5.2.4), and for comparison, the *hKLLK3* gene, which is up-regulated by

androgen (Riegman 1991), and the *FOLH1* gene, which is down-regulated by androgen (Israeli 1994). The results are shown in Table 5.4. One of the AREs detected in the *hKLK3* promoter region is known to be a functional PSA ARE sequence AGAACAgcaAGTGCT (Riegman 1991). The *hKLK3* promoter had approximately double the ARE to base pair ratio compared to the *ADAMTS15* and *FOLH1* promoters, and 1.5 times that of the *TIMP3* promoter. The *hKLK3* gene sequence had approximately 1.5 times the ratio found in the *ADAMTS15*, *TIMP3* and *FOLH1* gene sequences and approximately 3 times the ratio in the *ADAMTS1* gene sequence.

		<i>ADAMTS1</i>	<i>ADAMTS15</i>	<i>TIMP3</i>	<i>hKLK3</i>	<i>FOLH1</i>
	Gene Location	Chromosome 21q21.3	Chromosome 11q24.3	Chromosome 22q12.3	Chromosome 19q13.33	Chromosome 11p11.2
	Androgen Regulation	Not regulated	Down-regulated	Down-regulated	Up-regulated	Down-regulated
Promoter	Length (base pairs)	1,786	2,576	1,942	2,434	2,618
	AREs	0	1	1	2	1
	AREs per base pair	0	0.00039	0.00052	0.00082	0.00038
Sequence	Length (base pairs)	9,121	24,848	62,829	5,850	62,033
	AREs	2	12	31	4	25
	AREs per base pair	0.00022	0.00048	0.00049	0.00068	0.0004

Table 5.4: Summary of the ARE data for *ADAMTS1*, *ADAMTS15*, *TIMP3*, *hKLK3* and *FOLH1* genes.

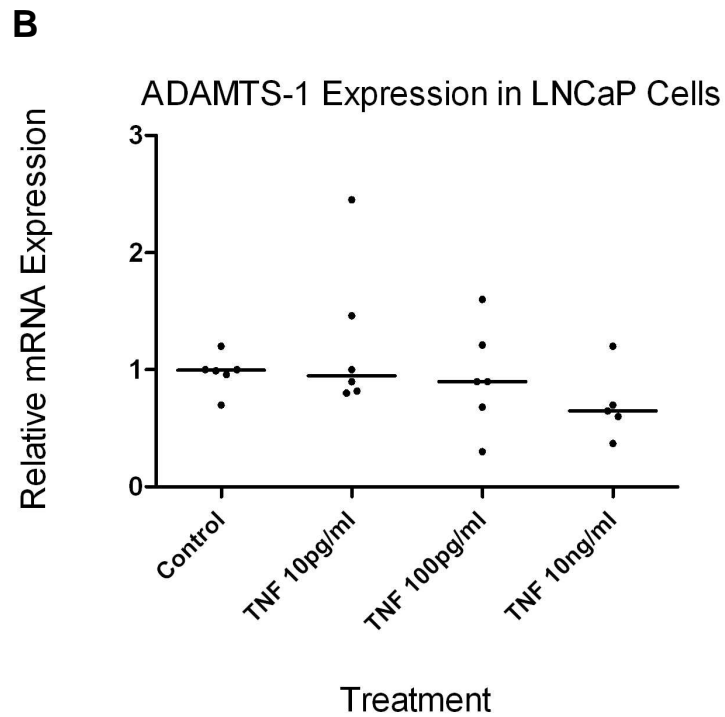
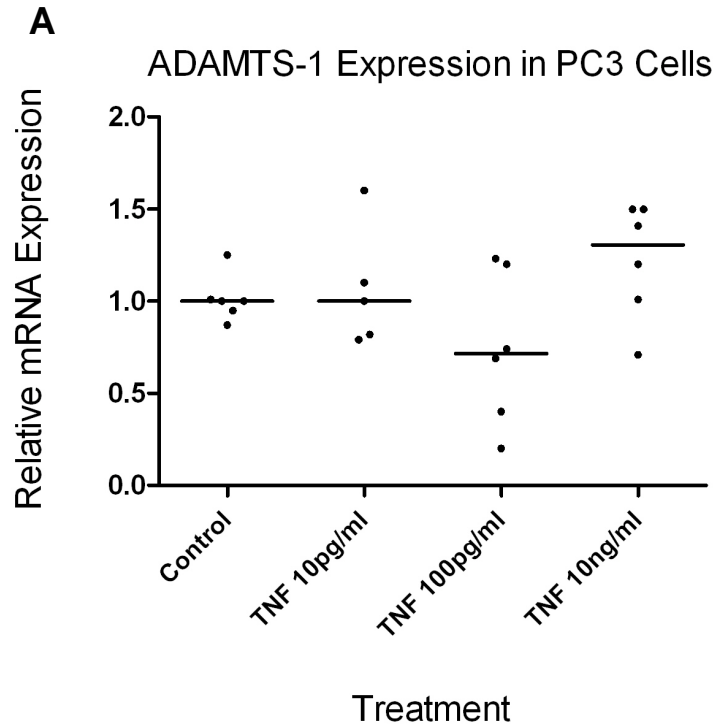
5.4 Regulation of ADAMTS-1 ADAMTS-15 and TIMP-3 mRNA Expression by TNF in PC3, LNCaP and Stromal Cells

Prostate cancer and stromal cells were treated with TNF to determine the effect on ADAMTS-1, -15, and TIMP-3 mRNA expression.

5.4.1 Regulation of ADAMTS-1 Expression by TNF

ADAMTS-1 expression was not regulated by TNF in PC3, LNCaP and BPH45 cells at treatment doses of 10pg/ml, 100pg/ml or 10ng/ml (Figure 5.8). The Kruskal-Wallis test

showed that there was no significant variance between the medians of experiments with PC3 cells ($p=0.1554$), LNCaP cells ($p=0.1842$) and BPH45 cells ($p=0.0856$).



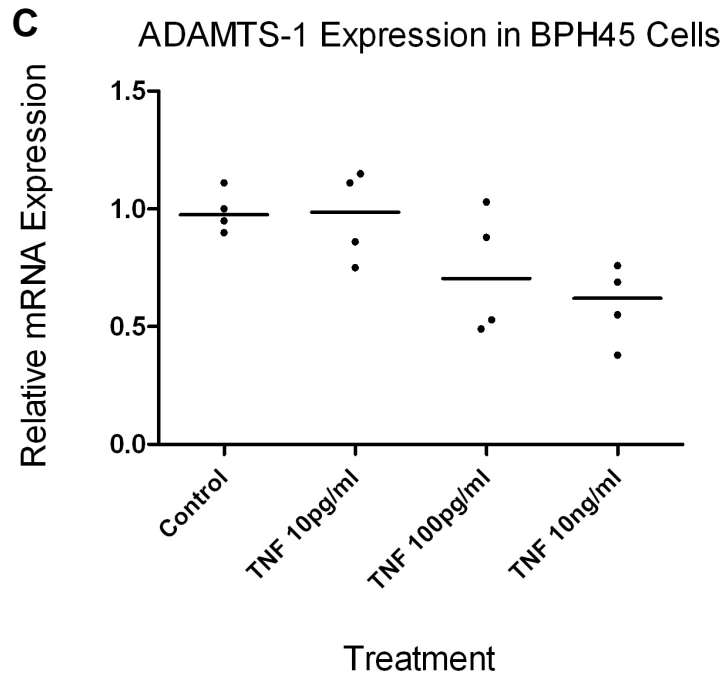


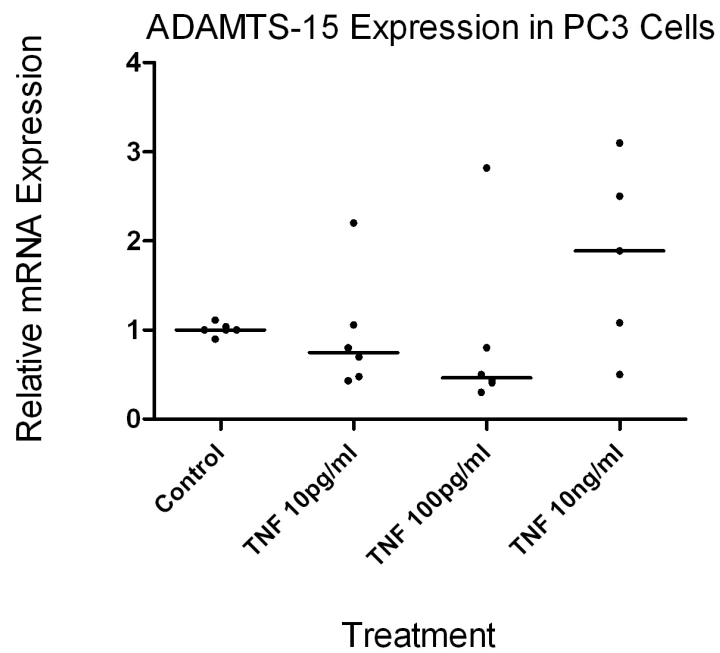
Figure 5.8: Expression of ADAMTS-1 mRNA in A) PC3, B) LNCaP and C) BPH45 cells treated with TNF. Cells were treated for 24 hours with the specified doses of TNF, lysed and cDNA was synthesized for analysis by real-time RT-PCR. Results were collated from 6 separate experiments (n=6) in A and B, and 4 separate experiments (n=4) in C. Each data point represents an individual sample of cDNA. The horizontal bars denote the median expression level for each treatment group. The expression levels of ADAMTS-1 mRNA in treated cells are shown as fold changes relative to controls. The Kruskal-Wallis test for variance of the medians and Dunn's multi-comparison test were used to analyse for differences between the groups. Asterisks were used to denote treatment groups in which difference in expression levels relative to control were statistically significant ($p < 0.05$ *, $p < 0.01$ **, $p < 0.001$ ***).

5.4.2 Regulation of ADAMTS-15 mRNA Expression by TNF

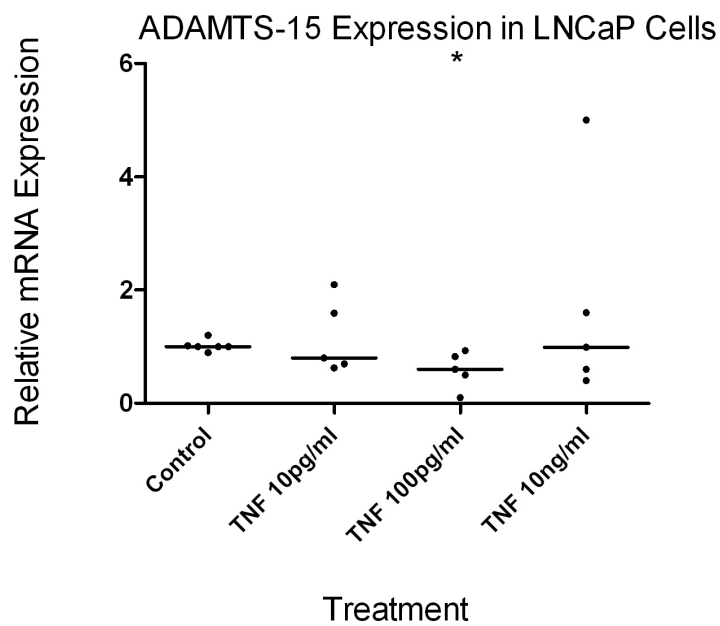
ADAMTS-15 expression was regulated by TNF in LNCaP and BPH45 cells but not in PC3 cells (Figure 5.9). The Kruskal-Wallis test showed no significant variance between

the medians of experiments with PC3 cells ($p=0.0806$) and LNCaP cells ($p=0.1070$), but a significant variance in BPH45 cells ($p=0.0043$). Dunn's post test showed that there was significant down-regulation of ADAMTS-15 in LNCaP cells at a treatment dose of 100pg/ml ($p<0.05$), and in BPH45 cells at a treatment dose of 10ng/ml ($p<0.05$).

A



B



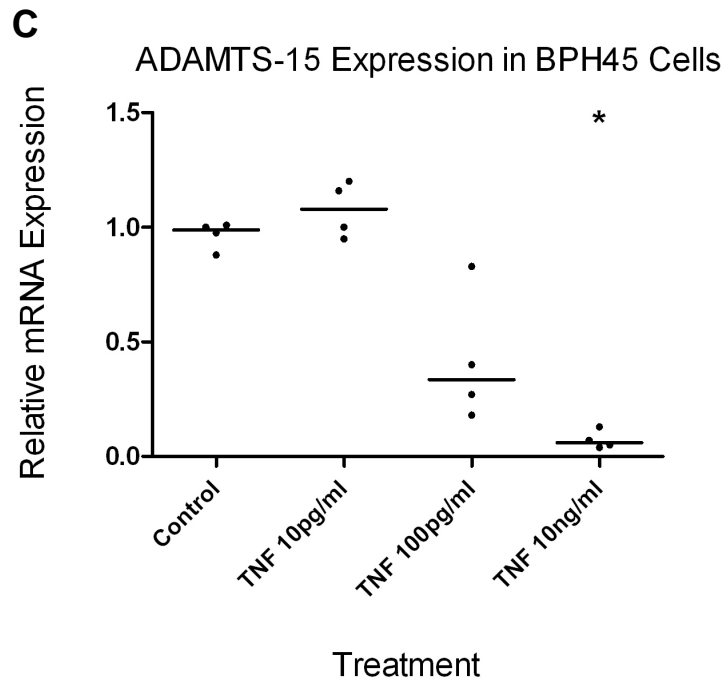
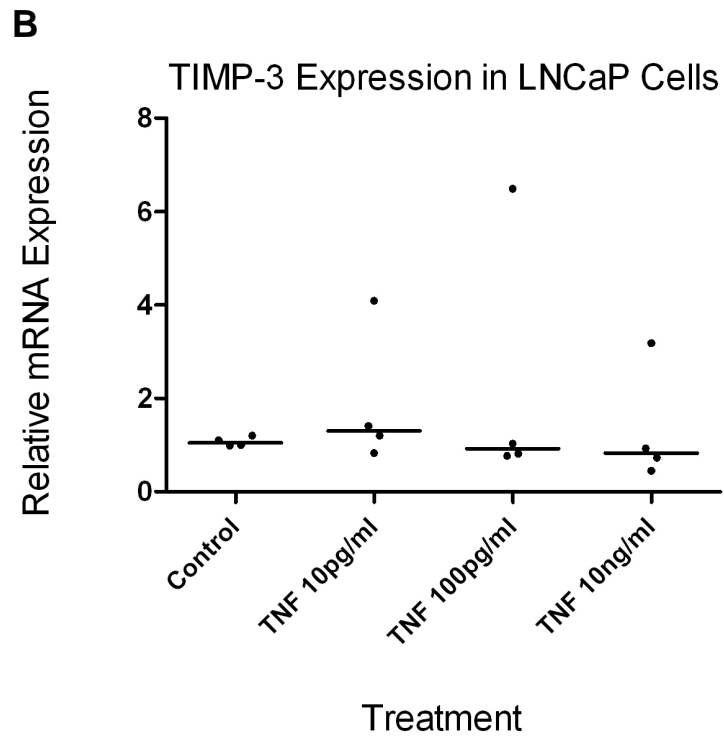
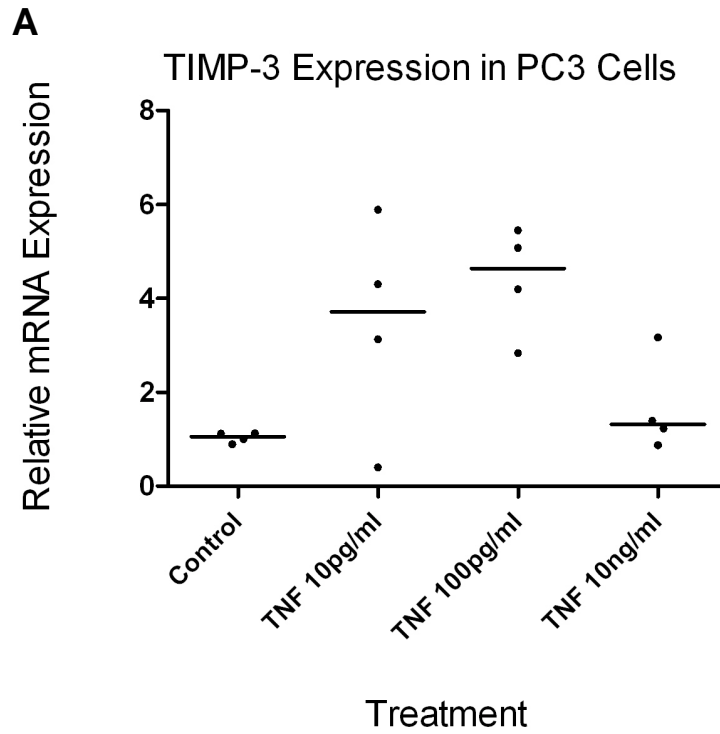


Figure 5.9: Expression of ADAMTS-15 mRNA in A) PC3, B) LNCaP and C) BPH45 cells treated with TNF. Cells were treated for 24 hours with the specified doses of TNF, lysed and cDNA was synthesized for analysis by real-time RT-PC. Results were collated from 6 separate experiments (n=6) in A and B, and 4 separate experiments (n=4) in C. Each data point represents an individual sample of cDNA. The horizontal bars denote the median expression level for each treatment group. The expression levels of ADAMTS-15 mRNA in treated cells are shown as fold changes relative to controls. The Kruskal-Wallis test for variance of the medians and Dunn's multi-comparison test were used to analyse for differences between the groups. Asterisks were used to denote treatment groups in which difference in expression levels relative to control were statistically significant ($p < 0.05$ *).

5.4.3 Regulation of TIMP-3 mRNA Expression by TNF

As with ADAMTS-15, TIMP-3 expression was down-regulated by TNF in BPH45 cells but not in PC3 and LNCaP cells (Figure 5.10). The Kruskal-Wallis test showed no

significant variance between the medians of experiments with PC3 cells ($p=0.0882$) and LNCaP cells ($p=0.4387$), but a significant variance in BPH45 cells ($p=0.0101$). Dunn's post test showed that there was significant down-regulation of TIMP-3 in BPH45 cells at a treatment dose of 10ng/ml ($p<0.01$).



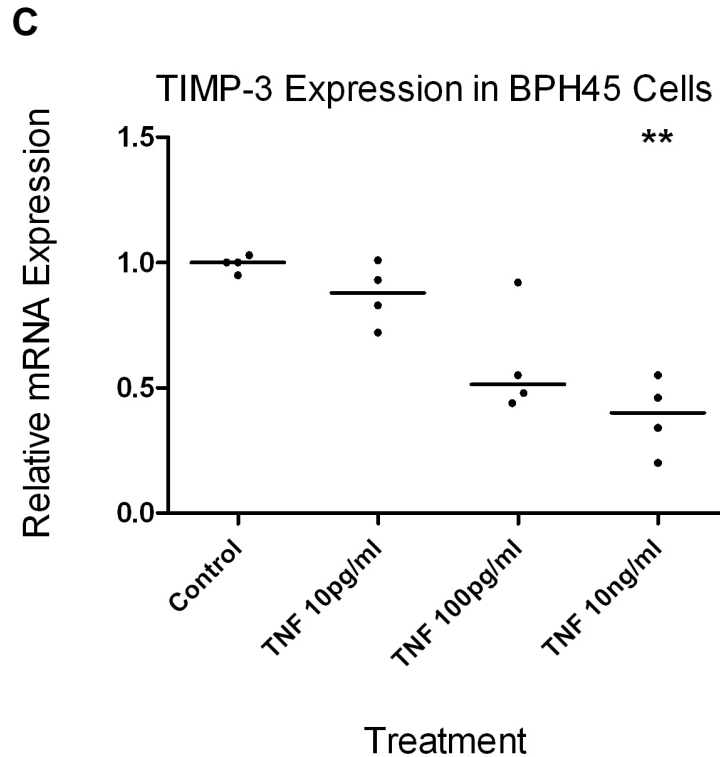


Figure 5.10: Expression of TIMP-3 mRNA in A) PC3, B) LNCaP and C) BPH45 cells treated with TNF. Cells were treated for 24 hours with the specified doses of TNF, lysed and cDNA was synthesized for analysis by real-time RT-PCR. Results were collated from 4 separate experiments ($n=4$). Each data point represents an individual sample of cDNA. The horizontal bars denote the median expression level for each treatment group. The expression levels of TIMP-3 mRNA in treated cells are shown as fold changes relative to controls. The Kruskal-Wallis test for variance of the medians and Dunn's multi-comparison test were used to analyse for differences between the groups. Asterisks were used to denote treatment groups in which difference in expression levels relative to control were statistically significant ($p<0.05$ *, $p<0.01$ **).

5.5 Discussion

In this chapter, the effects of DHT and TNF on expression of ADAMTS-1, -15 and TIMP-3 was analysed. The results are summarised in Table 5.6.

		ADAMTS-1	ADAMTS-15	TIMP-3
DHT	LNCaP	↔	↓	↓
TNF	PC3	↔	↔	↔
	LNCaP	↔	↓	↔
	BPH45	↔	↓	↓

Table 5.6: Summary of effect of DHT and TNF treatment on expression of ADAMTS-1, ADAMTS-15 and TIMP-3. Androgen-sensitive LNCaP cells were treated with DHT. PC3, LNCaP and BPH45 cells were treated with TNF. ↔ = Not regulated, ↓ = Down-regulated.

LNCaP androgen-sensitive cells were treated with DHT. DHT up-regulated PSA mRNA expression. DHT down-regulated the expression of ADAMTS-15 but had no effect on ADAMTS-1 expression. TIMP-3, an inhibitor of the ADAMTSs and other metalloproteinases, was also down-regulated by DHT. The non-steroidal AR inhibitor, flutamide did not inhibit the effect of DHT, but rather, had a similar effect of down-regulating ADAMTS-15 (Figure 5.3) and TIMP-3 (Figure 5.5). The mRNA expression data for PSA, ADAMTS-1, -15 and TIMP-3 showed variability in mRNA expression in response to DHT treatment between treatments (Figures 5.1, 5.2, 5.3, & 5.5). Previous reports have shown a similar degree of variability in ADAMTS and TIMP mRNA expression in cell lines between experiments, resulting in a wide range of expression levels (Gircz 2010; Stokes 2010). LNCaP cells in culture are an aggregate of several sub-populations of cells (Wan 2003), and different sub-clones of LNCaP cells show

varying response to androgen treatment (Iguchi 2007). Iguchi et al stimulated two different populations of LNCaP cells and found that one had a greater response to androgen in terms of proliferation and PSA expression. One or more of these factors could explain the wide range of expression levels. In keeping with its role as an androgen antagonist, flutamide has been shown to inhibit up-regulation of ADAMTS-1 by 100nM DHT in endometrial stromal cells at a concentration of 100nM (Wen 2006), and androgen receptor activation by 10pM DHT in PNT1A prostate epithelial cells at 10nM concentration (Avances 2001). Previous studies have reported that mutations in the ARs of prostate cancer cells could lead to aberrant activation by non-steroidal AR antagonists. LNCaP cells are known to have such a mutation in the LBD of the AR (Veldscholte 1992). This could account for the similar effect of DHT and flutamide on the LNCaP cells used in this study.

Androgen-regulated gene expression is mediated via the action of nuclear receptors. The activated AR binds to AREs in promoter regions of androgen regulated genes, where transcription factors are recruited by the receptor-ligand complex (Heinlein 2002). Transcription factors could either be co-activators or co-repressors. Recruitment of co-activators by the receptor will lead to increased transcription of mRNA, while recruitment of co-repressors leads to decreased transcription (Heinlein 2002). Further experiments were not performed to determine the mechanism of down-regulation of ADAMTS-15 by DHT. An *in silico* screen of the *ADAMTS1* and *ADAMTS15* genes for putative AREs found one ARE in the promoter region of *ADAMTS15* but none in the promoter region of *ADAMTS1*. Some AR co-repressors for example the transcription factor ERG, have been reported to effect down-regulation of androgen-regulated genes by forming complexes with ligand-activated AR and subsequent binding to AREs on androgen-repressed genes (Chng 2012). It is also possible that the down-regulation of

ADAMTS-15 by DHT is an indirect effect, and is mediated by interaction of other androgen regulated proteins with the transcription mechanism of *ADAMTS15* gene. Inhibition of protein synthesis by cyclohexamide attenuated AR mediated gene down-regulation (Prescott 2007), suggesting that AR acts via intermediary proteins to effect gene repression.

The search strategy used a matrix comprising nine ARE half-sites derived from six AREs that are known to functionally bind to AR. The search strategy identified putative AREs that had two half-sites (each with at least 80% similarity to any of the nine known half-sites) separated by a non-specific 3bp sequence. This strategy would therefore not detect putative non-canonical AREs with more or less than 15bp or putative 6bp ARE half-sites. In vitro studies have shown specific binding of AR to non-canonical AREs (Zhou 1997) and 6bp half-sites (Massie 2007), but functional binding and gene transcription has not been demonstrated. An analysis of the sequences of genomic AR binding sites showed that 27% were of the canonical sequence (Massie 2007). In a subsequent study by the same investigators, imposing a requirement of AR and RNA polymerase II co-binding found that 54% of identified sites were of the canonical format (Massie 2011). This indicates that binding to 6bp ARE half-sites does not necessarily lead to recruitment of the key components of the transcription mechanism. Seventy percent of the 6bp half-sites identified were located in close proximity to ETS transcription factor binding sites, and direct interaction between AR and ETS family transcription factors was required for binding at the 6bp half-sites (Massie 2007).

Several putative AREs were also found down-stream of the TSP of the *ADAMTS15* gene. This raises the possibility that one or more of these AREs could be acting as an enhancer. Unlike gene promoters, gene enhancers can be located many thousand bp upstream or downstream of the TSP (Kleinjan 2005). The *hKLK3* gene has such an

enhancer containing an ARE which is located 4,200 bp upstream of the TSP (Cleutjens 1997), and several studies have found that proportionately more AREs were located in the gene sequence than in the promoter region of androgen-regulated genes (Horie-Inoue 2004), which is in keeping with the findings in this study.

The significance of the ARE to base-pair ratio with respect to androgen up- or down-regulation is not known. Analysis of the gene sequences showed that the *hKLK3* promoter region had twice the density of putative AREs as the *FOLH1* and *ADAMTS15* promoters (Table 5.4). This may mean that more AREs are required to assemble co-activator complexes than are required for the assembly of co-repressor complexes. Further studies are required to determine if the putative AREs identified in this study are functional because *in silico* based methods can identify the presence of transcription factors associated with genes but do not test functionality (Wasserman 2004).

PC3, LNCaP and BPH45 cells were treated with TNF. TNF treatment down-regulated the expression of ADAMTS-15 in LNCaP and BPH45 cells. TNF also down-regulated TIMP-3 expression in BPH45 cells, but ADAMTS-1 expression was not modulated by TNF in any of the cell lines tested. TNF is a pro-inflammatory cytokine that may also be playing a role in prostate cancer progression. A study by Mizikami et al showed that malignant prostate epithelial cells strongly expressed TNF compared to normal epithelial cells (Mizokami 2000). This suggests that in addition to TNF produced by TAMs, tumour cells express TNF. Another study showed that TNF at a treatment dose of 200U/ml (equivalent of 12ng/ml) down-regulated AR, PSA and Epidermal Growth Factor receptor (EGFR) expression and up-regulated the expression of HLA Class I antigen in LNCaP cells (Sokoloff 1996). PC3 cells treated with TNF had down-regulated expression of MMP-2 (Gelatinase A), basic Fibroblast Growth Factor (bFGF)

and P-Cadherin. TNF treatment inhibited proliferation of LNCaP cells, but not PC3 cells (Sokoloff 1996).

Mozokami et al also showed that TNF treatment at a dose of 30ng/ml reduced the sensitivity of LNCaP cells to androgen stimulation by down-regulating AR expression, with the resulting cells forming new androgen-insensitive cell populations (Mizokami 2000). However, long term (> 3 months) treatment with 50ng/ml TNF produced LNCaP derived cells that had a greater rate of proliferation in response to DHT treatment compared to the parental LNCaP cells (Harada 2001). Results in this chapter showed that the effects of TNF were seen at doses of 100pg/ml and 10ng/ml (Figures 5.9 and 5.10). *In vivo* studies in the literature have produced mixed results, with TNF treatment having partial or no anti-tumour effect on prostate cancer xenografts (van Moorselaar 1991; van Moorselaar 1991). Clinical studies have shown that patients with advanced prostate cancer have elevated serum levels of TNF (Pfitzenmaier 2003; Michalaki 2004).

It is known that TNF could play either a pro- or anti-tumour role, depending on the site and stage of the cancer (Balkwill 2009). The body of evidence seems to suggest that TNF has anti-tumour activity in sarcomas, but minimal anti-tumour and sometimes pro-tumour activity in epithelial tumours like prostate cancer (Balkwill 2009).

It is not known with certainty the consequence of down-regulation of ADAMTS-15 and TIMP-3 in the TME. Evidence from breast cancer (Porter 2006) and colorectal cancer (Viloria 2009) suggests that ADAMTS-15 plays an anti-tumour role. TIMP-3 is an inhibitor of several MMPs, ADAMs and ADAMTSs, many of which degrade the ECM and promote prostate cancer cell invasion and metastases (Nemeth 2002; Udayakumar 2003; Aalinkeel 2004). ADAM-17 (TNF converting enzyme) is a metalloproteinase which sheds membrane-bound TNF into the ECM (Black 1997; Moss 1997). Down-

regulation of TIMP-3 by TNF could lead to an increase in ADAM-17 activity and initiate a vicious cycle creating a positive feed-back loop.

Down-regulation of TIMP-3 would lead to increased activity of ECM degrading MMPs and favour cancer cell invasion and metastasis. Decreased TIMP-3 expression would also lead to attenuation of its anti-angiogenic effect (Qi 2003) and favour metastasis. With these findings put together, the implication of the down-regulation of ADAMTS-15 and TIMP-3 by TNF in the TME is that TNF is likely playing a pro-tumour role in prostate cancer.

CHAPTER 6

KNOCK-DOWN OF ADAMTS-1 & -15 EXPRESSION & EFFECT ON PROLIFERATION, MIGRATION & INVASIVE POTENTIAL OF PC3 CELLS

CHAPTER 6:

KNOCK-DOWN OF ADAMTS-1 AND -15 EXPRESSION AND EFFECT ON PROLIFERATION, MIGRATION AND INVASIVE POTENTIAL OF PC3 CELLS

6.1 Introduction

Previous chapters in this thesis have reported on the expression of ADAMTS-1 and -15 in prostate cells and the effect of androgen and cytokine treatment on expression levels. In this chapter, results from functional assays following knock-down of ADAMTS-1 and -15 expression are presented. PC3 prostate cancer cells were used for the functional assays because of their high clonogenic and invasive properties. PC3 cells have proven metastatic potential and are representative of an advanced, poorly differentiated prostate adenocarcinoma (Kaighn 1979). PC3 cells express ADAMTS-1 and -15 (Cross 2005), and hence provided a good model system to determine the effects of ADAMTS-1 and -15 in prostate cancer progression.

Morbidity and mortality from prostate cancer is usually a consequence of local progression and metastasis of the primary tumour (Khafagy 2007). The cancer cells can invade locally; infiltrating surrounding tissues like the urethra, bladder and ureters, and eventually metastasize (Ware 1987). Metastatic spread could also occur to para-aortic lymph nodes lying adjacent to the ureters (Long 1999). Tumour infiltration of these structures could cause obstruction in the flow of urine, leading to renal failure and death (Mazur 1991; Paul 1994; Khafagy 2007). Prostate cancer also has a predilection to metastasize to bone, causing pain, pathologic fractures and spinal cord compression in the vertebrae. Metastases to the lungs and the liver could lead to respiratory and hepatic failure respectively (Long 1999; Khafagy 2007). Understanding the mechanisms by which cancer cells infiltrate surrounding tissue and metastasize is therefore of utmost importance.

The role of ADAMTS-1 and -15 in proliferation, migration and invasion were evaluated, as these are three important processes involved in tumour progression (Ware 1987; Arya 2006).

6.2 ADAMTS-1 and -15 Knock-down in PC3 Cells

A number of techniques have been used for transfection in mammalian cells. These include calcium phosphate co-precipitation (Graham 1973), lipid based transfection reagents (Chesnoy 2000) and electroporation (Chu 1987). These methods were evaluated to select the most suitable for introducing siRNA into PC3 cells to knock-down ADAMTS-1 and -15 expression.

6.2.1 Transient Knock-down

Transient knock-down can be achieved by transfecting siRNA targeted against the gene of interest into cells.

6.2.1.1 Metafectene Pro, Dharmafect 2 and Calcium Phosphate

PC3 cells were transfected according to the supplier's protocols as described in Section 2.18.3.1 for Metafectene Pro, Section 2.18.3.2 for Dharmafect 2 and Section 2.18.2 for calcium phosphate using the Profection kit (Promega) with the siGENOME (Dharmacon, Thermo Fisher) transient siRNA knock-down system (Section 2.19). According to the product data sheets, Metafectene Pro (Biontex) and Dharmafect 2 (Dharmacon, Thermo Fisher) are lipid based transfection reagents.

Knock-down of target siRNA was analysed by real-time RT-PCR at 72 hours post-transfection. ADAMTS-1 and -15 expression in non-targeting knock-down (NTC) PC3 cells was compared with expression in knock-down and WT cells. To monitor transfection efficiency, siGLO Red was transfected into separate cells using each of the transfection reagents. Transfection using each method was done in triplicate.

Using the expression of siGLO Red as an indicator, 72 hours was the approximate time that the effect of transfection peaked. Expression of siGLO Red was greatest in the cells that were transfected with Metafectene Pro, and least in the cells transfected with Dharmafect 2 (Figure 6.1). However, the cells transfected with Metafectene Pro did not appear healthy. They were rounded and remained loosely attached to the bottom of the tissue culture plate.

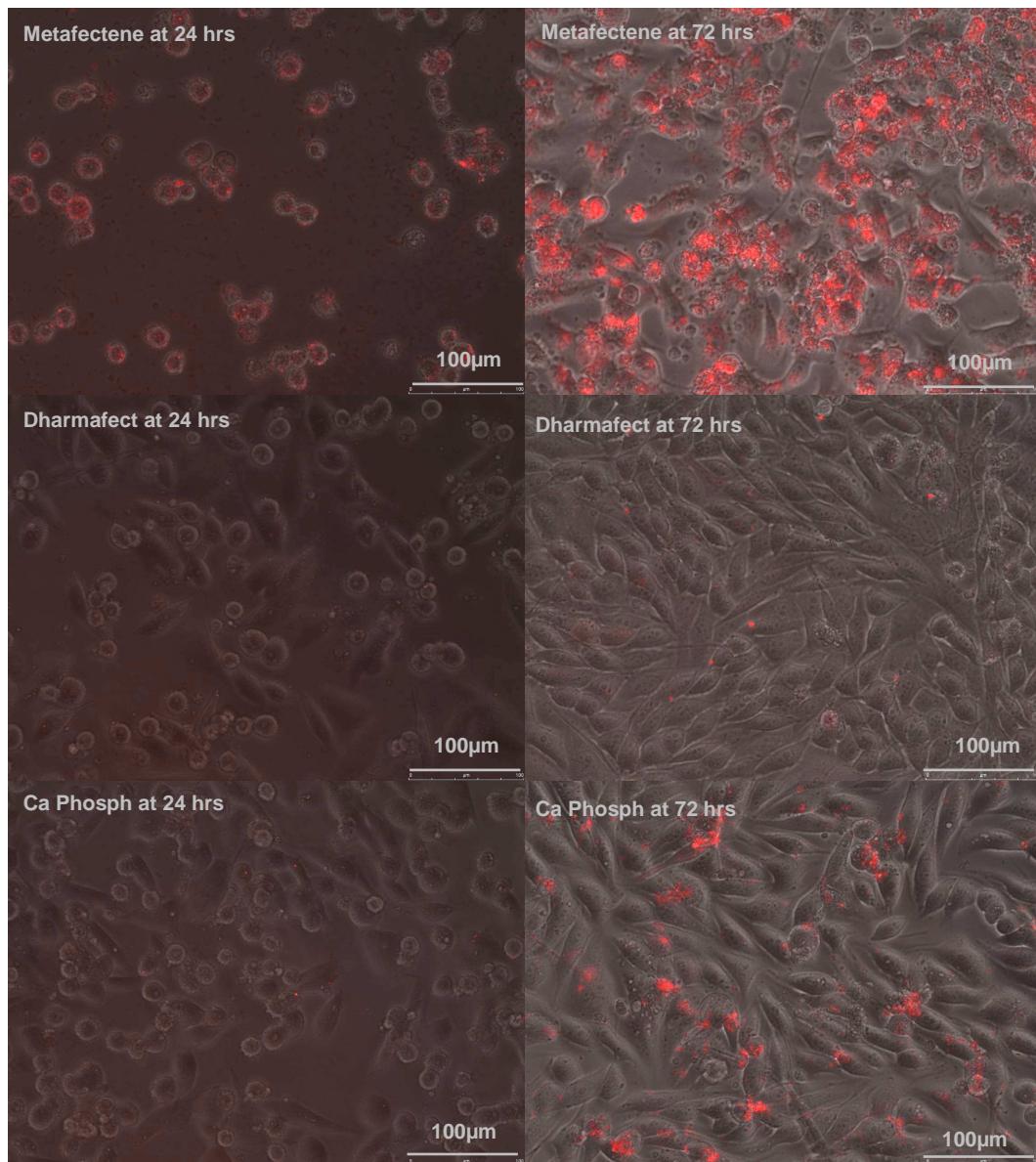


Figure 6.1: PC3 cells transfected with siGLO Red using Metafectene Pro, Dharmafect 2 and calcium phosphate transfection reagents as indicated on each photo-slide. Photo-

micrographs images were captured at 24 hours post-transfection and 72 hours post-transfection.

At 72 hours post-transfection, cells were lysed and samples prepared for real-time RT-PCR to determine expression levels of ADAMTS-1 and -15 mRNA. The results of transfection with these three agents were compared (Figure 6.2). The transfection process up-regulated ADAMTS-1 and -15 mRNA expression, evident by the higher expression of ADAMTS-1 and -15 in the non-targeting knock-down (NTC) cells compared to WT. Comparing the NTC with the knock-down cells, the highest transfection efficiency was seen with Metafectene Pro, followed by calcium phosphate. This was in keeping with the pattern of expression of siGLO Red seen in Figure 6.1. Transfection using Dharmafect 2 led to higher expression in the knock-down cells in one of the replicates of ADAMTS-1 knock-down (ATS1) and two replicates of ADAMTS-15 knock-down (ATS15). Transfection using Dharmafect 2 had previously produced as low as 80% knock-down of target genes in previous experiments (Sections 4.3.2 and 4.3.5).

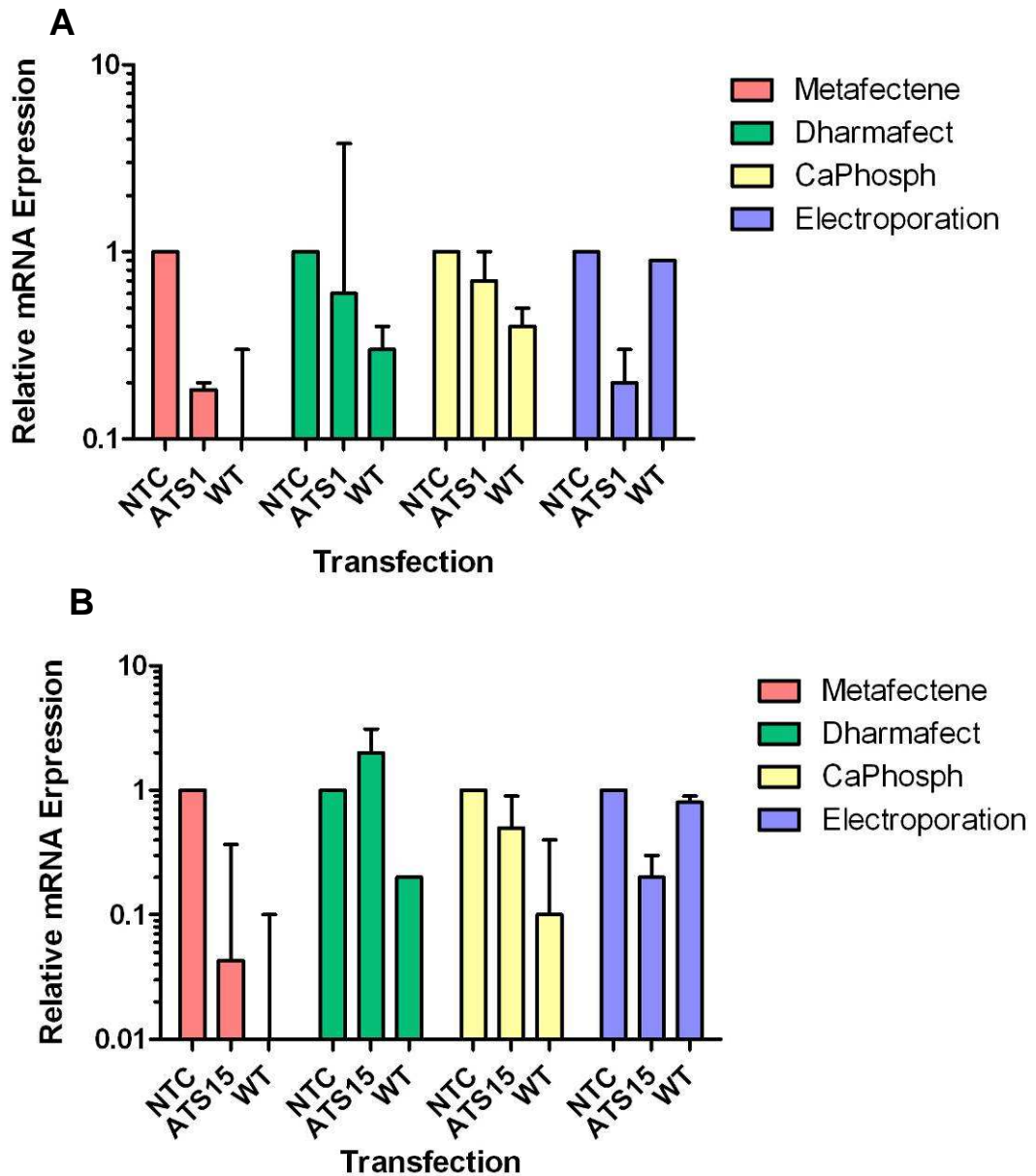


Figure 6.2: Transient transfection of PC3 cells with siRNA against ADAMTS-1 (A), and ADAMTS-15 (B). Knock-down of target siRNA was analysed by real-time RT-PCR at 72 hours post-transfection. Transfections were performed in triplicate. ADAMTS-1 expression (A) and ADAMTS-15 expression (B) were compared in non-targeting knock-down (NTC), ADAMTS-1 knock-down (ATS1), ADAMTS-15 knock-down (ATS15) and wild type (Gerhardt) PC3 cells. Median and range are displayed.

6.2.1.2 Electroporation

PC3 cells were transfected by electroporation using the Nucleofector II (Amaxa, Lonza) Kit-V which was optimised for PC3 cells by the supplier as described in Section 2.18.1 using the siGENOME (Dharmacon, Thermo Fisher) transient siRNA knock-down system (Section 2.19). Separate cells were also transfected with a non-targeting siRNA sequence (NTC). Knock-down of target siRNA was analysed by real-time RT-PCR at 72 hours post-transfection.

Cell attrition was not observed when cells were examined under the microscope at 24, 48, and 72 hours post-transfection. Electroporation resulted in knock-down of ADAMTS-1 and -15 mRNA in PC3 cells, with approximately 80% knock-down, as determined by real-time RT-PCR at 72 hours post-transfection (Figure 6.2).

6.2.2 Stable Knock-down

DNA coding for two shRNA sequences against ADAMTS-1 mRNA designated ATS1a and ATS1b were designed as described in Section 2.20. The oligonucleotides were annealed and inserted into the p-Silencer 4.1 CMV vector system (Invitrogen) using the supplier's protocol and used to transform TOP-10 competent *E.coli*. PC3 cells were transfected with DNA for either ATS1a or ATS1b by electroporation with the Nucleofector II kit (Amaxa, Lonza) as described in Section 2.18.1. An empty neomycin resistance vector (NTC) was transfected to be used as control. Successfully transfected cells were selected by growing in complete medium containing 12.5µg/ml puromycin (Invitrogen) for ATS1a or complete medium containing 500µg/ml geneticin for ATS1b in 100mm tissue culture dishes. These optimal concentrations of selection antibiotics were determined by a 'death curve'. WT PC3 cells were grown in wells containing increasing doses of the respective antibiotic. The lowest concentration of antibiotic that caused massive cell death of WT cells was selected. The antibiotic selection media

killed off cells that were not successfully expressing the puromycin or neomycin resistance genes, leaving scattered colonies of surviving cells in the dish. Clones were selected from the surviving cells using 3mm cloning discs (Sigma). The cell colonies were washed twice in PBS and trypsin-soaked cloning discs were placed on the each colony with sterile forceps for 5 minutes. The disks were picked up and placed into individual T25 flasks and the clones were left to proliferate, expanding into T75 flasks. The clones were kept under antibiotic selection pressure. Expression levels of ADAMTS-1 in the clones was analysed by real-time RT-PCR.

ATS1a and ATS1b knock-down cells produced viable clones that were expanded in culture. The NTC cells did not survive when grown in antibiotic selection media, suggesting that the neomycin resistance DNA was not being incorporated into the cellular DNA. WT PC3 cells were cloned in a similar manner as the transfected cells. Three clones were generated.

The ATS1a construct produced eight clones, while the ATS1b produced two. One of the WT clones was designated as the control, and the expression of ADAMTS-1 mRNA was determined in the other two WT clones and the ATS1a and ATS1b clones relative to the control. The most important finding was that the cloning process revealed that there was a wide range of expression between WT cells that were cloned from the same cell population (Figure 6.3). This made interpretation of the knock-down results difficult, as it was not possible to ascertain whether the differences in expression in the knock-down cells was due to a specific knock-down effect, or due to inherent differences in expression levels between clonal populations. Also, the difficulty in generating a non-targeting knock-down clone of cells to use as controls meant that the ATS1a and ATS1b clones could not be used in experiments to study the biological

functions of ADAMTS-1 in PC3 cells. For the same reasons, this knock-down system was not used for down-regulation of ADAMTS-15.

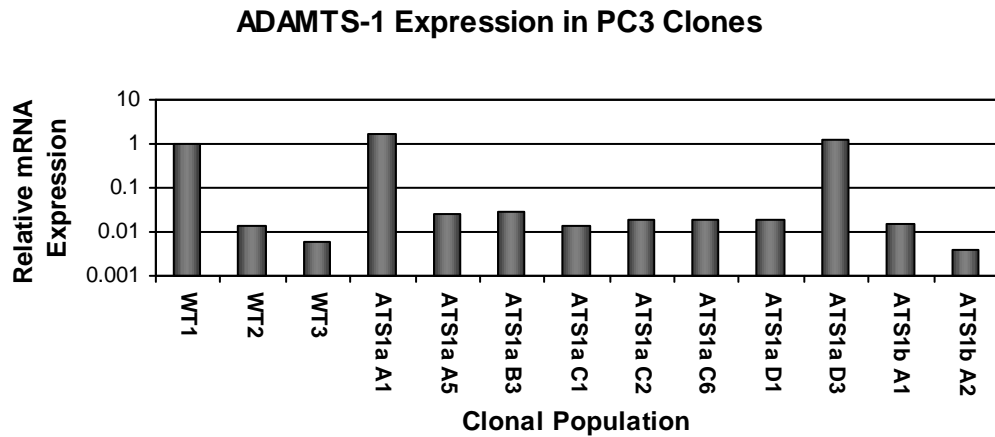


Figure 6.3: Expression levels of ADAMTS-1 mRNA in PC3 stable knock-down clones (ATS1a and ATS1b) relative to a WT PC3 cell clone (WT1). Stable transfection of DNA coding for short hairpin RNA (shRNA) against ADAMTS-1 was transfected into PC3 cells by electroporation. Following electroporation, the cells were plated in 100mm tissue culture dishes in complete medium for 24 hours. Medium was changed to antibiotic selection media and clones were selected and expanded from surviving colonies. Knock-down of target siRNA was analysed by real-time RT-PCR. Expression in two other WT clones (WT2 and WT3) was also determined. Results are from one experiment which is representative of 2 experiments.

6.3 Functional Assays

ADAMTS-1 and -15 expression was knocked down separately in PC3 cells using the transient siRNA knock-down procedure as described in Section 6.2.1.2. At 72 hours post transfection, levels of ADAMTS-1 and ADAMTS-15 expression in the ADAMTS-1 knock-down (ATS1kd) and ADAMTS-15 knock-down (ATS15kd) cells respectively was analysed relative to non-targeting control (NTC) cells using real-time RT-PCR. A

minimum of 70% knock-down was arbitrarily set for cells to be used in all of the functional assays reported below. Functional assays were commenced on Day 5 post-transfection, as previous experiments (Section 4.3.5) had shown that ADAMTS-15 protein expression was down-regulated at Day-5 post-transfection.

6.3.1 Proliferation

ADAMTSs are involved in ECM remodelling by cleaving proteoglycans (Jones 2005). The ECM acts as a reservoir for growth factors hence ECM degradation increases the bio-availability of growth factors sequestered in the ECM (Ruoslahti 1991; Schultz 2009). Down regulation of ADAMTS-1 and -15 could alter the rate of ECM proteolysis and cell proliferation.

6.3.1.1 Haemocytometer Cell Counts

Proliferation of PC3 ATS1kd and ATS15kd cells were compared to NTC cells by using direct cell counts to produce a growth curve (Jones, H.E. 1997; Wiepz 2006). Fifty thousand cells/well were plated in 12-well plates in quadruplicate in serum-free medium. Serum-free medium was used as there was no certainty that serum added to the media would not contain high enough concentrations of ADAMTS-1 or ADAMTS-15 to attenuate the effect of knock-down. At 24, 48, and 60 hours, cells were washed twice with phosphate buffered saline (PBS) and detached using trypsin-EDTA and counted using an Improved Neubauer haemocytometer (Hawksley). After each count, the cells were re-plated and incubated until the next time point.

The growth curve showed a progressive attrition of cells in all the ATS1kd, ATS15kd and NTC cells (Figure 6.4), suggesting that this method was not suitable for studying proliferation under the conditions used in our experiments. Possible reasons for the attrition of the cells were the effect of repeated trypsinisation on the cell membranes that had possibly not recovered from electroporation, and the use of serum-free medium for

the proliferation assay, which did not neutralise the trypsin when the cells were replated after each count.

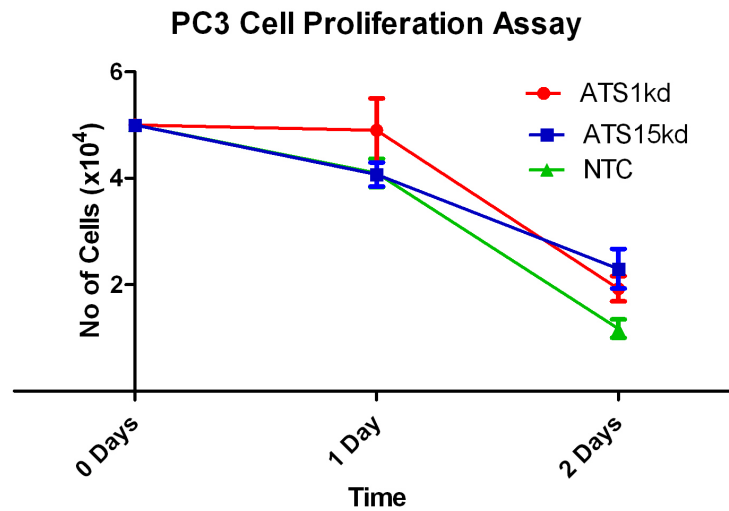


Figure 6.4: Cell proliferation assay comparing rate of proliferation in ADAMTS-1 knock-down (ATS1kd), ADAMTS-15 knock-down (ATS15kd) and non-targeting knock-down (NTC) PC3 cells using the haemocytometer count method. Knock-down levels were analysed by real-time RT-PCR at 72 hours post-transfection. At Day 5 post-transfection, 50,000 cells/well of each cell type were placed in 12-well plates in quadruplicate in serum-free medium. At 24, and 48 hours, cells were detached using trypsin-EDTA and counted using a haemocytometer. After each count, the cells were replated and incubated until the next time point. Mean (\pm) SEM is displayed. The assay was terminated at Day 2 due to the large attrition of cells.

6.3.1.2 MTT (3-[4,5-dimethylthiazol-2-yl]-2,5-diphenyl tetrazolium bromide) Assay

Proliferation of ATS1kd and ATS15kd cells were compared to NTC cells using an MTT assay (Sigma) as described in Section 2.23.2. Mitochondrial dehydrogenases of viable cells cleave the tetrazolium ring of MTT forming formazan crystals which change the colour of the solution from yellow to purple (Vistica 1991). Compared to direct cell

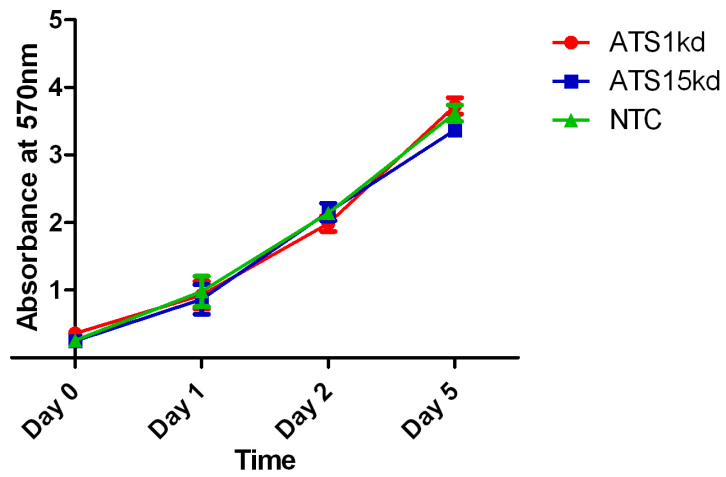
counts, the MTT assay is less labour intensive and avoids repeated trypsinisation (Wiepz 2006). Fifty thousand cells/well were plated in 12-well plates in triplicate. For each experiment, 4 sets of cells were plated, 1 set each to be counted on day 0, day 1, day 2 and day 5 of the experiment. The experiment was done three times (n=3).

Results from each experiment were plotted in the form of growth curves (Figure 6.5).

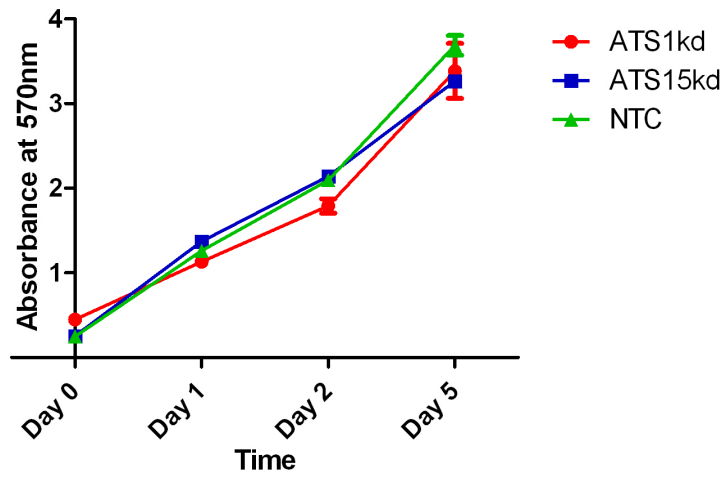
There were no significant differences in the rate of proliferation between ADAMTS-1 knock-down cells, ADAMTS-15 knock-down cells and non-targeting knock-down cells.

The experiment was not carried on beyond 5 days because using a transient knock-down system, the effect of knock-down is expected to decline with each successive cell cycle.

Experiment 1



Experiment 2



Experiment 3

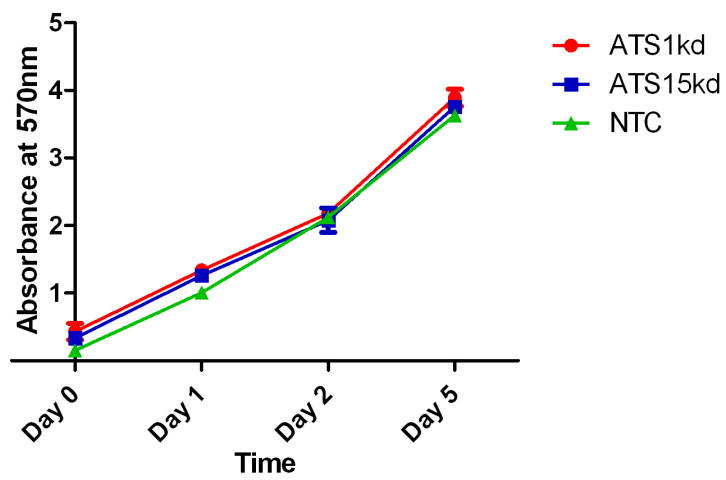


Figure 6.5: Cell proliferation assay comparing rate of proliferation in ADAMTS-1 knock-down (ATS1kd), ADAMTS-15 knock-down (ATS15kd) and non-targeting knock-down (NTC) PC3 cells using the MTT method. Knock-down levels were analysed by real-time RT-PCR at 72 hours post-transfection to ensure a minimum of 70% knock-down. At Day 5 post-transfection, 50,000 cells/well of each cell type were placed in 12-well plates in quadruplicate in serum-free medium. For each experiment, 4 sets of cells were plated, to be analysed on day 0, day 1, day 2 and day 5 of the experiment. At the designated time point, absorbance was measured using the protocol for the MTT assay. Absorbance was plotted against time. Mean (\pm) SEM is shown.

Cell Type	Time Point	P Value			Pooled
		Experiment 1	Experiment 2	Experiment 3	
ATS1kd	Day 1	0.86	0.14	0.05	0.84
	Day 2	0.26	0.05	0.48	0.1
	Day 5	0.56	0.43	0.14	0.87
ATS15kd	Day 1	0.73	0.12	0.06	0.67
	Day 2	0.91	0.57	0.83	0.93
	Day 5	0.14	0.03	0.32	0.09

Table 6.1: P values of proliferation assays done using the MTT method comparing ADAMTS-1 knock-down (ATS1kd) and ADAMTS-15 knock-down (ATS15kd) with non-targeting knock-down (NTC) PC3 cells. P values were calculated using the two-tailed unpaired t-test. P values for individual time points in each experiment are shown. Data from all three experiments were pooled and the resulting P values displayed.

6.3.2 Migration

For the purpose of this thesis, migration was defined as the movement of living cells in contact with a biologic or synthetic scaffold, from one position to another, with no physical barrier between the two positions. Motility of cancer cells is essential for

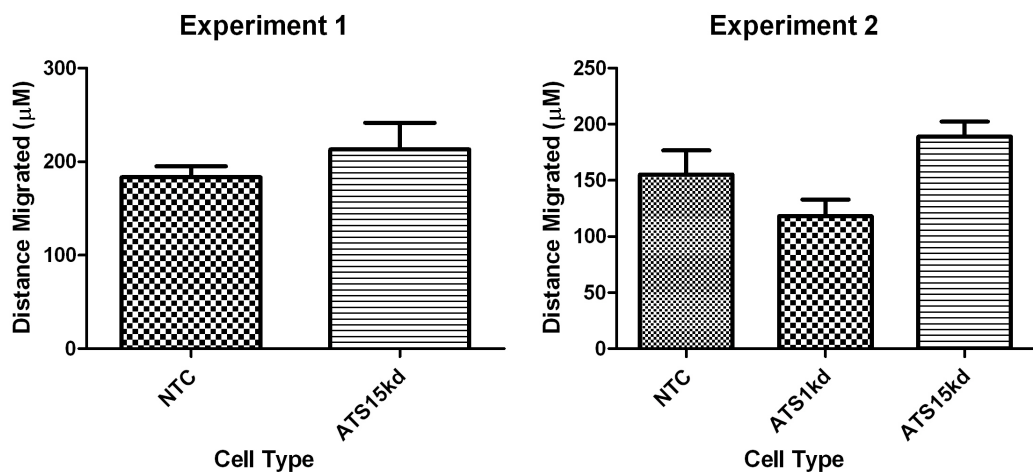
invasion and metastasis (Wolf 2003). Cell migration is a complex process requiring anterior protrusion and attachment to the ECM, localised ECM degradation and posterior detachment and retraction (Lauffenburger 1996). Gon-1, a homologue of ADAMTSs in *Caenorhabditis elegans*, mediates cell migration during gonadogenesis (Blelloch 1999). The proteoglycanase activity of ADAMTS-1 implies that it could be playing a role in ECM remodelling during migration. Also, ECM degradation could be releasing chemotactic factors that influence cell motility. ADAMTS-15 is predicted to be a proteoglycanase (Cal 2002) but its role in the ECM is not clear. The effect of ADAMTS-1 and -15 knock-down on migration was analysed using two methods, the wound healing (scratch) assay, and a modified Boyden chamber assay.

6.3.2.1 Migration using Scratch Assays

The scratch assay (O'Toole 1997; Cao 2006; Liang 2007) was used with some modifications as described in Section 2.24.1. One hundred thousand cells were plated in 12-well plates that had been pre-coated with Matrigel to act as a biological scaffold for the migrating cells. Assays were run for 24 hours. Six experiments were performed, four comparing ADAMTS-1 and -15 knock down cells with non-targeting knock-down cells, and two experiments each comparing either ADAMTS-1 or ADAMTS-15 knock-down cells with non-targeting knock-down cells. Each experiment was done in triplicate. Distance migrated was calculated by subtracting the width of the start gap from the width of the end gap as illustrated in Figure 2.7. The results of each experiment were plotted graphically (Figure 6.6) and the relative-fold difference in migration between the non-targeting knock-down and the ADAMTS knock-down cells was calculated by normalising the mean distance migrated in the non-targeting knock-down cells to 1. The relative-fold changes from Experiments 1 to 6 were pooled together and the two-tailed

paired t-test was used to analyse the results for significant differences in migration between the ADAMTS knock-down cells and the non-targeting knock-down cells.

Analysis of the pooled data from all six experiments showed no change in the migration of PC3 cells as a result of knock-down of ADAMTS-1 ($p=0.3163$) or ADAMTS-15 ($p=0.4006$).



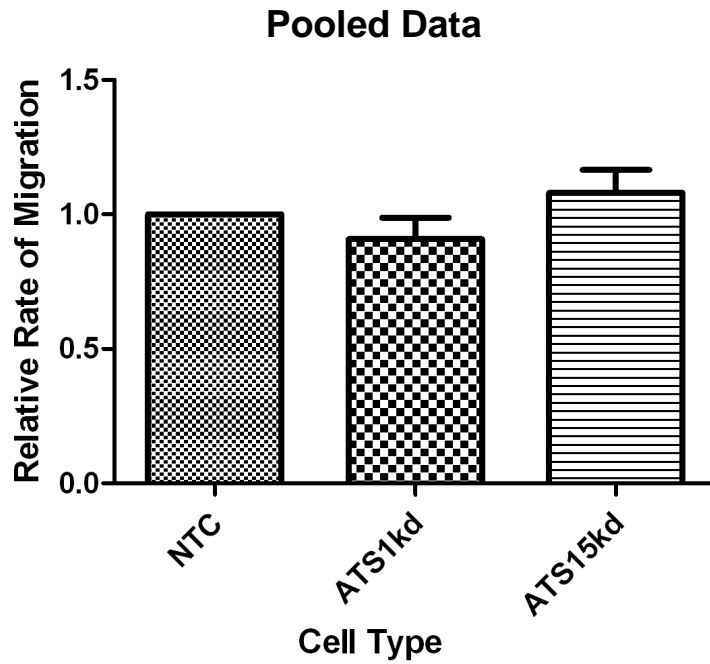
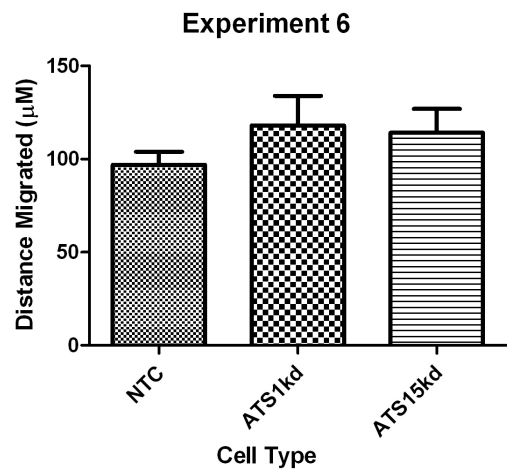
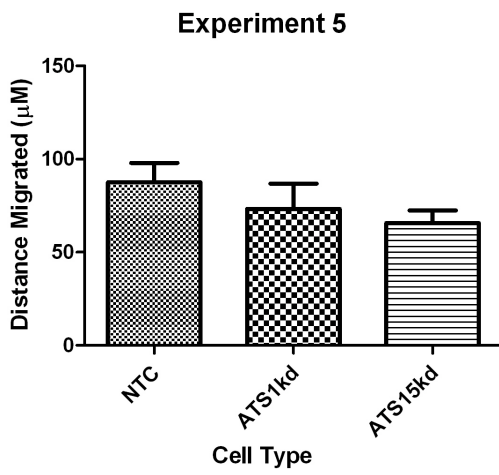
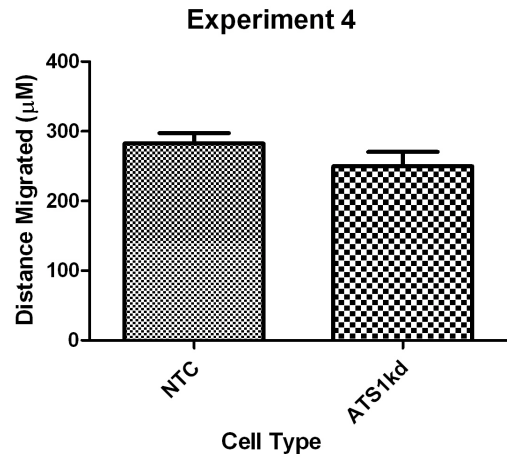
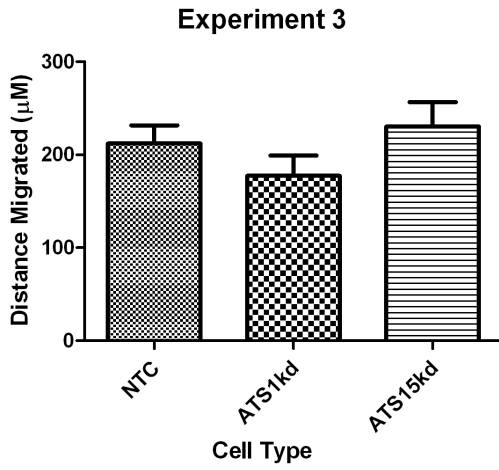


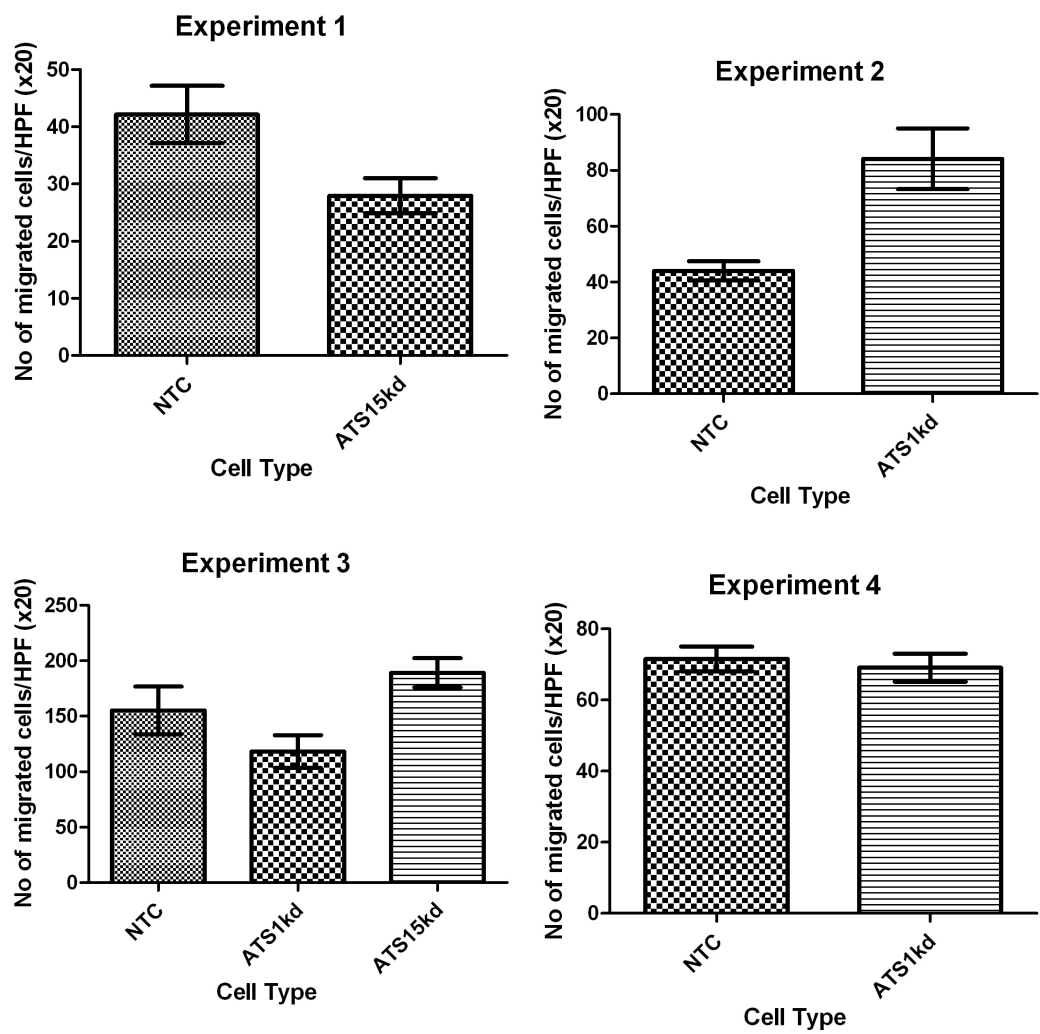
Figure 6.6: Cell migration assay comparing rate of migration in ADAMTS-1 knock-down (ATS1kd), ADAMTS-15 knock-down (ATS15kd) and non-targeting knock-down (NTC) PC3 cells using the scratch method. Six experiments were carried out, four comparing ADAMTS-1 and -15 knock down cells with non-targeting knock-down cells, and two experiments each comparing either ADAMTS-1 or ADAMTS-15 knock-down cells with non-targeting knock-down cells. Each experiment was done in triplicate. Distance migrated was plotted and the rate of migration of the knock-down cells relative to control in each experiment was calculated by normalising the distance migrated by the non-targeting knock-down cells to 1. Results of all six experiments were pooled to show relative-fold changes in migration (large graph at the bottom). The two-tailed paired t-test was used to analyse the results for significant differences in the relative migration of the ADAMTS knock-down cells compared to the non-targeting knock-down cells. Mean (\pm SEM) is shown.

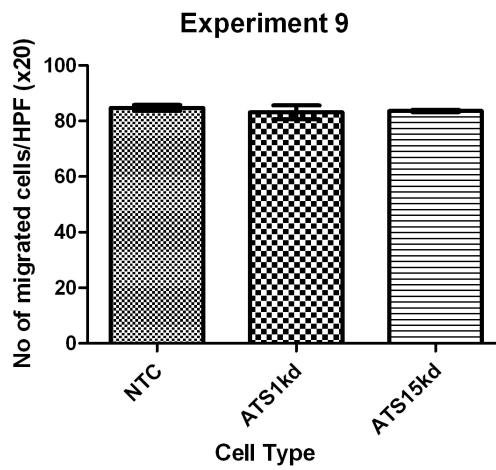
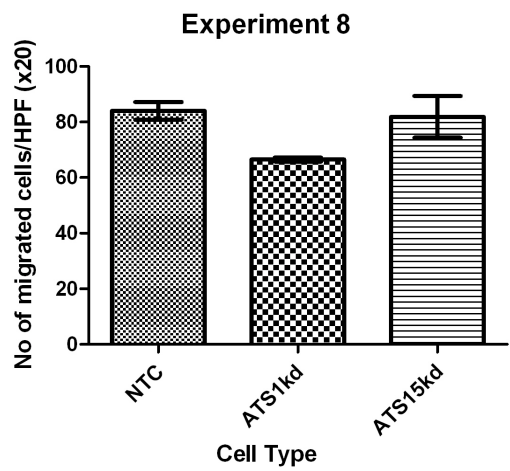
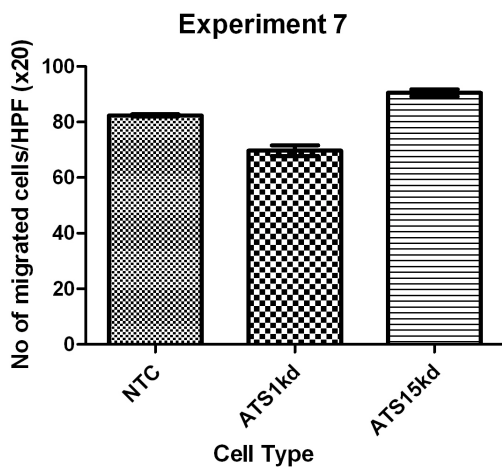
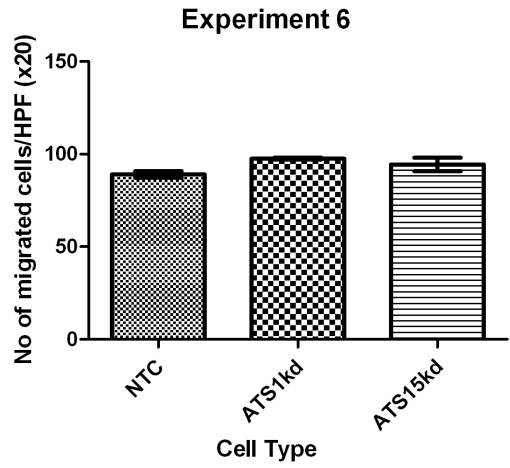
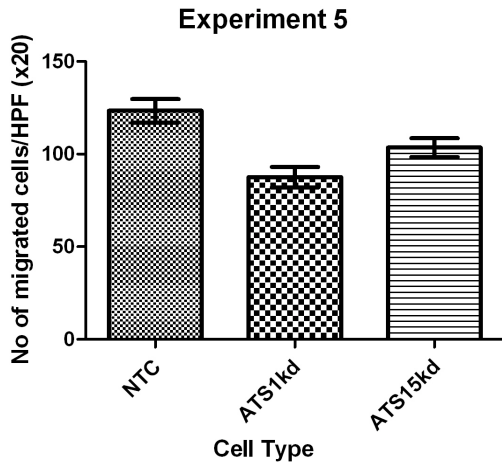
6.3.2.2 Migration using Boyden Chamber Assays

The modified Boyden chamber was adapted for use in migration assays (Albini 1987; Taniguchi 1989; Szpadarska 2001) as described in Section 2.24.2. Based on results of chemo-attraction assays reported in Section 3.5, 48 hour conditioned medium from prostatic stromal cells was placed in the lower chamber as a chemo-attractant as described in Figure 2.6. Seven-day conditioned medium was not used as there was evidence of nutritional depletion of the conditioned medium at 7 days. Assays were run for 6 hours.

Nine experiments were performed, six comparing ATS1kd cells and ATS15kd cells with NTC cells, two comparing ATS1kd cells with NTC cells and one comparing ATS15kd cells with NTC cells. Each experiment was done in triplicate. The results of

each experiment were plotted graphically (Figure 6.7). The relative difference in migration between the non-targeting knock-down and the ADAMTS knock-down cells was calculated by normalising the mean number of non-targeting knock-down cells to 1. Data from individual experiments were pooled and the two-tailed paired t-test was used to analyse the results for significant differences in the relative-fold changes in migration between the ADAMTS knock-down cells and the non-targeting knock-down cells. Analysis of the pooled data from all nine experiments showed no change in the migration of PC3 cells as a result of knock-down of ADAMTS-1 ($p=0.0649$) or ADAMTS-15 ($p=0.4696$).





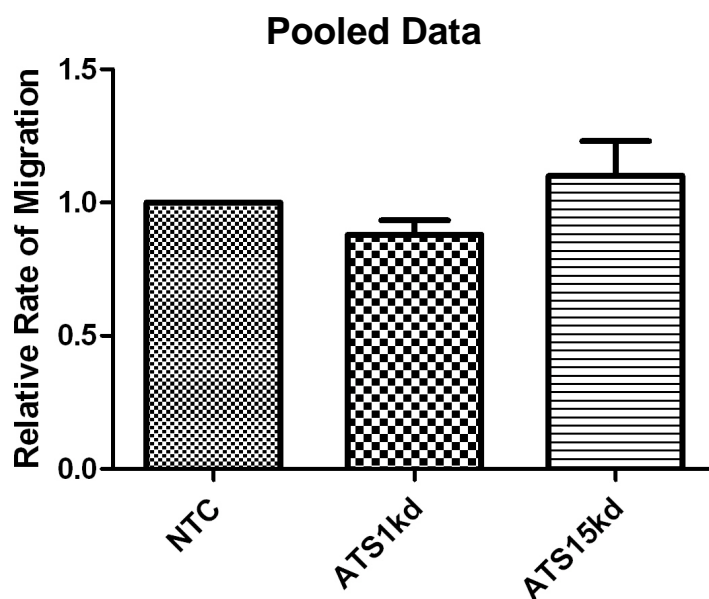


Figure 6.7: Cell migration assays comparing rate of migration in ADAMTS-1 knock-down (ATS1kd), ADAMTS-15 knock-down (ATS15kd) and non-targeting knock-down (NTC) PC3 cells using the modified Boyden chamber method. The number of cells migrating to the lower surface of the filter was counted at x20 magnification. Nine experiments were performed, six comparing ATS1kd cells and ATS15kd cells with NTC cells, two comparing ATS1kd cells with NTC cells and one comparing ATS15kd cells with NTC cells. Each experiment was done in triplicate. Number of cells migrating per high power field was plotted and the number of migrating knock-down cells relative to control in each experiment was calculated by normalising the number of migrating NTC cells to 1. Results of all the experiments were pooled to show relative changes in migration. The two-tailed paired t-test was used to analyse the results for significant differences in the relative migration of the ADAMTS knock-down cells compared to the non-targeting knock-down cells. Mean (\pm SEM) is shown.

6.3.3 Invasion

In addition to their ability to migrate, cancer cells require the ability to degrade the ECM proteins and proteoglycans that form structural barriers between tissue

compartments (Liotta 1986; Mareel 2003). For the purpose of this thesis, invasion refers to the movement of living cells in contact with a biological or synthetic scaffold, from one point to another, with a biological barrier separating the two points. Cancer cells of epithelial origin, like prostate cancer, have to breach the basement membrane underlying the epithelium in order to reach the stroma. They also have to penetrate the basement membrane encasing the endothelial cells in the vasculature in order to enter the circulation and metastasize to distant sites (Rowe 2008). Basement membranes are composed mainly of laminin and type IV collagen forming polymeric networks in a sheet-like structure (Kalluri 2003). Metalloproteinases have been implicated in the process of ECM and basement membrane degradation (Rowe 2009). The proteoglycanase properties of ADAMTS-1, and possibly ADAMTS-15, make them candidate proteinases for investigation into the mechanism of prostate cancer cell invasion.

6.3.3.1 Invasion using Boyden Chambers Assays

Invasion assays were adapted for modified Boyden chambers (Boyden 1962; Albini 1987; Taniguchi 1989; Szpaderska 2001; Albini 2007) as described in Section 2.25 using Transwell permeable polycarbonate 13mm filter wells with 8 μ m pore size (Corning, Fisher Scientific) coated with Matrigel as a biological barrier to cell migration. This experimental model mimics the process of invasion of the basement membrane. Two important variables of the invasion assay are the amount of Matrigel used to coat the filters, and the optimal length of time to run the assay. A novel method was devised to determine the assay duration for PC3 cells by allowing detection of invading cells in real-time. The polycarbonate filters were coated with 20 μ g of Matrigel. Some filters were also coated on the under-surface with Matrigel containing 50 μ g/ml of DQ-Gelatin. Based on results of chemo-attraction assays reported in Section

3.5, 48 hour conditioned medium from prostatic stromal cells was placed in the lower chamber as a chemo-attractant as described in Figure 2.6. Seven-day conditioned medium (Figure 2.8) was not used as there was evidence of nutritional depletion of the conditioned medium at 7 days. For the wells with the under-coating of DQ-Gelatin containing Matrigel, invading cells were detected by counting fluorescent spots as the invading cells proteolytically cleaved the DQ-Gelatin on the under-surface of the filter (Figure 2.8). For the wells with no DQ-Gelatin, the number of invading cells was counted either by staining the filters with haematoxylin and eosin (H&E), or with 4% (w/v) crystal violet in 95% (v/v) ethanol as described in Section 2.25.

Using the fluorescence method, the filters were examined under a fluorescence microscope every six hours. Fluorescent spots were first detected at 24 hours. The assay was continued and terminated at 48 hours. Figure 6.8 shows the appearance of the filter at 48 hours. In white light (Figure 6.8 A), it was not possible to tell which cells were above or below the polycarbonate filter. Under blue light (Figure 6.8 B), green fluorescent spots were seen which correspond to focal areas of proteolysis by invading cells. Figure 6.9 shows the appearance of invading cells on the polycarbonate filter after H&E staining.

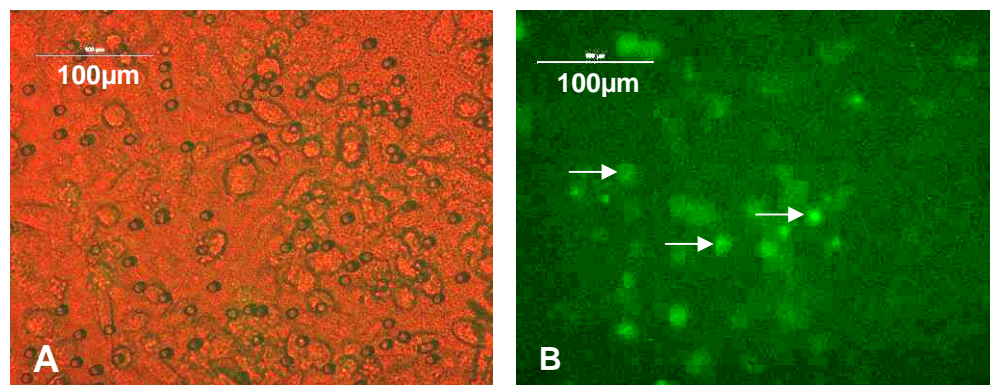


Figure 6.8: Counting invading cells after 48 hours using the fluorescence method at x 40 magnification. Invading cells can not be differentiated from non-invading cells when

the polycarbonate filter is viewed under white light in A. In blue light in B, the fluorescent spots (white arrows) emitted by the invading cells as DQ-Gelatin on the lower surface of the filter is cleaved was visualised and counted (See illustration in Figure 2.8).

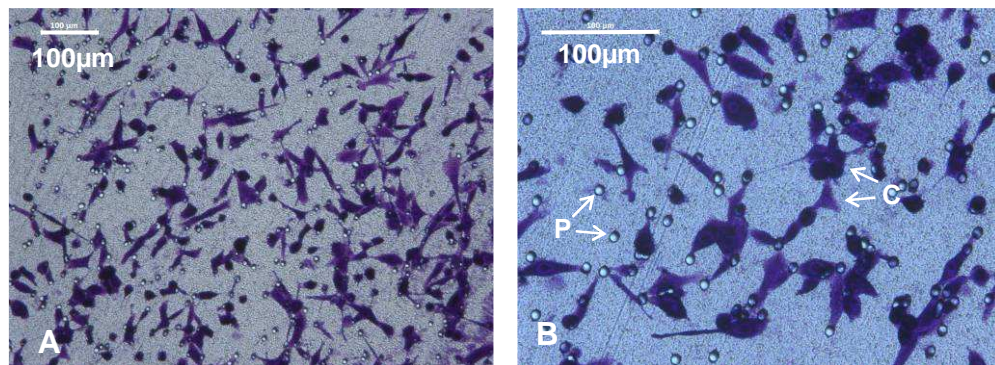


Figure 6.9: Counting invading PC3 cells after 24 hours using the H&E staining method. A, polycarbonate filter viewed at x 20 magnification and B, at x 40 magnification. Cells (C) can be differentiated from the 8µm filter pores (P).

To compare the fluorescence method with the conventional method of staining the filters before counting, invasion assays were set up as described above with triplicate wells for each counting method. The assay was run for 24 hours using 20µg of Matrigel to coat the filters. The results in Figure 6.10 showed that there was no significant difference in number of invading cells counted between the two methods using the unpaired t-test ($p=0.1704$). This implies that the fluorescent spots counted are due to proteolysis by a single cell.

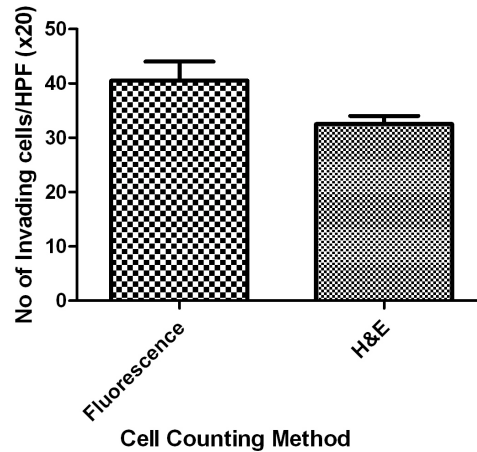
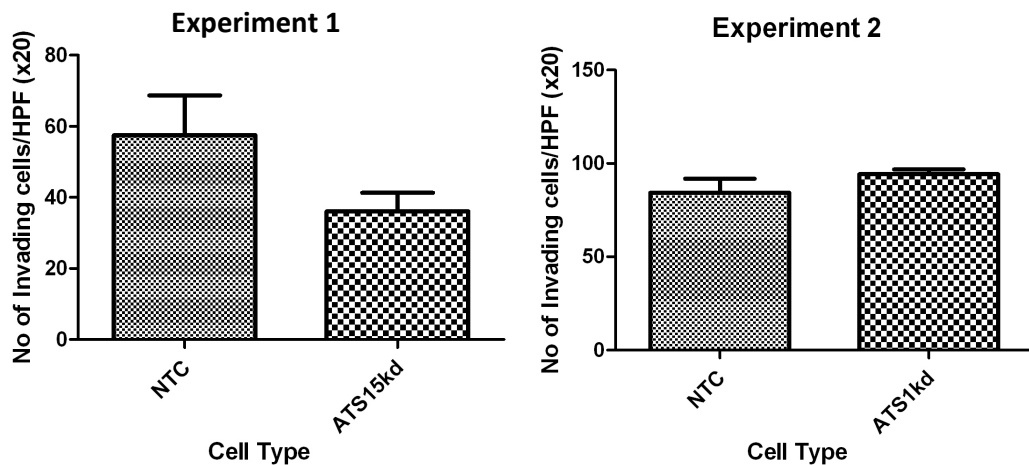
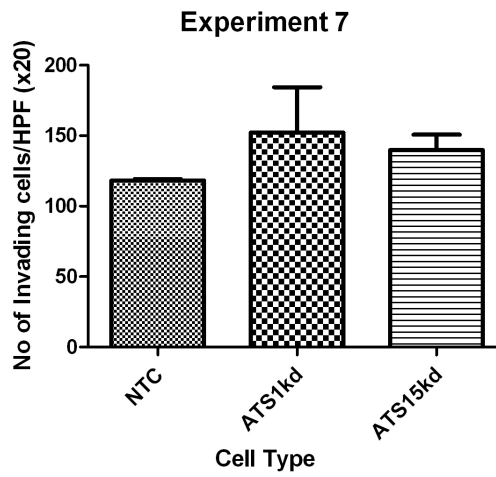
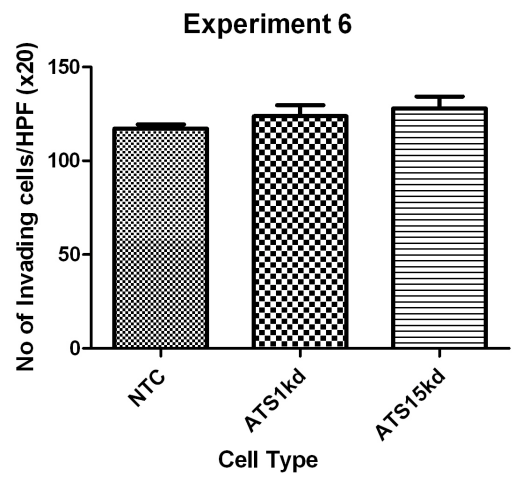
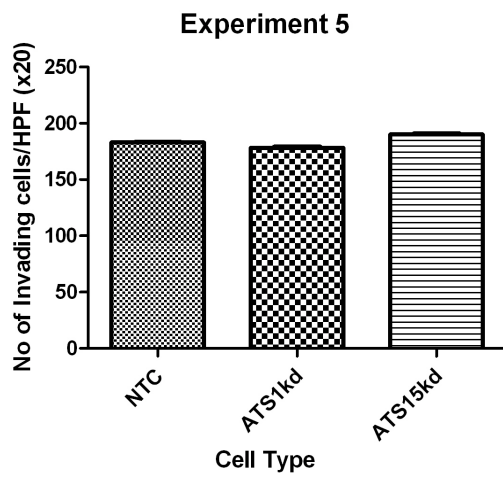
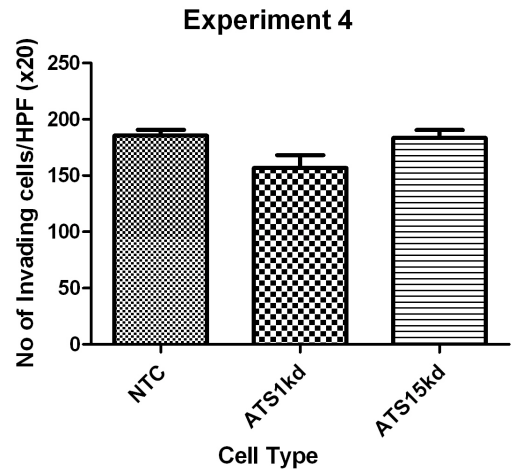
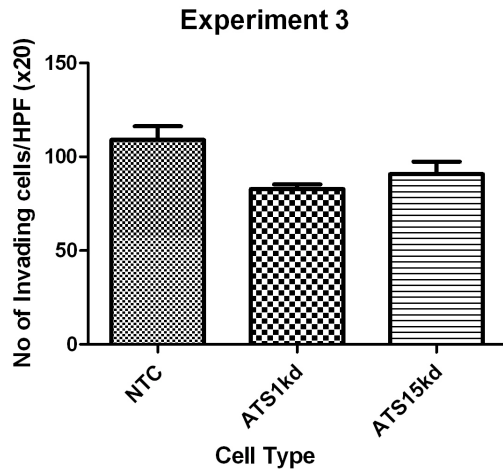


Figure 6.10: Modified Boyden chamber invasion assay comparing the fluorescence counting method with the H&E staining method. Six polycarbonate filters were coated with 20 μ g of Matrigel. Three of the filters were also coated on the under-surface with Matrigel containing 50 μ g/ml of DQ-Gelatin. The assay was stopped at 24 hours and the number of cells invading the Matrigel barrier was counted. The number of distinct fluorescent spots viewed under the microscope per high power field (hpf) was compared to the number of invading cells seen on the filters after staining with haematoxylin-eosin (H&E). Mean (\pm SEM) is shown.

The fluorescence method had shown evidence of proteolytic activity at the lower surface of the filters at 24 hours. Based on those results, the invasion assays were run for a duration of 24 hours. Polycarbonate filters were coated with 20 μ g Matrigel. Two hundred thousand PC3 cells were plated in the upper chamber of the transwell inserts in serum-free medium. Forty-eight hour conditioned medium from prostatic stromal cells was used as a chemo-attractant. The number of invading cells was counted either by staining the filters with haematoxylin and eosin (H&E), or with 4% (w/v) crystal violet in 95% (v/v) ethanol as described in Section 2.25. Four high power fields (hpf) were counted at magnification of x 20 and the mean was calculated.

Seven experiments were performed, five comparing ATS1kd cells and ATS15kd cells with NTC cells, one comparing ATS1kd cells with NTC cells and one comparing ATS15kd cells with NTC cells. Each experiment was done in triplicate. The results of each experiment were plotted graphically (Figure 6.11). The relative difference in migration between the non-targeting knock-down and ADAMTS the knock-down cells was calculated by normalising the mean number of non-targeting knock-down cells to 1. The relative changes were pooled together and the two-tailed, paired t-test was used to analyse the results for significant differences in the relative changes in migration between the ADAMTS knock-down cells and the non-targeting knock-down cells. Analysis of the pooled data from all seven experiments showed no change in the invasive potential of PC3 cells as a result of knock-down of ADAMTS-1 ($p=0.8336$) or ADAMTS-15 ($p=0.6281$).





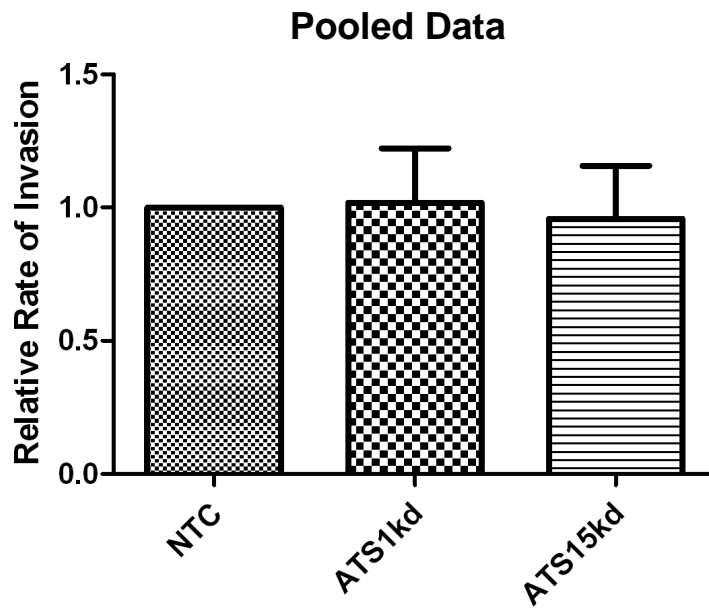


Figure 6.11: Invasion assays comparing invasive potential of ADAMTS-1 knock-down (ATS1kd), ADAMTS-15 knock-down (ATS15kd) and non-targeting knock-down (NTC) PC3 cells using the modified Boyden chamber method. The filters were coated with 20µg of Matrigel. Seven experiments were performed, five comparing ATS1kd cells and ATS15kd cells with NTC cells, one comparing ATS1kd cells with NTC cells and one comparing ATS15kd cells with NTC cells. Each experiment was done in triplicate. Number of cells invading per high power field was plotted and the number of invading knock-down cells relative to control in each experiment was calculated by normalising the number of invading NTC cells to 1. Results of all the experiments were pooled to show relative changes in invasion. The two-tailed paired t-test was used to analyse the results for significant differences in the relative invasion of the ADAMTS knock-down cells compared to the non-targeting knock-down cells. Mean (\pm SEM) is shown.

6.4 Discussion

This chapter described the use of calcium phosphate, lipid-based transfection reagents and electroporation for introducing siRNA and DNA into PC3 prostate cancer cells, and functional assays to analyse phenotypic changes.

siRNA against ADAMTS-1 and ADAMTS-15 were used to transiently knock-down expression in PC3 cells, and DNA coding an shRNA sequence against ADAMTS-1 was used in an attempt to produce stable knock-down cells.

Comparison of the transfection methods showed that the levels of knock-down achieved was variable between experiments. Metafectene Pro, a lipid-based reagent, produced the greatest knock-down effect but attrition of cells was high. Dharmafect 2, also lipid-based, produced inconsistent knock-down results but had no obvious effect on cell viability. Calcium phosphate transfection produced intermediate results and also did not have an obvious effect on cell viability. The Dharmafect 2 protocol utilised the greatest amount of siRNA (2.5µg for Dharmafect 2 compared with 0.5µg for Metafectene Pro and 0.4µg for calcium phosphate) per 30,000 cells transfected. The electroporation protocol required 2µg of siRNA for 1×10^6 PC3 cells, and produced high levels of knock-down, making it the best method to use when planning to perform experiments that required large cell numbers. For each of the transfection methods, comparing expression levels in WT and non-targeting knock-down cells suggested that the transfection process may have induced expression of ADAMTS-1 and -15 (Figure 6.2). The electroporation method produced the least of this non-specific effect. Based on these results, the electroporation method was chosen for knock-down of ADAMTS-1 and -15 for functional assays.

Stable knock-down of gene expression is preferable for functional studies because it allows for experiments to be optimised and repeated without performing transfection before each experiment. Attempts to produce stable knock-down of ADAMTS-1 in PC3 cells were unsuccessful. The protocol for the pSilencer 4.1-CMV knock-down system (Invitrogen) involved selecting clones of cells successfully expressing the selected antibiotic resistance gene. This created unexpected confounding factor in results

because WT PC3 cells had a wide range of ADAMTS-1 expression (Figure 6.4), for reasons not understood. Differences in expression between transfected cells and controls due to the variability could be mistaken for a specific knock-down effect. Presumably, if there is an inherent variability in ADAMTS-1 expression, there is likely to be variability in the expression of other proteins and molecules which could be influencing cell phenotype. Hence, differences in migration or invasion may not necessarily be due to ADAMTS-1 expression levels. This was coupled with the fact that cells transfected with the DNA for the control vector did not survive after transfection. It is unclear why the cells did not survive. The plans for producing stable knock-down PC3 cells were therefore abandoned in favour of a transient knock-down system.

Functional studies analysing the effect of ADAMTS-1 and ADAMTS-15 knock-down on PC3 cell proliferation, migration and invasion were performed using the siGENOME transient transfection system (Dharmacon, Thermo Fisher) with the electroporation method. The disadvantage of transient knock-down is that transfection of the cells with siRNA had to be done before each batch of experiments. Duration of knock-down was variable but up to 50% knock-down was seen at Day 14 post transfection in some experiments. Functional assays were started at Day 5, as western blotting showed attenuation of ADAMTS-15 protein expression at that time point (Section 4.3.5). The Boyden migration assay lasted 6 hours, the scratch migration assay and the Boyden invasion assay lasted 24 hours, and the proliferation assay lasted 5 days. Thus all the functional assays were completed within 10 days post transfection. The results of the functional studies showed that there was no effect of ADAMTS-1 or ADAMTS-15 knock-down on proliferation, migration and invasion of PC3 cells. A simple explanation for this would be that these biological functions are not dependent on ADAMTS-1 or -15 activity. However, it is possible that ADAMTS-1 and -15 activity are not manifested

in *in vitro* settings, but requires the complex interaction between cancer and stromal cells that can only be studied using *in vivo* models. In fact, a study on BZR lung cancer cells showed that ADAMTS-1 over-expression had no effect on proliferation, migration and invasion *in vitro*, but promoted tumour growth in mouse xenografts (Rocks 2008). The *in vitro* assays used by the authors were similar to those used in this study. ADAMTS-1 over-expression also induced a stromal reaction characterised by recruitment of α smooth muscle actin (α -SMA) positive cells and higher collagen, fibronectin, interleukin 1 β (IL-1 β), transforming growth factor β (TGF- β) and MMP-13 production (Rocks 2008). These findings provide further evidence of tumour-stromal interactions in cancer progression. It may be that knock-down or over-expression studies on ADAMTS-1 and -15 in prostate cancer cells using *in vivo* models could reveal important functions for these proteinases.

CHAPTER 7

GENERAL DISCUSSION, LIMITATIONS, FUTURE WORK & CONCLUSIONS

CHAPTER 7:

GENERAL DISCUSSION, LIMITATIONS, FUTURE WORK AND CONCLUSIONS

7.1 General Discussion and Limitations

The aim of this work was to demonstrate proteolytic activity in prostate cancer and stromal cells and to investigate the role of ADAMTS-1 and -15 proteinases in prostate cancer progression. ADAMTS-1 and -15 are the most highly expressed of the ADAMTSs proteins in prostate cell lines (Cross 2005). Due to the multi-domain structure of the ADAMTSs, these proteinases could be playing a number of roles. ADAMTS-1 has been more extensively studied than ADAMTS-15. The role of ADAMTS-1 as a proteolytic enzyme led to the hypothesis that ADAMTS-1 promotes prostate cancer progression by cleaving ECM components, releasing sequestered growth factors, and degrading the ECM to facilitate cancer cell migration and invasion. The function of ADAMTS-15 is not yet known. It is homologous with ADAMTS-1 (Cal 2002), which suggests that it may have proteoglycanase activity. However, reports have provided evidence that ADAMTS-15 is more likely playing an anti-tumour role in breast and colorectal cancers (Porter 2006; Vilorio 2009). This led to the hypothesis that ADAMTS-15 has an inhibitory effect on prostate cancer progression by attenuating cancer cell proliferation, migration and invasion.

Experiments in this study were designed firstly to show evidence of proteolytic activity in prostate cancer cells; secondly, to determine whether ADAMTS-1 and -15 expression is regulated by DHT and TNF; and thirdly, analyse the effect of ADAMTS-1 and -15 on prostate cancer cell proliferation, migration and invasion.

7.1.1 Proteolytic Activity of Prostate Cells

Imaging of multicellular tumour spheroids of prostate cancer and stromal cells showed evidence of proteolytic activity by invading and non-invading cells. Stromal cells emitted brighter fluorescence than cancer cells, indicating that stromal cells are active players in ECM remodelling. Co-cultures of cancer and stromal cells and chemotaxis assays showed that stromal cells released soluble chemotactic factors that attracted cancer cells to the stromal cells. The cross-talk between cancer and stromal cells is proving to be important in cancer progression. Although not analysed in this study, proteolysis is greatly enhanced in cancer cells co-cultured with stromal cells (Sameni 2003; Sloane 2005; Sloane 2006; Sameni 2009). Stromal cells have been shown to migrate and invade collectively with cancer cells and were found to be at the leading edge of the invading cell cluster (Gaggioli 2007; Gaggioli 2008). It is likely that stromal cells have a higher capacity for synthesis of ECM degrading proteinases, and cancer cells possibly are able to drive stromal cells to express higher levels of pro-tumour proteinases that facilitate tumour progression. Alternatively, prostate stromal cells may have the ability to alter cancer cell phenotype, and facilitate the progression of tumours by regulating the tumourigenic, migratory and invasive potential of cancer cells (Thalman 2010). The relative contribution of prostate cancer and stromal cells to ECM degradation warrants further study.

7.1.2 Detection of ADAMTS-1 and -15 Protein

Analysing protein expression of ADAMTS-1 and -15 presented a challenge during this study. Antibodies that were commercially available at the time of the study had not been validated in published reports to my knowledge. Generation of custom antibodies was considered to be beyond the scope of this study.

Because of the multi-domain structure of the ADAMTSs, the antibodies commercially available were raised against peptide sequences spanning a part of or a whole domain, or multiple domains. The propeptide domain of ADAMTSs is usually cleaved early in the Golgi apparatus before secretion (Bergeron 2000; Wang 2004), hence probing for the propeptide domain is a surrogate indicator of expression of the active proteinase. The catalytic domain, as the name implies, executes the proteolytic programme. Probing for this domain would give a more direct indication of the amount of active proteinase present. However other actions, for example anti-angiogenic activity as a result of VEGF binding, is effected by the thrombospondin and spacer domains in the C-terminus. The C-terminal domains are processed and cleaved off in the ECM (Rodriguez-Manzaneque 2000), and so probing for the C-terminal fragments would give only limited information on the expression levels and localisation of the catalytic domain.

The main aims of this study included the determination of the effect of androgen and cytokine stimulation on ADAMTS-1 and -15 expression, and to analyse the effect of knock-down on prostate cancer cell phenotype. Thus, the ideal antibody for these purposes would be a polyclonal antibody able to detect the full length protein, with bands of sufficient intensity to enable analyses of changes in expression due to treatment or knock-down. A search through the major antibody suppliers did not yield any anti-ADAMTS-1 or -15 antibodies with these desired specifications. Four antibodies were selected (two against ADAMTS-1 and two against ADAMTS-15). The anti-C-Terminal ADAMTS-1 antibody detected multiple bands, and the anti-catalytic domain antibody detected a band of approximately 50kDa, which was not attenuated with knock-down of ADAMTS-1 mRNA.

A considerable amount of effort was put into detection of ADAMTS-15 protein expression by western blotting using the anti-ADAMTS-15 antibody raised against the cysteine-rich domain. Techniques used included sample preparation by cell lysis, immunoprecipitation of cell lysate and conditioned medium, and heparin-agarose precipitation of cell lysate and conditioned medium. The bands detected using immunoprecipitation were found to be due to a protein from the protein A-agarose beads, most likely protein A. This was a source of error that precluded further immunoprecipitation experiments. No bands were detected with heparin-sepharose precipitation using this antibody. The anti-ADAMTS-15 propeptide antibody consistently detected a 50kDa band on western blots, which was attenuated by ADAMTS-15 knock-down. Fluorescence immunocytochemistry using this antibody showed decreased fluorescence in ADAMTS-15 knock-down cells.

The anti-ADAMTS-15 propeptide antibody was predicted by the supplier to detect ADAMTS-15 at a relative mass of 103kDa on western blotting. Western blot experiments detected bands of 50kDa which is about half the relative mass expected for the full length ADAMTS-15 protein, and twice the relative mass of the propeptide domain, which is approximately 22kDa. This suggests that ADAMTS-15 was processed post-translationally by proteolytic cleavage yielding an N-terminal fragment of 50kDa, implying that a cleavage site lies within the disintegrin-like domain of ADAMTS-15 (Figure 7.1c). The sequence homology of ADAMTS-15 and ADAMTS-1 (Cal 2002) suggests that the ADAMTS-15 disintegrin-like domain, where we predict a cleavage site lies, is a cysteine-rich domain with no disintegrin activity (Gerhardt 2007). ADAMTS proteinases are known to be C-terminally processed (Rodriguez-Manzaneque 2000; Kashiwagi 2004), and it is likely that the form of ADAMTS-15 detected as 50kDa has lost its C-terminal ancillary domains but retains the propeptide and catalytic

domains. The propeptide domain is thought to maintain the latency of the catalytic domain, and activation of the catalytic domain is mediated by cleavage by proprotein convertases such as furin (Bergeron 2000; Wang 2004). Retention of the propeptide implies that the catalytic domain of ADAMTS-15 remains inactive and thus proteolytic activity is muted. The full length ADAMTS-1 and the C-terminal region of ADAMTS-1 are reported to display pro and anti-metastatic properties respectively (Kuno 2004; Liu 2006). The C-terminal region containing three thrombospondin repeats and a spacer (Figure 7.1) is responsible for the anti-angiogenic properties of ADAMTS-1 (Kuno 2004). This region of ADAMTS-1 is very similar to the ADAMTS-15 C-terminal cleavage product that is predicted in this study (Figure 7.1), leaving propeptide and catalytic domains of 50kDa which was detected on the western blots. It is conceivable that the potential proteolytic activity of ADAMTS-15 is muted because the propeptide remains bound to the catalytic domain, and the C-terminal half of the molecule is released to function as an inhibitor of angiogenesis in the TME. It is generally accepted that prostate cancer angiogenesis correlates with disease severity (Weidner 1993; Revelos 2007). ADAMTS-15 could therefore be playing an anti-tumour role by inhibiting angiogenesis.

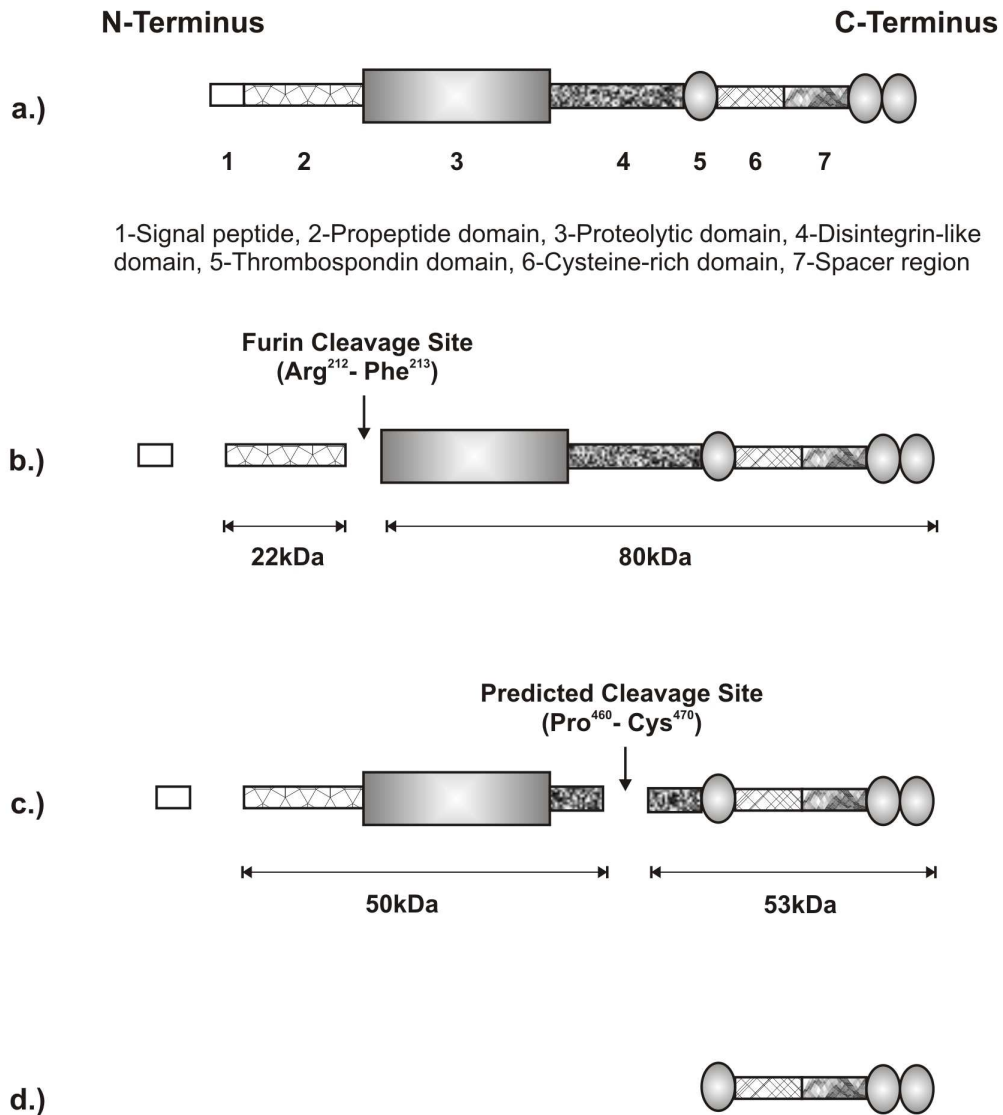


Figure 7.1: Domain structure of ADAMTS-15 and similarity of predicted cleavage products with ADAMTS-1. (a) is a schematic diagram of the domains of the full-length ADAMTS-15, (b) shows the furin cleavage site and the products that would result. Western blots did not detect a propeptide fragment of 22kDa as would be expected from cleavage at this site, (c) shows the approximate position of the predicted cleavage site that would produce a 50kDa propeptide fragment detected on western blots, and the structure of the C-terminal region that would be cleaved off. (d) Is a schematic diagram of the C-terminal region that is responsible for the anti-angiogenic activity of

ADAMTS-1. The predicted C-terminal cleavage product from ADAMTS-15 (c) is similar in structure to the anti-angiogenic region of ADAMTS-1.

Somatic mutations of *ADAMTS15* have been identified in breast and colorectal cancer cells (Sjoblom 2006; Wood 2007; Vilorio 2009). *ADAMTS15* mutations in colorectal cancer cells predict that shortened, mutant forms of ADAMTS -15 are produced (Vilorio 2009). No mutations of ADAMTS-15 have been reported in prostate cancer cells, but this could be a possible alternative explanation for the detection of a 50kDa ADAMTS-15 protein. Splice variants of ADAMTS-9, -13, -18 and -20 have been detected, which predict expression of proteins of varying lengths (Nicholson 2005). No such splice variants have been reported for ADAMTS-15, but alternative splicing could also explain the detection of a 50kDa form of ADAMTS-15.

7.1.3 Androgen Regulation of ADAMTS-15 and TIMP-3

The AR axis is important in prostate cancer pathophysiology. Normal prostate epithelial cells depend on androgen for growth stimulation (Sandberg 1980). Prostate cancer cells are initially dependent on androgen and regress when androgen stimulation is withdrawn (Huggins 1942; Lee, E.C. 2004). When hormone refractory cells evolve, AR signalling is still found to be active (Schroder 2008).

Hormone refractory progression is thought to be through one or a combination of the following mechanisms. 1.) Up-regulation of AR or co-regulator expression, causing increased sensitivity to the low concentrations of circulating androgen (Koivisto 1997; Gregory 2001; Linja 2001). 2.) Mutations in the AR, leading to ligand promiscuity and aberrant signalling by other steroid hormones, growth factors and antagonists such as Flutamide (Veldscholte 1990; Culig 1996; Taplin 1999; Zhao 2000; Hu 2009). 3.) Mutations in the AR causing the AR to be constitutively 'switched on' in a ligand-

independent manner (Hu 2009) 4.) Up-regulation of genes converting adrenal steroids to testosterone or de novo synthesis of testosterone by cancer cells and autocrine stimulation (Titus 2005; Stanbrough 2006; Mostaghel 2007; Locke 2008). The realisation that prostate cancer tumours progressing despite ADT, either in the form of medical or surgical castration, actually remain androgen dependent has led to a gradual change in terminology from 'hormone-refractory prostate cancer' (HRPC) to 'castration-resistant prostate cancer' (CRPC).

Because of the importance of AR signalling in prostate cancer progression, the effect of DHT on ADAMTS-1 and -15 was analysed. ADAMTS-15, but not ADAMTS-1 was regulated by DHT in LNCaP cells. DHT significantly down-regulated the expression of ADAMTS-15 approximately five-fold, with the maximal down-regulation at a concentration of 1nM. This concentration has been reported in previous studies to be the optimal concentration for DHT stimulated growth in LNCaP cells (Lee 1995; Okamoto 1997; Sherwood 1998). Thus the expression of ADAMTS-15 is lowest at a concentration of DHT that stimulates maximal proliferation. The implication of this is not clear but it suggests that low ADAMTS-15 expression is associated with increased LNCaP cell proliferation. TIMP-3 expression was also down-regulated by DHT, implying that DHT attenuates the inhibitory effect of TIMP-3 on metalloproteinases.

Long term management of prostate cancer usually involves androgen deprivation. Control of tumour growth at the cellular level may be partly due to higher expression of ADAMTS-15 and TIMP-3 expression in the androgen-deprived state. Androgen deprivation treatment causes depletion of circulating androgens, a situation which could increase ADAMTS-15 and TIMP-3 expression. This would conceivably result in down-regulation of proteolytic activity in the ECM and favour maintenance of normal prostate tissue architecture. The effect of flutamide was not in keeping with its function as an

AR antagonist (Peets 1974), as it did not reverse the effect of DHT. LNCaP cells have a mutation in the AR ligand binding domain in which threonine is changed to alanine at position 868 (T868A), leading to AR activation by flutamide (Veldscholte 1990; Culig 2001). The T877A mutation identified by Suzuki et al in AR from prostate cancer tumours was found to be identical to the T868A mutation in LNCaP cells (Suzuki 1996). Other AR mutations have been identified in tumours of patients with prostate cancer (Taplin 1995). Up to 68% of prostate cancer patients with disease progression while on treatment with flutamide experience disease remission when flutamide is withdrawn (Dupont 1993; Scher 1993; Herrada 1996; Sartor 2008). This phenomenon is known as the 'Anti-androgen Withdrawal Syndrome,' and provides clinical evidence that mutations in the AR of prostate cancer cells could lead to aberrant activation by flutamide.

Using an *in silico* method, the genes for ADAMTS-1 and ADAMTS-15 were screened for the presence of putative AREs. This revealed one ARE in the ADAMTS-15 gene promoter and 12 in the gene sequence. The presence of AREs provides a mechanism for the regulation of *ADAMTS15* expression by androgen. However, the effect of androgen could also occur via the action of intermediary androgen-regulated proteins that are involved in regulation of *ADAMTS15* transcription. Another possible explanation for the down-regulation by DHT of ADAMTS-15 and TIMP-3 mRNA expression could be that the action of DHT may be mediated through pathways that are independent of the AR, hence the inability of flutamide to antagonise this effect. Testosterone and DHT induce rapid increases in intracellular calcium in prostate cancer cells through non-genomic mechanisms (Lyng 2000; Sun 2006). Testosterone also induces rapid vasodilation that is not inhibited by flutamide (Yue 1995; Jones 2002; Tep-areenan 2002). This suggests

the possibility that calcium influx into LNCaP cells treated with DHT may be an alternative mechanism of ADAMTS-15 and TIMP-3 regulation.

7.1.4 TNF Regulation of ADAMTS-15 and TIMP-3

Cancer-related inflammation has been of interest to researchers for many years, dating back to Virchow in 1863 (Balkwill 2001). Virchow first identified the presence of inflammatory cells within tumours. TAMs secrete cyteine proteinases, MMPs, and an assorted array of cytokines including TNF, interleukins and interferons (Wahl 1998; Kuper 2000). TAM density in prostate tumours has been shown to predict disease progression in patients treated with hormone therapy (Nonomura 2011). The activity of TAMs could either be pro or anti-tumour. TAMs may be cytotoxic following activation (Brigati 2002; Tsung 2002), but on the other hand may produce angiogenic and lymphangiogenic proteinases and cytokines which promote tumour progression (Schoppmann 2002). Taking TNF as an example, binding and activation of the TNF receptor 1 (TNFR1) could induce pathways that lead to inflammation and cell survival via TNF receptor-associated factor 2 (TRAF2) pathway, or could induce apoptosis via the FAS-associated death domain (FADD) pathway (Balkwill 2009). The role of TNF in prostate cancer progression is not clear. Even though the name ‘tumour necrosis factor’ suggests anti-tumour activity, some studies have shown that the serum level of TNF required to cause decline in tumour growth could also be toxic to the patient (Balkwill 1992), and TNF may even promote tumour growth in certain situations (Malik 1992; Szlosarek 2006). Macrophages infiltrating the tumour site release cytokines locally as part of the inflammatory reaction to the presence of the tumour (Coussens 2002). This could explain the elevated levels of TNF in patients with advanced prostate cancer (Michalaki 2004).

Treatment of PC3, LNCaP and BPH45 cells with TNF showed that ADAMTS-15 mRNA expression was down-regulated by TNF in LNCaP and BPH45 cells, and TIMP-3 mRNA was down-regulated in BPH45 cells. It is not clear what pathway mediates the regulation of ADAMTS-15 and TIMP-3 but it is possibly via the action of nuclear factor- κ B (NF- κ B), a transcription factor that regulates the transcription of numerous genes including many proteinases (Hoffmann 2006). The online transcription factor tool CONSITE (www.phylofoot.org/consite) (Lenhard 2003) identified three NF- κ B binding sites in the *ADAMTS1* promoter, four in the *ADAMTS15* promoter, and four in the *TIMP3* promoter. ADAMTS-1 was not regulated by TNF, even though it has been regarded as an inflammation related proteinase (Kuno 1997).

Kuno et al found that ADAMTS-1 expression was up-regulated by IL-1 in colon carcinoma cells *in vitro* and by LPS in heart and kidney tissue *in vivo* (Kuno 1997). ADAMTS-1 expression was also up-regulated by IL-1 β in human uterine decidual stromal cells (Ng 2006) and by TNF in ARPE-19 retinal pigment epithelial cells (Bevitt 2003). Regulation of ADAMTS-1 by cytokines in prostate cancer cells has not been reported. It could be that ADAMTS-1 is regulated by cytokines other than TNF in the prostate cancer TME.

7.1.5 ADAMTS-1 and -15 Gene Silencing and Functional Assays

Silencing of gene expression using RNA interference is a valuable method of studying the function of specific proteins. RNA interference in the study of gene function began with the use of antisense RNA to knock-down gene expression (Izant 1984). Double-stranded RNA was later found to be more potent than single stranded antisense RNA at silencing gene expression (Fire 1998; Montgomery 1998), and has been adapted to the systems currently available (Sandy 2005). siRNA is introduced into the cell either directly by transfecting ready-made siRNA (transient transfection), or by transfecting

DNA coding for the desired siRNA sequence, which is incorporated into the nucleus and constitutively expresses the desired siRNA (stable transfection) (See Figure 2.4). Both systems have advantages and disadvantages. The main advantage of transient transfection is that it is relatively quick to set up, with the protocol involving fewer steps than are required for stable transfection. The disadvantage is that the effect of knock-down is progressively lost with each successive mitotic event due to dilution and degradation. This leaves a relatively short window for studying phenotypic changes due to gene silencing.

Stable knock-down generates clones of cells that constitutively express the desired siRNA along with resistance to a selected toxin and passes the trait to successive generations of daughter cells. Constant selection pressure has to be maintained using the toxin, usually an antibiotic. The constitutive expression of the siRNA enables long-term gene silencing, allowing *in vitro* and *in vivo* experiments to be performed over weeks and months. The protocol for stable transfection is longer, as more steps are required. Stable knock-down of ADAMTS-1 in PC3 cells was achieved in this study, but a source of error was detected.

Knock-down using the p-silencer system involved a cloning step after the cells were transfected and selected with antibiotics. Sub-clones of PC3 cells had wide variations in their expression levels for ADAMTS-1. Other proteins for example, osteoprotegerin (OPG), also show wide variations in expression even without any attempts being made to modulate expression (Dr Neil Cross, pers commun). Under these circumstances, experiments done with PC3 cells after any process of cloning is likely to be subject to error since there will not be certainty as to whether the differences in expression of the protein of interest is inherent to the cells as a result of being from different sub-clones, or as a result of modulation of expression. If the difference in expression is inherent, it

could be assumed that there may be inherent differences in expression of other proteins too. As such, any differences in phenotype may not be attributed solely to the activity of the silenced gene.

In this study, ADAMTS-1 and -15 expression was transiently down-regulated in PC3 cells using double-stranded siRNA. The *in vitro* assays used did not identify a role for ADAMTS-1 or -15 in proliferation, migration and invasion. It is possible that these results truly represent the situation in prostate cancer tumours *in vivo*. However, there are a number of alternative explanations for this. It is possible that *in vitro* assays do not sufficiently replicate the TME, and the presence of stromal cells, endothelial cells and inflammatory cells is required for activity of ADAMTS-1 and 15 to be manifested. Rocks et al found that ADAMTS-1 over-expression in BZR bronchial carcinoma cells had no effect on cell proliferation, migration and invasion using *in vitro* assays (Rocks 2008). *In vivo* assays in severe combined immunodeficiency (SCID) mice showed increased tumour sizes in ADAMTS-1 over-expressing BZR tumour xenografts and infiltration of host stromal cells. This implies that ADAMTS-1 activity in tumours is effected via recruitment of stromal cells, and explains why no effects were seen using monoculture *in vitro* assays. In contrast to these findings, ADAMTS-1 over-expression in SCP20 breast cancer cells (a derivative of the MBA-MD-231 cell line) did not lead to an increase in cell proliferation *in vivo* in nude mice (Lu 2009). No *in vivo* assays were performed in this study due to the fact that stable knock-down did not yield desirable results as explained earlier. Another possible explanation is that the sequence homology between ADAMTS-1 and -15 (Cal 2002) and the fact that both proteins evolved from the same ancestral ADAMTS protein could mean that they play mutually redundant roles in prostate cancer cells. Hence down-regulation of one or the other would lead to no phenotypic changes. Functional redundancy between other homologous ADAMTS

enzymes for example ADAMTS-4 and -5 in arthritis has not been demonstrated because *Adamts5* but not *Adamts1* or *Adamts4* knock-out mice are protected from developing arthritis (Glasson 2004; Glasson 2005; Little 2005; Stanton 2005), but redundancy between ADAMTS-1 and -15 has not been investigated. ADAMTS-1 and -15 are the most abundantly expressed ADAMTSs in prostate cells (Cross 2005), and so simultaneous knock-down may be required to reveal changes in phenotype.

7.1.6 Relevance of ADAMTS-15 Cleavage Products

Western blot experiments revealed what may well be a possible role for ADAMTS-15. If, as is predicted, ADAMTS-15 has a cleavage site at Pro⁴⁶⁰ – Cys⁴⁷⁰, the C-terminal fragment would be similar to the anti-angiogenic C-terminal of ADAMTS-1. Protein sequence alignment of Cys⁴⁷⁰ - Cys⁹⁵⁰ of ADAMTS-15 and His⁵⁵⁹ – Ser⁹⁶⁷ of ADAMTS-1 showed that 47% identity of 436 residues overlapped, with conservation of the cysteine residues predicting similar secondary structures (Figure 7.2).

```

ADAMTS-15, 456 SKPCP-YMQYCTKLWCCGTGKAKQCMVCQTRHFPWADGTSCGEGKLCLGKACVERHNLNKHR
ADAMTS-1, 496 SKHCPDAASTCSTLWCTGTSGGVLVCQTKHFPWADGTSCGEGKWCINGKCVNKTDRKHFD
** ** * ***** * ***** ***** * * **

ADAMTS-15, 515 VD--GSWAKWDPYGPCSRTCGGGVQLARRQCTNPTPANGGGKYCEGVRVKYRSCNLEPCPS
ADAMTS-1, 556 TPFHGSWGMWGPWGDCSRTCGGVQYTMRECDNFVPKNGGKYCEGKRVYRSCNLEDCED
*** * * * ***** * * * * ***** ** ***** **

ADAMTS-15, 573 SASGKSFREEQCEAFNGYNHSTNRLTLAVAWPKYSGVSPRDKCKLICRANGTGYFYVLA
ADAMTS-1, 616 N-NGKTFREEQCEAHNEFSKASFGSGPAVEWIPKYAGVSPDKRCKLICQAKGIGYFVLQ
** ***** * ** * *** ***** * ***** * * ** **

ADAMTS-15, 633 PKVVDGTLCSPDSTSVCVQGKCIKAGCDGNLGSKKRFDKCGVCGDNSKSCCKKVTGLFTKP
ADAMTS-1, 675 PKVVDGTPCSPDSTSVCVQGQCVKAGCDRIIDSKKRFDKCGVCGGNGSTCCKKISGSVTSA
***** ***** * ***** ** ***** ***** ** * *

ADAMTS-15, 693 MHGYNFVVIPAGASSIDIRQRGYKGLIGDDNYLALKNSQGKYLLNGHFVVSAVERDLVV
ADAMTS-1, 735 KPGYHDIITIPTGATNIEVKQRNRQRSRNGSFLAIKAADGTYILNGDYTLSTLEQDIMY
** ** ** * ** * ** * * * ** * * **

ADAMTS-15, 753 KGSLLRYSGTGTAVESLQASRPILEPLTVEVLSVGKMTPPRVRYSFYLPKEPREDKSSHP
ADAMTS-1, 795 KGVVLRYSGSSAALERIRSFSPLKEPLTIQVLTVGNALRPKIKYTYFVKKKKES-----
** ***** * * * ***** ** ** * * **

ADAMTS-15, 813 KDPRGPSVLHNSVLSLSSNQVEQPDDRPPARWVAGSWGPCSASCGSGLQKRAVDCRGSAGQ
ADAMTS-1, 849 -----FNAIPTFS-----AWVIEEWGECSKSCELGWORRLVECRDINGQ
* * ** ***** * * * * **

ADAMTS-15, 873 RTVPACDAAHRPVETQACGE-PCPTWELSAWSPCSSKSCGRGFQRRSLKCVGHGGRLLARD
ADAMTS-1, 888 -PASECAKEVKPASTRPCADHPCPOWLGEWSCSKTCGKYKKRSLKCLSHDGGVLSHE
* * * * ***** ** * *

ADAMTS-15, 932 QCNLHRKPQE-LDFCVLRPC
ADAMTS-1, 947 SCDPLKKPKHFDCTMAEC
* ** *** *

```

Figure 7.2: Protein sequence alignment of the C-terminal half of ADAMTS-15 and ADAMTS-1 showing the similarity between the predicted C-terminal cleavage product and the anti-angiogenic C-Terminal fragment of ADAMTS-1. The protein sequences were obtained from the Ensembl website (www.ensembl.org) and the sequences aligned using the online sequence alignment tool, SIM (www.expasy.ch/tools/sim-prot.html). The conserved cysteine residues are highlighted in grey.

The role of ADAMTS-15 in angiogenesis has not been investigated. ADAMTS-1 is known to be anti-angiogenic. Gustavsson et al have studied the expression of ADAMTS-1 in prostate cancer and the correlation with markers of angiogenesis and found that decreased ADAMTS-1 expression correlates with increased micro-vascular

density (MVD) (Gustavsson 2009). The role of ADAMTS-15 in angiogenesis in endothelial and prostate cancer cells deserves further study.

7.2 Future Work

The results from the experiments carried out during this study have answered some important questions. However some lines of investigation could not be pursued during the limited time period.

Given the chemotactic effect of stromal cell conditioned media on prostate cancer cells, and the reported role of epithelial-stromal cell interactions in cancer progression, an analysis of the changes in expression of ADAMTS-1 and -15 with stromal cell conditioned media would provide important information about possible mechanisms of regulation of ADAMTS expression. Three dimensional culture models more closely represent the *in vivo* environment than monolayer culture on plastic. The scratch migration assays and the Boyden chamber invasion assays used in this study employed the use of ECM gels to provide a biological scaffold and barrier respectively. Three dimensional models for functional assays could be further developed and validated for use in experiments in which monolayer culture would be inadequate.

The work in this thesis did not include an investigation of the role of ADAMTS-1 and -15 in angiogenesis, and also did not study the effect of simultaneous knock-down of ADAMTS-1 and -15. *In vivo* models were not used to study the effect of ADAMTS-1 and -15 knock-down on tumour progression. Future work should be directed towards the following goals. 1.) To analyse the effect of simultaneous knock-down of ADAMTS-1 and -15 on proliferation, migration and invasion and angiogenesis using *in vitro* and *in vivo* assays. 2.) To further characterise the cleavage products of ADAMTS-

15 to determine where the cleavage sites lie. 3.) Given the possibility that the cleavage products of ADAMTS-15 may have anti-angiogenic properties, the role of the fragments in angiogenesis should be investigated using *in vitro* and *in vivo* assays. A number of assays have been described for measuring angiogenesis and the effect of anti-angiogenic molecules (Staton 2004).

ADAMTS-15 was expressed in relatively small amounts in the PC3 and LNCaP cell lines used in this study. Real-time RT-PCR experiments yielded ΔC_T values of approximately 11 for ADAMTS-15 when normalised with GAPDH, and in western blotting experiments 100 μ g of protein was loaded in each lane for ADAMTS-15 bands to be detected. Therefore future functional assays could include an investigation of the effects of ADAMTS-15 over-expression on the phenotype of prostate cancer cells.

The Gleason score remains the most accurate predictor of prognosis in prostate cancer (Albertsen 1998; Buhmeida 2006). ADAMTS-1 expression is reported to have no correlation with Gleason score (Gustavsson 2009). Analysis of ADAMTS-1 and -15 expression in clinical samples was not undertaken during this study, due initially to difficulties encountered with validation of the ADAMTS-1 and -15 antibodies, and then because of time constraints. Immunohistochemistry for localisation and quantification of ADAMTS-15 would be a logical experimental step using the Abcam ab45047 antibody. Analysis of the correlation between ADAMTS-15 expression and Gleason score in prostate cancer tissue would determine whether this proteinase is a promising candidate diagnostic or prognostic marker. The use of fluorescence in-situ hybridisation can be explored for large through-put expression analyses, in conjunction with real-time RT-PCR and western blotting (Calvo 2003; Dressler 2005).

7.3 Conclusions

This thesis presents work aimed at analysing the role of ADAMTS-1 and -15 in prostate cancer progression. Prostate cancer and stromal cells execute proteolysis of ECM components as tumours grow, migrate and invade the surrounding ECM. Expression of ADAMTS-1 is not regulated by the prostate growth factor, DHT, in androgen sensitive LNCaP prostate cancer cells. Expression of ADAMTS-15 and the metalloproteinase inhibitor, TIMP-3 are down-regulated by DHT. This suggests that ADAMTS-15 and TIMP-3 expression do not favour prostate cancer progression. The action of DHT is possibly via binding of activated AR to AREs associated with the *ADAMTS15* and *TIMP3* genes. The cytokine, TNF, down-regulates ADAMTS-15 expression in LNCaP and stromal cells and TIMP-3 expression in stromal cells. ADAMTS-1 expression was not regulated by TNF. This implies that inflammation in the TME would down-regulate the expression of ADAMTS-15 and the metalloproteinase inhibitor, TIMP-3. These findings suggest an anti-tumour role for ADAMTS-15. However, knock-down of ADAMTS-1 and -15 expression in PC3 cells had no effect on proliferation, migration and invasion using *in vitro* assays, suggesting that cancer-stromal cell interactions may be required for effects of knock-down to be observed. Detection of a 50kDa pro-peptide containing fragment of ADAMTS-15 suggests the release of a C-terminal fragment with anti-angiogenic properties. These findings indicate that ADAMTS-15 may have an anti-tumour role for ADAMTS-15. This warrants further study of ADAMTS-15 in *in vivo* assays, with an emphasis on angiogenesis.

REFERENCES

9. REFERENCES

- Aalinkeel R, Nair M P, Sufrin G, Mahajan S D, Chadha K C, Chawda R P and Schwartz S A.** 2004. Gene expression of angiogenic factors correlates with metastatic potential of prostate cancer cells. *Cancer Res* 64(15): 5311-21.
- Abrahamsson P A.** 1999. Neuroendocrine differentiation in prostatic carcinoma. *Prostate* 39(2): 135-48.
- Adhami V M, Ahmad N and Mukhtar H.** 2003. Molecular targets for green tea in prostate cancer prevention. *J Nutr* 133(7 Suppl): 2417S-2424S.
- Adler H L, McCurdy M A, Kattan M W, Timme T L, Scardino P T and Thompson T C.** 1999. Elevated levels of circulating interleukin-6 and transforming growth factor-beta1 in patients with metastatic prostatic carcinoma. *J Urol* 161(1): 182-7.
- Ahlquist T, Lind G E, Costa V L, Meling G I, Vatn M, Hoff G S, Rognum T O, Skotheim R I, Thiis-Evensen E and Lothe R A.** 2008. Gene methylation profiles of normal mucosa, and benign and malignant colorectal tumors identify early onset markers. *Mol Cancer* 7: 94.
- Albertsen P C, Hanley J A, Gleason D F and Barry M J.** 1998. Competing risk analysis of men aged 55 to 74 years at diagnosis managed conservatively for clinically localized prostate cancer. *JAMA* 280(11): 975-80.
- Albini A and Benelli R.** 2007. The chemoinvasion assay: a method to assess tumor and endothelial cell invasion and its modulation. *Nat Protoc* 2(3): 504-11.
- Albini A, Iwamoto Y, Kleinman H K, Martin G R, Aaronson S A, Kozlowski J M and McEwan R N.** 1987. A rapid in vitro assay for quantitating the invasive potential of tumor cells. *Cancer Res* 47(12): 3239-45.
- Amin M B, Schultz D S, Zarbo R J, Kubus J and Shaheen C.** 1993. Computerized static DNA ploidy analysis of prostatic intraepithelial neoplasia. *Arch Pathol Lab Med* 117(8): 794-8.
- Anderson J, Abrahamsson P A, Crawford D, Miller K and Tombal B.** 2008. Management of advanced prostate cancer: can we improve on androgen deprivation therapy? *BJU Int* 101(12): 1497-501.
- Angelloz-Nicoud P and Binoux M.** 1995. Autocrine regulation of cell proliferation by the insulin-like growth factor (IGF) and IGF binding protein-3 protease system in a human prostate carcinoma cell line (PC-3). *Endocrinology* 136(12): 5485-92.
- Arya M, Bott S R, Shergill I S, Ahmed H U, Williamson M and Patel H R.** 2006. The metastatic cascade in prostate cancer. *Surg Oncol* 15(3): 117-28.
- Attiga F A, Fernandez P M, Weeraratna A T, Manyak M J and Patierno S R.** 2000. Inhibitors of prostaglandin synthesis inhibit human prostate tumor cell

invasiveness and reduce the release of matrix metalloproteinases. *Cancer Res* 60(16): 4629-37.

Aus G, Robinson D, Rosell J, Sandblom G and Varenhorst E. 2005. Survival in prostate carcinoma--outcomes from a prospective, population-based cohort of 8887 men with up to 15 years of follow-up: results from three countries in the population-based National Prostate Cancer Registry of Sweden. *Cancer* 103(5): 943-51.

Avances C, Georget V, Terouanne B, Orio F, Cussenot O, Mottet N, Costa P and Sultan C. 2001. Human prostatic cell line PNT1A, a useful tool for studying androgen receptor transcriptional activity and its differential subnuclear localization in the presence of androgens and antiandrogens. *Mol Cell Endocrinol* 184(1-2): 13-24.

Ayala A G, Ro J Y, Babaian R, Troncoso P and Grignon D J. 1989. The prostatic capsule: does it exist? Its importance in the staging and treatment of prostatic carcinoma. *Am J Surg Pathol* 13(1): 21-7.

Bailar J C, 3rd, Mellinger G T and Gleason D F. 1966. Survival rates of patients with prostatic cancer, tumor stage, and differentiation--preliminary report. *Cancer Chemother Rep* 50(3): 129-36.

Balk S P, Ko Y J and Bubley G J. 2003. Biology of prostate-specific antigen. *J Clin Oncol* 21(2): 383-91.

Balkwill F. 2006. TNF-alpha in promotion and progression of cancer. *Cancer Metastasis Rev* 25(3): 409-16.

Balkwill F. 2009. Tumour necrosis factor and cancer. *Nat Rev Cancer* 9(5): 361-71.

Balkwill F and Mantovani A. 2001. Inflammation and cancer: back to Virchow? *Lancet* 357(9255): 539-45.

Balkwill F R. 1992. Tumour necrosis factor and cancer. *Prog Growth Factor Res* 4(2): 121-37.

Bartsch G, Muller H R, Oberholzer M and Rohr H P. 1979. Light microscopic stereological analysis of the normal human prostate and of benign prostatic hyperplasia. *J Urol* 122(4): 487-91.

Bastard J P, Maachi M, Lagathu C, Kim M J, Caron M, Vidal H, Capeau J and Feve B. 2006. Recent advances in the relationship between obesity, inflammation, and insulin resistance. *Eur Cytokine Netw* 17(1): 4-12.

Baud V and Karin M. 2001. Signal transduction by tumor necrosis factor and its relatives. *Trends Cell Biol* 11(9): 372-7.

Ben-Shlomo Y, Evans S, Ibrahim F, Patel B, Anson K, Chinegwundoh F, Corbishley C, Dorling D, Thomas B, Gillatt D, Kirby R, Muir G, Nargund V, Popert R, Metcalfe C and Persad R. 2008. The risk of prostate cancer amongst black men in the United Kingdom: the PROCESS cohort study. *Eur Urol* 53(1): 99-105.

- Bergeron F, Leduc R and Day R.** 2000. Subtilase-like pro-protein convertases: from molecular specificity to therapeutic applications. *J Mol Endocrinol* 24(1): 1-22.
- Bernfield M, Gotte M, Park P W, Reizes O, Fitzgerald M L, Lincecum J and Zako M.** 1999. Functions of cell surface heparan sulfate proteoglycans. *Annu Rev Biochem* 68: 729-77.
- Berry S J, Coffey D S, Walsh P C and Ewing L L.** 1984. The development of human benign prostatic hyperplasia with age. *J Urol* 132(3): 474-9.
- Berthon P, Cussenot O, Hopwood L, Leduc A and Maitland N.** 1995. Functional expression of sv40 in normal human prostatic epithelial and fibroblastic cells - differentiation pattern of nontumorigenic cell-lines. *Int J Oncol* 6(2): 333-43.
- Beutler B and Cerami A.** 1986. Cachectin and tumour necrosis factor as two sides of the same biological coin. *Nature* 320(6063): 584-8.
- Bevitt D J, Mohamed J, Catterall J B, Li Z, Arris C E, Hiscott P, Sheridan C, Langton K P, Barker M D, Clarke M P and McKie N.** 2003. Expression of ADAMTS metalloproteinases in the retinal pigment epithelium derived cell line ARPE-19: transcriptional regulation by TNF α . *Biochim Biophys Acta* 1626(1-3): 83-91.
- Birney E, Andrews T D, Bevan P, Caccamo M, Chen Y, Clarke L, Coates G, Cuff J, Curwen V, Cutts T, Down T, Eyraas E, Fernandez-Suarez X M, Gane P, Gibbins B, Gilbert J, Hammond M, Hotz H R, Iyer V, Jekosch K, Kahari A, Kasprzyk A, Keefe D, Keenan S, Lehvaslaiho H, McVicker G, Melsopp C, Meidl P, Mongin E, Pettett R, Potter S, Proctor G, Rae M, Searle S, Slater G, Smedley D, Smith J, Spooner W, Stabenau A, Stalker J, Storey R, Ureta-Vidal A, Woodwark K C, Cameron G, Durbin R, Cox A, Hubbard T and Clamp M.** 2004. An overview of Ensembl. *Genome Res* 14(5): 925-8.
- Black P C, Mize G J, Karlin P, Greenberg D L, Hawley S J, True L D, Vessella R L and Takayama T K.** 2007. Overexpression of protease-activated receptors-1,-2, and-4 (PAR-1, -2, and -4) in prostate cancer. *Prostate* 67(7): 743-56.
- Black R A, Rauch C T, Kozlosky C J, Peschon J J, Slack J L, Wolfson M F, Castner B J, Stocking K L, Reddy P, Srinivasan S, Nelson N, Boiani N, Schooley K A, Gerhart M, Davis R, Fitzner J N, Johnson R S, Paxton R J, March C J and Cerretti D P.** 1997. A metalloproteinase disintegrin that releases tumour-necrosis factor- α from cells. *Nature* 385(6618): 729-33.
- Blelloch R and Kimble J.** 1999. Control of organ shape by a secreted metalloprotease in the nematode *Caenorhabditis elegans*. *Nature* 399(6736): 586-90.
- Bonkhoff H.** 1998. Neuroendocrine cells in benign and malignant prostate tissue: morphogenesis, proliferation, and androgen receptor status. *Prostate Suppl* 8: 18-22.
- Bordeaux J, Welsh A, Agarwal S, Killiam E, Baquero M, Hanna J, Anagnostou V and Rimm D.** 2010. Antibody validation. *Biotechniques* 48(3): 197-209.

Bostwick D G and Brawer M K. 1987. Prostatic intra-epithelial neoplasia and early invasion in prostate cancer. *Cancer* 59(4): 788-94.

Bostwick D G, de la Roza G, Dundore P, Corica F A and Iczkowski K A. 2003. Intraepithelial and stromal lymphocytes in the normal human prostate. *Prostate* 55(3): 187-93.

Bott S R, Arya M, Shergill I S and Williamson M. 2005. Molecular changes in prostatic cancer. *Surg Oncol* 14(2): 91-104.

Boyden S. 1962. The chemotactic effect of mixtures of antibody and antigen on polymorphonuclear leucocytes. *J Exp Med* 115: 453-66.

Bratt O. 2002. Hereditary prostate cancer: clinical aspects. *J Urol* 168(3): 906-13.

Bratt O. 2007. What should a urologist know about hereditary predisposition to prostate cancer? *BJU Int* 99(4): 743-7; discussion 747-8.

Brawer M K, Peehl D M, Stamey T A and Bostwick D G. 1985. Keratin immunoreactivity in the benign and neoplastic human prostate. *Cancer Res* 45(8): 3663-7.

Breslow N, Chan C W, Dhom G, Drury R A, Franks L M, Gellei B, Lee Y S, Lundberg S, Sparke B, Sternby N H and Tulinius H. 1977. Latent carcinoma of prostate at autopsy in seven areas. The International Agency for Research on Cancer, Lyons, France. *Int J Cancer* 20(5): 680-8.

Brew K, Dinakarpanthian D and Nagase H. 2000. Tissue inhibitors of metalloproteinases: evolution, structure and function. *Biochim Biophys Acta* 1477(1-2): 267-83.

Brigati C, Noonan D M, Albini A and Benelli R. 2002. Tumors and inflammatory infiltrates: friends or foes? *Clin Exp Metastasis* 19(3): 247-58.

Brinkmann A O, Blok L J, de Ruiter P E, Doesburg P, Steketee K, Berrevoets C A and Trapman J. 1999. Mechanisms of androgen receptor activation and function. *J Steroid Biochem Mol Biol* 69(1-6): 307-13.

Brooks J D 2007. Anatomy of the lower urinary tract and male genitalia. *Campbell-Walsh Urology*. K. L. R. Wein A.J., Novick A.C., Partin A.W., Peters C.A. Philadelphia, Saunders Elsevier. 1: 38-77.

Bubendorf L, Schopfer A, Wagner U, Sauter G, Moch H, Willi N, Gasser T C and Mihatsch M J. 2000. Metastatic patterns of prostate cancer: an autopsy study of 1,589 patients. *Hum Pathol* 31(5): 578-83.

Buhmeida A, Pyrhonen S, Laato M and Collan Y. 2006. Prognostic factors in prostate cancer. *Diagn Pathol* 1: 4.

- Burns-Cox N, Avery N C, Gingell J C and Bailey A J.** 2001. Changes in collagen metabolism in prostate cancer: a host response that may alter progression. *J Urol* 166(5): 1698-701.
- Byrne R L, Leung H and Neal D E.** 1996. Peptide growth factors in the prostate as mediators of stromal epithelial interaction. *Br J Urol* 77(5): 627-33.
- Cailleau R, Olive M and Cruciger Q V.** 1978. Long-term human breast carcinoma cell lines of metastatic origin: preliminary characterization. *In Vitro* 14(11): 911-5.
- Cal S, Arguelles J M, Fernandez P L and Lopez-Otin C.** 2001. Identification, characterization, and intracellular processing of ADAM-TS12, a novel human disintegrin with a complex structural organization involving multiple thrombospondin-1 repeats. *J Biol Chem* 276(21): 17932-40.
- Cal S, Obaya A J, Llamazares M, Garabaya C, Quesada V and Lopez-Otin C.** 2002. Cloning, expression analysis, and structural characterization of seven novel human ADAMTSs, a family of metalloproteinases with disintegrin and thrombospondin-1 domains. *Gene* 283(1-2): 49-62.
- Calvo B F, Levine A M, Marcos M, Collins Q F, Iacocca M V, Caskey L S, Gregory C W, Lin Y, Whang Y E, Earp H S and Mohler J L.** 2003. Human epidermal receptor-2 expression in prostate cancer. *Clin Cancer Res* 9(3): 1087-97.
- Camussi G, Albano E, Tetta C and Bussolino F.** 1991. The molecular action of tumor necrosis factor-alpha. *Eur J Biochem* 202(1): 3-14.
- Cao C, Sun Y, Healey S, Bi Z, Hu G, Wan S, Kouttab N, Chu W and Wan Y.** 2006. EGFR-mediated expression of aquaporin-3 is involved in human skin fibroblast migration. *Biochem J* 400(2): 225-34.
- Cao J, Hymowitz M, Conner C, Bahou W F and Zucker S.** 2000. The propeptide domain of membrane type 1-matrix metalloproteinase acts as an intramolecular chaperone when expressed in trans with the mature sequence in COS-1 cells. *J Biol Chem* 275(38): 29648-53.
- Cardoso L E, Falcao P G and Sampaio F J.** 2004. Increased and localized accumulation of chondroitin sulphate proteoglycans in the hyperplastic human prostate. *BJU Int* 93(4): 532-8.
- Chen D, Adenekan B, Chen L, Vaughan E D, Gerald W, Feng Z and Knudsen B S.** 2004. Syndecan-1 expression in locally invasive and metastatic prostate cancer. *Urology* 63(2): 402-7.
- Chen L M, Hodge G B, Guarda L A, Welch J L, Greenberg N M and Chai K X.** 2001. Down-regulation of prostatic serine protease: a potential invasion suppressor in prostate cancer. *Prostate* 48(2): 93-103.
- Chesnoy S and Huang L.** 2000. Structure and function of lipid-DNA complexes for gene delivery. *Annu Rev Biophys Biomol Struct* 29: 27-47.

- Chinegwundoh F, Enver M, Lee A, Nargund V, Oliver T and Ben-Shlomo Y.** 2006. Risk and presenting features of prostate cancer amongst African-Caribbean, South Asian and European men in North-east London. *BJU Int* 98(6): 1216-20.
- Chng K R, Chang C W, Tan S K, Yang C, Hong S Z, Sng N Y and Cheung E.** 2012. A transcriptional repressor co-regulatory network governing androgen response in prostate cancers. *EMBO J* 31(12): 2810-23.
- Chomczynski P and Sacchi N.** 1987. Single-step method of RNA isolation by acid guanidinium thiocyanate-phenol-chloroform extraction. *Anal Biochem* 162(1): 156-9.
- Chrambach A and Rodbard D.** 1971. Polyacrylamide gel electrophoresis. *Science* 172(982): 440-51.
- Chu G, Hayakawa H and Berg P.** 1987. Electroporation for the efficient transfection of mammalian cells with DNA. *Nucleic Acids Res* 15(3): 1311-26.
- Chuan Y C, Pang S T, Cedazo-Minguez A, Norstedt G, Pousette A and Flores-Morales A.** 2006. Androgen induction of prostate cancer cell invasion is mediated by ezrin. *J Biol Chem* 281(40): 29938-48.
- Chung L W, Baseman A, Assikis V and Zhau H E.** 2005. Molecular insights into prostate cancer progression: the missing link of tumor microenvironment. *J Urol* 173(1): 10-20.
- Civantos F, Marcial M A, Banks E R, Ho C K, Speights V O, Drew P A, Murphy W M and Soloway M S.** 1995. Pathology of androgen deprivation therapy in prostate carcinoma. A comparative study of 173 patients. *Cancer* 75(7): 1634-41.
- Claessens F and Gewirth D T.** 2004. DNA recognition by nuclear receptors. *Essays Biochem* 40: 59-72.
- Clark L C, Dalkin B, Krongrad A, Combs G F, Jr., Turnbull B W, Slate E H, Witherington R, Herlong J H, Janosko E, Carpenter D, Borosso C, Falk S and Rounder J.** 1998. Decreased incidence of prostate cancer with selenium supplementation: results of a double-blind cancer prevention trial. *Br J Urol* 81(5): 730-4.
- Cleland W W.** 1964. Dithiothreitol, a New Protective Reagent for Sh Groups. *Biochemistry* 3: 480-2.
- Cleutjens K B, van der Korput H A, van Eekelen C C, van Rooij H C, Faber P W and Trapman J.** 1997. An androgen response element in a far upstream enhancer region is essential for high, androgen-regulated activity of the prostate-specific antigen promoter. *Mol Endocrinol* 11(2): 148-61.
- Coffey R N, Watson R W, O'Neill A J, Mc Eleny K and Fitzpatrick J M.** 2002. Androgen-mediated resistance to apoptosis. *Prostate* 53(4): 300-9.

- Cohen J H, Kristal A R and Stanford J L.** 2000. Fruit and vegetable intakes and prostate cancer risk. *J Natl Cancer Inst* 92(1): 61-8.
- Colella R and Casey S F.** 2003. Decreased activity of cathepsins L + B and decreased invasive ability of PC3 prostate cancer cells. *Biotech Histochem* 78(2): 101-8.
- Colella R, Goodwyn E and Gopal P.** 2002. Increased cell density decreases cysteine proteinase inhibitor activity and increases invasive ability of two prostate tumor cell lines. *Cancer Lett* 185(2): 163-72.
- Colige A, Nuytinck L, Hausser I, van Essen A J, Thiry M, Herens C, Ades L C, Malfait F, Paepe A D, Franck P, Wolff G, Oosterwijk J C, Smitt J H, Lapiere C M and Nusgens B V.** 2004. Novel types of mutation responsible for the dermatosparactic type of Ehlers-Danlos syndrome (Type VIIC) and common polymorphisms in the ADAMTS2 gene. *J Invest Dermatol* 123(4): 656-63.
- Colige A, Sieron A L, Li S W, Schwarze U, Petty E, Wertelecki W, Wilcox W, Krakow D, Cohn D H, Reardon W, Byers P H, Lapiere C M, Prockop D J and Nusgens B V.** 1999. Human Ehlers-Danlos syndrome type VII C and bovine dermatosparaxis are caused by mutations in the procollagen I N-proteinase gene. *Am J Hum Genet* 65(2): 308-17.
- Colige A, Vandenberghe I, Thiry M, Lambert C A, Van Beeumen J, Li S W, Prockop D J, Lapiere C M and Nusgens B V.** 2002. Cloning and characterization of ADAMTS-14, a novel ADAMTS displaying high homology with ADAMTS-2 and ADAMTS-3. *J Biol Chem* 277(8): 5756-66.
- Collin S M, Martin R M, Metcalfe C, Gunnell D, Albertsen P C, Neal D, Hamdy F, Stephens P, Lane J A, Moore R and Donovan J.** 2008. Prostate-cancer mortality in the USA and UK in 1975-2004: an ecological study. *Lancet Oncol* 9(5): 445-52.
- Collins A T, Habib F K, Maitland N J and Neal D E.** 2001. Identification and isolation of human prostate epithelial stem cells based on alpha(2)beta(1)-integrin expression. *J Cell Sci* 114(Pt 21): 3865-72.
- Collins A T and Maitland N J.** 2006. Prostate cancer stem cells. *Eur J Cancer* 42(9): 1213-8.
- Colombel M, Filleur S, Fournier P, Merle C, Guglielmi J, Courtin A, Degeorges A, Serre C M, Bouvier R, Clezardin P and Cabon F.** 2005. Androgens repress the expression of the angiogenesis inhibitor thrombospondin-1 in normal and neoplastic prostate. *Cancer Res* 65(1): 300-8.
- Coughlin S R and Camerer E.** 2003. PARTicipation in inflammation. *J Clin Invest* 111(1): 25-7.
- Coussens L M and Werb Z.** 2002. Inflammation and cancer. *Nature* 420(6917): 860-7.
- Crissman J D, Sakr W A, Hussein M E and Pontes J E.** 1993. DNA quantitation of intraepithelial neoplasia and invasive carcinoma of the prostate. *Prostate* 22(2): 155-62.

Cross A K, Haddock G, Stock C J, Allan S, Surr J, Bunning R A, Buttle D J and Woodroffe M N. 2006. ADAMTS-1 and -4 are up-regulated following transient middle cerebral artery occlusion in the rat and their expression is modulated by TNF in cultured astrocytes. *Brain Res* 1088(1): 19-30.

Cross N A, Chandrasekharan S, Jokonya N, Fowles A, Hamdy F C, Buttle D J and Eaton C L. 2005. The expression and regulation of ADAMTS-1, -4, -5, -9, and -15, and TIMP-3 by TGFbeta1 in prostate cells: relevance to the accumulation of versican. *Prostate* 63(3): 269-75.

Culig Z, Hobisch A, Cronauer M V, Radmayr C, Hittmair A, Zhang J, Thurnher M, Bartsch G and Klocker H. 1996. Regulation of prostatic growth and function by peptide growth factors. *Prostate* 28(6): 392-405.

Culig Z, Hoffmann J, Erdel M, Eder I E, Hobisch A, Hittmair A, Bartsch G, Utermann G, Schneider M R, Parczyk K and Klocker H. 1999. Switch from antagonist to agonist of the androgen receptor bicalutamide is associated with prostate tumour progression in a new model system. *Br J Cancer* 81(2): 242-51.

Culig Z, Klocker H, Bartsch G and Hobisch A. 2001. Androgen receptor mutations in carcinoma of the prostate: significance for endocrine therapy. *Am J Pharmacogenomics* 1(4): 241-9.

Cunha G R, Ricke W, Thomson A, Marker P C, Risbridger G, Hayward S W, Wang Y Z, Donjacour A A and Kurita T. 2004. Hormonal, cellular, and molecular regulation of normal and neoplastic prostatic development. *J Steroid Biochem Mol Biol* 92(4): 221-36.

Cunha G R, Tuohimaa P and Visakorpi T. 2004. Steroids and prostate cancer. *J Steroid Biochem Mol Biol* 92(4): 219-20.

Davie E W. 2003. A brief historical review of the waterfall/cascade of blood coagulation. *J Biol Chem* 278(51): 50819-32.

Dawson R M C, Elliott D C, Elliott W H and Jones K M, Eds. 1986. Data for Biochemical Research. Oxford, Clarendon Press.

de Jong F H, Oishi K, Hayes R B, Bogdanowicz J F, Raatgever J W, van der Maas P J, Yoshida O and Schroeder F H. 1991. Peripheral hormone levels in controls and patients with prostatic cancer or benign prostatic hyperplasia: results from the Dutch-Japanese case-control study. *Cancer Res* 51(13): 3445-50.

De Marzo A M, Platz E A, Sutcliffe S, Xu J, Gronberg H, Drake C G, Nakai Y, Isaacs W B and Nelson W G. 2007. Inflammation in prostate carcinogenesis. *Nat Rev Cancer* 7(4): 256-69.

Demircan K, Gunduz E, Gunduz M, Beder L B, Hirohata S, Nagatsuka H, Cengiz B, Cilek M Z, Yamanaka N, Shimizu K and Ninomiya Y. 2009. Increased mRNA

expression of ADAMTS metalloproteinases in metastatic foci of head and neck cancer. *Head Neck* 31(6): 793-801.

Demircan K, Hirohata S, Nishida K, Hatipoglu O F, Oohashi T, Yonezawa T, Apte S S and Ninomiya Y. 2005. ADAMTS-9 is synergistically induced by interleukin-1beta and tumor necrosis factor alpha in OUMS-27 chondrosarcoma cells and in human chondrocytes. *Arthritis Rheum* 52(5): 1451-60.

Deng X, He G, Levine A, Cao Y and Mullins C. 2008. Adenovirus-mediated expression of TIMP-1 and TIMP-2 in bone inhibits osteolytic degradation by human prostate cancer. *Int J Cancer* 122(1): 209-18.

Doyle K M, Russell D L, Sriraman V and Richards J S. 2004. Coordinate transcription of the ADAMTS-1 gene by luteinizing hormone and progesterone receptor. *Mol Endocrinol* 18(10): 2463-78.

Drachenberg D E, Elgamal A A, Rowbotham R, Peterson M and Murphy G P. 1999. Circulating levels of interleukin-6 in patients with hormone refractory prostate cancer. *Prostate* 41(2): 127-33.

Dranoff G. 2004. Cytokines in cancer pathogenesis and cancer therapy. *Nat Rev Cancer* 4(1): 11-22.

Dressler L G, Berry D A, Broadwater G, Cowan D, Cox K, Griffin S, Miller A, Tse J, Novotny D, Persons D L, Barcos M, Henderson I C, Liu E T, Thor A, Budman D, Muss H, Norton L and Hayes D F. 2005. Comparison of HER2 status by fluorescence in situ hybridization and immunohistochemistry to predict benefit from dose escalation of adjuvant doxorubicin-based therapy in node-positive breast cancer patients. *J Clin Oncol* 23(19): 4287-97.

Dubail J, Kesteloot F, Deroanne C, Motte P, Lambert V, Rakic J M, Lapiere C, Nusgens B and Colige A. 2010. ADAMTS-2 functions as anti-angiogenic and anti-tumoral molecule independently of its catalytic activity. *Cell Mol Life Sci*.

Dunn J R, Panutsopoulos D, Shaw M W, Heighway J, Dormer R, Salmo E N, Watson S G, Field J K and Liloglou T. 2004. METH-2 silencing and promoter hypermethylation in NSCLC. *Br J Cancer* 91(6): 1149-54.

Dunn J R, Reed J E, du Plessis D G, Shaw E J, Reeves P, Gee A L, Warnke P and Walker C. 2006. Expression of ADAMTS-8, a secreted protease with antiangiogenic properties, is downregulated in brain tumours. *Br J Cancer* 94(8): 1186-93.

Dupont A, Gomez J L, Cusan L, Koutsilieris M and Labrie F. 1993. Response to flutamide withdrawal in advanced prostate cancer in progression under combination therapy. *J Urol* 150(3): 908-13.

Earnshaw W C, Martins L M and Kaufmann S H. 1999. Mammalian caspases: structure, activation, substrates, and functions during apoptosis. *Annu Rev Biochem* 68: 383-424.

Eeles R A, Kote-Jarai Z, Al Olama A A, Giles G G, Guy M, Severi G, Muir K, Hopper J L, Henderson B E, Haiman C A, Schleutker J, Hamdy F C, Neal D E, Donovan J L, Stanford J L, Ostrander E A, Ingles S A, John E M, Thibodeau S N, Schaid D, Park J Y, Spurdle A, Clements J, Dickinson J L, Maier C, Vogel W, Dork T, Rebbeck T R, Cooney K A, Cannon-Albright L, Chappuis P O, Hutter P, Zeegers M, Kaneva R, Zhang H W, Lu Y J, Foulkes W D, English D R, Leongamornlert D A, Tymrakiewicz M, Morrison J, Ardern-Jones A T, Hall A L, O'Brien L T, Wilkinson R A, Saunders E J, Page E C, Sawyer E J, Edwards S M, Dearnaley D P, Horwich A, Huddart R A, Khoo V S, Parker C C, Van As N, Woodhouse C J, Thompson A, Christmas T, Ogden C, Cooper C S, Southey M C, Lophatananon A, Liu J F, Kolonel L N, Le Marchand L, Wahlfors T, Tammela T L, Auvinen A, Lewis S J, Cox A, FitzGerald L M, Koopmeiners J S, Karyadi D M, Kwon E M, Stern M C, Corral R, Joshi A D, Shahabi A, McDonnell S K, Sellers T A, Pow-Sang J, Chambers S, Aitken J, Gardiner R A, Batra J, Kedda M A, Lose F, Polanowski A, Patterson B, Serth J, Meyer A, Luedeke M, Stefflova K, Ray A M, Lange E M, Farnham J, Khan H, Slavov C, Mitkova A, Cao G and Easton D F. 2009. Identification of seven new prostate cancer susceptibility loci through a genome-wide association study. *Nat Genet* 41(10): 1116-21.

Eeles R A, Kote-Jarai Z, Giles G G, Olama A A, Guy M, Jugurnauth S K, Mulholland S, Leongamornlert D A, Edwards S M, Morrison J, Field H I, Southey M C, Severi G, Donovan J L, Hamdy F C, Dearnaley D P, Muir K R, Smith C, Bagnato M, Ardern-Jones A T, Hall A L, O'Brien L T, Gehr-Swain B N, Wilkinson R A, Cox A, Lewis S, Brown P M, Jhavar S G, Tymrakiewicz M, Lophatananon A, Bryant S L, Horwich A, Huddart R A, Khoo V S, Parker C C, Woodhouse C J, Thompson A, Christmas T, Ogden C, Fisher C, Jamieson C, Cooper C S, English D R, Hopper J L, Neal D E and Easton D F. 2008. Multiple newly identified loci associated with prostate cancer susceptibility. *Nat Genet* 40(3): 316-21.

Elsasser-Beile U, Przytulski B, Gierschner D, Grussenmeyer T, Katzenwadel A, Leiber C, Deckart A and Wetterauer U. 2000. Comparison of the activation status of tumor infiltrating and peripheral lymphocytes of patients with adenocarcinomas and benign hyperplasia of the prostate. *Prostate* 45(1): 1-7.

Englaro W, Bahadoran P, Bertolotto C, Busca R, Derijard B, Livolsi A, Peyron J F, Ortonne J P and Ballotti R. 1999. Tumor necrosis factor alpha-mediated inhibition of melanogenesis is dependent on nuclear factor kappa B activation. *Oncogene* 18(8): 1553-9.

Epstein J I. 1996. The diagnosis and reporting of adenocarcinoma of the prostate in core needle biopsy specimens. *Cancer* 78(2): 350-6.

Escribano J M and Tabares E. 1987. Proteins specified by African swine fever virus: V. Identification of immediate early, early and late proteins. *Arch Virol* 92(3-4): 221-32.

Etminan M, FitzGerald J M, Gleave M and Chambers K. 2005. Intake of selenium in the prevention of prostate cancer: a systematic review and meta-analysis. *Cancer Causes Control* 16(9): 1125-31.

- Etminan M, Takkouche B and Caamano-Isorna F.** 2004. The role of tomato products and lycopene in the prevention of prostate cancer: a meta-analysis of observational studies. *Cancer Epidemiol Biomarkers Prev* 13(3): 340-5.
- Fajardo L F, Kwan H H, Kowalski J, Prionas S D and Allison A C.** 1992. Dual role of tumor necrosis factor-alpha in angiogenesis. *Am J Pathol* 140(3): 539-44.
- Fernandez-Catalan C, Bode W, Huber R, Turk D, Calvete J J, Lichte A, Tschesche H and Maskos K.** 1998. Crystal structure of the complex formed by the membrane type 1-matrix metalloproteinase with the tissue inhibitor of metalloproteinases-2, the soluble progelatinase A receptor. *EMBO J* 17(17): 5238-48.
- Festuccia C, Gravina G L, Angelucci A, Millimaggi D and Bologna M.** 2000. Culture conditions modulate cell phenotype and cause selection of subpopulations in PC3 prostate cancer cell line. *Anticancer Res* 20(6B): 4367-71.
- Fields G B, Netzel-Arnett S J, Windsor L J, Engler J A, Birkedal-Hansen H and Van Wart H E.** 1990. Proteolytic activities of human fibroblast collagenase: hydrolysis of a broad range of substrates at a single active site. *Biochemistry* 29(28): 6670-7.
- Fire A, Xu S, Montgomery M K, Kostas S A, Driver S E and Mello C C.** 1998. Potent and specific genetic interference by double-stranded RNA in *Caenorhabditis elegans*. *Nature* 391(6669): 806-11.
- Foley R, Lawler M and Hollywood D.** 2004. Gene-based therapy in prostate cancer. *Lancet Oncol* 5(8): 469-79.
- Forneris F, Wu J and Gros P.** 2012. The modular serine proteases of the complement cascade. *Curr Opin Struct Biol* 22(3): 333-41.
- Fowlkes J L, Enghild J J, Suzuki K and Nagase H.** 1994. Matrix metalloproteinases degrade insulin-like growth factor-binding protein-3 in dermal fibroblast cultures. *J Biol Chem* 269(41): 25742-6.
- Frederiks W M and Mook O R.** 2004. Metabolic mapping of proteinase activity with emphasis on in situ zymography of gelatinases: review and protocols. *J Histochem Cytochem* 52(6): 711-22.
- Freimann S, Ben-Ami I, Dantes A, Armon L, Ben Ya'cov-Klein A, Ron-El R and Amsterdam A.** 2005. Differential expression of genes coding for EGF-like factors and ADAMTS1 following gonadotropin stimulation in normal and transformed human granulosa cells. *Biochem Biophys Res Commun* 333(3): 935-43.
- Freshney R I** 2005. *Culture of animal cells : a manual of basic technique*. Hoboken, N.J., Wiley-Liss, Chichester : John Wiley [distributor].
- Friedrich B, Jung K, Lein M, Turk I, Rudolph B, Hampel G, Schnorr D and Loening S A.** 1999. Cathepsins B, H, L and cysteine protease inhibitors in malignant

prostate cell lines, primary cultured prostatic cells and prostatic tissue. *Eur J Cancer* 35(1): 138-44.

Fujikawa K, Suzuki H, McMullen B and Chung D. 2001. Purification of human von Willebrand factor-cleaving protease and its identification as a new member of the metalloproteinase family. *Blood* 98(6): 1662-6.

Fujita K, Ewing C M, Sokoll L J, Elliott D J, Cunningham M, De Marzo A M, Isaacs W B and Pavlovich C P. 2008. Cytokine profiling of prostatic fluid from cancerous prostate glands identifies cytokines associated with extent of tumor and inflammation. *Prostate* 68(8): 872-82.

Furuya S, Kumamoto Y, Yokoyama E, Tsukamoto T, Izumi T and Abiko Y. 1982. Alpha-adrenergic activity and urethral pressure in prostatic zone in benign prostatic hypertrophy. *J Urol* 128(4): 836-9.

Gaggioli C. 2008. Collective invasion of carcinoma cells: when the fibroblasts take the lead. *Cell Adh Migr* 2(1): 45-7.

Gaggioli C, Hooper S, Hidalgo-Carcedo C, Grosse R, Marshall J F, Harrington K and Sahai E. 2007. Fibroblast-led collective invasion of carcinoma cells with differing roles for RhoGTPases in leading and following cells. *Nat Cell Biol* 9(12): 1392-400.

Ganpule A P, Desai M R, Desai M M, Wani K D and Bapat S D. 2004. Natural history of lower urinary tract symptoms: preliminary report from a community-based Indian study. *BJU Int* 94(3): 332-4.

Gao G, Plaas A, Thompson V P, Jin S, Zuo F and Sandy J D. 2004. ADAMTS4 (aggrecanase-1) activation on the cell surface involves C-terminal cleavage by glycosylphosphatidyl inositol-anchored membrane type 4-matrix metalloproteinase and binding of the activated proteinase to chondroitin sulfate and heparan sulfate on syndecan-1. *J Biol Chem* 279(11): 10042-51.

Garcia Rodriguez L A and Gonzalez-Perez A. 2004. Inverse association between nonsteroidal anti-inflammatory drugs and prostate cancer. *Cancer Epidemiol Biomarkers Prev* 13(4): 649-53.

Gaylis F D, Keer H N, Wilson M J, Kwaan H C, Sinha A A and Kozlowski J M. 1989. Plasminogen activators in human prostate cancer cell lines and tumors: correlation with the aggressive phenotype. *J Urol* 142(1): 193-8.

Geiger B and Ayalon O. 1992. Cadherins. *Annu Rev Cell Biol* 8: 307-32.

Gerhardt S, Hassall G, Hawtin P, McCall E, Flavell L, Minshull C, Hargreaves D, Ting A, Pauptit R A, Parker A E and Abbott W M. 2007. Crystal structures of human ADAMTS-1 reveal a conserved catalytic domain and a disintegrin-like domain with a fold homologous to cysteine-rich domains. *J Mol Biol* 373(4): 891-902.

- Ghosh A, Wang X, Klein E and Heston W D.** 2005. Novel role of prostate-specific membrane antigen in suppressing prostate cancer invasiveness. *Cancer Res* 65(3): 727-31.
- Giovannucci E, Liu Y, Stampfer M J and Willett W C.** 2006. A prospective study of calcium intake and incident and fatal prostate cancer. *Cancer Epidemiol Biomarkers Prev* 15(2): 203-10.
- Giricz O, Lauer J L and Fields G B.** 2010. Variability in melanoma metalloproteinase expression profiling. *J Biomol Tech* 21(4): 194-204.
- Glasel J A.** 1995. Validity of nucleic acid purities monitored by 260nm/280nm absorbance ratios. *Biotechniques* 18(1): 62-3.
- Glasson S S, Askew R, Sheppard B, Carito B, Blanchet T, Ma H L, Flannery C R, Peluso D, Kanki K, Yang Z, Majumdar M K and Morris E A.** 2005. Deletion of active ADAMTS5 prevents cartilage degradation in a murine model of osteoarthritis. *Nature* 434(7033): 644-8.
- Glasson S S, Askew R, Sheppard B, Carito B A, Blanchet T, Ma H L, Flannery C R, Kanki K, Wang E, Peluso D, Yang Z, Majumdar M K and Morris E A.** 2004. Characterization of and osteoarthritis susceptibility in ADAMTS-4-knockout mice. *Arthritis Rheum* 50(8): 2547-58.
- Gleason D F.** 1966. Classification of prostatic carcinomas. *Cancer Chemother Rep* 50(3): 125-8.
- Glienke J, Schmitt A O, Pilarsky C, Hinzmann B, Weiss B, Rosenthal A and Thierauch K H.** 2000. Differential gene expression by endothelial cells in distinct angiogenic states. *Eur J Biochem* 267(9): 2820-30.
- Goulas A, Hatzichristou D G, Karakiulakis G, Mirtsou-Fidani V, Kalinderis A and Papakonstantinou E.** 2000. Benign hyperplasia of the human prostate is associated with tissue enrichment in chondroitin sulphate of wide size distribution. *Prostate* 44(2): 104-10.
- Graham F L and van der Eb A J.** 1973. Transformation of rat cells by DNA of human adenovirus 5. *Virology* 54(2): 536-9.
- Graham S D, Jr., Bostwick D G, Hoisaeter A, Abrahamsson P, Algaba F, di Sant'Agnese A, Mostofi F K and Napalkov P.** 1992. Report of the Committee on Staging and Pathology. *Cancer* 70(1 Suppl): 359-61.
- Grayhack J T and Kropp K.** 1965. Changes with Aging in Prostatic Fluid: Citric Acid, Acid Phosphatase and Lactic Dehydrogenase Concentration in Man. *J Urol* 93: 258-62.
- Gregory C W, He B, Johnson R T, Ford O H, Mohler J L, French F S and Wilson E M.** 2001. A mechanism for androgen receptor-mediated prostate cancer recurrence after androgen deprivation therapy. *Cancer Res* 61(11): 4315-9.

Grell M, Wajant H, Zimmermann G and Scheurich P. 1998. The type 1 receptor (CD120a) is the high-affinity receptor for soluble tumor necrosis factor. *Proc Natl Acad Sci U S A* 95(2): 570-5.

Guevara J, Jr., Herbert B H and Lee C. 1985. Two-dimensional electrophoretic analysis of human prostatic fluid proteins. *Cancer Res* 45(4): 1766-71.

Gupta A, Aragaki C, Gotoh M, Masumori N, Ohshima S, Tsukamoto T and Roehrborn C G. 2005. Relationship between prostate specific antigen and indexes of prostate volume in Japanese men. *J Urol* 173(2): 503-6.

Gupta S, Hastak K, Ahmad N, Lewin J S and Mukhtar H. 2001. Inhibition of prostate carcinogenesis in TRAMP mice by oral infusion of green tea polyphenols. *Proc Natl Acad Sci U S A* 98(18): 10350-5.

Gustavsson H, Wang W, Jennbacken K, Welen K and Damber J E. 2009. ADAMTS1, a putative anti-angiogenic factor, is decreased in human prostate cancer. *BJU Int* 104(11): 1786-90.

Haas G P, Delongchamps N, Brawley O W, Wang C Y and de la Roza G. 2008. The worldwide epidemiology of prostate cancer: perspectives from autopsy studies. *Can J Urol* 15(1): 3866-71.

Hamacher S, Matern S and Roeb E. 2004. [Extracellular matrix -- from basic research to clinical significance. An overview with special consideration of matrix metalloproteinases]. *Dtsch Med Wochenschr* 129(38): 1976-80.

Haqqi T M, Anthony D D, Gupta S, Ahmad N, Lee M S, Kumar G K and Mukhtar H. 1999. Prevention of collagen-induced arthritis in mice by a polyphenolic fraction from green tea. *Proc Natl Acad Sci U S A* 96(8): 4524-9.

Harada S, Keller E T, Fujimoto N, Koshida K, Namiki M, Matsumoto T and Mizokami A. 2001. Long-term exposure of tumor necrosis factor alpha causes hypersensitivity to androgen and anti-androgen withdrawal phenomenon in LNCaP prostate cancer cells. *Prostate* 46(4): 319-26.

Hashimoto G, Aoki T, Nakamura H, Tanzawa K and Okada Y. 2001. Inhibition of ADAMTS4 (aggrecanase-1) by tissue inhibitors of metalloproteinases (TIMP-1, 2, 3 and 4). *FEBS Lett* 494(3): 192-5.

Hatipoglu O F, Hirohata S, Cilek M Z, Ogawa H, Miyoshi T, Obika M, Demircan K, Shinohata R, Kusachi S and Ninomiya Y. 2009. ADAMTS1 is a unique hypoxic early response gene expressed by endothelial cells. *J Biol Chem* 284(24): 16325-33.

He K L and Ting A T. 2002. A20 inhibits tumor necrosis factor (TNF) alpha-induced apoptosis by disrupting recruitment of TRADD and RIP to the TNF receptor 1 complex in Jurkat T cells. *Mol Cell Biol* 22(17): 6034-45.

- Heidenreich A, Aus G, Bolla M, Joniau S, Matveev V B, Schmid H P and Zattoni F.** 2008. EAU guidelines on prostate cancer. *Eur Urol* 53(1): 68-80.
- Heinegard D.** 2009. Proteoglycans and more--from molecules to biology. *Int J Exp Pathol* 90(6): 575-86.
- Heinlein C A and Chang C.** 2002. Androgen receptor (AR) coregulators: an overview. *Endocr Rev* 23(2): 175-200.
- Held-Feindt J, Paredes E B, Blomer U, Seidenbecher C, Stark A M, Mehdorn H M and Mentlein R.** 2006. Matrix-degrading proteases ADAMTS4 and ADAMTS5 (disintegrins and metalloproteinases with thrombospondin motifs 4 and 5) are expressed in human glioblastomas. *Int J Cancer* 118(1): 55-61.
- Hellawell G O and Brewster S F.** 2002. Growth factors and their receptors in prostate cancer. *BJU Int* 89(3): 230-40.
- Herrada J, Dieringer P and Logothetis C J.** 1996. Characterization of patients with androgen-independent prostatic carcinoma whose serum prostate specific antigen decreased following flutamide withdrawal. *J Urol* 155(2): 620-3.
- Hienert G, Kirchheimer J C, Pfluger H and Binder B R.** 1988. Urokinase-type plasminogen activator as a marker for the formation of distant metastases in prostatic carcinomas. *J Urol* 140(6): 1466-9.
- Hoffmann A, Natoli G and Ghosh G.** 2006. Transcriptional regulation via the NF-kappaB signaling module. *Oncogene* 25(51): 6706-16.
- Horie-Inoue K, Bono H, Okazaki Y and Inoue S.** 2004. Identification and functional analysis of consensus androgen response elements in human prostate cancer cells. *Biochem Biophys Res Commun* 325(4): 1312-7.
- Horiguchi A, Chen D Y, Goodman O B, Jr., Zheng R, Shen R, Guan H, Hersh L B and Nanus D M.** 2008. Neutral endopeptidase inhibits prostate cancer tumorigenesis by reducing FGF-2-mediated angiogenesis. *Prostate Cancer Prostatic Dis* 11(1): 79-87.
- Horiguchi A, Zheng R, Goodman O B, Jr., Shen R, Guan H, Hersh L B and Nanus D M.** 2007. Lentiviral vector neutral endopeptidase gene transfer suppresses prostate cancer tumor growth. *Cancer Gene Ther* 14(6): 583-9.
- Horoszewicz J S, Leong S S, Kawinski E, Karr J P, Rosenthal H, Chu T M, Mirand E A and Murphy G P.** 1983. LNCaP model of human prostatic carcinoma. *Cancer Res* 43(4): 1809-18.
- Hu R, Dunn T A, Wei S, Isharwal S, Veltri R W, Humphreys E, Han M, Partin A W, Vessella R L, Isaacs W B, Bova G S and Luo J.** 2009. Ligand-independent androgen receptor variants derived from splicing of cryptic exons signify hormone-refractory prostate cancer. *Cancer Res* 69(1): 16-22.

Huggins C. 1942. Effect of Orchiectomy and Irradiation on Cancer of the Prostate. *Ann Surg* 115(6): 1192-200.

Hugosson J, Aus G, Lilja H, Lodding P and Pihl C G. 2004. Results of a randomized, population-based study of biennial screening using serum prostate-specific antigen measurement to detect prostate carcinoma. *Cancer* 100(7): 1397-405.

Huxley-Jones J, Clarke T K, Beck C, Toubaris G, Robertson D L and Boot-Handford R P. 2007. The evolution of the vertebrate metzincins; insights from *Ciona intestinalis* and *Danio rerio*. *BMC Evol Biol* 7: 63.

Iguchi K, Ishii K, Nakano T, Otsuka T, Usui S, Sugimura Y and Hirano K. 2007. Isolation and characterization of LNCaP sublines differing in hormone sensitivity. *J Androl* 28(5): 670-8.

Iruela-Arispe M L, Carpizo D and Luque A. 2003. ADAMTS1: a matrix metalloprotease with angioinhibitory properties. *Ann N Y Acad Sci* 995: 183-90.

Israeli R S, Powell C T, Corr J G, Fair W R and Heston W D. 1994. Expression of the prostate-specific membrane antigen. *Cancer Res* 54(7): 1807-11.

Iwamura M, Abrahamsson P A, Benning C M, Cockett A T and di Sant'Agnese P A. 1994. Androgen receptor immunostaining and its tissue distribution in formalin-fixed, paraffin-embedded sections after microwave treatment. *J Histochem Cytochem* 42(6): 783-8.

Izant J G and Weintraub H. 1984. Inhibition of thymidine kinase gene expression by anti-sense RNA: a molecular approach to genetic analysis. *Cell* 36(4): 1007-15.

Jacobs E J, Rodriguez C, Mondul A M, Connell C J, Henley S J, Calle E E and Thun M J. 2005. A large cohort study of aspirin and other nonsteroidal anti-inflammatory drugs and prostate cancer incidence. *J Natl Cancer Inst* 97(13): 975-80.

Janssens N, Janicot M, Perera T and Bakker A. 2004. Housekeeping genes as internal standards in cancer research. *Mol Diagn* 8(2): 107-13.

Jemal A, Bray F, Center M M, Ferlay J, Ward E and Forman D. 2011. Global cancer statistics. *CA Cancer J Clin* 61(2): 69-90.

Jenster G, van der Korput J A, Trapman J and Brinkmann A O. 1992. Functional domains of the human androgen receptor. *J Steroid Biochem Mol Biol* 41(3-8): 671-5.

Jiang C, Wang Z, Ganther H and Lu J. 2001. Caspases as key executors of methyl selenium-induced apoptosis (anoikis) of DU-145 prostate cancer cells. *Cancer Res* 61(7): 3062-70.

Jones G C and Riley G P. 2005. ADAMTS proteinases: a multi-domain, multi-functional family with roles in extracellular matrix turnover and arthritis. *Arthritis Res Ther* 7(4): 160-9.

- Jones H E, Eaton C L, Barrow D, Dutkowski C M, Gee J M and Griffiths K.** 1997. Comparative studies of the mitogenic effects of epidermal growth factor and transforming growth factor- α and the expression of various growth factors in neoplastic and non-neoplastic prostatic cell lines. *Prostate* 30(4): 219-31.
- Jones L J, Upson R H, Haugland R P, Panchuk-Voloshina N, Zhou M and Haugland R P.** 1997. Quenched BODIPY dye-labeled casein substrates for the assay of protease activity by direct fluorescence measurement. *Anal Biochem* 251(2): 144-52.
- Jones R D, English K M, Pugh P J, Morice A H, Jones T H and Channer K S.** 2002. Pulmonary vasodilatory action of testosterone: evidence of a calcium antagonistic action. *J Cardiovasc Pharmacol* 39(6): 814-23.
- Jonsson-Rylander A C, Nilsson T, Fritsche-Danielson R, Hammarstrom A, Behrendt M, Andersson J O, Lindgren K, Andersson A K, Wallbrandt P, Rosengren B, Brodin P, Thelin A, Westin A, Hurt-Camejo E and Lee-Sogaard C H.** 2005. Role of ADAMTS-1 in atherosclerosis: remodeling of carotid artery, immunohistochemistry, and proteolysis of versican. *Arterioscler Thromb Vasc Biol* 25(1): 180-5.
- Kaighn M E, Narayan K S, Ohnuki Y, Lechner J F and Jones L W.** 1979. Establishment and characterization of a human prostatic carcinoma cell line (PC-3). *Invest Urol* 17(1): 16-23.
- Kalluri R.** 2003. Basement membranes: structure, assembly and role in tumour angiogenesis. *Nat Rev Cancer* 3(6): 422-33.
- Kamada M, Mori H, Maeda N, Yamamoto S, Kunimi K, Takikawa M, Maegawa M, Aono T, Futaki S and Koide S S.** 1998. beta-Microseminoprotein/prostatic secretory protein is a member of immunoglobulin binding factor family. *Biochim Biophys Acta* 1388(1): 101-10.
- Kapuscinski J.** 1995. DAPI: a DNA-specific fluorescent probe. *Biotech Histochem* 70(5): 220-33.
- Kashiwagi M, Enghild J J, Gendron C, Hughes C, Caterson B, Itoh Y and Nagase H.** 2004. Altered proteolytic activities of ADAMTS-4 expressed by C-terminal processing. *J Biol Chem* 279(11): 10109-19.
- Kavanagh J P.** 1985. Sodium, potassium, calcium, magnesium, zinc, citrate and chloride content of human prostatic and seminal fluid. *J Reprod Fertil* 75(1): 35-41.
- Kawasaki H, Onuki R, Suyama E and Taira K.** 2002. Identification of genes that function in the TNF- α -mediated apoptotic pathway using randomized hybrid ribozyme libraries. *Nat Biotechnol* 20(4): 376-80.
- Kehinde E O, Mojiminiyi O A, Sheikh M, Al-Awadi K A, Daar A S, Al-Hunayan A, Anim J T and Al-Sumait A A.** 2005. Age-specific reference levels of serum prostate-specific antigen and prostate volume in healthy Arab men. *BJU Int* 96(3): 308-12.

Kemppainen J A, Langley E, Wong C I, Bobseine K, Kelce W R and Wilson E M. 1999. Distinguishing androgen receptor agonists and antagonists: distinct mechanisms of activation by medroxyprogesterone acetate and dihydrotestosterone. *Mol Endocrinol* 13(3): 440-54.

Kevorkian L, Young D A, Darrah C, Donell S T, Shepstone L, Porter S, Brockbank S M, Edwards D R, Parker A E and Clark I M. 2004. Expression profiling of metalloproteinases and their inhibitors in cartilage. *Arthritis Rheum* 50(1): 131-41.

Khafagy R, Shackley D, Samuel J, O'Flynn K, Betts C and Clarke N. 2007. Complications arising in the final year of life in men dying from advanced prostate cancer. *J Palliat Med* 10(3): 705-11.

Kirchheimer J C, Pfluger H, Ritschl P, Hienert G and Binder B R. 1985. Plasminogen activator activity in bone metastases of prostatic carcinomas as compared to primary tumors. *Invasion Metastasis* 5(6): 344-55.

Kleinjan D A and van Heyningen V. 2005. Long-range control of gene expression: emerging mechanisms and disruption in disease. *Am J Hum Genet* 76(1): 8-32.

Kleinman H K, McGarvey M L, Liotta L A, Robey P G, Tryggvason K and Martin G R. 1982. Isolation and characterization of type IV procollagen, laminin, and heparan sulfate proteoglycan from the EHS sarcoma. *Biochemistry* 21(24): 6188-93.

Klingler H C, Bretland A J, Reid S V, Chapple C R and Eaton C L. 1999. Regulation of prostatic stromal cell growth and function by transforming growth factor beta (TGFbeta). *Prostate* 41(2): 110-20.

Koistinen H, Paju A, Koistinen R, Finne P, Lovgren J, Wu P, Seppala M and Stenman U H. 2002. Prostate-specific antigen and other prostate-derived proteases cleave IGFBP-3, but prostate cancer is not associated with proteolytically cleaved circulating IGFBP-3. *Prostate* 50(2): 112-8.

Koivisto P, Kononen J, Palmberg C, Tammela T, Hyytinen E, Isola J, Trapman J, Cleutjens K, Noordzij A, Visakorpi T and Kallioniemi O P. 1997. Androgen receptor gene amplification: a possible molecular mechanism for androgen deprivation therapy failure in prostate cancer. *Cancer Res* 57(2): 314-9.

Kolonel L N, Altshuler D and Henderson B E. 2004. The multiethnic cohort study: exploring genes, lifestyle and cancer risk. *Nat Rev Cancer* 4(7): 519-27.

Kraus M, Ticha M and Jonakova V. 2001. Heparin-binding proteins of human seminal plasma homologous with boar spermadhesins. *J Reprod Immunol* 51(2): 131-44.

Kruger A, Soeltl R, Sopov I, Kopitz C, Arlt M, Magdolen V, Harbeck N, Gansbacher B and Schmitt M. 2001. Hydroxamate-type matrix metalloproteinase inhibitor batimastat promotes liver metastasis. *Cancer Res* 61(4): 1272-5.

Kuefer R, Day K C, Kleer C G, Sabel M S, Hofer M D, Varambally S, Zorn C S, Chinnaiyan A M, Rubin M A and Day M L. 2006. ADAM15 disintegrin is associated with aggressive prostate and breast cancer disease. *Neoplasia* 8(4): 319-29.

Kuno K, Bannai K, Hakozaiki M, Matsushima K and Hirose K. 2004. The carboxyl-terminal half region of ADAMTS-1 suppresses both tumorigenicity and experimental tumor metastatic potential. *Biochem Biophys Res Commun* 319(4): 1327-33.

Kuno K, Kanada N, Nakashima E, Fujiki F, Ichimura F and Matsushima K. 1997. Molecular cloning of a gene encoding a new type of metalloproteinase-disintegrin family protein with thrombospondin motifs as an inflammation associated gene. *J Biol Chem* 272(1): 556-62.

Kuno K and Matsushima K. 1998. ADAMTS-1 protein anchors at the extracellular matrix through the thrombospondin type I motifs and its spacing region. *J Biol Chem* 273(22): 13912-7.

Kuno K, Okada Y, Kawashima H, Nakamura H, Miyasaka M, Ohno H and Matsushima K. 2000. ADAMTS-1 cleaves a cartilage proteoglycan, aggrecan. *FEBS Lett* 478(3): 241-5.

Kuno K, Terashima Y and Matsushima K. 1999. ADAMTS-1 is an active metalloproteinase associated with the extracellular matrix. *J Biol Chem* 274(26): 18821-6.

Kuper H, Adami H O and Trichopoulos D. 2000. Infections as a major preventable cause of human cancer. *J Intern Med* 248(3): 171-83.

Kyprianou N, Tu H and Jacobs S C. 1996. Apoptotic versus proliferative activities in human benign prostatic hyperplasia. *Hum Pathol* 27(7): 668-75.

Laemmli U K. 1970. Cleavage of structural proteins during the assembly of the head of bacteriophage T4. *Nature* 227(5259): 680-5.

Langone J J. 1982. Applications of immobilized protein A in immunochemical techniques. *J Immunol Methods* 55(3): 277-96.

Lauffenburger D A and Horwitz A F. 1996. Cell migration: a physically integrated molecular process. *Cell* 84(3): 359-69.

Le Maire M, Kwee S, Andersen J P and Moller J V. 1983. Mode of interaction of polyoxyethyleneglycol detergents with membrane proteins. *Eur J Biochem* 129(3): 525-32.

Leav I, McNeal J E, Kwan P W, Komminoth P and Merk F B. 1996. Androgen receptor expression in prostatic dysplasia (prostatic intraepithelial neoplasia) in the human prostate: an immunohistochemical and in situ hybridization study. *Prostate* 29(3): 137-45.

- Lee C, Sutkowski D M, Sensibar J A, Zelner D, Kim I, Amsel I, Shaw N, Prins G S and Kozlowski J M.** 1995. Regulation of proliferation and production of prostate-specific antigen in androgen-sensitive prostatic cancer cells, LNCaP, by dihydrotestosterone. *Endocrinology* 136(2): 796-803.
- Lee D K and Chang C.** 2003. Molecular communication between androgen receptor and general transcription machinery. *J Steroid Biochem Mol Biol* 84(1): 41-9.
- Lee E C and Tenniswood M P.** 2004. Emergence of metastatic hormone-refractory disease in prostate cancer after anti-androgen therapy. *J Cell Biochem* 91(4): 662-70.
- Lee K O, Oh Y, Giudice L C, Cohen P, Peehl D M and Rosenfeld R G.** 1994. Identification of insulin-like growth factor-binding protein-3 (IGFBP-3) fragments and IGFBP-5 proteolytic activity in human seminal plasma: a comparison of normal and vasectomized patients. *J Clin Endocrinol Metab* 79(5): 1367-72.
- Lee M, Fridman R and Mobashery S.** 2004. Extracellular proteases as targets for treatment of cancer metastases. *Chem Soc Rev* 33(7): 401-9.
- Lee N V, Sato M, Annis D S, Loo J A, Wu L, Mosher D F and Iruela-Arispe M L.** 2006. ADAMTS1 mediates the release of antiangiogenic polypeptides from TSP1 and 2. *EMBO J* 25(22): 5270-83.
- Lee S O, Lou W, Hou M, de Miguel F, Gerber L and Gao A C.** 2003. Interleukin-6 promotes androgen-independent growth in LNCaP human prostate cancer cells. *Clin Cancer Res* 9(1): 370-6.
- Lee S O, Lou W, Hou M, Onate S A and Gao A C.** 2003. Interleukin-4 enhances prostate-specific antigen expression by activation of the androgen receptor and Akt pathway. *Oncogene* 22(39): 7981-8.
- Lee S O, Pinder E, Chun J Y, Lou W, Sun M and Gao A C.** 2008. Interleukin-4 stimulates androgen-independent growth in LNCaP human prostate cancer cells. *Prostate* 68(1): 85-91.
- Leitzmann M F, Stampfer M J, Ma J, Chan J M, Colditz G A, Willett W C and Giovannucci E.** 2002. Aspirin use in relation to risk of prostate cancer. *Cancer Epidemiol Biomarkers Prev* 11(10 Pt 1): 1108-11.
- Lenhard B, Sandelin A, Mendoza L, Engstrom P, Jareborg N and Wasserman W W.** 2003. Identification of conserved regulatory elements by comparative genome analysis. *J Biol* 2(2): 13.
- Lettesjo H, Nordstrom E, Strom H, Nilsson B, Glinghammar B, Dahlstedt L and Moller E.** 1998. Synovial fluid cytokines in patients with rheumatoid arthritis or other arthritic lesions. *Scand J Immunol* 48(3): 286-92.
- Lewis C E and Pollard J W.** 2006. Distinct role of macrophages in different tumor microenvironments. *Cancer Res* 66(2): 605-12.

- Li R, Wheeler T, Dai H, Frolov A, Thompson T and Ayala G.** 2004. High level of androgen receptor is associated with aggressive clinicopathologic features and decreased biochemical recurrence-free survival in prostate: cancer patients treated with radical prostatectomy. *Am J Surg Pathol* 28(7): 928-34.
- Liang C C, Park A Y and Guan J L.** 2007. In vitro scratch assay: a convenient and inexpensive method for analysis of cell migration in vitro. *Nat Protoc* 2(2): 329-33.
- Lilja H and Abrahamsson P A.** 1988. Three predominant proteins secreted by the human prostate gland. *Prostate* 12(1): 29-38.
- Lin M F, Meng T C, Rao P S, Chang C, Schonthal A H and Lin F F.** 1998. Expression of human prostatic acid phosphatase correlates with androgen-stimulated cell proliferation in prostate cancer cell lines. *J Biol Chem* 273(10): 5939-47.
- Lind G E, Kleivi K, Meling G I, Teixeira M R, Thiis-Evensen E, Rognum T O and Lothe R A.** 2006. ADAMTS1, CRABP1, and NR3C1 identified as epigenetically deregulated genes in colorectal tumorigenesis. *Cell Oncol* 28(5-6): 259-72.
- Lind T, Birch M A and McKie N.** 2006. Purification of an insect derived recombinant human ADAMTS-1 reveals novel gelatin (type I collagen) degrading activities. *Mol Cell Biochem* 281(1-2): 95-102.
- Lindmark R, Thoren-Tolling K and Sjoquist J.** 1983. Binding of immunoglobulins to protein A and immunoglobulin levels in mammalian sera. *J Immunol Methods* 62(1): 1-13.
- Linja M J, Savinainen K J, Saramaki O R, Tammela T L, Vessella R L and Visakorpi T.** 2001. Amplification and overexpression of androgen receptor gene in hormone-refractory prostate cancer. *Cancer Res* 61(9): 3550-5.
- Liotta L A.** 1986. Tumor invasion and metastases--role of the extracellular matrix: Rhoads Memorial Award lecture. *Cancer Res* 46(1): 1-7.
- Lippman S M, Klein E A, Goodman P J, Lucia M S, Thompson I M, Ford L G, Parnes H L, Minasian L M, Gaziano J M, Hartline J A, Parsons J K, Bearden J D, 3rd, Crawford E D, Goodman G E, Claudio J, Winquist E, Cook E D, Karp D D, Walther P, Lieber M M, Kristal A R, Darke A K, Arnold K B, Ganz P A, Santella R M, Albanes D, Taylor P R, Probstfield J L, Jagpal T J, Crowley J J, Meyskens F L, Jr., Baker L H and Coltman C A, Jr.** 2009. Effect of selenium and vitamin E on risk of prostate cancer and other cancers: the Selenium and Vitamin E Cancer Prevention Trial (SELECT). *JAMA* 301(1): 39-51.
- Little C B, Mittaz L, Belluoccio D, Rogerson F M, Campbell I K, Meeker C T, Bateman J F, Pritchard M A and Fosang A J.** 2005. ADAMTS-1-knockout mice do not exhibit abnormalities in aggrecan turnover in vitro or in vivo. *Arthritis Rheum* 52(5): 1461-72.

- Liu Y J, Xu Y and Yu Q.** 2006. Full-length ADAMTS-1 and the ADAMTS-1 fragments display pro- and antimetastatic activity, respectively. *Oncogene* 25(17): 2452-67.
- Livak K J and Schmittgen T D.** 2001. Analysis of relative gene expression data using real-time quantitative PCR and the 2(-Delta Delta C(T)) Method. *Methods* 25(4): 402-8.
- Llovera M, Garcia-Martinez C, Lopez-Soriano J, Carbo N, Agell N, Lopez-Soriano F J and Argiles J M.** 1998. Role of TNF receptor 1 in protein turnover during cancer cachexia using gene knockout mice. *Mol Cell Endocrinol* 142(1-2): 183-9.
- Loberg R D, Tantivejkul K, Craig M, Neeley C K and Pienta K J.** 2007. PAR1-mediated RhoA activation facilitates CCL2-induced chemotaxis in PC-3 cells. *J Cell Biochem* 101(5): 1292-300.
- Locke J A, Guns E S, Lubik A A, Adomat H H, Hendy S C, Wood C A, Ettinger S L, Gleave M E and Nelson C C.** 2008. Androgen levels increase by intratumoral de novo steroidogenesis during progression of castration-resistant prostate cancer. *Cancer Res* 68(15): 6407-15.
- Locksley R M, Killeen N and Lenardo M J.** 2001. The TNF and TNF receptor superfamilies: integrating mammalian biology. *Cell* 104(4): 487-501.
- Long M A and Husband J E.** 1999. Features of unusual metastases from prostate cancer. *Br J Radiol* 72(862): 933-41.
- Longpre J M and Leduc R.** 2004. Identification of prodomain determinants involved in ADAMTS-1 biosynthesis. *J Biol Chem* 279(32): 33237-45.
- Longpre J M, McCulloch D R, Koo B H, Alexander J P, Apte S S and Leduc R.** 2009. Characterization of proADAMTS5 processing by proprotein convertases. *Int J Biochem Cell Biol* 41(5): 1116-26.
- Louie A.** 2006. Design and characterization of magnetic resonance imaging gene reporters. *Methods Mol Med* 124: 401-17.
- Lu X, Wang Q, Hu G, Van Poznak C, Fleisher M, Reiss M, Massague J and Kang Y.** 2009. ADAMTS1 and MMP1 proteolytically engage EGF-like ligands in an osteolytic signaling cascade for bone metastasis. *Genes Dev* 23(16): 1882-94.
- Lubahn D B, Joseph D R, Sar M, Tan J, Higgs H N, Larson R E, French F S and Wilson E M.** 1988. The human androgen receptor: complementary deoxyribonucleic acid cloning, sequence analysis and gene expression in prostate. *Mol Endocrinol* 2(12): 1265-75.
- Lubahn D B, Joseph D R, Sullivan P M, Willard H F, French F S and Wilson E M.** 1988. Cloning of human androgen receptor complementary DNA and localization to the X chromosome. *Science* 240(4850): 327-30.

Luque A, Carpizo D R and Iruela-Arispe M L. 2003. ADAMTS1/METH1 inhibits endothelial cell proliferation by direct binding and sequestration of VEGF165. *J Biol Chem* 278(26): 23656-65.

Lyng F M, Jones G R and Rommerts F F. 2000. Rapid androgen actions on calcium signaling in rat sertoli cells and two human prostatic cell lines: similar biphasic responses between 1 picomolar and 100 nanomolar concentrations. *Biol Reprod* 63(3): 736-47.

Mabjeesh N J, Zhong H and Simons J W. 2002. Gene therapy of prostate cancer: current and future directions. *Endocr Relat Cancer* 9(2): 115-39.

Madaan S, Abel P D, Chaudhary K S, Hewitt R, Stott M A, Stamp G W and Lalani E N. 2000. Cytoplasmic induction and over-expression of cyclooxygenase-2 in human prostate cancer: implications for prevention and treatment. *BJU Int* 86(6): 736-41.

Malik S T. 1992. Tumour necrosis factor: roles in cancer pathophysiology. *Semin Cancer Biol* 3(1): 27-33.

Manaskova P, Liberda J, Ticha M and Jonakova V. 2002. Isolation of non-heparin-binding and heparin-binding proteins of boar prostate. *J Chromatogr B Analyt Technol Biomed Life Sci* 770(1-2): 137-43.

Manes S, Llorente M, Lacalle R A, Gomez-Mouton C, Kremer L, Mira E and Martinez A C. 1999. The matrix metalloproteinase-9 regulates the insulin-like growth factor-triggered autocrine response in DU-145 carcinoma cells. *J Biol Chem* 274(11): 6935-45.

Manzini G, Barcellona M L, Avitabile M and Quadrifoglio F. 1983. Interaction of diamidino-2-phenylindole (DAPI) with natural and synthetic nucleic acids. *Nucleic Acids Res* 11(24): 8861-76.

Marcelli M, Ittmann M, Mariani S, Sutherland R, Nigam R, Murthy L, Zhao Y, DiConcini D, Puxeddu E, Esen A, Eastham J, Weigel N L and Lamb D J. 2000. Androgen receptor mutations in prostate cancer. *Cancer Res* 60(4): 944-9.

Mareel M and Leroy A. 2003. Clinical, cellular, and molecular aspects of cancer invasion. *Physiol Rev* 83(2): 337-76.

Massie C E, Adryan B, Barbosa-Morais N L, Lynch A G, Tran M G, Neal D E and Mills I G. 2007. New androgen receptor genomic targets show an interaction with the ETS1 transcription factor. *EMBO Rep* 8(9): 871-8.

Massie C E, Lynch A, Ramos-Montoya A, Boren J, Stark R, Fazli L, Warren A, Scott H, Madhu B, Sharma N, Bon H, Zecchini V, Smith D M, Denicola G M, Mathews N, Osborne M, Hadfield J, Macarthur S, Adryan B, Lyons S K, Brindle K M, Griffiths J, Gleave M E, Rennie P S, Neal D E and Mills I G. 2011. The androgen receptor fuels prostate cancer by regulating central metabolism and biosynthesis. *EMBO J* 30(13): 2719-33.

- Masui T, Hosotani R, Tsuji S, Miyamoto Y, Yasuda S, Ida J, Nakajima S, Kawaguchi M, Kobayashi H, Koizumi M, Toyoda E, Tulachan S, Arie S, Doi R and Imamura M.** 2001. Expression of METH-1 and METH-2 in pancreatic cancer. *Clin Cancer Res* 7(11): 3437-43.
- Matrisian L M, Sledge G W, Jr. and Mohla S.** 2003. Extracellular proteolysis and cancer: meeting summary and future directions. *Cancer Res* 63(19): 6105-9.
- Matsudaira P.** 1987. Sequence from picomole quantities of proteins electroblotted onto polyvinylidene difluoride membranes. *J Biol Chem* 262(21): 10035-8.
- Mazur A W and Thompson I M.** 1991. Efficacy and morbidity of "channel" TURP. *Urology* 38(6): 526-8.
- Mazzola J L and Sirover M A.** 2003. Subcellular localization of human glyceraldehyde-3-phosphate dehydrogenase is independent of its glycolytic function. *Biochim Biophys Acta* 1622(1): 50-6.
- McClinton S, Miller I D and Eremin O.** 1990. An immunohistochemical characterisation of the inflammatory cell infiltrate in benign and malignant prostatic disease. *Br J Cancer* 61(3): 400-3.
- McCulloch D R, Harvey M and Herington A C.** 2000. The expression of the ADAMs proteases in prostate cancer cell lines and their regulation by dihydrotestosterone. *Mol Cell Endocrinol* 167(1-2): 11-21.
- McNeal J E.** 1972. The prostate and prostatic urethra: a morphologic synthesis. *J Urol* 107(6): 1008-16.
- McNeal J E.** 1981. The zonal anatomy of the prostate. *Prostate* 2(1): 35-49.
- McNeal J E, Hailot O and Yemoto C.** 1995. Cell proliferation in dysplasia of the prostate: analysis by PCNA immunostaining. *Prostate* 27(5): 258-68.
- McNeal J E, Redwine E A, Freiha F S and Stamey T A.** 1988. Zonal distribution of prostatic adenocarcinoma. Correlation with histologic pattern and direction of spread. *Am J Surg Pathol* 12(12): 897-906.
- Meyer F, Bairati I, Shadmani R, Fradet Y and Moore L.** 1999. Dietary fat and prostate cancer survival. *Cancer Causes Control* 10(4): 245-51.
- Michalaki V, Syrigos K, Charles P and Waxman J.** 2004. Serum levels of IL-6 and TNF-alpha correlate with clinicopathological features and patient survival in patients with prostate cancer. *Br J Cancer* 90(12): 2312-6.
- Michielsen P P, Francque S M and van Dongen J L.** 2005. Viral hepatitis and hepatocellular carcinoma. *World J Surg Oncol* 3: 27.

- Miller L R, Partin A W, Chan D W, Bruzek D J, Dobs A S, Epstein J I and Walsh P C.** 1998. Influence of radical prostatectomy on serum hormone levels. *J Urol* 160(2): 449-53.
- Mittaz L, Russell D L, Wilson T, Brasted M, Tkalcevic J, Salamonsen L A, Hertzog P J and Pritchard M A.** 2004. Adamts-1 is essential for the development and function of the urogenital system. *Biol Reprod* 70(4): 1096-105.
- Miyamoto S, Yano K, Sugimoto S, Ishii G, Hasebe T, Endoh Y, Kodama K, Goya M, Chiba T and Ochiai A.** 2004. Matrix metalloproteinase-7 facilitates insulin-like growth factor bioavailability through its proteinase activity on insulin-like growth factor binding protein 3. *Cancer Res* 64(2): 665-71.
- Mizokami A, Gotoh A, Yamada H, Keller E T and Matsumoto T.** 2000. Tumor necrosis factor-alpha represses androgen sensitivity in the LNCaP prostate cancer cell line. *J Urol* 164(3 Pt 1): 800-5.
- Mohler J, Bahnson R R, Boston B, Busby J E, D'Amico A, Eastham J A, Enke C A, George D, Horwitz E M, Huben R P, Kantoff P, Kawachi M, Kuettel M, Lange P H, Macvicar G, Plimack E R, Pow-Sang J M, Roach M, 3rd, Rohren E, Roth B J, Shrieve D C, Smith M R, Srinivas S, Twardowski P and Walsh P C.** 2010. NCCN clinical practice guidelines in oncology: prostate cancer. *J Natl Compr Canc Netw* 8(2): 162-200.
- Mohler J L, Gregory C W, Ford O H, 3rd, Kim D, Weaver C M, Petrusz P, Wilson E M and French F S.** 2004. The androgen axis in recurrent prostate cancer. *Clin Cancer Res* 10(2): 440-8.
- Monge A, Jagla M, Lapouge G, Sasorith S, Cruchant M, Wurtz J M, Jacqmin D, Bergerat J P and Ceraline J.** 2006. Unfaithfulness and promiscuity of a mutant androgen receptor in a hormone-refractory prostate cancer. *Cell Mol Life Sci* 63(4): 487-97.
- Montgomery M K and Fire A.** 1998. Double-stranded RNA as a mediator in sequence-specific genetic silencing and co-suppression. *Trends Genet* 14(7): 255-8.
- Montironi R, Scarpelli M, Sisti S, Braccischi A, Gusella P, Pisani E, Alberti R and Mariuzzi G M.** 1990. Quantitative analysis of prostatic intraepithelial neoplasia on tissue sections. *Anal Quant Cytol Histol* 12(5): 366-72.
- Moore B B, Arenberg D A, Stoy K, Morgan T, Addison C L, Morris S B, Glass M, Wilke C, Xue Y Y, Sitterding S, Kunkel S L, Burdick M D and Strieter R M.** 1999. Distinct CXC chemokines mediate tumorigenicity of prostate cancer cells. *Am J Pathol* 154(5): 1503-12.
- Moss M L, Jin S L, Milla M E, Bickett D M, Burkhart W, Carter H L, Chen W J, Clay W C, Didsbury J R, Hassler D, Hoffman C R, Kost T A, Lambert M H, Leesnitzer M A, McCauley P, McGeehan G, Mitchell J, Moyer M, Pahel G, Rocque W, Overton L K, Schoenen F, Seaton T, Su J L, Becherer J D and et al.**

1997. Cloning of a disintegrin metalloproteinase that processes precursor tumour-necrosis factor- α . *Nature* 385(6618): 733-6.

Mostaghel E A, Page S T, Lin D W, Fazli L, Coleman I M, True L D, Knudsen B, Hess D L, Nelson C C, Matsumoto A M, Bremner W J, Gleave M E and Nelson P S. 2007. Intraprostatic androgens and androgen-regulated gene expression persist after testosterone suppression: therapeutic implications for castration-resistant prostate cancer. *Cancer Res* 67(10): 5033-41.

Murphy G P, Busch C, Abrahamsson P A, Epstein J I, McNeal J E, Miller G J, Mostofi F K, Nagle R B, Nordling S, Parkinson C and et al. 1994. Histopathology of localized prostate cancer. Consensus Conference on Diagnosis and Prognostic Parameters in Localized Prostate Cancer. Stockholm, Sweden, May 12-13, 1993. *Scand J Urol Nephrol Suppl* 162: 7-42; discussion 115-27.

Nagler D K, Kruger S, Kellner A, Ziomek E, Menard R, Buhtz P, Krams M, Roessner A and Kellner U. 2004. Up-regulation of cathepsin X in prostate cancer and prostatic intraepithelial neoplasia. *Prostate* 60(2): 109-19.

Nakada M, Miyamori H, Kita D, Takahashi T, Yamashita J, Sato H, Miura R, Yamaguchi Y and Okada Y. 2005. Human glioblastomas overexpress ADAMTS-5 that degrades brevican. *Acta Neuropathol* 110(3): 239-46.

Nakashima J, Tachibana M, Ueno M, Miyajima A, Baba S and Murai M. 1998. Association between tumor necrosis factor in serum and cachexia in patients with prostate cancer. *Clin Cancer Res* 4(7): 1743-8.

Narod S A, Seth A and Nam R. 2008. Fusion in the ETS gene family and prostate cancer. *Br J Cancer* 99(6): 847-51.

Nef S and Parada L F. 2000. Hormones in male sexual development. *Genes Dev* 14(24): 3075-86.

Nelson J E and Harris R E. 2000. Inverse association of prostate cancer and non-steroidal anti-inflammatory drugs (NSAIDs): results of a case-control study. *Oncol Rep* 7(1): 169-70.

Nemeth J A, Yousif R, Herzog M, Che M, Upadhyay J, Shekarriz B, Bhagat S, Mullins C, Fridman R and Cher M L. 2002. Matrix metalloproteinase activity, bone matrix turnover, and tumor cell proliferation in prostate cancer bone metastasis. *J Natl Cancer Inst* 94(1): 17-25.

Ng Y H, Zhu H, Pallen C J, Leung P C and MacCalman C D. 2006. Differential effects of interleukin-1 β and transforming growth factor- β 1 on the expression of the inflammation-associated protein, ADAMTS-1, in human decidual stromal cells in vitro. *Hum Reprod* 21(8): 1990-9.

Nicholson A C, Malik S B, Logsdon J M, Jr. and Van Meir E G. 2005. Functional evolution of ADAMTS genes: evidence from analyses of phylogeny and gene organization. *BMC Evol Biol* 5(1): 11.

- Nishi N, Oya H, Matsumoto K, Nakamura T, Miyanaka H and Wada F.** 1996. Changes in gene expression of growth factors and their receptors during castration-induced involution and androgen-induced regrowth of rat prostates. *Prostate* 28(3): 139-52.
- Nonomura N, Takayama H, Nakayama M, Nakai Y, Kawashima A, Mukai M, Nagahara A, Aozasa K and Tsujimura A.** 2011. Infiltration of tumour-associated macrophages in prostate biopsy specimens is predictive of disease progression after hormonal therapy for prostate cancer. *BJU Int* 107(12): 4.
- Norata G D, Bjork H, Hamsten A, Catapano A L and Eriksson P.** 2004. High-density lipoprotein subfraction 3 decreases ADAMTS-1 expression induced by lipopolysaccharide and tumor necrosis factor-alpha in human endothelial cells. *Matrix Biol* 22(7): 557-60.
- O'Toole E A, Marinkovich M P, Peavey C L, Amieva M R, Furthmayr H, Mustoe T A and Woodley D T.** 1997. Hypoxia increases human keratinocyte motility on connective tissue. *J Clin Invest* 100(11): 2881-91.
- Okamoto M, Lee C and Oyasu R.** 1997. Autocrine effect of androgen on proliferation of an androgen responsive prostatic carcinoma cell line, LNCAP: role of interleukin-6. *Endocrinology* 138(11): 5071-4.
- Olsson M, Ekstrom L, Schulze J, Kjellman A, Akre O, Rane A and Gustafsson O.** 2010. Radical prostatectomy: influence on serum and urinary androgen levels. *Prostate* 70(2): 200-5.
- Olumi A F, Grossfeld G D, Hayward S W, Carroll P R, Tlsty T D and Cunha G R.** 1999. Carcinoma-associated fibroblasts direct tumor progression of initiated human prostatic epithelium. *Cancer Res* 59(19): 5002-11.
- Osborn J L, Getzenberg R H and Trump D L.** 1995. Spinal cord compression in prostate cancer. *J Neurooncol* 23(2): 135-47.
- Osman I, Dai J, Mikhail M, Navarro D, Taneja S S, Lee P, Christos P, Shen R and Nanus D M.** 2006. Loss of neutral endopeptidase and activation of protein kinase B (Akt) is associated with prostate cancer progression. *Cancer* 107(11): 2628-36.
- Ostrowski W S and Kuciel R.** 1994. Human prostatic acid phosphatase: selected properties and practical applications. *Clin Chim Acta* 226(2): 121-9.
- Ottewell P D, Monkkonen H, Jones M, Lefley D V, Coleman R E and Holen I.** 2008. Antitumor effects of doxorubicin followed by zoledronic acid in a mouse model of breast cancer. *J Natl Cancer Inst* 100(16): 1167-78.
- Patel H R, Mirsadraee S and Emberton M.** 2003. The patient's dilemma: prostate cancer treatment choices. *J Urol* 169(3): 828-33.

- Paul A B, Love C and Chisholm G D.** 1994. The management of bilateral ureteric obstruction and renal failure in advanced prostate cancer. *Br J Urol* 74(5): 642-5.
- Peehl D M.** 2005. Primary cell cultures as models of prostate cancer development. *Endocr Relat Cancer* 12(1): 19-47.
- Peets E A, Henson M F and Neri R.** 1974. On the mechanism of the anti-androgenic action of flutamide (alpha-alpha-alpha-trifluoro-2-methyl-4'-nitro-m-propionotoluidide) in the rat. *Endocrinology* 94(2): 532-40.
- Pfitzenmaier J, Vessella R, Higano C S, Noteboom J L, Wallace D, Jr. and Corey E.** 2003. Elevation of cytokine levels in cachectic patients with prostate carcinoma. *Cancer* 97(5): 1211-6.
- Platz E A, Rohrmann S, Pearson J D, Corrada M M, Watson D J, De Marzo A M, Landis P K, Metter E J and Carter H B.** 2005. Nonsteroidal anti-inflammatory drugs and risk of prostate cancer in the Baltimore Longitudinal Study of Aging. *Cancer Epidemiol Biomarkers Prev* 14(2): 390-6.
- Podvinec M, Kaufmann M R, Handschin C and Meyer U A.** 2002. NUBIScan, an in silico approach for prediction of nuclear receptor response elements. *Mol Endocrinol* 16(6): 1269-79.
- Ponten J and Macintyre E H.** 1968. Long term culture of normal and neoplastic human glia. *Acta Pathol Microbiol Scand* 74(4): 465-86.
- Porter S, Clark I M, Kevorkian L and Edwards D R.** 2005. The ADAMTS metalloproteinases. *Biochem J* 386(Pt 1): 15-27.
- Porter S, Scott S D, Sassoon E M, Williams M R, Jones J L, Girling A C, Ball R Y and Edwards D R.** 2004. Dysregulated expression of adamalysin-thrombospondin genes in human breast carcinoma. *Clin Cancer Res* 10(7): 2429-40.
- Porter S, Span P N, Sweep F C, Tjan-Heijnen V C, Pennington C J, Pedersen T X, Johnsen M, Lund L R, Romer J and Edwards D R.** 2006. ADAMTS8 and ADAMTS15 expression predicts survival in human breast carcinoma. *Int J Cancer* 118(5): 1241-7.
- Powell A K, Yates E A, Fernig D G and Turnbull J E.** 2004. Interactions of heparin/heparan sulfate with proteins: appraisal of structural factors and experimental approaches. *Glycobiology* 14(4): 17R-30R.
- Prescott J, Jariwala U, Jia L, Cogan J P, Barski A, Pregizer S, Shen H C, Arasheben A, Neilson J J, Frenkel B and Coetzee G A.** 2007. Androgen receptor-mediated repression of novel target genes. *Prostate* 67(13): 1371-83.
- Pulukuri S M, Gondi C S, Lakka S S, Jutla A, Estes N, Gujrati M and Rao J S.** 2005. RNA interference-directed knockdown of urokinase plasminogen activator and urokinase plasminogen activator receptor inhibits prostate cancer cell invasion, survival, and tumorigenicity in vivo. *J Biol Chem* 280(43): 36529-40.

Qi J H, Ebrahim Q, Moore N, Murphy G, Claesson-Welsh L, Bond M, Baker A and Anand-Apte B. 2003. A novel function for tissue inhibitor of metalloproteinases-3 (TIMP3): inhibition of angiogenesis by blockage of VEGF binding to VEGF receptor-2. *Nat Med* 9(4): 407-15.

Qian J, Wollan P and Bostwick D G. 1997. The extent and multicentricity of high-grade prostatic intraepithelial neoplasia in clinically localized prostatic adenocarcinoma. *Hum Pathol* 28(2): 143-8.

Radonic A, Thulke S, Mackay I M, Landt O, Siegert W and Nitsche A. 2004. Guideline to reference gene selection for quantitative real-time PCR. *Biochem Biophys Res Commun* 313(4): 856-62.

Ratnikov B, Deryugina E, Leng J, Marchenko G, Dembrow D and Strongin A. 2000. Determination of matrix metalloproteinase activity using biotinylated gelatin. *Anal Biochem* 286(1): 149-55.

Rawlings N D, Morton F R, Kok C Y, Kong J and Barrett A J. 2008. MEROPS: the peptidase database. *Nucleic Acids Res* 36(Database issue): D320-5.

Rawlings N D, Morton, F.R. & Barrett, A.J. . 2006. MEROPS: the peptidase database. . *Nucleic Acids Res* 34: D270-D272.

Raymond S and Weintraub L. 1959. Acrylamide gel as a supporting medium for zone electrophoresis. *Science* 130: 711.

Rehn A P, Birch M A, Karlstrom E, Wendel M and Lind T. 2007. ADAMTS-1 increases the three-dimensional growth of osteoblasts through type I collagen processing. *Bone* 41(2): 231-8.

Revelos K, Petraki C, Scorilas A, Stefanakis S, Malovrouvas D, Alevizopoulos N, Kanellis G, Halapas A and Koutsilieris M. 2007. Correlation of androgen receptor status, neuroendocrine differentiation and angiogenesis with time-to-biochemical failure after radical prostatectomy in clinically localized prostate cancer. *Anticancer Res* 27(5B): 3651-60.

Rhodes T, Girman C J, Jacobsen S J, Roberts R O, Guess H A and Lieber M M. 1999. Longitudinal prostate growth rates during 5 years in randomly selected community men 40 to 79 years old. *J Urol* 161(4): 1174-9.

Ricciardelli C, Mayne K, Sykes P J, Raymond W A, McCaul K, Marshall V R and Horsfall D J. 1998. Elevated levels of versican but not decorin predict disease progression in early-stage prostate cancer. *Clin Cancer Res* 4(4): 963-71.

Ricciardelli C, Quinn D I, Raymond W A, McCaul K, Sutherland P D, Stricker P D, Grygiel J J, Sutherland R L, Marshall V R, Tilley W D and Horsfall D J. 1999. Elevated levels of peritumoral chondroitin sulfate are predictive of poor prognosis in patients treated by radical prostatectomy for early-stage prostate cancer. *Cancer Res* 59(10): 2324-8.

Riddick A C, Shukla C J, Pennington C J, Bass R, Nuttall R K, Hogan A, Sethia K K, Ellis V, Collins A T, Maitland N J, Ball R Y and Edwards D R. 2005.

Identification of degradome components associated with prostate cancer progression by expression analysis of human prostatic tissues. *Br J Cancer* 92(12): 2171-80.

Riegman P H, Vlietstra R J, van der Korput J A, Brinkmann A O and Trapman J. 1991. The promoter of the prostate-specific antigen gene contains a functional androgen responsive element. *Mol Endocrinol* 5(12): 1921-30.

Rios-Doria J, Day K C, Kuefer R, Rashid M G, Chinnaiyan A M, Rubin M A and Day M L. 2003. The role of calpain in the proteolytic cleavage of E-cadherin in prostate and mammary epithelial cells. *J Biol Chem* 278(2): 1372-9.

Roberts R O, Jacobson D J, Girman C J, Rhodes T, Lieber M M and Jacobsen S J. 2002. A population-based study of daily nonsteroidal anti-inflammatory drug use and prostate cancer. *Mayo Clin Proc* 77(3): 219-25.

Robinson-Rechavi M, Escriva Garcia H and Laudet V. 2003. The nuclear receptor superfamily. *J Cell Sci* 116(Pt 4): 585-6.

Robinson-Rechavi M and Laudet V. 2003. Bioinformatics of nuclear receptors. *Methods Enzymol* 364: 95-118.

Roche P J, Hoare S A and Parker M G. 1992. A consensus DNA-binding site for the androgen receptor. *Mol Endocrinol* 6(12): 2229-35.

Rocks N, Paulissen G, El Hour M, Quesada F, Crahay C, Gueders M, Foidart J M, Noel A and Cataldo D. 2008. Emerging roles of ADAM and ADAMTS metalloproteinases in cancer. *Biochimie* 90(2): 369-79.

Rocks N, Paulissen G, Quesada-Calvo F, Munaut C, Gonzalez M L, Gueders M, Hacha J, Gilles C, Foidart J M, Noel A and Cataldo D D. 2008. ADAMTS-1 metalloproteinase promotes tumor development through the induction of a stromal reaction in vivo. *Cancer Res* 68(22): 9541-50.

Rocks N, Paulissen G, Quesada Calvo F, Polette M, Gueders M, Munaut C, Foidart J M, Noel A, Birembaut P and Cataldo D. 2006. Expression of a disintegrin and metalloprotease (ADAM and ADAMTS) enzymes in human non-small-cell lung carcinomas (NSCLC). *Br J Cancer* 94(5): 724-30.

Rodriguez-Manzaneque J C, Carpizo D, Plaza-Calonge Mdel C, Torres-Collado A X, Thai S N, Simons M, Horowitz A and Iruela-Arispe M L. 2009. Cleavage of syndecan-4 by ADAMTS1 provokes defects in adhesion. *Int J Biochem Cell Biol* 41(4): 800-10.

Rodriguez-Manzaneque J C, Milchanowski A B, Dufour E K, Leduc R and Iruela-Arispe M L. 2000. Characterization of METH-1/ADAMTS1 processing reveals two distinct active forms. *J Biol Chem* 275(43): 33471-9.

- Rodriguez-Manzaneque J C, Westling J, Thai S N, Luque A, Knauper V, Murphy G, Sandy J D and Iruela-Arispe M L.** 2002. ADAMTS1 cleaves aggrecan at multiple sites and is differentially inhibited by metalloproteinase inhibitors. *Biochem Biophys Res Commun* 293(1): 501-8.
- Romanov V I, Whyard T, Adler H L, Waltzer W C and Zucker S.** 2004. Prostate cancer cell adhesion to bone marrow endothelium: the role of prostate-specific antigen. *Cancer Res* 64(6): 2083-9.
- Rowe R G and Weiss S J.** 2008. Breaching the basement membrane: who, when and how? *Trends Cell Biol* 18(11): 560-74.
- Rowe R G and Weiss S J.** 2009. Navigating ECM barriers at the invasive front: the cancer cell-stroma interface. *Annu Rev Cell Dev Biol* 25: 567-95.
- Ruoslahti E and Yamaguchi Y.** 1991. Proteoglycans as modulators of growth factor activities. *Cell* 64(5): 867-9.
- Russell D L, Doyle K M, Ochsner S A, Sandy J D and Richards J S.** 2003. Processing and localization of ADAMTS-1 and proteolytic cleavage of versican during cumulus matrix expansion and ovulation. *J Biol Chem* 278(43): 42330-9.
- Sahai E and Marshall C J.** 2003. Differing modes of tumour cell invasion have distinct requirements for Rho/ROCK signalling and extracellular proteolysis. *Nat Cell Biol* 5(8): 711-9.
- Sakko A J, Ricciardelli C, Mayne K, Suwivat S, LeBaron R G, Marshall V R, Tilley W D and Horsfall D J.** 2003. Modulation of prostate cancer cell attachment to matrix by versican. *Cancer Res* 63(16): 4786-91.
- Sakko A J, Ricciardelli C, Mayne K, Tilley W D, Lebaron R G and Horsfall D J.** 2001. Versican accumulation in human prostatic fibroblast cultures is enhanced by prostate cancer cell-derived transforming growth factor beta1. *Cancer Res* 61(3): 926-30.
- Sakr W A, Haas G P, Cassin B F, Pontes J E and Crissman J D.** 1993. The frequency of carcinoma and intraepithelial neoplasia of the prostate in young male patients. *J Urol* 150(2 Pt 1): 379-85.
- Sameni M, Cavallo-Medved D, Dosescu J, Jedeszko C, Moin K, Mullins S R, Olive M B, Rudy D and Sloane B F.** 2009. Imaging and quantifying the dynamics of tumor-associated proteolysis. *Clin Exp Metastasis* 26(4): 299-309.
- Sameni M, Dosescu J, Moin K and Sloane B F.** 2003. Functional imaging of proteolysis: stromal and inflammatory cells increase tumor proteolysis. *Mol Imaging* 2(3): 159-75.
- Sandberg A A.** 1980. Endocrine control and physiology of the prostate. *Prostate* 1(2): 169-84.

Sandy J D, Westling J, Kenagy R D, Iruela-Arispe M L, Verscharen C, Rodriguez-Mazaneque J C, Zimmermann D R, Lemire J M, Fischer J W, Wight T N and Clowes A W. 2001. Versican V1 proteolysis in human aorta in vivo occurs at the Glu441-Ala442 bond, a site that is cleaved by recombinant ADAMTS-1 and ADAMTS-4. *J Biol Chem* 276(16): 13372-8.

Sandy P, Ventura A and Jacks T. 2005. Mammalian RNAi: a practical guide. *Biotechniques* 39(2): 215-24.

Sanz L, Calvete J J, Mann K, Gabius H J and Topfer-Petersen E. 1993. Isolation and biochemical characterization of heparin-binding proteins from boar seminal plasma: a dual role for spermadhesins in fertilization. *Mol Reprod Dev* 35(1): 37-43.

Sartor A O, Tangen C M, Hussain M H, Eisenberger M A, Parab M, Fontana J A, Chapman R A, Mills G M, Raghavan D and Crawford E D. 2008. Antiandrogen withdrawal in castrate-refractory prostate cancer: a Southwest Oncology Group trial (SWOG 9426). *Cancer* 112(11): 2393-400.

Schalken J A and van Leenders G. 2003. Cellular and molecular biology of the prostate: stem cell biology. *Urology* 62(5 Suppl 1): 11-20.

Scher H I and Kelly W K. 1993. Flutamide withdrawal syndrome: its impact on clinical trials in hormone-refractory prostate cancer. *J Clin Oncol* 11(8): 1566-72.

Schoppmann S F, Birner P, Stockl J, Kalt R, Ullrich R, Caucig C, Kriehuber E, Nagy K, Alitalo K and Kerjaschki D. 2002. Tumor-associated macrophages express lymphatic endothelial growth factors and are related to peritumoral lymphangiogenesis. *Am J Pathol* 161(3): 947-56.

Schroder F H. 2008. Progress in understanding androgen-independent prostate cancer (AIPC): a review of potential endocrine-mediated mechanisms. *Eur Urol* 53(6): 1129-37.

Schroder F H, Hermanek P, Denis L, Fair W R, Gospodarowicz M K and Pavone-Macaluso M. 1992. The TNM classification of prostate cancer. *Prostate Suppl* 4: 129-38.

Schultz G S and Wysocki A. 2009. Interactions between extracellular matrix and growth factors in wound healing. *Wound Repair Regen* 17(2): 153-62.

Seidenfeld J, Samson D J, Hasselblad V, Aronson N, Albertsen P C, Bennett C L and Wilt T J. 2000. Single-therapy androgen suppression in men with advanced prostate cancer: a systematic review and meta-analysis. *Ann Intern Med* 132(7): 566-77.

Shariat S F, Svatek R S, Kabbani W, Walz J, Lotan Y, Karakiewicz P I and Roehrborn C G. 2008. Prognostic value of syndecan-1 expression in patients treated with radical prostatectomy. *BJU Int* 101(2): 232-7.

Sherwood E R, Van Dongen J L, Wood C G, Liao S, Kozlowski J M and Lee C. 1998. Epidermal growth factor receptor activation in androgen-independent but not

androgen-stimulated growth of human prostatic carcinoma cells. *Br J Cancer* 77(6): 855-61.

Shindo T, Kurihara H, Kuno K, Yokoyama H, Wada T, Kurihara Y, Imai T, Wang Y, Ogata M, Nishimatsu H, Moriyama N, Oh-hashii Y, Morita H, Ishikawa T, Nagai R, Yazaki Y and Matsushima K. 2000. ADAMTS-1: a metalloproteinase-disintegrin essential for normal growth, fertility, and organ morphology and function. *J Clin Invest* 105(10): 1345-52.

Sjoblom T, Jones S, Wood L D, Parsons D W, Lin J, Barber T D, Mandelker D, Leary R J, Ptak J, Silliman N, Szabo S, Buckhaults P, Farrell C, Meeh P, Markowitz S D, Willis J, Dawson D, Willson J K, Gazdar A F, Hartigan J, Wu L, Liu C, Parmigiani G, Park B H, Bachman K E, Papadopoulos N, Vogelstein B, Kinzler K W and Velculescu V E. 2006. The consensus coding sequences of human breast and colorectal cancers. *Science* 314(5797): 268-74.

Sloane B F, Sameni M, Podgorski I, Cavallo-Medved D and Moin K. 2006. Functional imaging of tumor proteolysis. *Annu Rev Pharmacol Toxicol* 46: 301-15.

Sloane B F, Yan S, Podgorski I, Linebaugh B E, Cher M L, Mai J, Cavallo-Medved D, Sameni M, Dosesu J and Moin K. 2005. Cathepsin B and tumor proteolysis: contribution of the tumor microenvironment. *Semin Cancer Biol* 15(2): 149-57.

Smith P K, Krohn R I, Hermanson G T, Mallia A K, Gartner F H, Provenzano M D, Fujimoto E K, Goeke N M, Olson B J and Klenk D C. 1985. Measurement of protein using bicinchoninic acid. *Anal Biochem* 150(1): 76-85.

Sobin L H, Hermanek P and Hutter R V. 1988. TNM classification of malignant tumors. A comparison between the new (1987) and the old editions. *Cancer* 61(11): 2310-4.

Soda H, Raymond E, Sharma S, Lawrence R, Davidson K, Oka M, Kohno S, Izbicka E and Von Hoff D D. 2000. Effects of androgens on telomerase activity in normal and malignant prostate cells in vitro. *Prostate* 43(3): 161-8.

Soejima K, Mimura N, Hirashima M, Maeda H, Hamamoto T, Nakagaki T and Nozaki C. 2001. A novel human metalloprotease synthesized in the liver and secreted into the blood: possibly, the von Willebrand factor-cleaving protease? *J Biochem* 130(4): 475-80.

Soff G A, Sanderowitz J, Gately S, Verrusio E, Weiss I, Brem S and Kwaan H C. 1995. Expression of plasminogen activator inhibitor type 1 by human prostate carcinoma cells inhibits primary tumor growth, tumor-associated angiogenesis, and metastasis to lung and liver in an athymic mouse model. *J Clin Invest* 96(6): 2593-600.

Sokoloff M H, Tso C L, Kaboo R, Taneja S, Pang S, deKernion J B and Beldegrun A S. 1996. In vitro modulation of tumor progression-associated properties of hormone refractory prostate carcinoma cell lines by cytokines. *Cancer* 77(9): 1862-72.

Soloway M S, Chodak G, Vogelzang N J, Block N L, Schellhammer P F, Smith J A, Jr., Scott M, Kennealey G and Gau T C. 1991. Zoladex versus orchiectomy in treatment of advanced prostate cancer: a randomized trial. Zoladex Prostate Study Group. *Urology* 37(1): 46-51.

Somerville R P, Longpre J M, Jungers K A, Engle J M, Ross M, Evanko S, Wight T N, Leduc R and Apte S S. 2003. Characterization of ADAMTS-9 and ADAMTS-20 as a distinct ADAMTS subfamily related to *Caenorhabditis elegans* GON-1. *J Biol Chem* 278(11): 9503-13.

Song W, Dong Z, Jin T, Mantellini M G, Nunez G and Nor J E. 2008. Cancer gene therapy with iCaspase-9 transcriptionally targeted to tumor endothelial cells. *Cancer Gene Ther* 15(10): 667-75.

Sparano J A, Bernardo P, Stephenson P, Gradishar W J, Ingle J N, Zucker S and Davidson N E. 2004. Randomized phase III trial of marimastat versus placebo in patients with metastatic breast cancer who have responding or stable disease after first-line chemotherapy: Eastern Cooperative Oncology Group trial E2196. *J Clin Oncol* 22(23): 4683-90.

Stanbrough M, Bubley G J, Ross K, Golub T R, Rubin M A, Penning T M, Febbo P G and Balk S P. 2006. Increased expression of genes converting adrenal androgens to testosterone in androgen-independent prostate cancer. *Cancer Res* 66(5): 2815-25.

Stanton H, Rogerson F M, East C J, Golub S B, Lawlor K E, Meeker C T, Little C B, Last K, Farmer P J, Campbell I K, Fourie A M and Fosang A J. 2005. ADAMTS5 is the major aggrecanase in mouse cartilage in vivo and in vitro. *Nature* 434(7033): 648-52.

Staton C A, Stribbling S M, Tazzyman S, Hughes R, Brown N J and Lewis C E. 2004. Current methods for assaying angiogenesis in vitro and in vivo. *Int J Exp Pathol* 85(5): 233-48.

Steers W D. 2001. 5alpha-reductase activity in the prostate. *Urology* 58(6 Suppl 1): 17-24; discussion 24.

Steiner G, Tohidast-Akrad M, Witzmann G, Vesely M, Studnicka-Benke A, Gal A, Kunaver M, Zenz P and Smolen J S. 1999. Cytokine production by synovial T cells in rheumatoid arthritis. *Rheumatology (Oxford)* 38(3): 202-13.

Steiner M S. 1993. Role of peptide growth factors in the prostate: a review. *Urology* 42(1): 99-110.

Stewart R J, Panigrahy D, Flynn E and Folkman J. 2001. Vascular endothelial growth factor expression and tumor angiogenesis are regulated by androgens in hormone responsive human prostate carcinoma: evidence for androgen dependent destabilization of vascular endothelial growth factor transcripts. *J Urol* 165(2): 688-93.

Stokes A, Joutsa J, Ala-Aho R, Pitchers M, Pennington C J, Martin C, Premachandra D J, Okada Y, Peltonen J, Grenman R, James H A, Edwards D R

and Kahari V M. 2010. Expression profiles and clinical correlations of degradome components in the tumor microenvironment of head and neck squamous cell carcinoma. *Clin Cancer Res* 16(7): 2022-35.

Su S C, Mendoza E A, Kwak H I and Bayless K J. 2008. Molecular profile of endothelial invasion of three-dimensional collagen matrices: insights into angiogenic sprout induction in wound healing. *Am J Physiol Cell Physiol* 295(5): C1215-29.

Sugita H, Osaka S, Toriyama M, Osaka E, Yoshida Y, Ryu J, Sano M, Sugitani M and Nemoto N. 2004. Correlation between the histological grade of chondrosarcoma and the expression of MMPs, ADAMTSs and TIMPs. *Anticancer Res* 24(6): 4079-84.

Sun Y H, Gao X, Tang Y J, Xu C L and Wang L H. 2006. Androgens induce increases in intracellular calcium via a G protein-coupled receptor in LNCaP prostate cancer cells. *J Androl* 27(5): 671-8.

Suzuki H, Akakura K, Komiya A, Aida S, Akimoto S and Shimazaki J. 1996. Codon 877 mutation in the androgen receptor gene in advanced prostate cancer: relation to antiandrogen withdrawal syndrome. *Prostate* 29(3): 153-8.

Szlosarek P, Charles K A and Balkwill F R. 2006. Tumour necrosis factor-alpha as a tumour promoter. *Eur J Cancer* 42(6): 745-50.

Szpaderska A M and Frankfater A. 2001. An intracellular form of cathepsin B contributes to invasiveness in cancer. *Cancer Res* 61(8): 3493-500.

Tamura K, Furihata M, Tsunoda T, Ashida S, Takata R, Obara W, Yoshioka H, Daigo Y, Nasu Y, Kumon H, Konaka H, Namiki M, Tozawa K, Kohri K, Tanji N, Yokoyama M, Shimazui T, Akaza H, Mizutani Y, Miki T, Fujioka T, Shuin T, Nakamura Y and Nakagawa H. 2007. Molecular features of hormone-refractory prostate cancer cells by genome-wide gene expression profiles. *Cancer Res* 67(11): 5117-25.

Taniguchi S, Tatsuka M, Nakamatsu K, Inoue M, Sadano H, Okazaki H, Iwamoto H and Baba T. 1989. High invasiveness associated with augmentation of motility in a fos-transferred highly metastatic rat 3Y1 cell line. *Cancer Res* 49(23): 6738-44.

Taplin M E, Bubley G J, Ko Y J, Small E J, Upton M, Rajeshkumar B and Balk S P. 1999. Selection for androgen receptor mutations in prostate cancers treated with androgen antagonist. *Cancer Res* 59(11): 2511-5.

Taplin M E, Bubley G J, Shuster T D, Frantz M E, Spooner A E, Ogata G K, Keer H N and Balk S P. 1995. Mutation of the androgen-receptor gene in metastatic androgen-independent prostate cancer. *N Engl J Med* 332(21): 1393-8.

Taplin M E and Ho S M. 2001. Clinical review 134: The endocrinology of prostate cancer. *J Clin Endocrinol Metab* 86(8): 3467-77.

Tauber P F, Zaneveld L J, Propping D and Schumacher G F. 1975. Components of human split ejaculates. I. Spermatozoa, fructose, immunoglobulins, albumin, lactoferrin, transferrin and other plasma proteins. *J Reprod Fertil* 43(2): 249-67.

Tep-areenan P, Kendall D A and Randall M D. 2002. Testosterone-induced vasorelaxation in the rat mesenteric arterial bed is mediated predominantly via potassium channels. *Br J Pharmacol* 135(3): 735-40.

Tetu B, Srigley J R, Boivin J C, Dupont A, Monfette G, Pinault S and Labrie F. 1991. Effect of combination endocrine therapy (LHRH agonist and flutamide) on normal prostate and prostatic adenocarcinoma. A histopathologic and immunohistochemical study. *Am J Surg Pathol* 15(2): 111-20.

Thalmann G N, Rhee H, Sikes R A, Pathak S, Multani A, Zhau H E, Marshall F F and Chung L W. 2010. Human prostate fibroblasts induce growth and confer castration resistance and metastatic potential in LNCaP Cells. *Eur Urol* 58(1): 162-71.

Thalmann G N, Sikes R A, Wu T T, Degeorges A, Chang S M, Ozen M, Pathak S and Chung L W. 2000. LNCaP progression model of human prostate cancer: androgen-independence and osseous metastasis. *Prostate* 44(2): 91-103 Jul 1;44(2).

Thiery J P. 2003. Epithelial-mesenchymal transitions in development and pathologies. *Curr Opin Cell Biol* 15(6): 740-6.

Ticha M, Zelezna B, Jonakova V and Filka K. 1994. Immobilization of heparin on polyacrylamide derivatives. *J Chromatogr B Biomed Appl* 656(2): 423-6.

Titus M A, Schell M J, Lih F B, Tomer K B and Mohler J L. 2005. Testosterone and dihydrotestosterone tissue levels in recurrent prostate cancer. *Clin Cancer Res* 11(13): 4653-7.

Tomita K, van Bokhoven A, van Leenders G J, Ruijter E T, Jansen C F, Bussemakers M J and Schalken J A. 2000. Cadherin switching in human prostate cancer progression. *Cancer Res* 60(13): 3650-4.

Tomlins S A, Bjartell A, Chinnaiyan A M, Jenster G, Nam R K, Rubin M A and Schalken J A. 2009. ETS gene fusions in prostate cancer: from discovery to daily clinical practice. *Eur Urol* 56(2): 275-86.

Tomlins S A, Rhodes D R, Perner S, Dhanasekaran S M, Mehra R, Sun X W, Varambally S, Cao X, Tchinda J, Kuefer R, Lee C, Montie J E, Shah R B, Pienta K J, Rubin M A and Chinnaiyan A M. 2005. Recurrent fusion of TMPRSS2 and ETS transcription factor genes in prostate cancer. *Science* 310(5748): 644-8.

Torres-Collado A X, Kisiel W, Iruela-Arispe M L and Rodriguez-Manzaneque J C. 2006. ADAMTS1 interacts with, cleaves, and modifies the extracellular location of the matrix inhibitor tissue factor pathway inhibitor-2. *J Biol Chem* 281(26): 17827-37.

Towbin H, Staehelin T and Gordon J. 1979. Electrophoretic transfer of proteins from polyacrylamide gels to nitrocellulose sheets: procedure and some applications. *Proc Natl Acad Sci U S A* 76(9): 4350-4.

Tracey K J. 1992. TNF and other cytokines in the metabolism of septic shock and cachexia. *Clin Nutr* 11(1): 1-11.

Trapman J and Cleutjens K B. 1997. Androgen-regulated gene expression in prostate cancer. *Semin Cancer Biol* 8(1): 29-36.

Trapman J, Klaassen P, Kuiper G G, van der Korput J A, Faber P W, van Rooij H C, Geurts van Kessel A, Voorhorst M M, Mulder E and Brinkmann A O. 1988. Cloning, structure and expression of a cDNA encoding the human androgen receptor. *Biochem Biophys Res Commun* 153(1): 241-8.

Tsopanoglou N E and Maragoudakis M E. 2004. Role of thrombin in angiogenesis and tumor progression. *Semin Thromb Hemost* 30(1): 63-9.

Tsung K, Dolan J P, Tsung Y L and Norton J A. 2002. Macrophages as effector cells in interleukin 12-induced T cell-dependent tumor rejection. *Cancer Res* 62(17): 5069-75.

Twillie D A, Eisenberger M A, Carducci M A, Hsieh W S, Kim W Y and Simons J W. 1995. Interleukin-6: a candidate mediator of human prostate cancer morbidity. *Urology* 45(3): 542-9.

Udayakumar T S, Chen M L, Bair E L, Von Bredow D C, Cress A E, Nagle R B and Bowden G T. 2003. Membrane type-1-matrix metalloproteinase expressed by prostate carcinoma cells cleaves human laminin-5 beta3 chain and induces cell migration. *Cancer Res* 63(9): 2292-9.

van Moorselaar R J, Hendriks B T, van Stratum P, van der Meide P H, Debruyne F M and Schalken J A. 1991. Synergistic antitumor effects of rat gamma-interferon and human tumor necrosis factor alpha against androgen-dependent and -independent rat prostatic tumors. *Cancer Res* 51(9): 2329-34.

van Moorselaar R J, van Stratum P, Borm G, Debruyne F M and Schalken J A. 1991. Differential antiproliferative activities of alpha- and gamma-interferon and tumor necrosis factor alone or in combinations against two prostate cancer xenografts transplanted in nude mice. *Prostate* 18(4): 331-44.

Van Wart H E and Birkedal-Hansen H. 1990. The cysteine switch: a principle of regulation of metalloproteinase activity with potential applicability to the entire matrix metalloproteinase gene family. *Proc Natl Acad Sci U S A* 87(14): 5578-82.

Vankemmelbeke MN B D. 2001. ADAMTSs: Multidomain and multifunctional proteinases. *Recent Res Developments Biophys Biochem* 1: 9-33.

- Vankemmelbeke M N, Jones G C, Fowles C, Ilic M Z, Handley C J, Day A J, Knight C G, Mort J S and Buttle D J.** 2003. Selective inhibition of ADAMTS-1, -4 and -5 by catechin gallate esters. *Eur J Biochem* 270(11): 2394-403.
- Vazquez F, Hastings G, Ortega M A, Lane T F, Oikemus S, Lombardo M and Iruela-Arispe M L.** 1999. METH-1, a human ortholog of ADAMTS-1, and METH-2 are members of a new family of proteins with angio-inhibitory activity. *J Biol Chem* 274(33): 23349-57.
- Veldscholte J, Berrevoets C A, Ris-Stalpers C, Kuiper G G, Jenster G, Trapman J, Brinkmann A O and Mulder E.** 1992. The androgen receptor in LNCaP cells contains a mutation in the ligand binding domain which affects steroid binding characteristics and response to antiandrogens. *J Steroid Biochem Mol Biol* 41(3-8): 665-9.
- Veldscholte J, Ris-Stalpers C, Kuiper G G, Jenster G, Berrevoets C, Claassen E, van Rooij H C, Trapman J, Brinkmann A O and Mulder E.** 1990. A mutation in the ligand binding domain of the androgen receptor of human LNCaP cells affects steroid binding characteristics and response to anti-androgens. *Biochem Biophys Res Commun* 173(2): 534-40.
- Verma P and Dalal K.** 2011. ADAMTS-4 and ADAMTS-5: key enzymes in osteoarthritis. *J Cell Biochem* 112(12): 3507-14.
- Viloria C G, Obaya A J, Moncada-Pazos A, Llamazares M, Astudillo A, Capella G, Cal S and Lopez-Otin C.** 2009. Genetic inactivation of ADAMTS15 metalloprotease in human colorectal cancer. *Cancer Res* 69(11): 4926-34.
- Vistica D T, Skehan P, Scudiero D, Monks A, Pittman A and Boyd M R.** 1991. Tetrazolium-based assays for cellular viability: a critical examination of selected parameters affecting formazan production. *Cancer Res* 51(10): 2515-20.
- Wahl L M and Kleinman H K.** 1998. Tumor-associated macrophages as targets for cancer therapy. *J Natl Cancer Inst* 90(21): 1583-4.
- Walsh P C, Lepor H and Eggleston J C.** 1983. Radical prostatectomy with preservation of sexual function: anatomical and pathological considerations. *Prostate* 4(5): 473-85.
- Wan X S, Zhou Z, Steele V, Kopelovich L and Kennedy A R.** 2003. Establishment and characterization of sublines of LNCaP human prostate cancer cells. *Oncol Rep* 10(5): 1569-75.
- Wang J, Cai Y, Ren C and Ittmann M.** 2006. Expression of variant TMPRSS2/ERG fusion messenger RNAs is associated with aggressive prostate cancer. *Cancer Res* 66(17): 8347-51.
- Wang P, Tortorella M, England K, Malfait A M, Thomas G, Arner E C and Pei D.** 2004. Proprotein convertase furin interacts with and cleaves pro-ADAMTS4 (Aggrecanase-1) in the trans-Golgi network. *J Biol Chem* 279(15): 15434-40.

- Wang W, Bergh A and Damber J E.** 2005. Cyclooxygenase-2 expression correlates with local chronic inflammation and tumor neovascularization in human prostate cancer. *Clin Cancer Res* 11(9): 3250-6.
- Wang Z B, Liu Y Q and Cui Y F.** 2005. Pathways to caspase activation. *Cell Biol Int* 29(7): 489-96.
- Ware J L.** 1987. Prostate tumor progression and metastasis. *Biochim Biophys Acta* 907(3): 279-98.
- Wasserman W W and Sandelin A.** 2004. Applied bioinformatics for the identification of regulatory elements. *Nat Rev Genet* 5(4): 276-87.
- Weber B H, Vogt G, Pruett R C, Stohr H and Felbor U.** 1994. Mutations in the tissue inhibitor of metalloproteinases-3 (TIMP3) in patients with Sorsby's fundus dystrophy. *Nat Genet* 8(4): 352-6.
- Weidner N, Carroll P R, Flax J, Blumenfeld W and Folkman J.** 1993. Tumor angiogenesis correlates with metastasis in invasive prostate carcinoma. *Am J Pathol* 143(2): 401-9.
- Wen J, Zhu H, Murakami S, Leung P C and MacCalman C D.** 2006. Regulation of A Disintegrin And Metalloproteinase with ThromboSpondin repeats-1 expression in human endometrial stromal cells by gonadal steroids involves progestins, androgens, and estrogens. *J Clin Endocrinol Metab* 91(12): 4825-35.
- Wiepz G J, Edwin F, Patel T and Bertics P J.** 2006. Methods for determining the proliferation of cells in response to EGFR ligands. *Methods Mol Biol* 327: 179-87.
- Williams H and Powell I J.** 2009. Epidemiology, pathology, and genetics of prostate cancer among African Americans compared with other ethnicities. *Methods Mol Biol* 472: 439-53.
- Williamson R A, Marston F A, Angal S, Koklitis P, Panico M, Morris H R, Carne A F, Smith B J, Harris T J and Freedman R B.** 1990. Disulphide bond assignment in human tissue inhibitor of metalloproteinases (TIMP). *Biochem J* 268(2): 267-74.
- Wilson E M and French F S.** 1976. Binding properties of androgen receptors. Evidence for identical receptors in rat testis, epididymis, and prostate. *J Biol Chem* 251(18): 5620-9.
- Wilson M J, Norris H, Kapoor D, Woodson M, Limas C and Sinha A A.** 1993. Gelatinolytic and caseinolytic proteinase activities in human prostatic secretions. *J Urol* 149(3): 653-8.
- Wise G J, Marella V K, Talluri G and Shirazian D.** 2000. Cytokine variations in patients with hormone treated prostate cancer. *J Urol* 164(3 Pt 1): 722-5.
- Wolf B B and Green D R.** 1999. Suicidal tendencies: apoptotic cell death by caspase family proteinases. *J Biol Chem* 274(29): 20049-52.

Wolf K and Friedl P. 2009. Mapping proteolytic cancer cell-extracellular matrix interfaces. *Clin Exp Metastasis* 26(4): 289-98.

Wolf K, Mazo I, Leung H, Engelke K, von Andrian U H, Deryugina E I, Strongin A Y, Brocker E B and Friedl P. 2003. Compensation mechanism in tumor cell migration: mesenchymal-amoeboid transition after blocking of pericellular proteolysis. *J Cell Biol* 160(2): 267-77.

Wong C P, Bray T M and Ho E. 2009. Induction of proinflammatory response in prostate cancer epithelial cells by activated macrophages. *Cancer Lett* 276(1): 38-46.

Wood L D, Parsons D W, Jones S, Lin J, Sjoblom T, Leary R J, Shen D, Boca S M, Barber T, Ptak J, Silliman N, Szabo S, Dezso Z, Ustyanksky V, Nikolskaya T, Nikolsky Y, Karchin R, Wilson P A, Kaminker J S, Zhang Z, Croshaw R, Willis J, Dawson D, Shipitsin M, Willson J K, Sukumar S, Polyak K, Park B H, Pethiyagoda C L, Pant P V, Ballinger D G, Sparks A B, Hartigan J, Smith D R, Suh E, Papadopoulos N, Buckhaults P, Markowitz S D, Parmigiani G, Kinzler K W, Velculescu V E and Vogelstein B. 2007. The genomic landscapes of human breast and colorectal cancers. *Science* 318(5853): 1108-13.

Wu C P and Gu F L. 1991. The prostate in eunuchs. *Prog Clin Biol Res* 370: 249-55.

Wu Y, Wu J, Lee D Y, Yee A, Cao L, Zhang Y, Kiani C and Yang B B. 2005. Versican protects cells from oxidative stress-induced apoptosis. *Matrix Biol* 24(1): 3-13.

Xu J, Dimitrov L, Chang B L, Adams T S, Turner A R, Meyers D A, Eeles R A, Easton D F, Foulkes W D, Simard J, Giles G G, Hopper J L, Mahle L, Moller P, Bishop T, Evans C, Edwards S, Meitz J, Bullock S, Hope Q, Hsieh C L, Halpern J, Balise R N, Oakley-Girvan I, Whittemore A S, Ewing C M, Gielzak M, Isaacs S D, Walsh P C, Wiley K E, Isaacs W B, Thibodeau S N, McDonnell S K, Cunningham J M, Zarfes K E, Hebbing S, Schaid D J, Friedrichsen D M, Deutsch K, Kolb S, Badzioch M, Jarvik G P, Janer M, Hood L, Ostrander E A, Stanford J L, Lange E M, Beebe-Dimmer J L, Mohai C E, Cooney K A, Ikonen T, Baffoe-Bonnie A, Fredriksson H, Matikainen M P, Tammela T, Bailey-Wilson J, Schleutker J, Maier C, Herkommer K, Hoegel J J, Vogel W, Paiss T, Wiklund F, Emanuelsson M, Stenman E, Jonsson B A, Gronberg H, Camp N J, Farnham J, Cannon-Albright L A and Seminara D. 2005. A combined genomewide linkage scan of 1,233 families for prostate cancer-susceptibility genes conducted by the international consortium for prostate cancer genetics. *Am J Hum Genet* 77(2): 219-29.

Yilmaz M and Christofori G. 2010. Mechanisms of motility in metastasizing cells. *Mol Cancer Res* 8(5): 629-42.

Yu W H, Yu S, Meng Q, Brew K and Woessner J F, Jr. 2000. TIMP-3 binds to sulfated glycosaminoglycans of the extracellular matrix. *J Biol Chem* 275(40): 31226-32.

- Yuan X and Balk S P.** 2009. Mechanisms mediating androgen receptor reactivation after castration. *Urol Oncol* 27(1): 36-41.
- Yue P, Chatterjee K, Beale C, Poole-Wilson P A and Collins P.** 1995. Testosterone relaxes rabbit coronary arteries and aorta. *Circulation* 91(4): 1154-60.
- Zegarra-Moro O L, Schmidt L J, Huang H and Tindall D J.** 2002. Disruption of androgen receptor function inhibits proliferation of androgen-refractory prostate cancer cells. *Cancer Res* 62(4): 1008-13.
- Zeng W, Corcoran C, Collins-Racie L A, Lavallie E R, Morris E A and Flannery C R.** 2006. Glycosaminoglycan-binding properties and aggrecanase activities of truncated ADAMTSs: comparative analyses with ADAMTS-5, -9, -16 and -18. *Biochim Biophys Acta* 1760(3): 517-24.
- Zhao X Y, Malloy P J, Krishnan A V, Swami S, Navone N M, Peehl D M and Feldman D.** 2000. Glucocorticoids can promote androgen-independent growth of prostate cancer cells through a mutated androgen receptor. *Nat Med* 6(6): 703-6.
- Zheng X, Chung D, Takayama T K, Majerus E M, Sadler J E and Fujikawa K.** 2001. Structure of von Willebrand factor-cleaving protease (ADAMTS13), a metalloprotease involved in thrombotic thrombocytopenic purpura. *J Biol Chem* 276(44): 41059-63.
- Zhou Z, Corden J L and Brown T R.** 1997. Identification and characterization of a novel androgen response element composed of a direct repeat. *J Biol Chem* 272(13): 8227-35.
- Zhu M L and Kyprianou N.** 2010. Role of androgens and the androgen receptor in epithelial-mesenchymal transition and invasion of prostate cancer cells. *FASEB J* 24(3): 769-77.
- Zhu Y S, Cai L Q, You X, Cordero J J, Huang Y and Imperato-McGinley J.** 2003. Androgen-induced prostate-specific antigen gene expression is mediated via dihydrotestosterone in LNCaP cells. *J Androl* 24(5): 681-7.
- Zucker S, Cao J and Chen W T.** 2000. Critical appraisal of the use of matrix metalloproteinase inhibitors in cancer treatment. *Oncogene* 19(56): 6642-50.

APPENDIX

APPENDIX A

Peer-Reviewed Publication:

Androgen regulates *ADAMTS15* gene expression in prostate cancer cells. *Cancer Investigation*. Molokwu CN, Adeniji OO, Chandrasekharan S, Hamdy FC, Buttle DJ. 2010; 28(7):698710.

Cancer Investigation, 28:698–710, 2010
ISSN: 0735-7907 print / 1532-4192 online
Copyright © Informa Healthcare USA, Inc.
DOI: 10.3109/07357907.2010.489538

informa
healthcare

ORIGINAL ARTICLE
Cellular and Molecular Biology

Androgen Regulates *ADAMTS15* Gene Expression in Prostate Cancer Cells

Chidi N. Molokwu,^{1,2} Olajumoke O. Adeniji,² Shankar Chandrasekharan,^{1,2} Freddie C. Hamdy,^{1,3} and David J. Buttle²

Academic Urology Unit, University of Sheffield Medical School, Sheffield, United Kingdom,¹ Academic Unit of Molecular Medicine and Rheumatology, University of Sheffield Medical School, Sheffield, United Kingdom,² Nuffield Department of Surgery, John Radcliffe Hospital, University of Oxford, Oxford, United Kingdom³

ABSTRACT

Prostate cancer is a major cause of mortality, largely as a consequence of metastases and transformation to androgen-independent growth. Metalloproteinases are implicated in cancer progression. A disintegrin and metalloproteinase with thrombospondin motifs (ADAMTS) are expressed in prostate cancer cells, with ADAMTS-1 and ADAMTS-15 being the most abundant. ADAMTS-15 but not ADAMTS-1 expression was downregulated by androgen in LNCaP prostate cancer cells, possibly through androgen response elements associated with the gene. ADAMTS-15 expression is predictive for survival in breast cancer, and the situation may be similar in prostate cancer, as androgen independence is usually due to aberrant signaling through its receptor.

INTRODUCTION

Prostate cancer is the most common cancer in men in the Western world and second only to lung cancer as a cause of cancer death in men (1, 2). Approximately 30% of men diagnosed with prostate cancer will die of the disease (3), usually as a result of metastases. The exact mechanisms by which cancer cells invade and metastasize are not clear, but some metalloproteinases are thought to play roles in the process of cancer progression (4, 5).

Prostate epithelial cells depend on androgens for proliferation (6). Testosterone from the circulation is converted in the prostate by 5- α -reductase to dihydrotestosterone (DHT), the androgen that is most active in prostate tissue (7, 8). Androgen deprivation therapy (ADT) in the form of surgical or medical castration is used in the management of locally advanced, metastatic, or

relapsing disease. Androgen deprivation leads to reduction in the size of local tumors and the size and number of metastatic deposits (9). ADT reduces serum androgen concentration from about 2 nM to undetectable levels (10, 11), which has an adverse effect on hormone-sensitive prostate cancer cell survival and slows the development and progression of prostate cancer.

Androgen-regulated gene expression is mediated via the action of nuclear receptors. The activated androgen receptor translocates from the cytoplasm to the nucleus, where it binds to androgen response elements (AREs) located in proximity to androgen-regulated genes. AREs are 15-base-pair (15-bp) DNA sequences comprising two 6-bp half-sites separated by a 3-bp spacer. The sequence 5'-GGA/TACAnnnTGTTCT-3' has been described as the consensus ARE (12), but there is considerable variation in the sequence and configuration of AREs located in association with androgen-responsive genes (13).

A disintegrin and metalloproteinase with thrombospondin motifs (ADAMTSs) are a group of proteolytic enzymes belonging to family M12 in protease clan MA of the MEROPS database (www.merops.sanger.ac.uk) (14) and thus are homologous to a disintegrin and metalloproteinase and matrix metalloproteinases (15). There are 19 ADAMTS enzymes in the human genome, which play diverse roles in the tissues in which they are expressed (16). ADAMTS-1 is essential for normal development of the urogenital tract in mice (17) and for ovulation (18), and ADAMTS-1 and ADAMTS-8 have antiangiogenic

Keywords: Bladder & prostate cancer, Gene expression, Growth factors & receptor, Tumor cell biology, Tumor suppressors
Correspondence to:
Dr. David J. Buttle
Academic Unit of Molecular Medicine and Rheumatology
University of Sheffield Medical School
Beech Hill Road, Sheffield S10 2RX, United Kingdom
email: d.j.buttle@sheffield.ac.uk

properties (19). ADAMTS-5 has been implicated in cartilage breakdown in arthritis (20, 21). ADAMTS-2, ADAMTS-3, and ADAMTS-14 are procollagen *N*-peptidases (22), and ADAMTS-13 has been identified as the von Willebrand factor cleaving protease that is an important part of the blood coagulation cascade (23). Expression levels of ADAMTS proteases in prostate cancer and stromal cells have been reported previously (24). ADAMTS-1 and ADAMTS-15 were the most abundantly expressed in each of the prostate cancer and stromal cell lines investigated, but their role in prostate cancer development and progression is not known.

Owing to homology with ADAMTS-1, ADAMTS-15 is predicted to have proteoglycanase properties (25). However the ADAMTSs undergo C-terminal proteolytic processing (26), which affects their localization and activities, and the multiple domains could be playing different roles, as is the case with ADAMTS-1, in which the proteolytic domain is responsible for aggrecanase activity, while the C-terminal domains are required for antiangiogenic activity (27).

Decreased ADAMTS-15 expression in malignant breast tumors correlates with poor patient prognosis (28), suggesting that ADAMTS-15 may be playing a protective role in breast cancer patients. As is the case with prostate cancer, breast cancer is a disease in which hormone deprivation plays a role in management, with the use of estrogen receptor antagonists in patients with estrogen-receptor-positive tumors (29).

In order to further understand the potential roles of ADAMTS-1 and ADAMTS-15 in prostate cancer progression, we set out to test the hypothesis that the expression of ADAMTS-1 and ADAMTS-15 is regulated by androgens in prostate cancer cells. Owing to their possible proteolytic and antiangiogenic effects, such a scenario might suggest that these proteases play important roles in prostate cancer progression.

MATERIALS AND METHODS

Cell culture

The androgen-sensitive LNCaP prostate cancer cell line (30) was used to test the effects of DHT on ADAMTS expression. The cells were plated into 24-well culture plates at a density of 1×10^4 cells/well for RNA extraction and in 6-well culture plates at 5×10^4 cells/well for protein extraction. Cells were grown to approximately 60% confluence in Dulbecco's modification of Eagle's medium supplemented with 10% fetal calf serum, 100 units/mL penicillin, 100 μ g/mL streptomycin, and 0.25 μ g/mL amphotericin B, at 37°C in a humidified atmosphere of 5% CO₂. Medium was changed to serum-free DCCM (Biological Industries, Kibbutz Beit HaEmek, Israel), supplemented with 2 mM L-glutamine, and cells were allowed to acclimatize to the new medium for 48 hr. The medium was then removed, and cells were treated in fresh DCCM medium for 24 hr with DHT (Sigma) or with flutamide (Sigma, Poole, UK), a nonsteroidal androgen receptor antagonist. LNCaP cell proliferation is maximally stimulated by DHT at concentrations between 1 and 10 nM (8, 30–32). To cover the range between castrate levels and

maximal DHT stimulation, treatment doses of 0.1, 1.0, and 10 nM DHT were used. To determine whether an excess of flutamide would inhibit the effect of DHT, LNCaP cells were also treated with 1 μ M flutamide or 10 nM DHT + 1 μ M flutamide. DHT and flutamide were dissolved in 0.1% ethanol. The control arm was treated with 0.001% ethanol, as this was the final concentration of ethanol in the treatment arms.

RNA extraction and cDNA synthesis

For mRNA expression analysis, DHT treatment was carried out for 24 hr. This time point was used because previous experiments analyzing regulation of ADAMTS-15 had shown responsive changes in expression by this time point (24). The medium was removed, and TRI Reagent (Sigma) was applied to the wells to lyse the cells, using the supplier's protocol. The resulting cell lysate was stored at -80°C , awaiting RNA extraction. Total RNA was reverse-transcribed to cDNA with reverse transcriptase II (Invitrogen, Paisley, UK) using the supplier's protocol. Reactions for cDNA synthesis were run on a GeneAmp PCR System 9700 (Applied Biosystems). The thermal cycle was set at 25°C for 2 min, 42°C for 50 min, and 70°C for 15 min and was then cooled to 4°C. Furthermore, cDNA was stored at -20°C until ready for use in real-time reverse-transcriptase polymerase chain reactions (RT-PCRs).

Real-time RT-PCR

Real-time RT-PCR was run in 10- μ L reactions in duplicate, using 384-well plates on the ABI Prism 7900HT sequence detector with SDS 2.1 software (Applied Biosystems). TaqMan gene expression assays (Applied Biosystems) were used. Each assay contained a proprietary primer probe with a 6-carboxyfluorescein reporter and a quencher. Further, 5 μ L of TaqMan master mix (Applied Biosystems, Warrington, UK), 0.5 μ L of TaqMan gene expression assay, 2.5 μ L of diethylpyrocarbonate-treated water, and 2 μ L of cDNA were mixed in each well. The thermal cycle was set at 95°C for 5 min, and then 40 cycles were set at 95°C for 15 s and 60°C for 60 s. Independent cDNA samples were also analyzed using SYBR Green assays (Applied Biosystems). Each reaction consisted of 5 μ L of 2 \times SYBR Green mastermix as supplied, 50–1,000 nM of each primer, and 1 μ L of cDNA and made up to a final reaction volume of 10 μ L with diethylpyrocarbonate-treated water.

Glyceraldehyde-3-phosphate dehydrogenase (GAPDH) or RNA polymerase II (RNAP) were used as the endogenous housekeeping genes to normalize between samples (33). Assay IDs of TaqMan assays were as follows: Hs00199608_mL for ADAMTS-1, Hs00373520_mL for ADAMTS-15, Hs00426859_gL for prostate-specific antigen (PSA), Hs99999905_mL for GAPDH, and Hs00992801_mL for RNAP. Primer sequences for SYBR Green experiments were as follows: for ADAMTS-1, forward 5'-GCACTGCAAGGCGTAGGAC and reverse 5'-AAGCATGGTTTCCACATAGCG; for ADAMTS-15, forward 5'-TCCTCTTACCAGGCAGGAC and reverse 5'-GGTCACACATGGTACCCACATCA; and for

Table 1. Sequence Data for siGENOME SMARTpool siRNA From Dharmacon, Showing the Sequence ID and the Nucleotide Sequence for Each of the siRNA Duplexes

Gene	SMARTpool ID	Sense/Antisense	Sequence
ADAMTS15	D-005766-01	Sense	5'-GCGCGGACCGGAACAUUAAU
		Antisense	5'-UAAUGUCCAGGUCCGCGCUU
	D-005766-03	Sense	5'-CUGCGACGCGUCUUCUAUUUU
		Antisense	5'-AAUAGAAGCAGCGUCGAGUU
	D-005766-04	Sense	5'-CCAAGCGUUUCGUGUCUAAUU
		Antisense	5'-AUAGACACGAAACGCUUGUUU
	D-005766-05	Sense	5'-GCAAGAAGGUGACUGGACUUU
		Antisense	5'-AGUCCAGUCACCUUCUUGCUU

GAPDH, forward 5'-GCTCCTCTGTTCGACAGTCA and reverse 5'-AACTTCCCCATGGTGTCTGA. Expression levels of mRNA in the treated cells relative to the control cells were determined using the $2^{-\Delta\Delta Ct}$ method (34). This allowed the normalization of the expression levels of the gene of interest in individual experiments.

Protein extraction

For protein extraction, cells were treated with DHT and flutamide for 72 hr, after which medium was removed and cells were gently washed with phosphate-buffered saline. Tris-buffered saline was mixed with 0.01% Triton X-100 at 4°C in a volume ratio of 100:1 with protease inhibitor cocktail (Sigma) containing 4-(2-aminoethyl)benzenesulfonyl fluoride, pepstatin A, bestatin, leupeptin, aprotinin, and trans-epoxysuccinyl-L-leucylamido(4-guanido)-butane (E-64) according to the supplier's protocol. Each well was applied with 200 μ L of the mixture for 1 hr at 4°C to lyse the cells. The lysate was centrifuged at $12,000 \times g$ for 10 min at 4°C. The supernatant was removed and saved, while the pellet containing cell debris was discarded. The supernatant was stored at -40°C, awaiting protein quantification and Western blotting. Protein quantification was achieved using the MicroBCA assay (Pierce, Loughborough, UK) according to the manufacturer's protocol.

Characterization of an antibody to the propeptide of ADAMTS-15

We are unaware of any publications describing the specificity of an antibody to ADAMTS-15. It was therefore essential that we first characterized a commercial antibody before we could go on to use it in this study. This was achieved by siRNA knockdown of ADAMTS-15 expression and then analysis of changes in protein expression by Western blotting, using a rabbit antibody directed against the propeptide of ADAMTS-15 (Abcam, Cambridge, UK, ab45047). In addition, siGENOME SMARTpool siRNA against ADAMTS-15 was synthesized by Dharmacon (Epsom, UK). Each SMARTpool siRNA vial contained a pool of four different siRNA sequences directed against the gene of interest (Table 1). GAPDH was knocked down to serve as a positive control, and a nontargeting siRNA sequence (NTC) bearing no identity to any sequence in the human genome was transfected into cells in a separate set of wells as a negative

control. The sequences of the positive and the negative control were proprietary. GAPDH and NTC experiments were carried out using siCONTROL GAPD (cat. no. D-001140-01-05) and siCONTROL nontargeting siRNA (cat. no. D-001206-13) respectively. The cells were transfected in DharmaFECT 2 Transfection Reagent (Dharmacon) according to the manufacturer's protocol. The androgen-independent, LNCaP-derived C4-2b4 cell line (35) was used for validating the anti-ADAMTS-15 antibody. The cells were detached using trypsin-EDTA, and a small amount of serum-containing medium was added to the cell suspension to inactivate the trypsin. The cells were centrifuged at $1,000 \times g$ for 5 min, and the medium was removed from the cell pellet. The cells were resuspended in the medium containing 10% (v/v) fetal calf serum without antibiotics and counted. Wells of a 96-well polystyrene plate were used to prepare the reagents for the transfections. In one well, 2.5 μ g of siRNA was added to 10 μ L of serum-free medium, and in a separate well, 0.4 μ L of DharmaFECT 2 was added to 19.6 μ L of serum-free medium. The contents of the first well were added to the second, and the mixture was left at ambient temperature for 20 min, before being placed into the wells of a 48-well plate. A total of 3×10^4 cells were added to each of the wells containing the siRNA mixture, and the final volume of each well was made up to 200 μ L with the medium containing no antibiotics. Knockdown of target siRNA was analyzed by real-time RT-PCR at 72 hr posttransfection, and protein knockdown was analyzed at 120 hr posttransfection by Western blotting as described below.

Protein samples were prepared by heating to 95°C for 5–10 min in reducing sample buffer [62.5 mM Tris-HCl; 25% (v/v) glycerol; 2% (w/v) sodium dodecyl sulfate; 0.01% bromophenol blue; 350 mM dithiothreitol, pH 6.8]. Sodium dodecyl sulfate-polyacrylamide gel electrophoresis was performed using 10% (w/v) polyacrylamide gels. Each well was loaded with 100 μ g of protein, and the gels were electrophoresed for 1 hr at a constant voltage of 200 V. Protein from the gel was then transferred to a polyvinylidene fluoride membrane at a constant current of 400 A for 10 min at pH 11.0. The membrane was blocked for 1 hr in blocking buffer [6% (w/v) casein, 0.05% Tween-20 in TBS (TBST)]. After blocking, the membrane was probed for 6 hr using the rabbit anti-ADAMTS-15 antibody (Abcam, ab45047) raised against the propeptide of ADAMTS-15, at a dilution of 1:5,000 (200 ng/mL) in blocking buffer. After three washes in TBST, the membrane was probed for 1 hr with

a horseradish-peroxidase-conjugated (HRP-conjugated) swine antirabbit IgG antibody (Dako Cytomation, P0399, Ely, UK) at a dilution of 1:3,000 (113 ng/mL). HRP detection was done with ECL Plus Western blotting detection kit (Amersham, Little Chalfont, UK) according to the manufacturer's protocol. Hyperfilm ECL (Amersham) X-ray film was used to expose and develop the membranes.

For reprobing, the polyvinylidene fluoride membranes were washed three times in TBST and stripped of anti-ADAMTS-15 antibody by agitation at 4°C for 6 hr in TBST brought to pH 2.0 with HCl. GAPDH was probed with rabbit polyclonal anti-GAPDH IgG (Abcam, ab9485) at a dilution of 1:1,000 (1 µg/mL). Secondary antibody probing and HRP detection were done as described earlier.

Densitometry

Bands detected on X-ray films from Western blotting experiments were semiquantitatively analyzed by densitometry using a GS-710 Calibrated Imaging Densitometer (Bio-Rad, Hemel Hempstead, UK) running on Quantity One version 4.5.1 software (Bio-Rad). A boundary was drawn around each band for analysis. The adjusted area and density (volume) of the band from each treatment sample was compared with the band from the control sample, measured as optical density × mm², and was defined by the software as the sum of the intensities of the pixels (in optical density) within a volume boundary multiplied by the area of a single pixel (in mm²) minus the background volume.

ADAMTS15 gene analysis

The genomic sequences of the *ADAMTS1* and *ADAMTS15* genes were obtained from the Ensembl genome database, Release 49 (www.ensembl.org) (36). The Ensembl online tool was used to determine the 5'-flanking sequence containing the gene regulatory region, the transcription start point (TSP), and the gene sequence with intron and exon information. Using an *in silico* approach with the online nuclear receptor binding site search tool NUBIScan version 2.0 (www.nubiscan.unibas.ch) (37), a matrix was created consisting of the following nine ARE half-sites: AGAACA, TGTACC, TGTACA, TGTTCT, GGTACA, AGTGCT, TGGTCA, AGTTCT, and AGTACG. Each half-site has previously been shown to be functional (13). A search strategy was designed to search for putative AREs composed of direct repeats (DRs), inverted repeats (IRs), and everted repeats (ERs) of these half-sites interposed by a nonspecific 3-bp sequence, forming a complete 15-bp ARE. A threshold score of 0.8 was set to minimize false-positive predictions. This threshold setting ensured that only putative AREs with sequences corresponding to 80–100% similarity with the half-sites in the matrix were detected. The frequency and position of AREs that met the search criteria were recorded. For comparison, the promoter regions and sequences of PSA (human kallikrein 3, *hKLK3*) and prostate-specific membrane antigen (folate hydrolase 1, *FOLH1*) genes were also analyzed using the same strategy. *hKLK3* gene expression is known to be upregulated by androgen, and the promoter region contains the functional ARE (AGAACA_{gca}AGTGCT) at -170 bp from the TSP (38). The

expression of the *FOLH1* gene is downregulated by androgen (39).

Statistical analyses

The Kruskal–Wallis test was used to identify significant differences between the medians of each treatment group. Differences in expression levels were tested for significance with the Dunn's multiple-comparison test, which analyzes differences in rank sum between each treatment group and control. The Grubb's test was used to identify and remove outlying samples where appropriate. All tests were performed on GraphPad Prism 5.0 (GraphPad Software Inc.). Statistically significant differences were defined by $p \leq .05$.

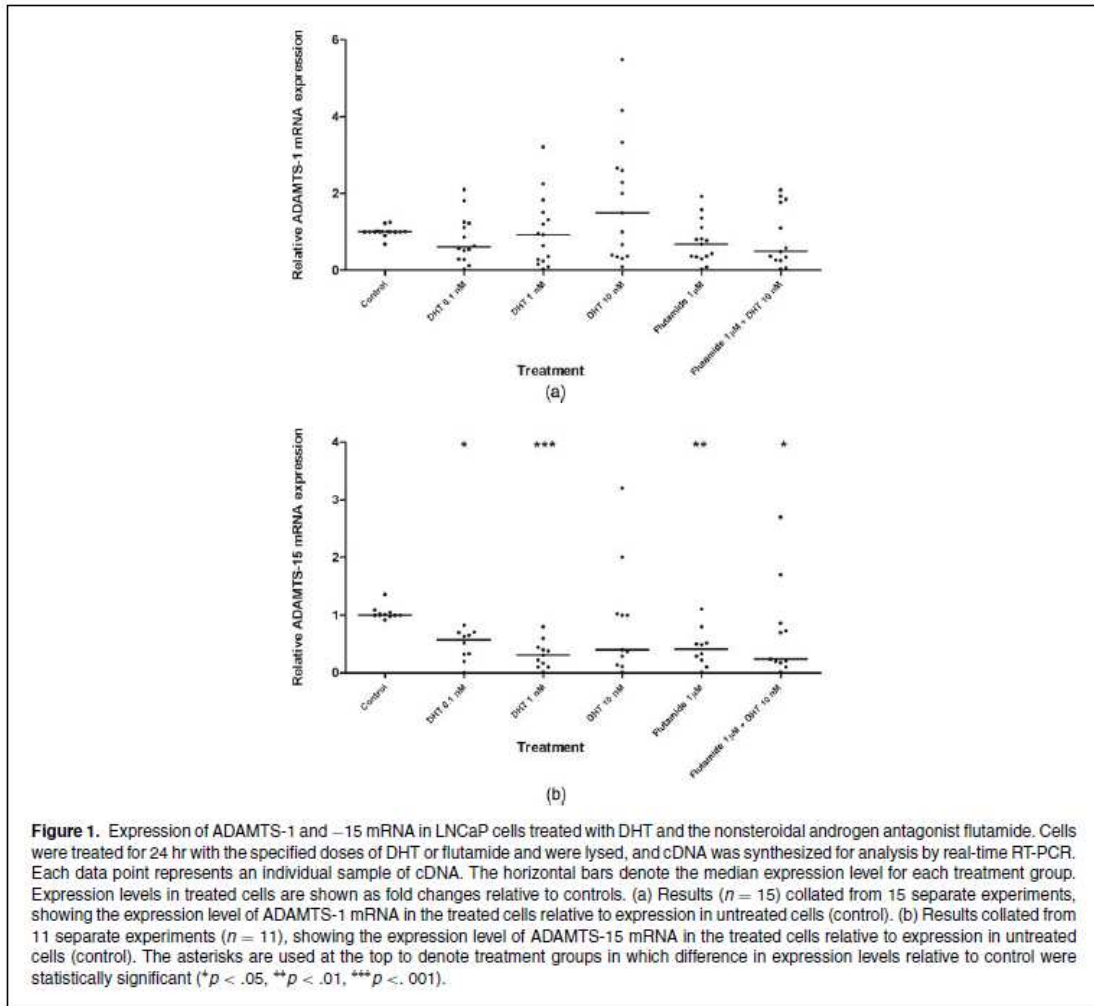
RESULTS

Regulation of *ADAMTS-1* and *ADAMTS-15* mRNA expression by DHT

The effect of DHT and flutamide on expression of *ADAMTS-1* and *ADAMTS-15* mRNA was analyzed using real-time RT-PCR. DHT treatment did not significantly regulate expression of *ADAMTS-1* mRNA at any of the concentrations used [Figure 1(a)]. In contrast to this, DHT treatment downregulated the expression of *ADAMTS-15* mRNA. *ADAMTS-15* mRNA was downregulated by 40% and 70% with treatments of 0.1 and 1 nM DHT respectively [Figure 1(b)]. The Kruskal–Wallis test demonstrated that the medians had a significantly different variance ($p = .0022$). Dunn's multiple-comparison test was used to analyze differences in rank sum between each treatment group and control. *ADAMTS-15* mRNA expression was significantly downregulated with treatments of 0.1 nM DHT ($p < .05$), 1 nM DHT ($p < .001$), 1 µM flutamide ($p < .01$), and 10 nM DHT with 1 µM flutamide ($p < .05$). Comparing the 10 nM DHT treatment group with the 10 nM DHT plus 1 µM flutamide treatment group showed no significant difference in *ADAMTS-15* expression. Grubb's test was applied to the 10 nM DHT treatment group to identify and remove an outlying sample, after which the difference in the median *ADAMTS-15* mRNA expression between the control and the 10 nM DHT group was significant ($p < .05$). Independent cDNA samples ($n = 5$) from LNCaP cells treated with DHT and flutamide were analyzed using SYBR Green assays. Results from these experiments also showed downregulation of *ADAMTS-15* mRNA by DHT that was not inhibited by flutamide (data not shown). As a positive control, regulation of PSA mRNA by DHT was also analyzed. As expected, PSA mRNA expression was upregulated by DHT in a dose-dependent manner. Compared with control, PSA mRNA was upregulated 4-fold by 0.1 nM DHT, 9-fold by 1 nM DHT, and 45-fold by 10 nM DHT (data not shown).

Antibody validation

As we failed to find characterization of *ADAMTS-15* antibodies in the literature, we undertook an investigation of the utility of one such antibody, ab45047, raised against a region

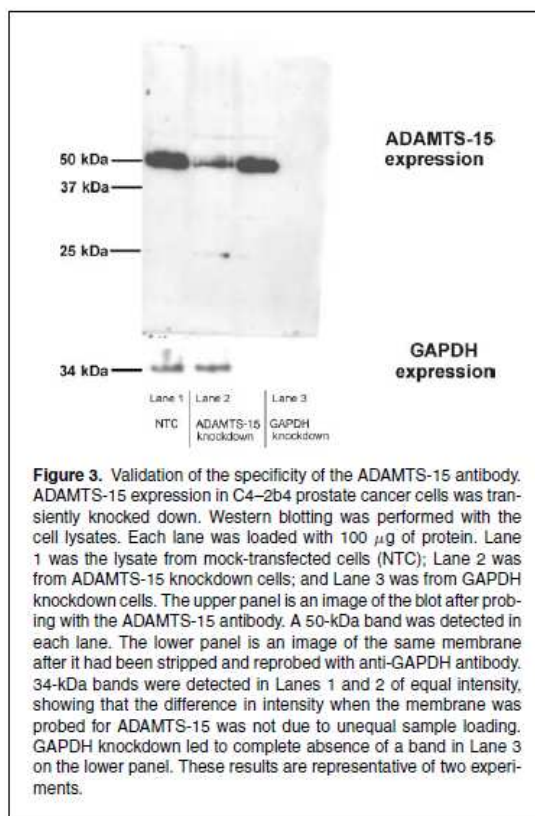
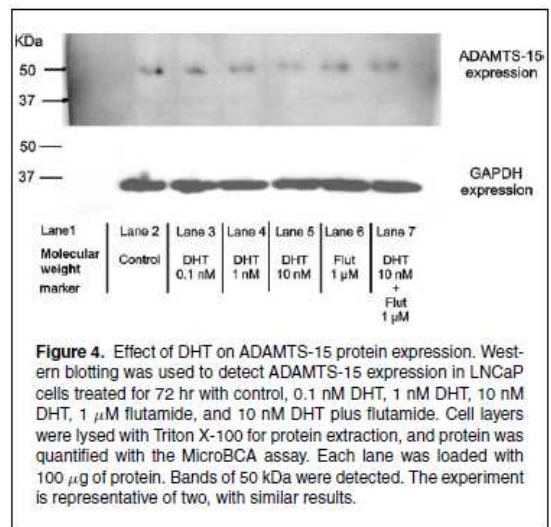
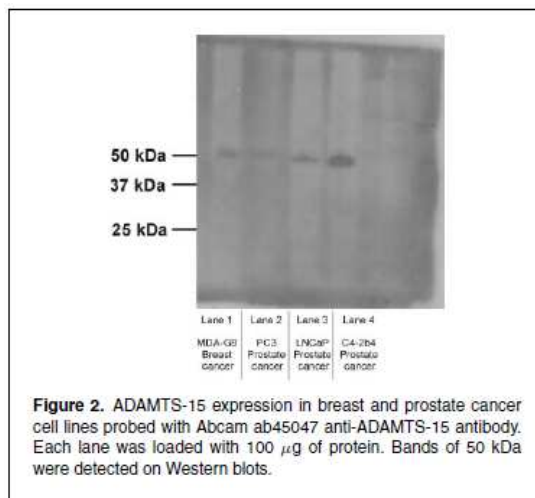


of the propeptide of ADAMTS-15. C4-2b4 cells expressed more ADAMTS-15 than did LNCaP cells in preliminary experiments (Figure 2), making the effect of knockdown more readily detectable on a Western blot. We therefore utilized the former cell line in these characterization studies. ADAMTS-15 mRNA expression in C4-2b4 prostate cancer cells was inhibited by 80% ($\pm 10\%$, $n = 3$) by siRNA specific for ADAMTS-15. Protein expression was analyzed by Western blotting. Bands of 50 kDa were detected in all the lanes, but the band was attenuated in the cells treated with ADAMTS-15 siRNA. Densitometric analysis of the 50-kDa band showed that its expression was knocked down by over 80% (Figure 3). To control for errors in sample loading, the membrane was stripped and then reprobed with anti-GAPDH antibody. Bands of 34 kDa were detected

with equal intensity in the NTC and ADAMTS-15 knockdown lanes. The band was absent in the GAPDH knockdown lane (Figure 3). The detection of downregulated expression of the 50-kDa band by the antibody in the cells treated with siRNA to the *ADAMTS15* gene verified the specificity of the antibody and illustrated that the major product from these cells was a form of the enzyme of approximately 50 kDa.

Regulation of ADAMTS-15 protein expression by DHT

To analyze the effect of DHT stimulation on ADAMTS-15 protein expression, LNCaP cells were treated with DHT with and without flutamide for 72 hr. Western blotting with the



anti-ADAMTS-15 antibody revealed a 50-kDa band in all the lanes (Figure 4). These bands were analyzed by densitometry, and in keeping with the mRNA data, ADAMTS-15 protein was downregulated by DHT in a dose-dependent manner (Table 2). This effect was not inhibited by flutamide. In fact, as had been observed at the mRNA level, treatment with flutamide alone also caused downregulation of ADAMTS-15 protein.

Putative androgen response elements

The *ADAMTS15* gene has not been previously described as an androgen-regulated gene. Using the NUBIScan online nuclear receptor binding site search tool, the *ADAMTS15* gene promoter and gene sequence were screened to identify putative AREs. We identified 1 ARE in the *ADAMTS15* promoter and 12 AREs in the gene sequence. ADAMTS-1 mRNA expression was not regulated by DHT in our experiments. The *ADAMTS1* gene had no putative AREs in the promoter region but had two in the gene sequence. Table 3 gives the position, orientation, sequence, and score for the putative AREs identified. For comparison, we performed the same search on the *hKLK3* gene, which is upregulated by androgen, and on the *FOLH1* gene, which is downregulated by androgen (Table 4). Figure 5 shows a schematic representation of the AREs identified in the *ADAMTS1*, *ADAMTS15*, and *hKLK3* genes. The ARE detected at position 169 of the *hKLK3* promoter region is known to be the functional PSA ARE sequence AGAACAgcaAGT-GCT (35). The *hKLK3* promoter had approximately double the ARE-to-bp ratio compared with the *ADAMTS15* and *FOLH1* promoters, and the *hKLK3* gene sequence had approximately 1.5 times the ratio found in the *ADAMTS15* and *FOLH1* gene sequences and approximately 3 times the ratio in the *ADAMTS1* gene sequence.

Table 2. Densitometric Analysis of Bands Detected on Western Blots Performed on Samples From Two Experiments, with Adjusted Volume of the Bands Quantified and Compared With Control

	Lane 1 Control	Lane 2 DHT 0.1 nM	Lane 3 DHT 1 nM	Lane 4 DHT 10 nM	Lane 5 Flutamide 1uM	Lane 6 DHT 10 nM + Flutamide 1 uM
Experiment 1						
Adjusted densitometric volume (OD mm ²)	0.2025	0.1238	0.0905	0.0483	0.0659	0.055
Adjusted volume relative to control	1	0.6	0.4	0.2	0.3	0.3
Experiment 2						
Adjusted densitometric volume (OD mm ²)	0.2038	0.2231	0.0217	0.0022	0.05	0.0093
Adjusted volume relative to control	1	1.1	0.1	0.01	0.2	0.05

Table 3. Position, Orientation, Sequence, and Similarity Score of the AREs Detected in the *ADAMTS1* and *ADAMTS15* Genes

	Position (Strand)	Repeat Orientation	ARE Sequence	Score
<i>ADAMTS1</i>				
Promoter	-	-	-	-
Sequence	4933 (-)	DR	GGTGCTacaTGTGCT	0.82
	7676 (+)	DR	TGGTCAcaTGTCT	0.81
<i>ADAMTS15</i>				
Promoter	-2319 (+)	ER	GGAACAtaaGGTGCG	0.81
Sequence	914 (+)	DR	AGCACCCcgAGTACT	0.81
	914 (+)	ER	AGCACCCcgAGTACT	0.88
	914 (+)	IR	AGCACCCcgAGTACT	0.81
	928(-)	DR	AGTACTcggGGTGCT	0.88
	2357 (+)	ER	GGCACAgctAGTCCC	0.81
	6884 (-)	DR	AGTGTCTctgAGTGCA	0.87
	6893 (-)	DR	AGTGCCgagAGTGCT	0.84
	7038 (+)	IR	TGTGCTgccTGGACT	0.86
	12880 (-)	DR	TGTCCCcacAGTGCC	0.81
	16123 (+)	DR	TGAACCGttAGTTCA	0.82
	16123 (-)	ER	TGAACCGttAGTTCA	0.89
	19163 (+)	IR	AGCACTctcTGAAct	0.81
	19177 (-)	DR	AGTTCAgagAGTGCT	0.90
	24790 (+)	IR	AGTGCAactTGCACC	0.84

Note: For the orientation, DR, ER, and IR denote direct repeat, everted repeat, and inverted repeat respectively.

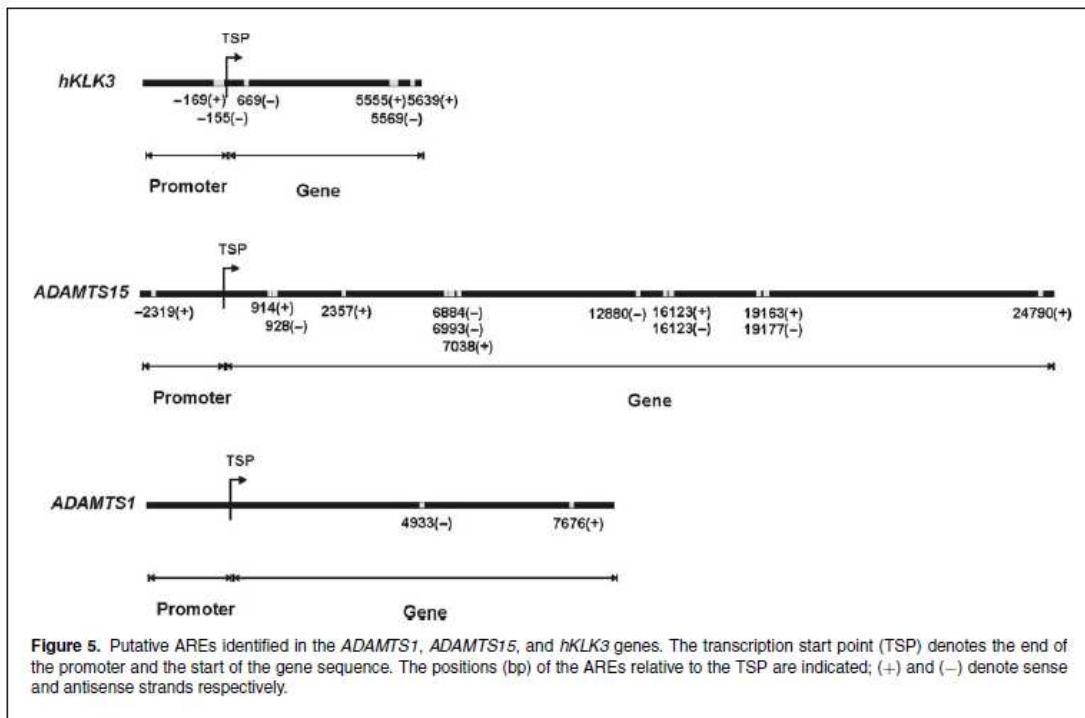
Table 4. Summary of the ARE Data for *ADAMTS1*, *ADAMTS15*, *hKlK3*, and *FOLH1* Genes

	<i>ADAMTS1</i>	<i>ADAMTS15</i>	<i>hKlK3</i>	<i>FOLH1</i>
Gene location	21q21.3	11q24.3	19q13.33	11p11.2
Androgen regulation	Not regulated	Downregulated	Upregulated	Downregulated
Promoter				
Length (bp)	1,786	2,576	2,434	2,618
AREs	0	1	2	1
AREs per bp	0	0.00039	0.00082	0.00038
Sequence				
Length (bp)	9,121	24,848	5,850	62,033
AREs	2	12	4	25
AREs per bp	0.00022	0.00048	0.00068	0.0004

DISCUSSION

Hormone therapy for locally advanced and metastatic prostate cancer essentially consists of lowering circulating androgen concentration in order to silence androgen receptor signaling. In our experiments, we analyzed the expression of *ADAMTS-1* and *ADAMTS-15* under different concentrations

of DHT in an androgen-responsive cell line, LNCaP. *ADAMTS-1* mRNA expression was not significantly regulated by DHT. By contrast, DHT downregulated the expression of *ADAMTS-15* mRNA and protein. The *ADAMTS15* gene has not previously been reported to be androgen regulated. It is known to be expressed in prostate cancer cell lines (24), and its expression in breast cancer is a good indicator of patient survival (28). This

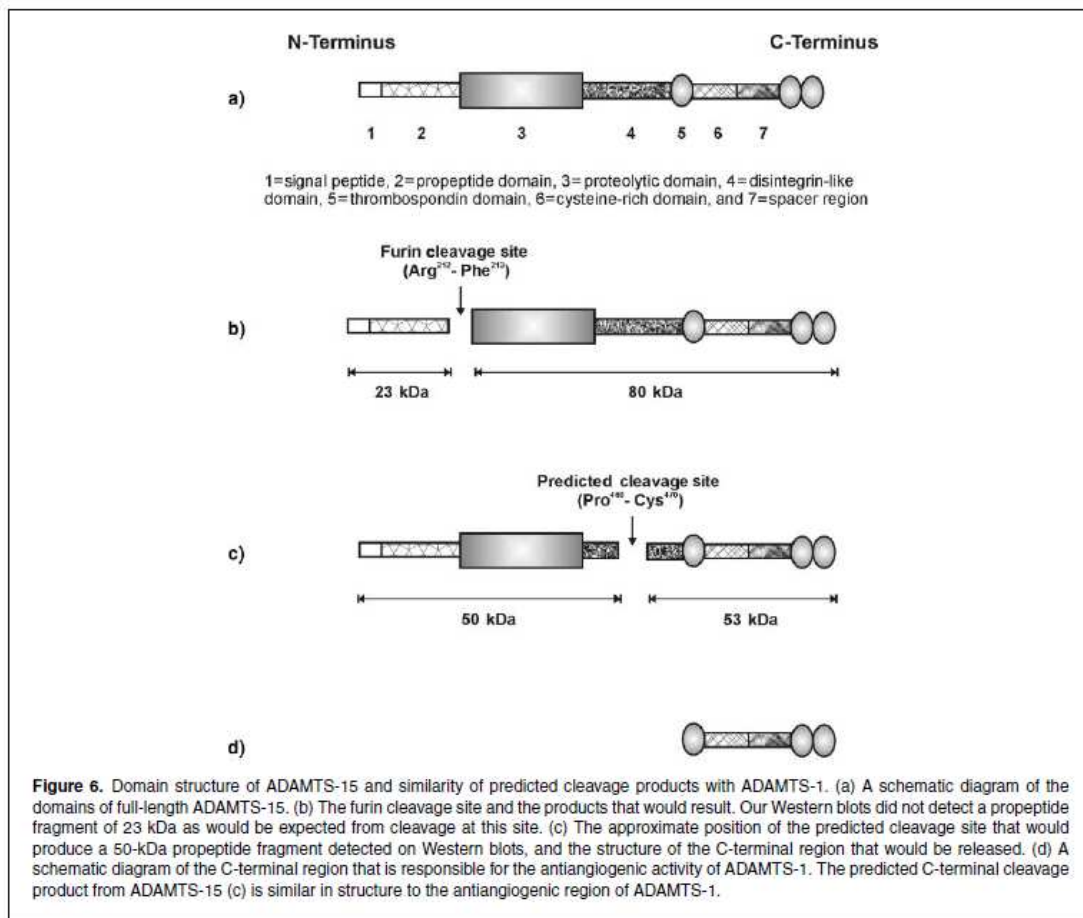


raises the possibility that ADT could be upregulating *ADAMTS15* expression in prostate cancer cells and inhibiting tumor progression, at least until the cells become androgen independent. The relationship between tumor expression of *ADAMTS15* and survival has not yet been studied in prostate cancer patients.

Our experiments also showed that rather than inhibiting the action of DHT, flutamide actually had a similar effect as DHT in downregulating *ADAMTS15* expression. This supports previous findings that mutations in the androgen receptor of prostate cancer cells could lead to aberrant activation by adrenal steroids and nonsteroidal androgen receptor antagonists (40–42). LNCaP cells have a mutation in the androgen receptor ligand-binding domain in which threonine is changed to alanine at position 877 (T877A), leading to androgen receptor activation by flutamide (40). Other androgen receptor mutations have been identified in tumors of patients with prostate cancer (43). Up to 68% of prostate cancer patients with disease progression while on treatment with flutamide experience disease remission when flutamide is withdrawn (44–47). This phenomenon, known as the flutamide withdrawal syndrome, provides clinical evidence that mutations in the androgen receptor of prostate cancer cells could lead to aberrant activation by flutamide.

Activated androgen receptors bind to AREs in promoter regions of androgen-regulated genes, where transcription factors are recruited by the receptor–ligand complex (48). Transcrip-

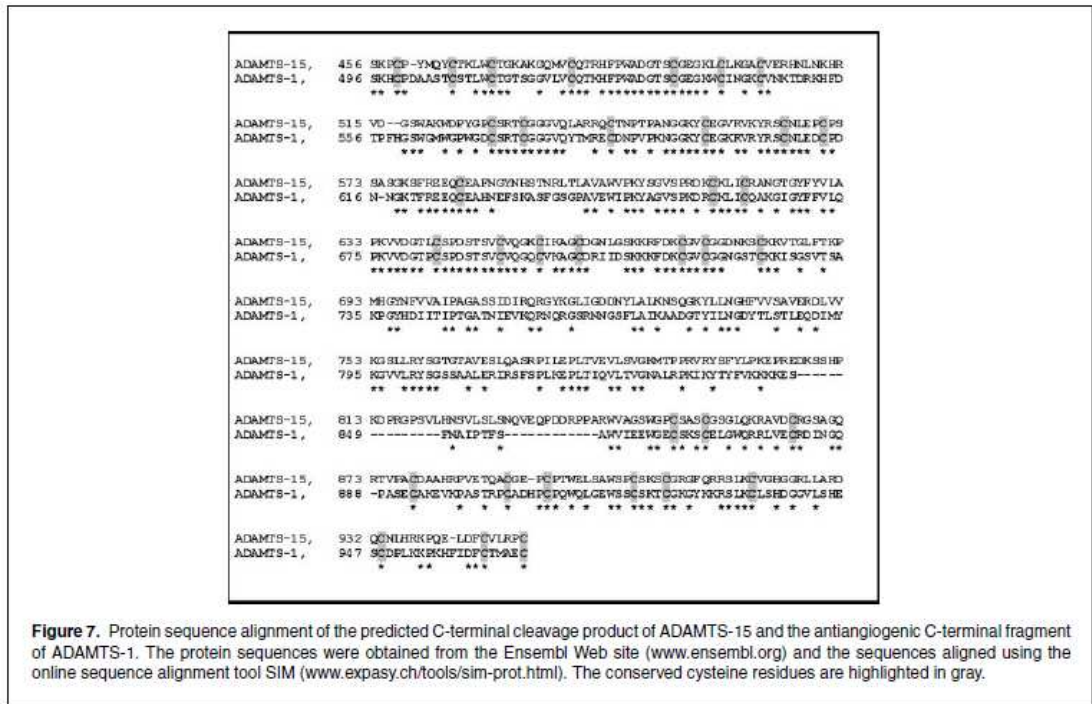
tion factors could be either coactivators or corepressors. Recruitment of coactivators by the receptor will lead to increased transcription of mRNA, while recruitment of corepressors leads to decreased transcription (48). Using an *in silico* approach we screened the *ADAMTS1* and *ADAMTS15* genes for putative AREs. One ARE was found in the promoter region of *ADAMTS15* but none in the promoter region of *ADAMTS1*. We also found several putative AREs downstream of the TSP of the *ADAMTS15* gene. This raises the possibility that one or more of these AREs could be acting as an enhancer. Unlike gene promoters, gene enhancers can be located many thousand bp upstream or downstream of the TSP (49). The *hKLK3* gene has such an enhancer containing an ARE that is located 4,200 bp upstream of the TSP (50), and several studies have found that proportionately more AREs are located in the gene sequence than in the promoter region of androgen-regulated genes (51), which is in keeping with our findings. The significance of the ARE to bp ratio with respect to androgen upregulation or downregulation is not known. Our analysis showed that the *hKLK3* promoter region had twice the density of putative AREs as the *FOLH1* and *ADAMTS15* promoters (Table 4). This may mean that more AREs are required to assemble coactivator complexes than are required for the assembly of corepressor complexes. A similar search for other transcription factor binding sites in the promoter regions of *ADAMTS1*,



ADAMTS15, *hKLK3*, and *FOLH1* did not identify differences between the androgen upregulated (*hKLK3*) and the androgen downregulated (*ADAMTS15* and *FOLH1*) genes. However the androgen-regulated genes (*ADAMTS15*, *hKLK3*, and *FOLH1*) had the myocyte enhancer factor 2 (MEF2) and the chorion factor 2 transcription factor binding sites in their promoter regions. The MEF2 and the chorion factor 2 transcription factors synergistically regulate gene expression (52). In addition to regulating myocyte differentiation, MEF2 maintains vascular integrity by promoting endothelial cell survival and proliferation (53). It is acknowledged that *in-silico*-based methods can identify the presence of transcription factors associated with genes but do not show functionality (54). Further studies are required to determine if the putative AREs identified in this study are functional.

The ADAMTS-15 antibody used in our experiments was described by the supplier as being directed against the propeptide

domain of ADAMTS-15 and predicted a relative mass of 103 kDa on Western blotting. Our Western blot experiments (Figures 2–4) detected bands of 50 kDa from the cell and ECM lysate, which is about half the relative mass expected for the full length ADAMTS-15 protein and twice the relative mass of the propeptide domain, which is approximately 23 kDa. No bands were detected from the conditioned medium. The 50-kDa band was attenuated when ADAMTS-15 was knocked down with siRNA targeting ADAMTS-15 mRNA. This suggests that ADAMTS-15 was processed posttranslationally by proteolytic cleavage yielding an N-terminal fragment of 50 kDa, implying that the cleavage site lies within the disintegrin-like domain of ADAMTS-15 [Figure 6(c)]. Analysis of the X-ray crystal structure of the ADAMTS-1 disintegrin-like domain has shown that this domain is actually a cysteine-rich domain that fails to superimpose on the structures of the disintegrin domains of ADAM-10, VAP-1, and trimestatin (55). The sequence



similarity of ADAMTS-15 and ADAMTS-1 (25) suggests that the ADAMTS-15 disintegrin-like domain, where we predict the cleavage site lies, is also a cysteine-rich domain with no disintegrin activity.

ADAMTS enzymes are known to be C-terminally processed (26, 56), and it is likely that the form of ADAMTS-15 we detected has lost its C-terminal ancillary domains but retains the propeptide and catalytic domains. The propeptide domain is thought to maintain the latency of the catalytic domain, and activation of the catalytic domain is mediated by cleavage by pro-protein convertases such as furin (16). Retention of the propeptide implies that the catalytic domain of ADAMTS-15 remains inactive, and thus the proteolytic activity is muted. It is possible that a catalytically active form of ADAMTS-15, with the propeptide removed, is also expressed by LNCaP cells, as such a form would not have been detected by the antibody used in our study. Analogously, the full length ADAMTS-1 and the C-terminal region of ADAMTS-1 are reported to display prometastatic and antimetastatic properties respectively (27, 57). The C-terminal region containing three thrombospondin repeats and a spacer (Figure 6) is responsible for the antiangiogenic properties of ADAMTS-1 (57). This region of ADAMTS-1 is very similar to the C-terminal region that we predict is cleaved from ADAMTS-15 (Figures 6 and 7), leaving the propeptide and the catalytic domain of 50 kDa that we detected on our Western blots. It is conceivable that the potential proteolytic ac-

tivity of the form of ADAMTS-15 that we have identified is muted because the propeptide remains bound to the catalytic domain, and the C-terminal half of the molecule is released to function as an inhibitor of angiogenesis in the tumor microenvironment. Somatic mutations of *ADAMTS15* have been identified in breast and colorectal cancer cells (58–60). Analysis of the *ADAMTS15* mutations in colorectal cancer cells predict that shortened, mutant forms of ADAMTS-15 are produced (60). No mutations of ADAMTS-15 have been reported in prostate cancer cells, but in addition to proteolytic processing, this could be another possible explanation for the detection of a 50-kDa ADAMTS-15 protein.

It is generally accepted that prostate and breast cancer angiogenesis correlates with disease severity (61–63), and as noted earlier, breast cancer patients with relatively higher tumor expression of ADAMTS-15 have better survival (28). Patients undergoing ADT eventually progress to hormone refractory prostate cancer (HRPC). In HRPC, by mechanisms which are not yet clearly understood, androgen receptor signaling resumes despite diminished levels of circulating androgen (64). On the basis of our findings, this is likely to result in downregulation of ADAMTS-15 in the tumor microenvironment, contributing to the poor prognosis of patients who develop HRPC.

In conclusion, we have shown that ADAMTS-15 expression is downregulated by androgen, suggesting that ADT leads to

increased expression of ADAMTS-15 in the tumor microenvironment, and mutations in the androgen receptor leading to an androgen-independent state may result in constitutive downregulation of ADAMTS-15. Its role in breast cancer suggests that ADAMTS-15 has a cancer-repressive role.

ACKNOWLEDGMENTS

The authors would like to thank Dr. Colby Eaton for providing the C4-2b4 prostate cancer cells and Dr. Ingunn Holen for providing the MDA-G8 breast cancer cells used in the experimental work.

Declaration of interest: The authors report no conflict of interest. The authors alone are responsible for the content and writing of this paper.

REFERENCES

1. Ferlay, J.; Autier, P.; Boniol, M.; Heanue, M.; Colombet, M.; Boyle, P. Estimates of the cancer incidence and mortality in Europe in 2006. *O. Annncol* **2007**, *18*(3), 581–592.
2. Jemal, A.; Siegel, R.; Ward, E.; Hao, Y.; Xu, J.; Thun, M.J. Cancer statistics. *Cancer, C.A. J Clin* **2009**, *59*(4), 225–249.
3. Aus, G.; Robinson, D.; Rosell, J.; Sandblom, G.; Varenhorst, E.; R. South-Eastregion C. Prostatecancer Group. Survival in prostate carcinoma – outcomes from a prospective, population-based cohort of 8887 men with up to 15 years of follow-up: results from three countries in the population-based P. Nationalrostate R. Canceregistry of Sweden. *Cancer* **2005**, *103*(5), 943–951.
4. Egeblad, M.; Werb, Z. New functions for the matrix metalloproteinases in cancer progression. *R. Natev Cancer* **2002**, *2*(3), 161–174.
5. Rocks, N.; Paulissen, G.; El Hour, M.; Quesada, F.; Crahay, C.; Gueders, M.; Foidart, J.M.; Noel, A.; Cataldo, D. Emerging roles of ADAM and ADAMTS metalloproteinases in cancer. *Biochimie* **2008**, *90*(2), 369–379.
6. Sandberg, A.A. Endocrine control and physiology of the prostate. *Prostate* **1980**, *1*, 169–184.
7. Steers, W.D. 5 α -Reductase activity in the prostate. *Urology* **2001**, *58*(6 Suppl. 1), 17–24.
8. Zhu, Y.S.; Cai, L.Q.; You, X.; Cordero, J.J.; Huang, Y.; Imperato-McGinley, J. Androgen-induced prostate-specific antigen gene expression is mediated via dihydrotestosterone in LNCaP cells. *J Androl* **2003**, *24*(5), 681–687.
9. Huggins, C. Effect of orchiectomy and irradiation on cancer of the prostate. *S. Annuig* **1942**, *115*(6), 1192–1200.
10. de Jong, F.H.; Oishi, K.; Hayes, R.B.; Bogdanowicz, J.F.; Raatgever, J.W.; van der Maas, P.J.; Yoshida, O.; Schroeder, F.H. Peripheral hormone levels in controls and patients with prostatic cancer or benign prostatic hyperplasia: results from the Dutch-Japanese case-control study. *R. Canceres* **1991**, *57*(13), 3445–3450.
11. Anderson, J.; Abrahamsson, P.A.; Crawford, D.; Miller, K.; Tombal, B. Management of advanced prostate cancer: can we improve on androgen deprivation therapy? *Int. B.J.U* **2008**, *101*(12), 1497–1501.
12. Roche, P.J.; Hoare, S.A.; Parker, M.G. A consensus DNA-binding site for the androgen receptor. *E. Molndocrinol* **1992**, *6*(12), 2229–2235.
13. Monge, A.; Jagla, M.; Lapouge, G.; Satorith, S.; Cruchant, M.; Wurtz, J.M.; Jacqmin, D.; Bergerat, J.P.; Céraline, J. Unfaithfulness and promiscuity of a mutant androgen receptor in a hormone-refractory prostate cancer. *M. Cellol S. Lifeci* **2006**, *63*(4), 487–497.
14. Rawlings, N.D.; Morton, F.R.; Kok, C.Y.; Kong, J.; Barrett, A.J. MEROPS: the peptidase database. *A. Nucleicoids Res* **2008**, *36*, D320–D325.
15. Nicholson, A.C.; Malik, S.B.; Logsdon, J.M.; Van Meir, E.; Functional, G. evolution of ADAMTS genes: evidence from analyses of phylogeny and gene organization. *Evol. B.M.C Biol* **2005**, *5*(1), 11–23.
16. Porter, S.; Clark, I.M.; Kevorkian, L.; Edwards, D.R.; Clark, I.M.; Kevorkian, L.; Edwards, D.R. A. D. A. M. TheTS metalloproteinases. *J. Biochem* **2005**, *386*(1), 15–27.
17. Shindo, T.; Kurihara, H.; Kuno, K.; Yokoyama, H.; Wada, T.; Kurihara, Y.; Imai, T.; Wang, Y.; Ogata, M.; Nishimatsu, H.; Moriyama, N.; Oh-hashii, Y.; Morita, H.; Ishikawa, T.; Nagai, R.; Yazaki, Y.; Matsumura, K. ADAMTS-1: a metalloproteinase-disintegrin essential for normal growth, fertility and organ morphology and function. *J. I. Cllnvest* **2000**, *105*(10), 1345–1352.
18. Russell, D.L.; Doyle, K.M.; Ochsner, S.A.; Sandy, J.D.; Richards, J.S. Processing and localization of ADAMTS-1 and proteolytic cleavage of versican during cumulus matrix expansion and ovulation. *J. C. Biolhem* **2003**, *278*(43), 42330–42339.
19. Vázquez, F.; Hastings, G.; Ortega, M.-A.; Lane, T.F.; Oikemus, S.; Lombardo, M.; Iruela-Arispe, M.L. METH-1, a human ortholog of ADAMTS-1, and METH-2 are members of a new family of proteins with angio-inhibitory activity. *J. C. Biolhem* **1999**, *274*(33), 23349–23357.
20. Stanton, H.; Rogerson, F.M.; East, C.J.; Golub, S.B.; Lawlor, K.E.; Meeker, C.T.; Little, C.B.; Last, K.; Farmer, P.J.; Campbell, I.K.; Fourie, A.M.; Fosang, A.J. ADAMTS5 is the major aggrecanase in mouse cartilage in vivo and in vitro. *Nature* **2005**, *434*(7033), 648–652.
21. Glasson, S.S.; Askew, R.; Sheppard, B.; Carito, B.; Blanchet, T.; Ma, H.-L.; Flannery, C.R.; Peluso, D.; Kanki, K.; Yang, Z.; Majumdar, M.K.; Morris, E.A. Deletion of active ADAMTS-5 prevents cartilage degradation in a murine model of osteoarthritis. *Nature* **2005**, *434*(7033), 644–648.
22. Collge, A.; Vandenberghe, I.; Thiry, M.; Lambert, C.A.; van Beeumen, J.; Li, S.W.; Prockop, D.J.; Lapière, C.M.; Nusgens, B.V. Cloning and characterization of ADAMTS-14, a novel ADAMTS displaying high homology with ADAMTS-2 and ADAMTS-3. *J. C. Biolhem* **2002**, *277*(8), 5756–5766.
23. Fujikawa, K.; Suzuki, H.; McMullen, B.; Chung, D. Purification of human von Willebrand factor-cleaving protease and its identification as a new member of the metalloproteinase family. *Blood* **2001**, *98*(6), 1662–1666.
24. Cross, N.A.; Chandrasekharan, S.; Jokonya, N.; Fowles, A.; Hamdy, F.C.; Buttle, D.J.; Eaton, C.L. The expression and regulation of ADAMTS-1, ADAMTS-4, ADAMTS-5, ADAMTS-9, and ADAMTS-15, and TIMP-3 by TGF β 1 in prostate cells: relevance to the accumulation of versican. *Prostate* **2005**, *63*(3), 269–275.
25. Cal, S.; Obaya, A.J.; Llamazares, M.; Garabaya, C.; Quesada, V.; López-Otín, C. Cloning, expression analysis, and structural characterization of seven novel human ADAMTSs, a family of metalloproteinases with disintegrin and thrombospondin-1 domains. *Gene* **2002**, *283*(1–2), 49–62.
26. Jones, G.C.; Riley, G.P. ADAMTS proteinases: a multi-domain, multi-functional family with roles in extracellular matrix turnover and arthritis. *R. Arthritises Ther* **2005**, *7*(4), 160–169.
27. Liu, Y.J.; Xu, Y.; Yu, Q. A. D. A. M. Full-lengthTS-1 and the ADAMTS-1 fragments display pro- and antimetastatic activity, respectively. *Oncogene* **2006**, *25*(17), 2452–2467.
28. Porter, S.; Span, P.N.; Sweep, F.C.; Tjan-Heijnen, V.C.G.; Pennington, C.J.; Pedersen, T.X.; Johnsen, M.; Lund, L.R.; Rømer, J.; Edwards, D.R. ADAMTS8 and ADAMTS15 expression predicts

- survival in human breast carcinoma. *J. Int Cancer* **2006**, *118*(5), 1241–1247.
29. Pearson, O.H.; Manni, A.; Arafah, B.M. Antiestrogen treatment of breast cancer: an overview. *R. Canceres* **1982**, *42*(8 Suppl.), 3424S–3429S.
 30. Horoszewicz, J.S.; Leong, S.S.; Kawinski, E. LNCaP model of human prostatic carcinoma. *R. Canceres* **1983**, *43*(4), 1809–1818.
 31. Lin, M.F.; Meng, T.C.; Rao, P.S.; Chang, C.; Schonthal, A.H.; Lin, F.F. Expression of human prostatic acid phosphatase correlates with androgen-stimulated cell proliferation in prostate cancer cell lines. *J. C. Biolhem* **1998**, *273*(10), 5939–5947.
 32. Sherwood, E.R.; Van Dongen, J.L.; Wood, C.G.; Liao, S.; Kozlowski, J.M.; Lee, C. Epidermal growth factor receptor activation in androgen-independent but not androgen-stimulated growth of human prostatic carcinoma cells. *J. Br Cancer* **1998**, *77*(6), 855–861.
 33. Radonić, A.; Thulke, S.; Mackay, I.M.; Landt, O.; Slegert, W.; Nitsche, A. Guideline to reference gene selection for quantitative real-time PCR. *Biochem. R. R. Biophys Commun* **2004**, *313*(4), 856–862.
 34. Livak, K.J.; Schmittgen, T.D. Analysis of relative gene expression data using real-time quantitative PCR and the 2^{-ΔΔC_T} method. *Methods* **2001**, *25*(4), 402–408.
 35. Thalmann, G.N.; Sikes, R.A.; Wu, T.T.; Degeorges, A.; Chang, S.M.; Ozen, M.; Pathak, S.; Chung, L.W. LNCaP progression model of human prostate cancer: androgen-independence and osseous metastasis. *Prostate* **2000**, *44*(2), 91–103.
 36. Birney, E.; Andrews, T.D.; Bevan, P.; Caccamo, M.; Chen, Y.; Clarke, L.; Coates, G.; Cuff, J.; Curwen, V.; Cutts, T.; Down, T.; Eyra, E.; Fernandez-Suarez, X.M.; Gane, P.; Gibbins, B.; Gilbert, J.; Hammond, M.; Hotz, H.R.; Iyer, V.; Jekosch, K.; Kahari, A.; Kasprzyk, A.; Keefe, D.; Keenan, S.; Lehtvasalho, H.; McVicker, G.; Melsopp, C.; Meidl, P.; Mongin, E.; Pettett, R.; Potter, S.; Proctor, G.; Rae, M.; Searle, S.; Slater, G.; Smedley, D.; Smith, J.; Spooner, W.; Stabenau, A.; Stalker, J.; Storey, R.; Ureta-Vidal, A.; Woodward, K.C.; Cameron, G.; Durbin, R.; Cox, A.; Hubbard, T.; Clamp, M. An overview of Ensembl. *R. Genomes* **2004**, *14*(5), 925–928.
 37. Podvinec, M.; Kaufmann, M.; Handschin, C.; Meyer, U. NUBIScan, an in silico approach for prediction of nuclear receptor response elements. *E. Molndocrinol* **2002**, *16*(6), 1269–1279.
 38. Riegman, P.H.; Vlietstra, R.J.; van der Korput, J.A.; Brinkmann, A.O.; Trapman, J. The promoter of the prostate-specific antigen gene contains a functional androgen responsive element. *E. Molndocrinol* **1991**, *5*(12), 1921–1930.
 39. Israeli, R.S.; Powell, C.T.; Corr, J.G.; Fair, W.R.; Heston, W.D. Expression of the prostate-specific membrane antigen. *R. Canceres* **1994**, *54*(7), 1807–1811.
 40. Veldscholte, J.; Berrevoets, C.A.; Ris-Stalpers, C. The androgen receptor in LNCaP cells contains a mutation in the ligand binding domain which affects steroid binding characteristics and response to antiandrogens. *J. B. Steroidiochem B. Moliol* **1992**, *47*(3–8), 665–669.
 41. Culig, Z.; Hobisch, A.; Cronauer, M.V.; Cato, A.C.; Hittmair, A.; Radmayr, C.; Eberle, J.; Bartsch, G.; Klocker, H. Mutant androgen receptor detected in an advanced-stage prostatic carcinoma is activated by adrenal androgens and progesterone. *E. Molndocrinol* **1993**, *7*(12), 1541–1550.
 42. Zhao, X.Y.; Malloy, P.J.; Krishnan, A.V.; Swami, S.; Navone, N.M.; Peehl, D.M.; Feldman, D. Glucocorticoids can promote androgen-independent growth of prostate cancer cells through a mutated androgen receptor. *M. Nated* **2000**, *6*(6), 703–706.
 43. Taplin, M.E.; Bubley, G.J.; Shuster, T.D.; Frantz, M.E.; Spooner, A.E.; Ogata, G.K.; Keer, H.N.; Balk, S.P. Mutation of the androgen-receptor gene in metastatic androgen-independent prostate cancer. *N. J. Engl Med* **1995**, *332*(21), 1393–1388.
 44. Sartor, A.O.; Tangen, C.M.; Hussain, M.H.; Eisenberger, M.A.; Parab, M.; Fontana, J.A.; Chapman, R.A.; Mills, G.M.; Raghavan, D.; Crawford, E.D.; O. Southwestncology Group. Antiandrogen withdrawal in castrate-refractory prostate cancer: a O. Southwestncology Group trial (SWOG 9426). *Cancer* **2008**, *112*(11), 2393–2400.
 45. Scher, H.I.; Kelly, W.K. Flutamide withdrawal syndrome: its impact on clinical trials in hormone-refractory prostate cancer. *J. O. Clinncol* **1993**, *11*(8), 1566–1572.
 46. Herrada, J.; Dieringer, P.; Logothetis, C.J. Characterization of patients with androgen-independent prostatic carcinoma whose serum prostate specific antigen decreased following flutamide withdrawal. *J. Urol* **1996**, *155*(2), 620–623.
 47. Dupont, A.; Gomez, J.L.; Cusan, L.; Koutsilieris, M.; Labrie, F. Response to flutamide withdrawal in advanced prostate cancer in progression under combination therapy. *J. Urol* **1993**, *150*(3), 908–913.
 48. Heinelein, C.A.; Chang, C. Androgen receptor (AR) coregulators: an overview. *R. Endocrev* **2002**, *23*(2), 175–200.
 49. Kleinjan, D.A.; van Heyningen, V. Long-range control of gene expression: emerging mechanisms and disruption in disease. *J. Am G. Hument* **2005**, *76*(1), 8–32.
 50. Cleutjens, K.B.; van der Korput, H.A.; van Eekelen, C.C.; van Rooij, H.C.; Faber, P.W.; Trapman, J. An androgen response element in a far upstream enhancer region is essential for high, androgen-regulated activity of the prostate-specific antigen promoter. *E. Molndocrinol* **1997**, *11*(2), 148–161.
 51. Horie-Inoue, K.; Bono, H.; Okazaki, Y.; Inoue, S. Identification and functional analysis of consensus androgen response elements in human prostate cancer cells. *B. Biochemiophys C. Resomun* **2004**, *325*(4), 1312–1317.
 52. Tanaka, K.K.; Bryantsev, A.L.; Cripps, R.M. Myocyte enhancer factor 2 and chorion factor 2 collaborate in activation of the myogenic program in *Drosophila*. *C. Molell Biol* **2008**, *28*(5), 1616–1629.
 53. Potthoff, M.J.; Olson, E.N. MEF2: a central regulator of diverse developmental programs. *Development* **2007**, *134*(23), 4131–4140.
 54. Wasserman, W.W.; Sandelin, A. Applied bioinformatics for the identification of regulatory elements. *R. Natev Genet* **2004**, *5*(4), 276–287.
 55. Gerhardt, S.; Hassall, G.; Hawtin, P.; McCall, E.; Flavell, L.; Minshull, C.; Hargreaves, D.; Ting, A.; Pauptit, R.A.; Parker, A.E.; Abbott, W.M. Crystal structures of human ADAMTS-1 reveal a conserved catalytic domain and a disintegrin-like domain with a fold homologous to cysteine-rich domains. *J. B. Moliol* **2007**, *373*(4), 891–902.
 56. Kashiwagi, M.; Enghild, J.J.; Gendron, C.; Hughes, C.; Caterson, B.; Itoh, Y.; Nagase, H. Altered proteolytic activities of ADAMTS-4 expressed by C-terminal processing. *J. C. Biolhem* **2004**, *279*(11), 10109–10119.
 57. Kuno, K.; Bannai, K.; Hakozaaki, M.; Matsushima, K.; Hirose, K. The carboxyl-terminal half region of ADAMTS-1 suppresses both tumorigenicity and experimental tumor metastatic potential. *B. Biochemiophys C. Resomun* **2004**, *319*(4), 1327–1333.
 58. Sjöblom, T.; Jones, S.; Wood, L.D.; Parsons, D.W.; Lin, J.; Barber, T.D.; Mandelker, D.; Leary, R.J.; Ptak, J.; Silliman, N.; Szabo, S.; Buckhaults, P.; Farrell, C.; Meeh, P.; Markowitz, S.D.; Willis, J.; Dawson, D.; Willson, J.K.; Gazdar, A.F.; Hartigan, J.; Wu, L.; Liu, C.; Parmigiani, G.; Park, B.H.; Bachman, K.E.; Papadopoulos, N.; Vogelstein, B.; Kinzler, K.W.; Velculescu, V.E. The consensus coding sequences of human breast and colorectal cancers. *Science* **2006**, *314*(5797), 268–274.
 59. Wood, L.D.; Parsons, D.W.; Jones, S.; Lin, J.; Sjöblom, T.; Leary, R.J.; Shen, D.; Boca, S.M.; Barber, T.; Ptak, J.; Silliman, N.; Szabo, S.; DeZso, Z.; Ustyanksky, V.; Nikolskaya, T.; Nikolsky, Y.; Karchin, R.; Wilson, P.A.; Kaminker, J.S.; Zhang, Z.; Croshaw, R.; Willis, J.; Dawson, D.; Shipitsin, M.; Willson, J.K.; Sukumar, S.; Polyak, K.; Park, B.H.; Pethiyagoda, C.L.; Pant, P.V.; Ballinger, D.G.; Sparks, A.B.; Hartigan, J.; Smith, D.R.; Suh, E.; Papadopoulos, N.;

- Buckhaults, P.; Markowitz, S.D.; Parmigiani, G.; Kinzler, K.W.; Velculescu, V.E.; Vogelstein, B. The genomic landscapes of human breast and colorectal cancers. *Science* **2007**, *318*(5853), 1108–1113.
60. Viloria, C.G.; Obaya, A.J.; Moncada-Pazos, A.; Llamazares, M.; Astudillo, A.; Capellá, G.; Cal, S.; López-Otín, C. Genetic inactivation of ADAMTS15 metalloprotease in human colorectal cancer. *R. Canceres* **2009**, *69*(11), 4926–4934.
61. Weidner, N.; Carroll, P.R.; Flax, J.; Blumenfeld, W.; Folkman, J. Tumor angiogenesis correlates with metastasis in invasive prostate carcinoma. *J. Am Pathol* **1993**, *143*(2), 401–409.
62. Revelos, K.; Petraki, C.; Scorilas, A.; Stefanakis, S.; Malovrouvas, D.; Alevizopoulos, N.; Kanellis, G.; Halapas, A.; Koutsilieris, M. Correlation of androgen receptor status, neuroendocrine differentiation and angiogenesis with time-to-biochemical failure after radical prostatectomy in clinically localized prostate cancer. *R. Anticanceres* **2007**, *27*(5B), 3651–3660.
63. van 't Veer, L.J.; Dai, H.; van de Vijver, M.J.; He, Y.D.; Hart, A.A.M.; Mao, M.; Peterse, H.L.; van der Kooy, K.; Marton, M.J.; Witteveen, A.T.; Schreiber, G.J.; Kerkhoven, R.M.; Roberts, C.; Linsley, P.S.; Bernards, R.; Friend, S.H. Gene expression profiling predicts clinical outcome of breast cancer. *Nature* **2002**, *415*(6871), 530–536.
64. Yuan, X.; Balk, S.P. Mechanisms mediating androgen receptor reactivation after castration. *O. Uroincol* **2009**, *27*(1), 36–41.

APPENDIX B

Copyright Permissions:

WOLTERS KLUWER HEALTH LICENSE TERMS AND CONDITIONS

This is a License Agreement between Chidi Molokwu ("You") and Wolters Kluwer Health ("Wolters Kluwer Health") provided by Copyright Clearance Center ("CCC"). The license consists of your order details, the terms and conditions provided by Wolters Kluwer Health, and the payment terms and conditions.

All payments must be made in full to CCC. For payment instructions, please see information listed at the bottom of this form.

License Number	2450180590550
License date	Jun 15, 2010
Licensed content publisher	Wolters Kluwer Health
Licensed content publication	American Journal of Surgical Pathology, The
Licensed content title	Zonal Distribution of Prostatic Adenocarcinoma: Correlation with Histologic Pattern and Direction of Spread
Licensed content author	John McNeal, Elise Redwine, Fuad Freiha, et al
Licensed content date	Jan 1, 1988
Volume Number	12
Issue Number	12
Type of Use	Dissertation/Thesis
Requestor type	Individual
Title of your thesis / dissertation	Analysis of the Functional Role of ADAMTS-1 and -15 in Prostate Cancer Progression
Expected completion date	Jul 2010
Estimated size(pages)	250

Billing Type	Invoice
Billing Address	Academic Urology Unit, D-Floor University of Sheffield Medical School Sheffield, other S10 2RX United Kingdom
Customer reference info	
Total	0.00 GBP
Terms and Conditions	

Terms and Conditions

1. A credit line will be prominently placed and include: for books - the author(s), title of book, editor, copyright holder, year of publication; For journals - the author(s), title of article, title of journal, volume number, issue number and inclusive pages.
2. The requestor warrants that the material shall not be used in any manner which may be considered derogatory to the title, content, or authors of the material, or to Wolters Kluwer/Lippincott, Williams & Wilkins.
3. Permission is granted for one time use only as specified in your correspondence. Rights herein do not apply to future reproductions, editions, revisions, or other derivative works. Once term has expired, permission to renew must be made in writing.
4. Permission granted is non-exclusive, and is valid throughout the world in the English language and the languages specified in your original request.
5. Wolters Kluwer Health/ Lippincott, Williams & Wilkins, cannot supply the requestor with the original artwork or a "clean copy."
6. The requestor agrees to secure written permission from the author (for book material only).
7. Permission is valid if the borrowed material is original to a LWW imprint (Lippincott-Raven Publishers, Williams & Wilkins, Lea & Febiger, Harwal, Igaku-Shoin, Rapid Science, Little Brown & Company, Harper & Row Medical, American Journal of Nursing Co, and Urban & Schwarzenberg - English Language).
8. If you opt not to use the material requested above, please notify Rightslink within 90 days of the original invoice date.
9. Other Terms and Conditions:

v1.0

Gratis licenses (referencing \$0 in the Total field) are free. Please retain this printable license for your reference. No payment is required.

If you would like to pay for this license now, please remit this license along with your payment made payable to "COPYRIGHT CLEARANCE CENTER" otherwise you will be invoiced within 48 hours of the license date. Payment should be in the form of a check or money order referencing your account number and this invoice number RLNK10799789.

Once you receive your invoice for this order, you may pay your invoice by credit card. Please follow instructions provided at that time.

**Make Payment To:
Copyright Clearance Center
Dept 001
P.O. Box 843006
Boston, MA 02284-3006**

For suggestions or comments regarding this order, contact Rightslink Customer Support: customer care@copyright.com or +1-877-622-5543 (toll free in the US) or +1-978-646-2777.



Subject: **Copyright Information Request**

From: **C N Molokwu** <C.Molokwu@sheffield.ac.uk>
Date: 4 May 2010 21:21
To: PermissionsUK@wiley.com

Dear Sir/Madam,

I am a PhD student at the University of Sheffield in the UK. I am presently writing my thesis.

I have used the book titled 'Prostate Cancer' edited by Marc S. Ernstoff, John A. Heaney and Richard E. Peschel, published 1998, ISBN 0-63204-317-2.

In Chapter 2 'Pathology of Prostate Cancer' by David G Bostwick, page 30, Figure 2-9, is a drawing of the Gleason grades originally drawn by D.F. Gleason. I have been trying unsuccessfully to find out who the copyright holder is, and if I may use the image in my thesis.

Please could you give me any information on this image, and if Blackwell holds the copyright, how I may obtain permission to use the image.

Thank you for your help.

Yours sincerely,

Chidi Molokwu.

From: **Permission Requests - UK** <permissionsuk@wiley.com>
Date: 20 May 2010 15:12
To: C N Molokwu <C.Molokwu@sheffield.ac.uk>

Dear Chidi Molokwu

Thank you for your email request. Permission is granted for you to use the material below for your thesis/dissertation subject to the usual acknowledgements and on the understanding that you will reapply for permission if you wish to distribute or publish your thesis/dissertation commercially.

Kind Regards

Katie B Wade
Permissions Assistant
Wiley-Blackwell
9600 Garsington Road
Oxford OX4 2DQ
UK
Tel: +44 (0) 1865 476149
Fax: +44 (0) 1865 471158
Email: katie.wade@wiley.com

From: **C N Molokwu** <C.Molokwu@sheffield.ac.uk>
Date: 9 March 2010 12:45
Subject: Copyright Permission
To: terese.winslow@mindspring.com

Dear Terese Winslow,

I am a PhD student at the University of Sheffield in the United Kingdom. I am writing my thesis titled 'The Role of ADAMTS-1 and -15 in Prostate Cancer Progression'. During my studies, I came across two of your images on the National Cancer Institute website (Images attached). I would like to use them in my thesis if you would be kind enough to grant me permission. Are there any formal request procedures to be followed? Please let me know.

Thanks for your help.

Yours faithfully,

Chidi Molokwu

From: **Terese Winslow** <terese.winslow@mindspring.com>
Date: 9 March 2010 13:46
Subject: Re: Copyright Permission
To: C N Molokwu <C.Molokwu@sheffield.ac.uk>

Dear Chidi Molokwu,

Thank you for contacting me. You have my permission. Please send me your address and the approximate number of copies to be printed. Will the thesis be posted online? Make sure name credit is written as shown on the art and be sure to contact me again for any other usage.

Best regards,
Terese

Terese Winslow
Medical Illustrator
714 South Fairfax Street
Alexandria, Virginia 22314
Phone: 703-836-9121
Fax: 703-836-3715
terese.winslow@mindspring.com
www.teresewinslow.com

From: **C N Molokwu** <C.Molokwu@sheffield.ac.uk>
Date: 9 March 2010 18:30
Subject: Re: Copyright Permission
To: Terese Winslow <terese.winslow@mindspring.com>

Dear Terese,

Thanks for you reply.

My address is

Chidi Molokwu
21 Cherry Tree Grove
Duncroft
Doncaster DN7 4NU
United Kingdom

Seven copies of the thesis will be printed. One copy each will be available at the University of Sheffield and the Royal College of Physicians & Surgeons of Glasgow libraries. The other copies will be kept by my supervisors and myself. Theses from the University of Sheffield are not usually posted online but this procedure may change by the time I submit. Would you require that they are not placed online?

Name credit will be given as it appears on the images. Do you require the line 'US Govt has certain rights' be included or can this be blanked out?

In the image showing the stages of prostate cancer, with your permission, would like to blank out the headings 'Stage I', 'Stage II', 'Stage III', 'Stage IV' at the top of each image. This is because the staging system has been superceded by the TNM staging classification for tumours.

Thanks again for your help.

Regards,

Chidi Molokwu

APPENDIX C

LIST OF SUPPLIERS

Abcam, 330 Cambridge Science Park, Cambridge, United Kingdom CB4 0FL

Phone: 01223696000, Fax: 01223771600, E-mail: orders@abcam.com

www.abcam.com

AGFA, Vantage West, Great West Road, Brentford, Middlesex, United Kingdom TW8

9AX

Phone: 02082314983, Fax: 08009172032, E-mail: graphic@agfa.com

www.agfa.com

Alpha Laboratories Ltd, 40 Parham Drive, Eastleigh, Hampshire, United Kingdom

SO50 4NU

Phone: 0800387732, Fax: 0800614249, E-mail: sales@alphalabs.co.uk

www.alphalabs.co.uk

Applied Biosystems, Lingley House, 120 Birchwood Boulevard, Warrington, United

Kingdom WA3 7QH

Phone: 01925 28 2670, Fax: 01925 28 2503, E-mail:

uk.orders@eur.appliedbiosystems.com

www.appliedbiosystems.com

Bachem (UK) Ltd, Delph Court, Sullivans Way, St. Helens, Merseyside, United

Kingdom WA9 5GL

Phone: 01744612108, Fax: 01744730064

www.bachem.com

BD Biosciences, Edmund Halley Road, Oxford Science Park, Oxford, United Kingdom

OX4 4DQ

Phone: 01865781666, Fax: 01865781627,

E-mail: BDUK_Customerservice@europe.bd.com

www.bdbiosciences.com

Bioline Ltd, Unit 16, The Edge Business Centre, Humber Road, London, United Kingdom NW2 6EW

Phone: 0208 830 5300, Fax: 0208 452 2822, E-mail: orders.uk@bioline.com

Biological Industries Ltd, Kibbutz Beit-Haemek, 25115, Israel

Phone: +972(0)49960595, Fax: +972(0)49968896, E-mail: info@bioind.com

www.bioind.com

Biontex Laboratories GmbH, im Innovations- und Gründerzentrum Biotechnologie (Soda), Am Klopferspitz 19, 82152 Martinsried/Planegg, Germany

Phone: +498932479950, Fax: +498932479952, E-Mail: contact@biontex.com

www.biontex.com

Bio-Rad Laboratories Ltd, Bio-Rad House, Maxted Road, Hemel Hempstead, Hertfordshire, United Kingdom HP2 7DX

Phone: 02083282000, Fax: 02083282550, E-mail: uk.lsg.marketing@bio-rad.com

www.bio-rad.com

BioSource Europe, S.A., Rue de l'Industrie 8, B-1400 Nivelles, Belgium

Phone: +3267889900, Fax: +3267889996

www.biosource.com

Dako UK Ltd, Cambridge House, St Thomas Place, Ely, Cambridgeshire, United Kingdom CB7 4EX

Phone: 01353669911, Fax: 01353667309, E-mail: info.uk@dako.com

www.dako.co.uk

GE Healthcare Life Sciences, Amersham Place, Little Chalfont, Buckinghamshire, United Kingdom HP7 9NA

Phone: 0800515313, Fax: 0800616927, Email: Orders.GB@ge.com

www.gelifesciences.com

GraphPad Software, Inc, 2236 Avenida de la Playa, La Jolla, CA 92037 USA

Phone: +18584545577, Fax: +18584544150, E-mail: sales@graphpad.com

www.graphpad.com

Hawksley, Marlborough Road, Lancing Business Park, Lancing, Sussex, United

Kingdom BN15 8TN

Phone: 01903752815, Fax: 01903766050, E-mail: enquiries@hawksley.co.uk

www.hawksley.co.uk

Invitrogen Ltd, 3 Fountain Drive, Inchinnan Business Park, Paisley, United Kingdom

PA4 9RF

Phone: 0141 814 6100, Fax: 0141 814 6260, E-mail: ukorders@invitrogen.com

www.invitrogen.com

Lonza Biologics Plc, 228 Bath Road, Slough, Berkshire, United Kingdom SL1 4DX

Phone: 01753777000, Fax: 01753777001, E-mail: contact.slough@lonza.com

www.lonza.com

Millipore (U.K.) Ltd, Suite 3 & 5, Building 6, Croxley Green Business Park

Watford, United Kingdom WD18 8YH

Phone: 08709004645 Fax: 087090046 44 E-mail: UKcustomerservice@millipore.com

www.millipore.com

Molecular Devices (UK) Ltd, 660 - 665 Eskdale Road, Winnersh Triangle,

Wokingham, Berkshire, United Kingdom RG41 5TS

Phone: 01189448000, Fax: 01189448001

www.moleculardevices.com

Perbio Science UK Ltd, Unit 9, Atley Way, North Nelson Industrial Estate,
Cramlington, Northumberland, United Kingdom NE23 1WA
Phone: 0800 252 185, Fax: 0800 085 8772, Email: perbio.orders@thermofisher.com
www.perbio.com

Promega UK, Delta House, Southampton Science Park, Southampton,
United Kingdom SO16 7NS
Phone: 012380760225, Fax: 012380767014, E-mail: ukcustserve@promega.com
www.promega.com

Qiagen, Qiagen House, Fleming Way, Crawley, West Sussex, United Kingdom RH10
9NQ
Phone: 01293422999, Fax: 01293422922, Email: customercare-uk@qiagen.com
www.qiagen.com

R&D Systems Europe Ltd, 19 Barton Lane, Abingdon Science Park, Abingdon United
Kingdom OX14 3NB
Phone: 01235529449, Fax: 01235533420
www.rndsystems.com

Sigma-Aldrich Company Ltd, The Old Brickyard, New Road, Gillingham, Dorset,
United Kingdom SP8 4XT
Phone: 0800 717181, Fax: 0800 378785, E-mail: ukorders@sial.com
www.sigmaaldrich.com

Thermo Fisher Scientific UK, Bishop Meadow Road, Loughborough, Leicestershire,
United Kingdom
Phone: 01509231166, Fax: 01509231893, E-mail: sales@fisher.co.uk
www.fisher.co.uk